

Bacteria-initiated self-healing concrete
Influence of chloride ions, carbonation and mechanical load

Binti Md Yunus, B.

DOI

[10.4233/uuid:ebc7e6c4-c699-423e-98d6-42a4840c59b0](https://doi.org/10.4233/uuid:ebc7e6c4-c699-423e-98d6-42a4840c59b0)

Publication date

2023

Document Version

Final published version

Citation (APA)

Binti Md Yunus, B. (2023). *Bacteria-initiated self-healing concrete: Influence of chloride ions, carbonation and mechanical load*. [Dissertation (TU Delft), Delft University of Technology].
<https://doi.org/10.4233/uuid:ebc7e6c4-c699-423e-98d6-42a4840c59b0>

Important note

To cite this publication, please use the final published version (if applicable).
Please check the document version above.

Copyright

Other than for strictly personal use, it is not permitted to download, forward or distribute the text or part of it, without the consent of the author(s) and/or copyright holder(s), unless the work is under an open content license such as Creative Commons.

Takedown policy

Please contact us and provide details if you believe this document breaches copyrights.
We will remove access to the work immediately and investigate your claim.

BACTERIA-INITIATED SELF-HEALING CONCRETE
INFLUENCE OF CHLORIDE IONS, CARBONATION AND MECHANICAL
LOAD

Dissertation

for the purpose of obtaining the degree of doctor
at Delft University of Technology
by the authority of the Rector Magnificus prof. dr.ir. T.H.J.J. van der Hagen,
Chair of the Board for Doctorates
to be defended publicly on
Monday 27 February 2023 at 10:00 o'clock

by

Balqis MD YUNUS

Master of Science in Civil Engineering, Universiti Teknologi MARA, Malaysia
born in Kuala Lumpur, Malaysia

This dissertation has been approved by the promotor.

Composition of the doctoral committee:

Rector Magnificus	chairperson
Prof. dr. ir. E. Schlangen	Delft University of Technology, promotor
Prof. dr. H. M. Jonkers	Delft University of Technology, promotor

Independent members:

Prof. dr. H. Mohd Saman	Universiti Teknologi MARA, Malaysia
Prof. dr. S. Kessler	University of Hamburg, Germany
Prof. dr. ir. N. De Belie	Ghent University, Belgium
Prof. dr. ir. P.C. Louter	Delft University of Technology
Prof. dr. ir. K. van Breugel	Delft University of Technology



Keywords: bacterial concrete, self-healing concrete, microcracks, chloride, combined-load

Printed by: Ipskamp printing

Cover by:

Copyright © 2023 by Balqis Md Yunus

ISBN

An electronic copy of this dissertation is available at

<http://repository.tudelft.nl/>

Contents

1	General introduction.....	1
1.1	Research motivation.....	2
1.2	Scientific gap.....	4
1.3	Research objectives.....	4
1.4	Scope of work.....	5
1.5	Thesis structure.....	5
2	Literature review.....	8
2.1	Introduction and research significance.....	9
2.2	Durability and service life of concrete.....	10
2.2.1	Environmental loading.....	11
2.2.2	Deterioration mechanism.....	12
2.3	Transport mechanism in concrete.....	13
2.3.1	Chloride transport in concrete.....	15
2.3.2	Carbonation of concrete.....	16
2.4	Capillary pores and micro cracks in concrete.....	17
2.5	Self-healing of cement-based materials.....	19
2.5.1	Microbial applications in cement-based materials.....	21
2.5.2	Field applications of bacteria-based repair systems.....	24
2.6	Concluding remarks.....	25
3	Test methods to determine durability of concrete under compressive load-induced damage.....	27
3.1	Introduction.....	28
3.2	Permeability of cracked concrete.....	28
3.3	Permeability of stressed concrete.....	29
3.4	Cracking and failure in compression.....	31
3.5	Analysis of load-induced damage.....	31
3.6	Service life of concrete under combined mechanical load and environmental actions.....	32
3.7	Proposed combined method.....	33
3.7.1	Description of test rig for compression.....	33
3.7.2	Method for preparation of samples.....	35
3.7.3	Vacuum saturation test.....	36
3.7.4	Chloride circulation setups.....	37

3.8	Determination of chloride profiles	38
3.8.1	Laser Induced Breakdown Spectroscopy, LIBS	38
3.8.2	Photometric Determination	39
3.9	Conclusions.....	41
4	Chloride resistance of concrete with compressive load-induced cracks.	42
4.1	Introduction	43
4.2	Materials	43
4.3	Specimen under combined loads	44
4.4	Sampling techniques	46
4.4.1	LIBS sampling method	46
4.4.2	Sampling method for photometric determination.....	48
4.5	Results and discussion	48
4.5.1	LIBS measurement and results	48
4.5.2	Photometric determination.....	53
4.6	Summary of LIBS and photometric determination	57
4.7	Conclusions.....	58
5	Strength development of concrete containing bacteria-based self-healing agent	59
5.1	Introduction and research significance.....	60
5.2	Bacteria-based self-healing concrete	60
5.2.1	Slump test.....	62
5.2.2	Setting time of concrete.....	62
5.2.3	Strength development	63
5.3	Mortar containing bacteria-based healing agent	64
5.4	Bacteria-based self-healing agent constituents.....	65
5.4.1	Influence of bacteria-based self-healing agent on properties of fresh mortar mix	66
5.4.2	Hydration and strength development	66
5.5	Conclusions.....	67
6	Chloride transport under compressive load in bacteria-based self-healing concrete.....	68
6.1	Introduction	69
6.2	Experimental program and used methods	70
6.2.1	Bacterial specimen preparation	70
6.2.2	Testing methods	70
6.2.3	Chloride profiles determination	71

6.2.4	Determination of the concrete self-healing process.....	72
6.3	Results and data collections	74
6.3.1	Chloride ingress in bacteria-based healing agent containing specimens	74
6.3.2	Chloride ingress in reference specimens.....	75
6.3.3	Estimation of chloride diffusion coefficients	76
6.3.4	Microscopic observation of mineral formation	78
6.3.5	Oxygen consumption of concrete specimens	79
6.4	Discussion	80
6.5	Conclusions.....	82
7	Durability improvement via bacteria-based self-healing of cracked mortars under compression-, carbonation- and chloride-loaded conditions.	83
7.1	Introduction	84
7.2	Materials and methods.....	85
7.2.1	Pre-conditioning of mortar specimens	85
7.2.2	Healing treatment procedure and selection of bio-healing agent.....	86
7.3	Evaluation of healing efficiency	87
7.3.1	Chloride ingress in cracked mortar	87
7.3.2	Carbonation rate of cracked specimen.....	90
7.3.3	Pore volume assessment	90
7.3.4	Optical observations by ESEM and stereomicroscopy	91
7.3.5	Oxygen consumption analysis.....	92
7.4	Results and discussion	93
7.4.1	Crack opening displacement.....	93
7.4.2	Crack-healing capacity	94
7.4.3	EDS mapping analysis.....	97
7.4.4	Carbonation.....	101
7.4.5	Gas expansion pycnometer.....	102
7.4.6	Optical observation of bacterial imprints	103
7.4.7	Oxygen consumption test	106
7.5	Conclusions.....	109
8	Conclusions and prospects.....	110
8.1	General conclusions	111
8.2	Future perspectives	113

References	115
A Test methods to determine durability of concrete under combined environmental actions and mechanical load: final report of RILEM TC 246-TDC	125
B Recommendation of RILEM TC 246-TDC: test methods to determine durability of concrete under combined environmental actions and mechanical load	139
Summary	149
Samenvatting	152
Curriculum vitae	155
List of publication	156

ACKNOWLEDGEMENT

In the end, it's not the years in your life that count. It's the life in your years.

-Abraham Lincoln-

The research work reported in this thesis was sponsored by Ministry of Education (MOE), Malaysia, Universiti Teknologi MARA (UiTM), Malaysia and Delft University of Technology (TU Delft). This research was carried out in the Section of Materials and Environment at the Faculty of Civil Engineering and Geosciences of TU Delft. MOE, UiTM and DCMat, TU Delft are gratefully acknowledged for the financial and the technical support.

Alhamdulillah, all praises is due to Allah S.W.T., the Mighty and the Wise to realize the success of my doctoral degree. Without His blessings and His grace this thesis can never be completed.

I see my PhD successions as a growing baby. We have the same feeling at the beginning of “our” journey, thinking about how to survive in this new expedition that full with unexpected. We need people around, to keep us “calm”. Through continuous loves and guidance, we gradually acquiring the skills to “survive”. There are many great people who had sincerely supported me technically, physically and mentality.

Firstly, I would like to express my deepest appreciation to my first promotor, Erik (Prof. Schlangen). During my first year, Erik had spent a lot of time not only to familiar me with the research area but also on ways of living in Delft. The same year he was appointed as a head of microlab, but he still remains the same as he is easy to approach and access. Concerning that I need more people and room for discussion, he had introduced me to Henk (Prof. Jonkers), who is my second promotor. Words cannot express my gratitude to Henk for his constructive comments and suggestions that always made ongoing improvements to my research works. I was extremely lucky that they both completely understand my roles as a PhD candidate and a mother of two kids during my research work at TU Delft. Their immense knowledge and bountiful experience have encouraged me in all the time of my academic research and daily life.

I am deeply indebted to Gerrit Nagtegaal for his valuable experience and brilliant solution in comprehending my “crazy” ideas for the experimental setup. This endeavor would not have been possible without the time and energy he has spent. Special thanks to Arjan for his assistance in living bacteria discoveries, John for his never missed safety and regulations reminder for working in chemical lab and Maiko and Ton for their kind support in providing me the materials to make concrete.

Special word to the Bio-team member; Senot, Renee, Eirini, Damian, Virginie and Lupita. Thank you for the bundle of knowledge sharing via monthly meeting. Also, I am grateful to Branko, Jose, Farhad, Zichao Pan and Dong Hua for an intensive chloride discussions and Bei Wu for his assistance with my carbonation chamber setups. My heartfelt thanks to Agus and Adhi for their time and energy to assist me on my concrete lab work during my antenatal period. Lourdes, Stefan (Bianca), Renee, Xu Ma, Mladena, who had sometimes made my lunch time more merrier. Thank you to Marija (and Patrick) for the companionship. Not to

forget, I must thank my officemate, Shizhe Zhang for the endnote course! And the rest of the PhD candidates and colleagues at the department of Materials & Environment (MicroLab), Xiao Wei (and Rosie), Gao Peng, Tianshi Lu, (for an exciting tour in Beijing) Hitham, Claudia for never ending support.

I would also like to extend my thanks to all Malaysian living in Delft during the period of March 2013 until February 2017. Thank you for making my days in Delft not too far from Malaysia with the languages we talked and the food we cooked. My sincere thanks to Zura and family, I will never forget your warm welcome and hospitality upon our arrival in Delft. To Roslinda (M. Fauzi), M. Zairul, Munirah (M.Farabi) and Basyarah (Shahril) for being so nice and helpful during my antenatal time in Delft. Thank you for this pleasing family friendship.

I owe to my parents, Norsiah and Md Yunus for their time and energy in taking care of my family and me during my confinement time in Delft. No matter what was the decision I have made in my life, both of you never objected and support me to the fullest. Thank you to my parents-in-law for their long-distance encouragement and prays. To my sisters and brothers and my family in law, thank you for the unfailing support although we were far from distance.

I save the last word of my acknowledgement for the best 'companion' in my PhD journey, my husband, Suryamin for his continued and unwavering love, support and encouragement to stay close in all ups and downs moments. To my eldest son, Alaudeen, he is the subject of this story. We came to Delft when he was 3 months old. I see his growth as my Ph.D development, we both have struggled to develop our skills ultimately and finally we have been through the process magnificently! Also, to all my children Amandha, Achraaf and Adleyaa who joined us when I was writing my thesis, thank you for giving me unlimited happiness and pleasure. I feel blessed to have all of you by my side on the day that I will end my PhD journey. Although my journey is very "far" to reach, the adorable in every one of you have provided me strength in pursuing this work till the end.

PhD journey is an exciting term that contributes to the best lesson and many sweet memories in life. This accomplished mission has shape me into a better and mature person in both career and life. As I reflect on my journey, I am humbled and touched by the outpouring of love and support that I have received. I am forever grateful to Allah SWT, my promotors, my small and big families and will continue to strive for an excellence performance in all my future endeavors.

Balqis Md Yunus

Shah Alam,
January 30, 2023

1 .

General introduction

Motivation is what gets you started, habit is what keeps you going.

-Jim Rohn-

In practice, it was observed that the lifespan of reinforced concrete structure as designed according to the codes is often too short particularly in aggressive environment. As a consequence, the maintenance and repair costs in subsequent years over the project lifespan have become extremely high. Thus, it is necessary to develop sustainable concrete and make it more durable. The solution to this is to bio-mimic nature by making self-healed concrete materials to make service life design even more realistic.

The chapter starts with the research motivation and background of the research. Furthermore, the objectives, scope of the study and summaries of thesis structures of all chapters are presented.

1.1 Research motivation

A mixture of cement, water, fine aggregate and coarse aggregate, also universally known as concrete, is a versatile construction material that is used as a main building material since the midst of the nineteenth century. Concrete becomes monolith when the cement and water fill the spaces between the aggregates and hardens after a certain period of curing [1]. Concrete elements that are subjected to a substantial tensile load can easily break. Therefore, concrete is usually strengthened with steel bars to increase the tensile capacity. It is imperative for concrete structures to maintain the required strength and durability during the specified lifespan.

Durability of concrete is its ability to withstand the continuous interaction with the environment or any process of degradation. The detrimental action can be direct or indirect from various forms of distress due to chemical, thermal and mechanical stress [2]. In general, the potentially most destructive factor for the steel in concrete is the presence of chloride, carbon dioxide, oxygen and sulphate and other aggressive agents.

Chloride ions can destroy the passive oxide film on steel, leading to localised corrosion of steel reinforcement and subsequently become a significant threat to reinforced concrete, especially for structures in marine environments [2]. The condition may become worse if high levels of chloride contamination accompany the carbonation. Carbonation is a chemical reaction between atmospheric carbon dioxide (CO_2) and the calcium bearing phases present in hydrated cement. In concrete containing Portland cement, the reaction is mainly on carbonation of calcium hydroxide ($\text{Ca}(\text{OH})_2$), however, calcium silicate hydrate (C-S-H) will also be carbonated if $\text{Ca}(\text{OH})_2$ becomes depleted. The pH of the pore water in carbonated concrete drops from 12.6 – 13.5 to about 7 – 8.3 resulting in rupture of passivation layer around the embedded steel, initiating steel corrosion [2-5].

Permeability is influenced by the pore volume, size and continuity in the pore system. The pore's connection can be in the zone near the interface between the cement paste and the aggregate and also within the bulk of the hardened cement paste. It is primarily the total volume of the pores that is important in regard to the strength and durability of the concrete [6]. When the concrete dries out, it will cause a volume change in concrete. Volume changes in concrete may result in cracks.

For a variety of reasons, particularly aesthetics purpose, cracks can be undesirable to concrete structures [7]. From a structural point of view, the formation of cracks in concrete can be regarded as an intrinsic feature and may not jeopardize the structural integrity of an element. From a durability point of view, cracks increase the permeability and the diffusivity of concrete by interlinking with existing pores in concrete, making the transport of chloride ions or carbon dioxides into the interior of concrete relatively easy [4] as represented in Figure 1.1.

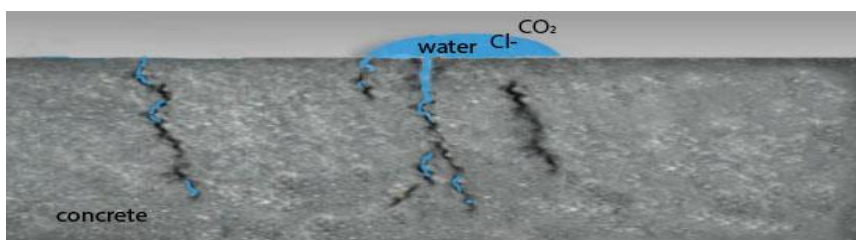


Figure 1.1 Cracks and capillary pores in concrete

The crack and pore structure undergoes changes due to continuing hydration, even more significant under mechanical stress [8]. In this condition, pores become interconnected because of the formation of new micro-cracks and the growth of existing cracks. In case these micro-cracks form a continuous network of cracks, deleterious substances, particularly chloride and carbon dioxide, may easily permeate into the concrete [9]. Consequently, the degradation processes of the concrete may occur and affect the durability of the concrete within the expected service life, or even worse, reduce the concrete structures lifespan. Indeed, mutual interacting effects of mechanical stress-induced cracks and ingress of attacking agents must be taken into serious consideration.

Previous studies have indicated that the service life under these combined mechanical and environmental loads is considerably shorter than under the effect of separate individual actions [10]. It is not clear from published literature at which stress level, the access of chloride and carbon dioxide into concrete is affected. Similar studies have found that the permeability of concrete was considerably affected only at higher stress level [9],[11-13]. This work, however, was undertaken in the absence of a standard testing method and several ingress influencing parameters were not taken into consideration, such as environmental intermittency, temperature, relative humidity, etc where not all of which can be identical in different research studies performed.

Because of all these complexities, the durability potential of concrete is considered difficult to assess and frequently it turns out that a substantial expense on repair and maintenance of structures are needed. The increasing amount of money spent each year on maintenance and repairs clearly demonstrate a demand for higher quality and more durable concrete structures.

Practical experience and experimental investigation demonstrate that cement is capable to heal cracks in fractured concrete by autogenous healing, likely improving its water tightness. The autogenous healing of cracks in concrete is initially fast and then the rate decreases. In aging concrete structures autogenous healing may not seem to be available. This might also be the case in young concrete with high densities of cracks. However, with current research invention the self-healing in concrete can be feasible throughout the service life of concrete structures. One of the potential materials is some selected bacteria with a suitable organic compound to act as a self-healing agent in concrete. Different types or group of bacteria may require different environments and nutrients for their growth and to produce limestone. Sometimes the coupled agents may leave effects on the properties of cement-based materials. Therefore, it is very important to always check the effect of bacterial agent on the fresh properties of cementitious materials.

The inclusion of a healing agent in concrete can also be considered as a protective measure. The integration of a bacteria-based self-healing agent in the concrete matrix results in efficient sealing of cracks [14],[15]. Although it may not completely prevent chloride penetration or other ingress of aggressive substances, it is expected to reduce the ingress significantly. This will reduce the risk of degradation of the concrete and extend the service life, resulting in reduction of the maintenance and repair cost. In case self-healing materials are used, it will be essential that they are reliable in order to allow an economical and sustainable construction of concrete structures.

1.2 Scientific gap

Bacteria-based self-healing concrete was invented in 2006 at Delft University of Technology, the Netherlands [16-18]. Bacteria-based self-healing agents contain harmless bacteria and the nutrients they will need to feed. They are added into concrete and remain dormant until the water seeps into the cracks and activates them. After germination, the bacteria feed on the nutrients to produce limestone and thus bridge the cracks [19].

This novel type of self-healing concrete has shown promising performance by improving the liquid-tightness of cracked concrete [19],[20]. Self-healing of existing or predefined cracks is a well-known phenomenon. However, the possibility for self-healing to occur under stress has received little attention. Concrete in real structures is always in some state of stress. Thus, it is essential to consider specimen under stress conditions for more realistic characterisation of durability. The next challenge is to investigate the healing agent-containing specimens subjected to chloride and carbonation for its crack-healing potential under compressive load-induced cracks and predefined cracks.

Previously, most self-healing studies used standard mortars where the results are more indicative of the chemical resistance of cement paste instead of the physical structure of the hardened cement paste in the actual concrete. Moreover, many studies of concrete durability focused on sound (uncracked) concrete while cracking is more influential in increasing the rate of mass transport that affects the service life of concrete. Other important knowledge in this field concerns specific healing agents that could influence the ingress of harmful agents (e.g. chloride ions and carbon dioxide). This knowledge is not only important for establishing realistic test methods for determining concrete durability, but it suggests that the real concrete behaviour is more complex. Therefore, not all knowledge gaps will be addressed in this thesis, only those that are listed below:

- Crack-healing potential of bacteria-based self-healing concrete subjected to compression load-induced cracking and chloride attack in a synergistic manner.
- Crack-healing capacity of cracked mortar being exposed to chloride and carbon dioxide.

1.3 Research objectives

Considering the urgent need for sustainable and durable structures, and the crack-healing potential of bacteria-based concrete which can improve durability performance of the concrete, the main research question of this thesis can be formulated as follows:

To what extent can a bacteria-based self-healing agent enhance the lifespan of concrete structures subjected to chloride and carbon dioxide?

To answer this research question, the following key questions were investigated: -

- *What is the influence of bacteria-based self-healing agent on the fresh properties of cementitious materials?*
- *How does mechanical stress affect the chloride transport in ordinary concrete with and without bacterial healing agent?*
- *How resistant is the bacterial concrete subjected to chloride and load-induced cracks?*

- *What is the healing potential of the biogenic healing agent in cracked specimen exposed to carbonation and chloride attack?*

1.4 Scope of work

A standard testing method for durability assessment of concrete under combined chloride penetration and mechanical loading is being developed under RILEM TC 246-TDC surveillance. A number of test series are performed on ordinary concrete which acted as control specimens. A similar approach is applied to self-healing concrete and both results are compared for healing potential evaluation under chloride and carbon dioxide environments. Considering various influencing parameters, this research mainly focuses on fully water saturated specimens for the diffusion test except for carbonation tested samples. Furthermore, due to experimental constraints only a single batch of concrete specimen under compressive load and chloride loading are being investigated. In addition to that, the following restrictions apply:

- Standard mortar mixture is according to NEN-EN 196-1
- Addition healing agent content of 15 kg/m³ for concrete and mortar
- Type of cement used was Portland cement CEM I 42.5 for all mixtures

The quantification of chlorine in the tested samples was performed by Laser-Induced Breakdown Spectroscopy (LIBS) and Photometric determination after chemical extraction. Energy Disperse Spectroscopy (EDS) was used to measure the chloride distribution by element mapping analysis on cracked mortar samples. Carbonation front on the crack surface and exposed surface of mortar specimens were revealed by means of phenolphthalein solution. Environmental Scanning Electron Microscopy (ESEM) and Fourier-Transform Infrared (FT-IR) spectrometry were employed to analyse and characterize mineral precipitates on cracked surfaces of samples. Oxygen consumption of water-immersed control- and bacteria-based healing agent-containing concrete and mortar samples were quantified by optical oxygen microsensors (micro-optodes) for establishing metabolic activity of bacteria.

1.5 Thesis structure

This thesis is sectioned into four parts as represented in Figure 1.2. After this Introductory Chapter, a critical review on fundamental parameters influencing durability performance of concrete is given in **Chapter 2** based on literature survey. The chapter explains the transport mechanisms of chloride ions and carbon dioxide in concrete, pore structures and cracks and provides a small introduction to self-healing materials.

Chapter 3 introduces the test method for the purpose of concrete durability evaluation under combined environmental and mechanical stress to be discussed in Part III chapters. The test method is devised by RILEM Technical Committee 246-TDC. The procedure is focused on the method to inhibit the damage due to both crack formation and ingress of chloride. An overview of mechanical stresses affecting concrete permeability is also presented. The Chapter provides a realistic test approach for concrete durability evaluation.

Chapter 4 realizes the proposed method through several test series on normal concrete. In this method, concrete specimens are subjected to two different stress levels of compression load while simultaneously being exposed to chloride solution. The chloride diffusion coefficient of specimens subjected to these conditions is determined. The Chapter concludes by quantifying the effect of chloride transport in concrete subjected to different compressive load levels.

Chapter 5 reviews the application of bacteria-based self-healing agent in cement-based materials. The influence of bio-healing agent on fresh properties and early-strength development of concrete and mortar is investigated experimentally. The Chapter closes with a discussion on the material's feasibility in cement-based materials without significant impact on the overall performance of the system.

A similar experimental investigation is performed in **Chapter 6** on the bacterial concrete. The results observed are compared with the outcome of the chloride diffusion coefficients obtained in Chapter 5. The healing potential is verified in the Chapter's concluding remarks.

Chapter 7 investigates the influence of bio-healing agent on carbonation and chloride penetration in cracked mortars. Experimental investigations on chloride distribution and carbonation front are presented. Formation of calcium carbonate minerals at cracks surface due to microbial activity is investigated. In summary, the Chapter quantifies the healing capacity of concrete samples by comparing those with and without healing agent.

Finally, conclusions are drawn, and potential prospects are presented in **Chapter 8**. The main and key research questions are briefly summarized. The Chapter completes the thesis aim by corroborating the feasibilities of bacteria-based self-healing agent in concrete under chloride and carbonation environments and highlighting the influence of combined environmental and mechanical loads on durability of concrete.

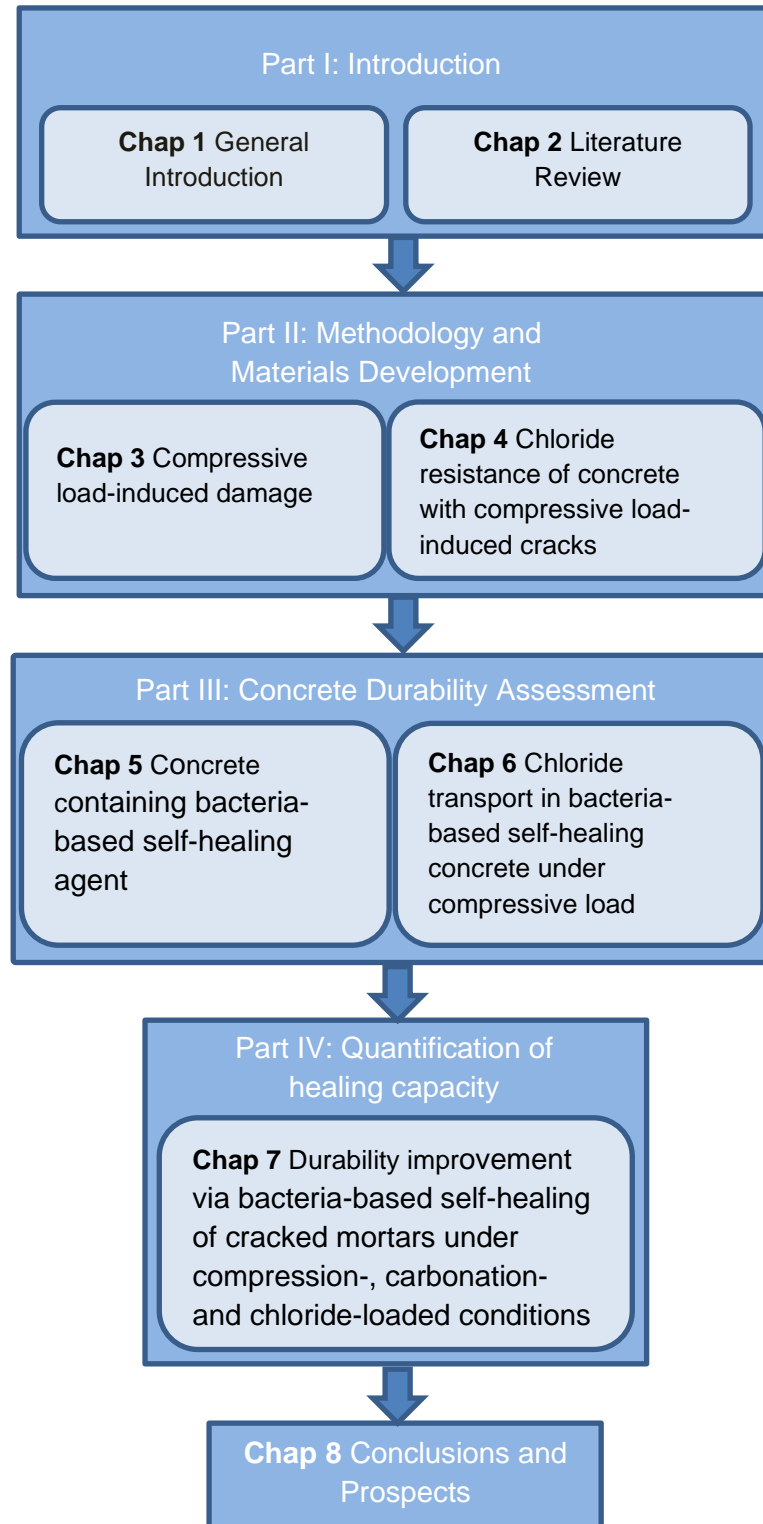


Figure 1.2 Outline of the thesis

2.

Literature review

Example is not the main thing in influencing others. It is the only thing.

-Albert Schweitzer-

Chloride and carbonation are harmful long-term deterioration processes to reinforced concrete structures. The ingress of these harmful agents involves a number of transport mechanisms that are influenced by cracks and the pore system in the concrete. The current Chapter provides insight into the underlying mechanisms and newly invented self-healing materials to improve the service performance of concrete structures.

The survey begins with discussions on the research significance (2.1) and followed by a description of durability and service life of concrete (2.2). The important mechanisms for chloride and carbonation transport in concrete are presented in section 2.3. In section 2.4, the most important influencing factors of the aggressive agent transport by capillary pores and micro cracks are presented and discussed. It is followed by a general description of self-healing phenomena of cement-based materials (2.5) and reviews of current knowledge on the application of bacteria in concrete for the durability improvement. Finally, the chapter gives a summary and highlights (2.6) which will be reviewed in the following chapters.

2.1 Introduction and research significance

Concrete is the most essential building material and has become worldwide domination in construction. Figure 2.1 illustrates one of the exclusive formability of structural concrete with remarkable architectural challenges in the current applications. From the image, structural building construction designs, in general, need to fulfil the necessity of these three aspects: engineering, science and technology and art. In order to fulfil these aspects, the structure must meet the conditions of safety, serviceability, economy and functionality. The success of this design task ultimately involves the process of choosing the right materials and proportioned elements of the structure.



Figure 2.1 Marina Bay Sands, Singapore

The stage design philosophy and concepts of reinforced concrete structures involve the strength design and load design for structural elements, and limit stress design for durability. In terms of service life, the load can be viewed as the aggressiveness of the environment and the resistance as the inherent durability of the material. In time, the load increased and/or the durability decreased, at the time the two just balance each other; this is a so-called limit state [21]. Ultimate limit state (ULS) required the actual load or working load to be multiplied by factor of safety in the final stage of the load design due to direct danger for human lives or extreme economic losses is at stake [22]. In contrast, design for the Serviceability Limit State (SLS) involves making reliable predictions of the instantaneous and time-dependent deterioration of the structures. The non-linear behaviour of concrete due to cracking makes this more difficult. Therefore, in severe environmental loading, several protective measures are being considered in designing the structures.

The application of protective measures can be obviously observed in marine structures. Marine structures are considered to be built with crack-free design and protected by a protective membrane to limit the ingress of harmful substances. In the case of bridge decks, application of straight structure component is important to prevent excessive negative moments. The bridge deck structures are also covered by a protective membrane or coatings to prevent surface cracks in the shear plane of corbels. In extreme cases that involve various nonlinearities in structures, these protective measures applied are generally not sufficient enough to achieve minimal required protection provided to the structures [23]. Consequently, this research is attempts to develop a concrete with inbuilt protective measures (self-healing concrete) that can enhance safety and serviceability of the structures and reduce repair and maintenance costs on infrastructure works significantly.

2.2 Durability and service life of concrete

Workability, strength and durability are the main factors being considered in designing concrete structures. Workability of concrete is measured on fresh concrete immediately after the concrete mixing, while the strength of concrete is measured on hardened concrete normally after 28 days of curing. However, estimating concrete durability is more complicated as it measures the length of design service life. In the codes of practice for structural design, the concrete durability is calculated by using deemed-to-satisfy approach, with requirements for minimum concrete cover and suitable concrete composition in order to limit permeability for harmful substances. This relates with the provisions of resistance to the aggressivity of the service environment. The provisions only provide qualitative definitions of exposure, which were later found to be insufficiently defining the design life with respect to durability [22]. An important index in designing a specified service life is by considering the ageing and degradation of the concrete structures. The two-phase modelling of structural degradation is illustrated in Figure 2.2. The length of technical service life is determined by the expected structural exposure time and conditions which are mostly governed by the concrete quality, loading, relative humidity, concrete permeability, cracks, temperature, thickness of the concrete cover, ageing effects etc.

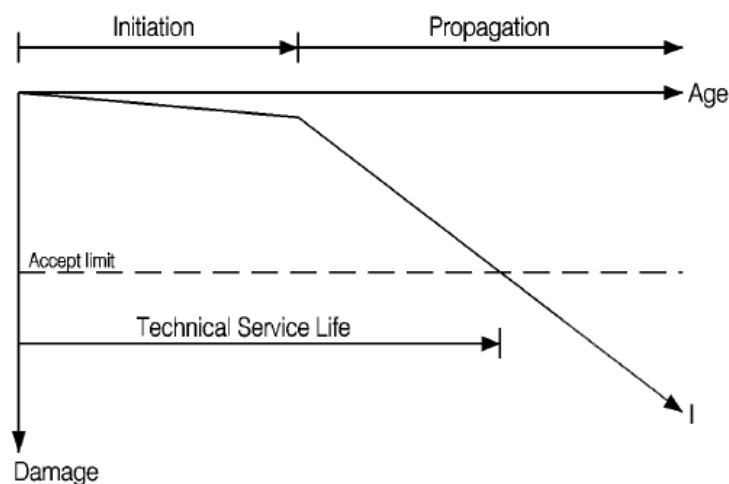


Figure 2.2 Technical service life of concrete structures [22]

Concrete is made of materials with time-dependent properties. Each material has different susceptibilities to premature degradation. Hence, the selection of suitable material is extremely important. Wrongly specified materials could be one of the causes for premature concrete structural failure. Furthermore, different concrete composition will lead to different environmental sensitivities. If the environmental exposure is not well-understood, it could be another influential factor of premature degradation of concrete structures.

Process of concrete degradation involves deterioration of microstructure and destabilization of the material which mostly refer to the initiation and development of steel corrosion in concrete [24, 25]. The sources of concrete degradation are classified on the basis of multiple distress forms due to mechanical, chemical and thermal stress environment as shown in Figure 2.3 [26]. In practice, the concrete structures are subjected to the combination of these multi-stresses forms [25]. This means that service life prediction based on results obtained from simple laboratory tests without considering multi-loads effects can be liberal or overestimate. When the service life is affected, it will expose the unsafe condition to the users

of the structures. For these reasons, it has been considered necessary to study multi-loads effects for the realistic service life design.

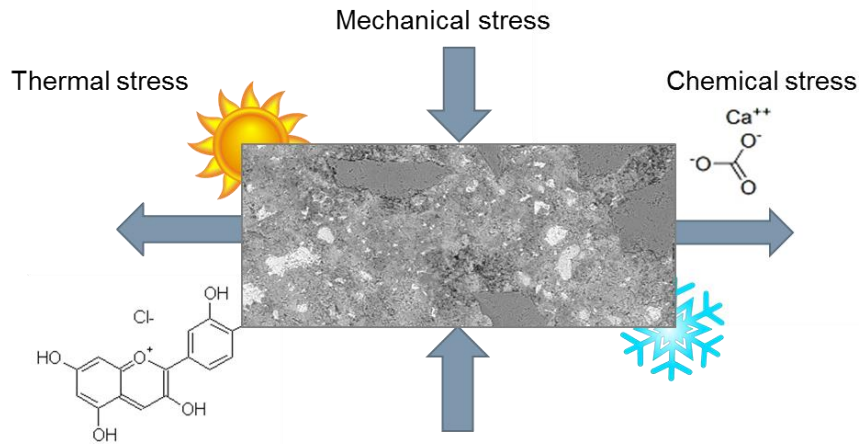


Figure 2.3 Basis forms of distress in concrete degradation

2.2.1 Environmental loading

The continuous interaction of the concrete with the environment makes this material frequently discussed as a system rather than a material [27]. Performance of structural concrete is not only determined by the material properties of its components, but the condition of the structure in its environment as a whole [22]. Chloride transport is the result of a driving force measured by the environment that produces a particular chloride content on the concrete surface [28]. An example of this is when the reinforced concrete is exposed to sea water. Permeable concrete allows chloride ions (in sea water) ingress which after some time will result in deterioration of the protective passivity oxide layer of the steel bars embedded in the concrete [29]. Consequently, initiate the occurrence of corrosion when the chloride content at the steel surface increases with time due to chloride ions building up at the concrete surface and their subsequent transport into the bulk [28].

The corrosion process is an electrochemical process that requires an aqueous environment and in an atmospheric environment. This involves the transfer of electrons between a metal surface and an aqueous electrolyte solution. Sea water is an efficient electrolyte. One of the important causes for reinforcing steel corrosion in reinforced concrete structure is the presence of chloride ion close to embedded steel. In addition to that, the passive film can be destroyed when the pH value due to carbonation of the cement paste drops below a pH-value of 9. The most severe conditions in practice are due to alternate wetting and drying exposure cycles of concrete structures. In the submerged zone, a layer of brucite may precipitate and initiate deposition of a layer of calcium carbonate which indirectly protects the reinforced concrete from the attacks by magnesium, chloride and sulphate ions and carbonization. Above the seawater surface, the process of salt crystallization from saturated seawater in the concrete pores and then drying up may cause mechanical damage. Therefore, the higher corrosive effects of steel reinforcing bars can be observed in the tidal and splash zones in the marine environment [30-32]. Reinforced concrete permanently submerged in seawater may allow substantial penetration of chloride, but significant corrosion may not occur due to insufficient level of oxygen supply in comparison to the higher oxygen supply in the reinforced concrete in the tidal zone [33]. Many possible mechanisms of chloride ion interaction

with the reinforcement and passive layer have been reported but until now none of them is generally adopted. These situations explain that the exposed environments could be beyond the expectations and hard to estimate by the structural designer since no design codes have been developed to take into account of all these uncertainties.

In comparison, the research presented here suggests that an autonomic self-healing in such reinforced concretes is seen to potentially reduce or even minimize the halting corrosion processes. This technology is expected to reduce corrosion in a cost-effective manner without compromising the constructability of a structure or requiring the development of new design codes. Therefore, it is important to initially understand the self-healing phenomena in a plain concrete (without steel reinforcement) subjected to mild marine environment (submerged zone) and ending with full-scale field trials, will be necessary in future research.

2.2.2 Deterioration mechanism

In general, neither weakening of the material nor the deterioration of the structure can be precisely detected during the initiation phase. As a consequence, the mechanisms and effects are difficult to model even though a few intrinsic protective barriers have already been affected by aggressive media at this point. In propagation phase, the damage is more visible through the indication of function loss by dividing it into several events as illustrated in Figure 2.4. Points 1 and 2 suggest the boundary of structure serviceability. Point 3 indicates the ultimate limit state level and at point 4, collapse event is expected to occur [22].

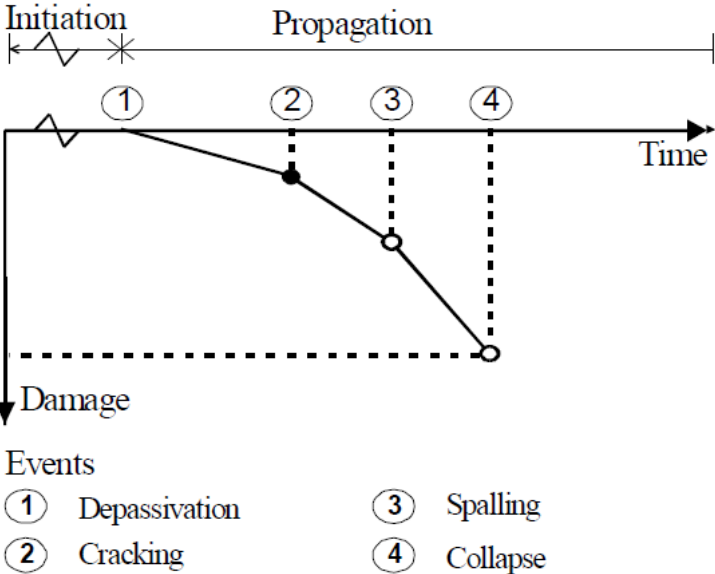


Figure 2.4 Corrosion dependent events with respect to service life [22].

Chloride ingress and carbonation are the phenomena that could represent deterioration mechanisms related to service life. The protective layer on the surface of reinforcing steel can be destroyed by the action of chloride ions or when the alkalinity environment drops to pH-value of 9 due to carbonation of the cement paste. These aggressive agents will induce depassivation of steel when the concentration of chloride or carbonation at the surface of the steel reinforcement is higher than the critical threshold value with enough moisture and

oxygen. It is important to note that the absence of passivation will continue the degradation of steel from surface what breaches the initiation phase. At this stage, the structure is considered to fail [28]. Chlorides are directly responsible for the initiation of corrosion but not in the rate of corrosion after initiation as the main rate-controlling factors depend on the availability of oxygen, and the pH, temperature, relative humidity and electrical resistivity of the concrete. Formation of expansive rust products by corrosion leads to internal stress within the concrete that is sufficient to cause cracking of the concrete cover. If corrosion products react further with dissolved oxygen after cracking, it expands, inducing internal stresses that, once they exceed the tensile strength of concrete, spalling of the concrete cover will occur [22, 34, 35]. If this stage becomes apparent, the building or structure may not be safe for occupants.

A significant parameter to prevent such events to occur is concrete cover [22]. Concrete cover is designed to prevent the steel bar from corrosion due to environmental effects. The concrete quality and thickness of the cover determine its effectiveness [29, 36]. In the case of propagation, the phase can be terminated by providing denser and crack-free concrete cover which eliminates the ingress of aggressive agents into concrete.

The degradation processes also strongly relate to the transport phenomena in concrete [2]. Thus, consideration of durability requires knowledge of the transport mechanisms of aggressive compounds into and within the concrete. However, a thorough investigation of corrosion effects on reinforcement falls outside the scope of this thesis. Moreover, to avoid complex analysis of the mechanisms involved, the subsequent concrete durability study therefore focuses primarily on the chloride ingress and carbonation in plain concrete (without steel bar) and mortar.

2.3 Transport mechanism in concrete

The interpretation of penetrability in concrete is essentially related to critical assessment of transport rate of aggressive elements in concrete [2, 37]. The ease of movement liquids and gases movement through concrete can be controlled in different ways, but all the transport properties depend mainly on the hydrated cement paste structure or its self-healing capacity [2]. Depending on the changes of the pore system in concrete with time due to continuous cement hydration, transport mechanisms are limited to permeation, diffusion, capillary sorption and migration as presented in Table 2.1. The entrance or movement of fluids through concrete may also consist of several combined mechanisms depending on the type of structures [38].

Table 2.1 Modes of transport mechanism in concrete

Transport Mechanism	Description
Permeation	<ul style="list-style-type: none"> ▪ Movement of liquids or gases through a substance under differential pressure. ▪ Primarily in structures submitted to high pressure, however not limited to structures under low pressure.
Diffusion	<ul style="list-style-type: none"> ▪ Ionic movement due to a concentration difference. ▪ Diffusing substance transports from zones with higher concentration to zones with lower concentration ▪ Typically, in structures exposed to severe environment that have higher ions concentration outside the concrete than inside.
Capillary sorption	<ul style="list-style-type: none"> ▪ The transport of chlorides by moisture differential in the concrete pores that are exposed to the ambient medium. ▪ It can occur only in partially dry or partly saturated concrete and almost impossible in completely dry concrete or in saturated concrete [2]. ▪ Limited to structure subjected to wet-dry cycles.
Migration	<ul style="list-style-type: none"> ▪ Transport of ions due to differences in electrical potential. ▪ Chloride ions migrate to zone with positive potential. ▪ The transport mechanism has been applied in NT Build 492 [39].

Among the above mechanisms, diffusion and capillary sorption are the predominant transport mechanisms for the chloride ingress in cement-based materials, which are the main interest in this research. Diffusion is the principal mode of chloride transport in concrete [9]. Fick's Law of diffusion is mathematically modelled to describe the relation of diffusive flux to the concentration field [40]. In one-dimensional diffusion (steady-state diffusion), the law is given:

$$J = -D \frac{dC}{dx} \quad (2.1)$$

Where J is the diffusion flux, D is the diffusion coefficient, C is the concentration of chloride in solution at a location x . This equation is independent on time and only practical after steady-state conditions have been achieved. For a non-steady state process, the concentration is a function of both time and position. Fick's second law describes the change of the ionic concentration C at a location x in a unit volume of time as:

$$\frac{\partial C}{\partial t} = D \left(\frac{\partial^2 C}{\partial x^2} \right) \quad (2.2)$$

With regard to simple geometry and boundary conditions, an analytical solution to Equation 2.2 can be applied for a semi-infinite medium by using the boundary condition as $C(x=0, t > 0) = C_s$ (the value of surface chloride concentration is constant at C_s) and the initial condition as $C(x > 0, t = 0) = C_0$ (the initial value of chloride concentration in the specimen is C_0), chloride ingress in concrete is given as [41]:

$$C_{(x,t)} = C_0 + (C_s - C_0) \cdot \left[1 - \operatorname{erf} \left(\frac{x}{2\sqrt{Dt}} \right) \right] \quad (2.3)$$

Where $C_{(x,t)}$ is the chloride concentration at a location x measure from exposure surface after a certain exposure time t and $\operatorname{erf}(z)$ is the error function which can be expressed as:

$$\operatorname{erf}(z) = \frac{2}{\sqrt{\pi}} \int_0^z \exp(-y^2) dy \quad (2.4)$$

Equation 2.3 has been broadly used to define the diffusion of chloride ions in concrete. However, chloride ingress in concrete remains a complex process due to the uncertainty of input variables such as time-dependent changes and chloride binding [2].

2.3.1 Chloride transport in concrete

Chloride ions can enter the concrete through diffusion, capillary absorption and hydrostatic pressure. As the pores remain saturated in the bulk of the concrete, the chloride ion movement is mostly influenced by concentration gradient (diffusion). In addition to diffusion coefficient through the pore solution, physical characteristics of the capillary pore structure also plays a role in controlling the diffusion rate due to liquid and solid components in concrete [42]. A multitude of experimental works of concrete resistance towards chloride ingress have been proposed and used to allow an appropriate consideration of multi-mechanistic transport mechanism triggered by concentration gradient and physical characteristics of the capillary pore structure for designing reinforced concrete [43].

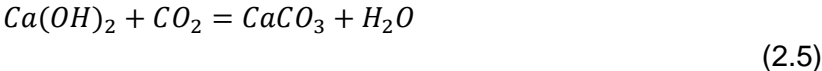
The presence of chloride ions in concrete can be from chloride-containing admixtures applied e.g. as accelerator in mixtures. In fresh concrete, sources of chloride ions could be from contaminated water, aggregates or admixtures while in hardened concrete, chloride sources are generally from the environment, for instance application of de-icing salts, air-borne chloride or direct exposure to sea water in marine environments [2]. Chloride ions can be found in two forms in concrete which are bound and free chlorides. In general, only a small portion of chloride ions from the total amount in concrete is dissolved in the pore solution which can destroy the protective film and cause rebar corrosion [29]. The acid solubility method quantifies the total of bound and free chloride ions (total chloride) in the concrete, while the water extraction method only computes free ions soluble in pore water. The bound chlorides can be easily determined by extracting the value from acid-soluble method with water-soluble method and this binding reduces the rate of diffusion.

The chloride binding capacity is controlled by the hydration degree of cement and also cementing materials used in the concrete. The chloride binding capacity of the concrete may influence the rate of chloride transport in some serious cracking conditions such as large crack width or high crack density [44]. However, the chloride binding capacity is negligible when steady-state conditions have been reached and therefore can be ignored in the calculation of

the diffusion coefficient. If a steady state condition has not been reached, then the binding capacity should be taken into account [43]. As the exact influence of chloride binding is unclear, the influence of chloride binding is less important in comparison to permeability towards resistance of chloride in concrete [45].

2.3.2 Carbonation of concrete

Carbonation is typically defined as the chemical reaction between the hydration products of the cement in concrete and carbon dioxide from the air which are converted to calcium carbonate, in accordance with the reaction [46];



In properly consolidated concrete, the carbonation penetration is restricted. Concrete with low water-to-cement ratio and minimal concrete cover generally needs more than 100 years for carbonation to reach the steel in concrete and destroy the passive film [47]. The rate of carbonation is affected by factors associated with the concrete and the external environment. This process requires the presence of a certain amount of water and relative humidity ranging from 40% to 90% that enable the carbon dioxide to penetrate through the voids in the hydrated cement paste [48].

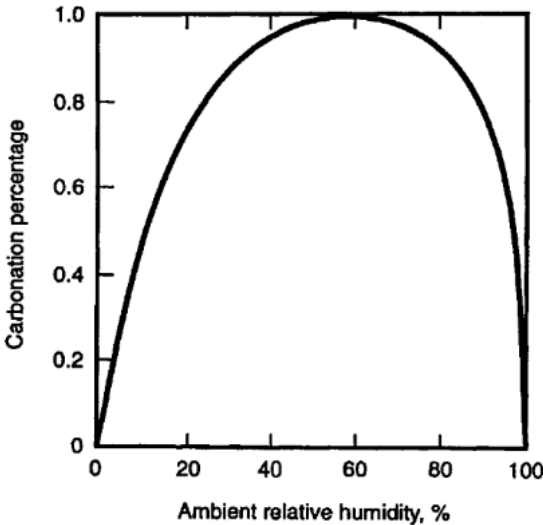
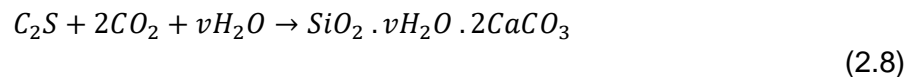
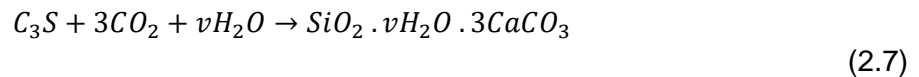
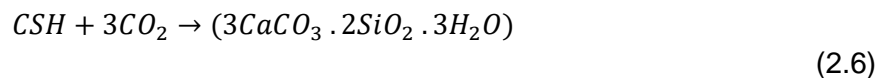


Figure 2.5 Influence on carbonation of concrete by ambient relative humidity [3].

The relation between concrete carbonation percentage and ambient relative humidity is given in Figure 2.5. It shows that at low relative humidities, calcium hydroxide tends to react very slowly with carbon dioxide and that the reaction becomes faster at a relative humidity above 50 % when a thin film of water is expected to be present on the calcium hydroxide particles. In addition, the water-to-cement ratio of the concrete can influence the rate of carbonation in concrete [49]. The importance of carbonation phenomenon is the reduction of concrete alkalinity to a pH of almost 8, thereby permitting the corrosion of the embedded steel.

Steel is passive and protected from corrosion due to the high content of calcium hydroxide in concrete. The steel passivation layer requires a high pH between 12 and 14.

When the carbonation front reaches the steel bar, the passive film will lose thermodynamic stability and initiates an active corrosion. In addition to the corrosion of steel bar, carbonation has several other effects on the permeability and pore structure of concrete which has a remarkable influence on most of the transport properties. Carbonation is conditional on the diffusivity of the cement paste, which in turn is a function of the pore system [50]. The continuous process of carbonation may lead to a reduction in pore volume due to excessive calcium carbonate produced compared to the products of the original reactants. This reduction may slightly vary with different types of binder used and can be more noticeable in low quality concrete with higher porosity [51]. This phenomenon can also be observed with the other hydration products namely calcium silicate hydrate also known as CSH and residual unhydrated cement compounds specifically tricalcium silicate (C_3S) and dicalcium silicate (C_2S) react with CO_2 in the following reactions given by Papadakis et al. 1991 [4];



2.4 Capillary pores and micro cracks in concrete

Lime, silica alumina and iron oxide are the main compounds in Portland cement. These compounds are ground and heated in the kiln at high temperatures of up to about $1450^\circ C$ to produce a series of more complex products known as clinker. The four main phases regarded to cement clinker are Tricalcium silicate (C_3S), Dicalcium silicate (C_2S), Tricalcium aluminate (C_3A) and Tetracalcium aluminoferrite (C_4AF). C_3S or also called as alite is the most reactive and contributes to early strength, while belite denoted as C_2S in above contributes more to long-term strength by being slower-reacting. The products of hydration of cement exist when cement is brought into contact with water. By hydrolysis process of C_3S and C_2S , calcium silicate hydrates (C-S-H) compounds are formed with the precipitation of crystalline calcium hydroxide ($Ca(OH)_2$) [2, 52, 53].

CSH is occupying 50 to 60% of the solids hydrated paste volume, making the most important phase in Portland cement. Hexagonal $Ca(OH)_2$ morphology or also known as portlandite makes 20 to 25% of the solid hydrated paste volume [53]. In general, 40% of Portland cement weight of water is required to hydrate and 25% of this is required for chemical reactions which is non-vaporizable. The other 15% is absorbed onto the internal surfaces of the C-S-H gel, known as gel water and is vaporizable under severe conditions. The hydrated cement paste is a porous material with a very wide range of pore distribution in more than 6 orders of magnitude. Setzer in 1997 [54], had classified the pore size into micro gel pores (<1 nm), meso gel pores (<30 nm), micro capillaries (<1 μm), meso capillaries (<30 μm) and macro capillaries (<1 mm). Figure 2.6 represents the size distribution of solid phases and voids in the hydrated cement paste. The shrinkage of the C-S-H gel creates voids, known as capillary voids. Capillary voids are irregular in shape [53]. These capillary voids will fill with excessive water of highly alkalinity and is normally considered as the pore solution. The matrix capillary water of young concrete is characterized by its pH values is typically between 11 and 13 [2].

The capillary voids in concrete have an important influence on its transport properties [8]. Concrete with a low water-cement ratio has fewer capillary pores and the pores are very fine which are easily filled up within a few days by hydration products of cement. However, if there is inadequate water, un-reacted particles of cement would remain. Denser matrix increases the resistance of concrete to the attack of deleterious solutions. Introduction of larger size aggregates may increase the permeability significantly as the spaces will not get filled up by products of hydration. This will contribute to the development of micro-cracks especially in the interfacial transition zone known as ITZ in which the porosity is reported to be much bigger than the capillary pores.

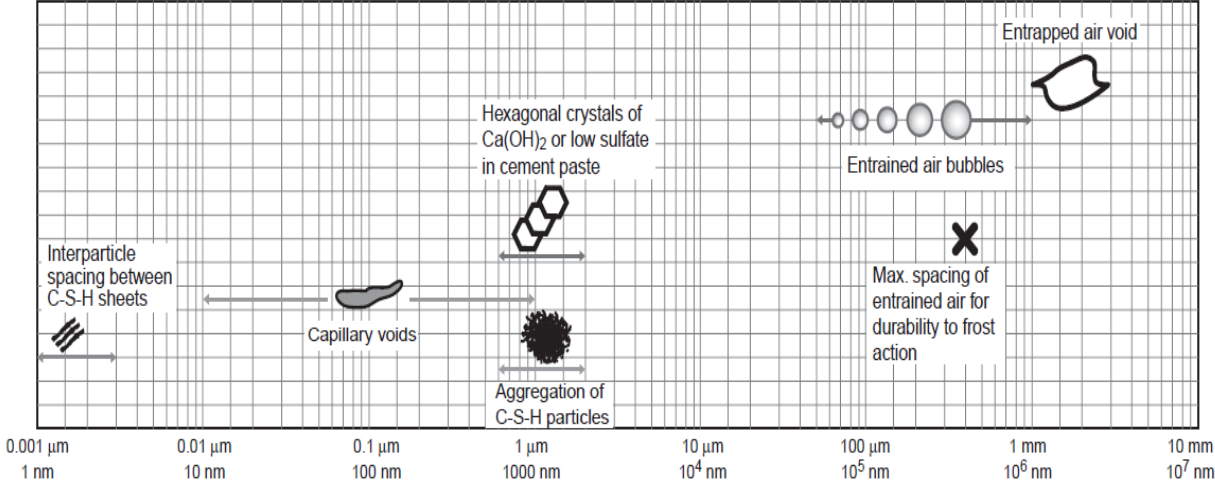


Figure 2.6 Logarithmic scale of solids and pores in hardened cement paste [53].

ITZ is a paste region surrounding each aggregate grain in concrete. ITZ is highly porous and prone to cracking due to mechanical incompatibility between the natural aggregate and the hardened cement paste [8, 26]. As it is vulnerable to the ingress of aggressive substances into concrete, ITZ becomes the basis of many transport models for concrete [55]. The diagrammatic image of the ITZ and bulk cement paste in concrete is shown in Figure 2.7 [2, 8]. Cracks often start and propagate preferably in the ITZ [56]. Fatigue load may cause multiple micro-cracks in concrete [2]. In initial stage, micro-cracks are so fine that they may not increase the permeability. However, the propagation of micro-cracks with time due to drying shrinkage, thermal shrinkage, and externally applied loads may jeopardize the tightness of the structure.

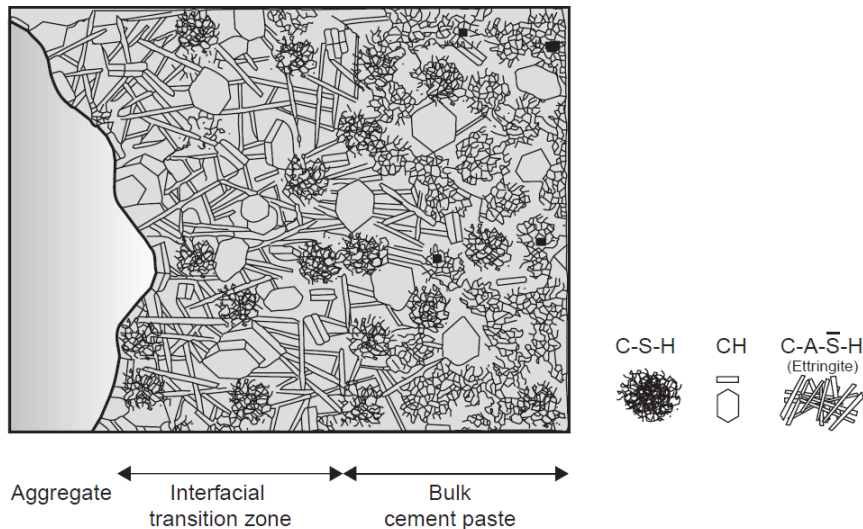


Figure 2.7 Interfacial transition zone and bulk cement paste in concrete [53]

Micro-cracking is a general feature of an ordinary concrete and has a large influence on concrete mechanical properties including deformation, permeability and strength characteristics [57]. Maximum tolerable crack widths specified by construction codes are in the range of 200 μm to 300 μm [58]. The crack width should not exceed a certain critical crack width value for direct impact on the concrete permeability capacity [27]. Presence of cracks can be resulting from environmental or mechanical loadings [38]. Their occurrence is not harmful to the durability of concrete as long as the cracks are small and stable. With regards to reinforced concrete structures, micro-cracks may not cause immediate structural failure which links to safety problems. However, if micro-cracks form a continuous network of cracks, it may provide the onset for deterioration that leads to permeability issues and ultimately steel bar corrosion protection [2, 49].

The reason for premature deterioration can be very complex. Therefore, there is a large number of durability enhancing measures used to counteract the problem. The most prominent ones used are high performance concrete, permeability controlled formwork liners, self-compacting concrete and stainless steel reinforcement. However, these specific measures require specialised expertise and experience and are expectedly more expensive than traditional measures [21]. Consequently, the development of materials aiming at increasing the service life of concrete structures that would contribute to reasonable and affordable costs of maintenance and repair works is urgently needed for reliable structures in the future.

2.5 Self-healing of cement-based materials

Human beings and animals have inborn self-healing in their body systems. Most of the time, injuries and wounds are treated immediately without involving any serious surgery. Therefore, self-healing in a system or material refers to the ability of it to sense and heal the 'damage' itself. Self-healing targets complete recovery of functional properties. As an example, in concrete, self-sealing of cracks reduces permeability and increases water tightness without necessarily recovering its original strength [59]. In this case, self-sealing is not defined as self-healing. By RILEM definition, self-healing is any recovery process and performance improvements by the material itself which had reduced performance due to previous adverse actions in the concrete. Self-healing materials can be categorized into two groups which are

by using own generic material known as autogenous-healing or with engineered material additions known as autonomic-healing. The kinetics of autogenous-healing is initially fast and then slows significantly over time as it mainly depends on continued hydration of the unhydrated cement and natural carbonation in concrete [38, 60]. Autonomous healing is sectioned by passive and active modes. In passive mode, the autonomous-healing will respond to an external stimulus without the demand for human intervention, whereas in active mode, autonomous-healing requires intervention in order to complete the healing process [15].

When water becomes supersaturated with regard to calcium and carbonate ions, both ions can actively precipitate calcium carbonate together with calcium hydroxide minerals, making deposits inside the cracks in concrete as illustrated in Figure 2.8 [27]. This process can cause the self-healing of fractures under specific conditions. Adding a self-healing agent to the concrete mix will enhance its already present autogenous healing capacity.

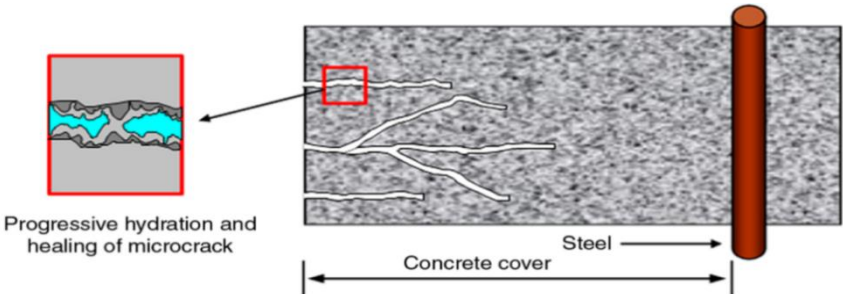


Figure 2.8 Autogenous-healing of microcracks in concrete cover by hydration process [61].

Recently, similar healing capability has been invented for concrete materials and structures through robust engineering evolution to reduce maintenance and repair costs. This invention is known as self-healing materials and smart structures. Bacteria-based self-healing concrete has been proposed as an environmentally-friendly method for enhancing the crack-healing system in concrete which eventually protects the steel reinforcement from further external chemical attack. Both the bacteria and nutrients that are embedded in the concrete should immediately react and start to multiply and precipitate minerals such as calcium carbonate (CaCO_3) upon concrete cracking and water ingress and thereby filling the crack [17]. The process shown in Figure 2.9 shows the bacterial metabolic conversion of nutrients into limestone blocking the crack.

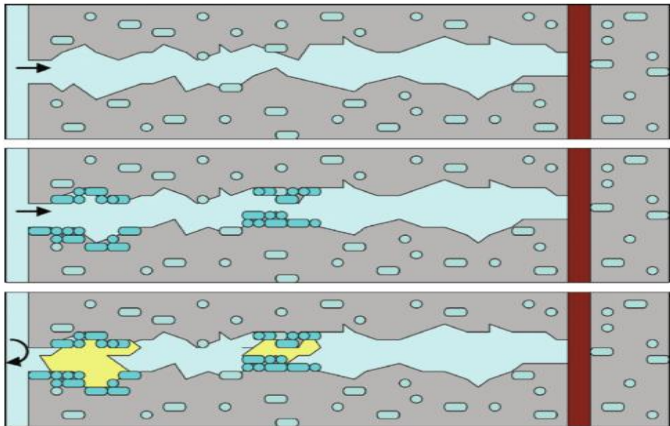


Figure 2.9 Scenario of crack-healing by concrete-immobilized bacteria [17].

2.5.1 Microbial applications in cement-based materials

Several types of bacteria-based self-healing concrete have been investigated and developed in recent years. With specific combinations of metabolic pathways and micro-environmental conditions, bacteria can influence the precipitation of calcium carbonate resulting in the sealing of cracks. The potential of bacteria to act as self-healing agent in concrete appears to be beneficial and has proven to be a promising sustainable repair methodology in a number of laboratory investigations. Microbial mineral precipitation was initially used in the heavy oil industry for selectively plugging reservoir zones of high water permeability [62]. In the following decade practical application of microbial mineral precipitation in building structures and monuments was initially reported by Islam and Bang, 1993 [63]. Furthermore the applicability of microbial mineral precipitation for sand consolidation [64-66] and deposition of calcite by bacteria within the pores and cracks in concrete as surface treatment or healing system in concrete was also investigated [67-69].

Biocementation and crack remediation

Bacteria treatment has exhibited high potential for decreasing the permeability properties of cementitious materials through precipitation of calcium carbonate, a process that increases the density of the porous concrete matrix [70]. This technique has been studied by Ramachandran et al., 2001 [68] in which calcite deposition induced by *Bacillus pasteurii* was applied by using various concentrations of bacteria and urea and loading these in cracks of different dimensions in mortar cubes. The sealing in shallower cracks was observed to be more efficient in comparison to deeper cracks due to active growth of bacteria by the presence of oxygen. Bang et al., 2001 [67] used polyurethane (PU) to immobilize whole cells of *Bacillus pasteurii* and found PU as an effective improvement method in microbiologically-induced calcite precipitation (MICP) for remediation of concrete cracks. Both authors concluded that the MICP technique was effective to remediate cracks in building materials. The conclusion was in good accordance with studies done by Achal et al., 2010, 2013 [71, 72], who observed positive effects of *Bacillus* sp. CT-5 on development of mortar compressive strength and permeation properties. The authors examined the calcite production ability of *Sporosarcina pasteurii* featuring high urease activity using corn steep liquor as nutrient source and compared with standard nutrient broth. The study was aimed to reduce the permeability of concrete by conducting water impermeability test and rapid chloride permeability test. As a result, a significant improvement in surface permeability resistance of concrete towards water and chloride penetration was observed [73].

In a Belgian study, bacteria and urea were externally applied on degraded limestone and cement-based materials as surface protection for reducing the water absorption [66, 69, 74]. The bacteria of the *Bacillus sphaericus* and *Bacillus lentus* species were examined for calcite deposition on limestone through the process of ureolytic calcium precipitation. The hydrolysis of urea into carbonate and ammonium is catalysed by the enzyme urease. The deposition of a carbonate layer on the surface by a biofilm was initially proposed in a study by Dick et al., 2006 [66]. Further investigation of the effect of biodeposition treatment on durability aspects was studied by De Muynck et al., 2008 [69]. Using a modified treatment procedure, he demonstrated an increased resistance of mortar specimens towards water and gas permeability. Moreover, as calcium carbonate was mainly deposited at the surface, the biodeposition treatment on cement-based materials was regarded as a coating system.

Bacterial treatment of cementitious materials

In addition to external application, the effects of incorporating bacteria into cement mortar and concrete mixtures have also been investigated. Bacteria that have been added into the concrete to remediate the cracks should not negatively affect the concrete strength properties. As a further extension to this research, the roles of bacteria on the durability properties in cementitious structures were studied. Different researchers from all over the world have been evaluating different types of the bacteria and metabolic pathways used. Ghosh et al., 2005 [75, 76] described the addition effects of thermophilic anaerobic bacteria of the *Shewanella* species on compressive strength of mortar cubes and found that the strength of mortar cubes increased at all levels of cell concentration. In addition to that, no improvement in strength of mortar was recorded with the addition of *Escherichia coli* (a low urease active species) to the mortar mixture. It was concluded that different types of bacteria in different environments exhibit different levels of urease activity.

In more recent studies, an attempt was made to use ureolytic bacteria with other supplementary cementing material. Achal et al., 2011 [77] investigated the potential of *Bacillus megaterium* to enhance the durability of fly-ash amended concrete. The bacterial cells were grown in nutrient containing urea (NBU) media and added to cement mortar during wet mixing. All the samples were cured in NBU media for 28 days. The biocalcification by *B. megaterium* demonstrated considerable improvement on compressive strength and water impermeability of fly-ash amended concrete. A similar experiment was also conducted using a different bacterium, i.e. *Sporosarcina pasteurii* on fly ash-amended concrete [78]. That study revealed the significant role of the urease-producing bacterium *S. pasteurii* in increasing the compressive strength of fly ash concrete with simultaneous reduction in water absorption and chloride permeability. Related findings were also reported for silica fume concrete in which a significantly improved durability of construction materials or structures was claimed [79].

Development of bacteria-based self-healing concrete

In the newly developed bacteria-based self-healing agent by Jonkers and Schlangen, 2008 [80], the same advantages of MICP technique were afforded by using alkali-resistant spore-forming bacteria of the genus *Bacillus* and more specifically related to the species *Bacillus pseudofirmus* and *Bacillus cohnii*. These types of bacteria are able to survive in high-alkalinity and temperature conditions and were together with suitable nutrients used as self-healing agent to increase the self-healing capacity of concrete. In this case, autonomous active crack remediation is done by the hardened mortar or concrete with the aid of bacteria. The bacteria can be viable for periods up to 200 years and able to survive until the moment that self-healing is required [15]. The bacteria spores are quite similar to plant seeds. They feature a very thick cell wall which makes them well-resisted against deficiency, aggressive chemicals or extreme mechanical loads. Like a seed, the spore will patiently wait for the suitable environment to grow. Under favourable conditions, the bacteria will be activated from its dormant state to germinate and will multiply again. In this way, the drawback of urea hydrolysis resulting in formation of ammonia leading to excessive environmental nitrogen loading can be avoided [17, 20].

In principle, the healing particles can be mixed in the concrete in the same way as aggregate particles. However, the inclusions must be strong enough to resist forces imposed during mixing and placing of the concrete and should be weak enough to break open on intersection with a crack [27]. This healing particle contains selected bacteria and organic

mineral precursors which are converted by active bacteria to calcium carbonate-based minerals upon activation by ingress of water through the crack. Among the precursor compounds selected, calcium lactate showed marginal effects on setting and compressive strength development of cement-based materials. This process of microbial calcium carbonate formation is relatively fast and consumes oxygen. The life cycle of bacteria spore formation is diagrammatically illustrated in Figure 2.10 by Richard van de Pol in *Betoniek* magazine, 2009 [81].

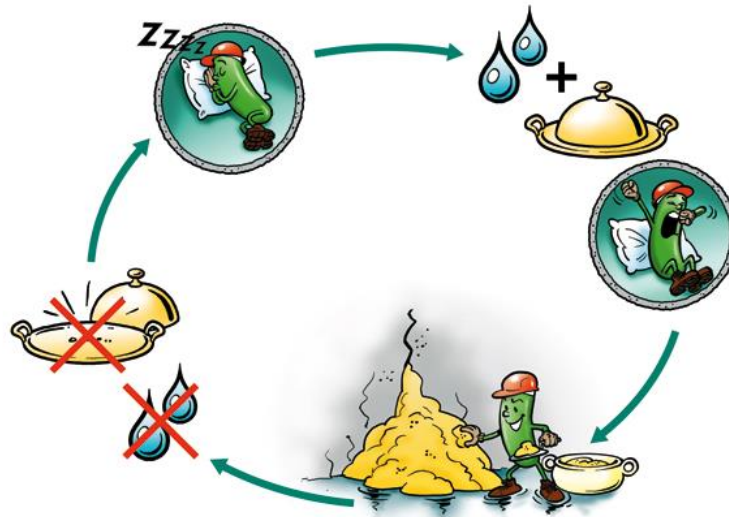


Figure 2.10 Life cycle of bacteria-based self-healing agent [81].

Sierra Beltran et al., 2014 [82], described mechanical properties, self-healing capacity and bonding behaviour of a sustainable bio-based mortar repair system. The bacteria *Bacillus cohnii* with a nutrient source of calcium lactate are embedded in lightweight aggregates (LWA) prior to addition to the concrete mix. It has been shown that the unprotected spores will not normally survive for longer periods in the concrete matrix due to on-going hydration of cement. For this reason, Jonkers, 2011 [83] and Wiktor et al., 2011 [14] immobilized the bacterial spores in porous expanded clay particles prior to adding them to the concrete mix. This procedure resulted in a bacterial spore viability of more than 6 months which was proven by in situ oxygen consumption measurements. This bio-based agent (LWA particles loaded with bacterial spores and nutrients and with sizes ranging between 0.25 and 2 mm) was added to the strain-hardening cement-based composite (SHCC) and the metabolic activity of bacteria was monitored. Outcomes indicated that this SHCC type of material with bio-based healing agent fulfils the requirements of a structural repair mortar in terms of compressive and bonding strength. In follow-up research by same authors [84], the self-healing capacity of this SHCC was investigated with respect to regain of mechanical properties lost by cracking. A slightly better recovery of both flexural strength and deflection capacity in comparison to mixtures without bio-based healing agent was observed after pre-loading and healing the SHCC material. According to the authors, the amount of calcium carbonate precipitated in the bio-based specimens did not substantially differ from control specimens as only superficial crack closure in the crack mouth region was observed. The self-healing capacity of this bacteria-based strain hardening repair mortar is currently being further investigated in pending studies.

2.5.2 Field applications of bacteria-based repair systems

The present production of bacteria-based self-healing agent has been up scaled by the Delft University of Technology now since more than five years ago. The self-healing concrete technology has since been transformed from fundamental research to practical applications. Figure 2.11 exemplifies the first field application of a bacteria-based self-healing repair system applied in the form of a liquid suspension as a protective layer on the cracked and water permeable roof of a first-aid emergency post in Galder, near Breda, The Netherlands. The cracked building which was built and treated with the bacteria-based repair system in 2009 remained waterproof as to date (Building from Waste: Recovered Materials in Architecture and Construction).

In October 2014, the bacteria-based liquid system developed by the Delft University of Technology was applied to repair a cracked and leaking parking deck as shown in Figure 2.12. The details of the treatments and the tests performed for this pilot study was reported by Tziviloglou et al.,2016 [85]. Two repeated treatments were conducted throughout the investigation. Water permeability tests showed that permeability significantly decreased particularly after the second treatment due to formation of limestone in the crack as evidenced by ESEM observations of drilled samples after the treatment.

From the field applications described above, it can be concluded that the bacteria-based repair system is reliable for applications in real structures suffering from cracking and water leakage problems. However, to what extent the limestone formation also results in more durable structures (e.g. protection of the embedded steel reinforcement against corrosion) and eventually extended service life of a structure remains to be investigated. From a sustainability point of view, extension of service life would not only reduce use of primary resources but will also decrease cost of ownership of the building due to decreased need for manual repair and increased service life. [27].



Figure 2.11 First aid emergency post in Galder, the Netherlands.

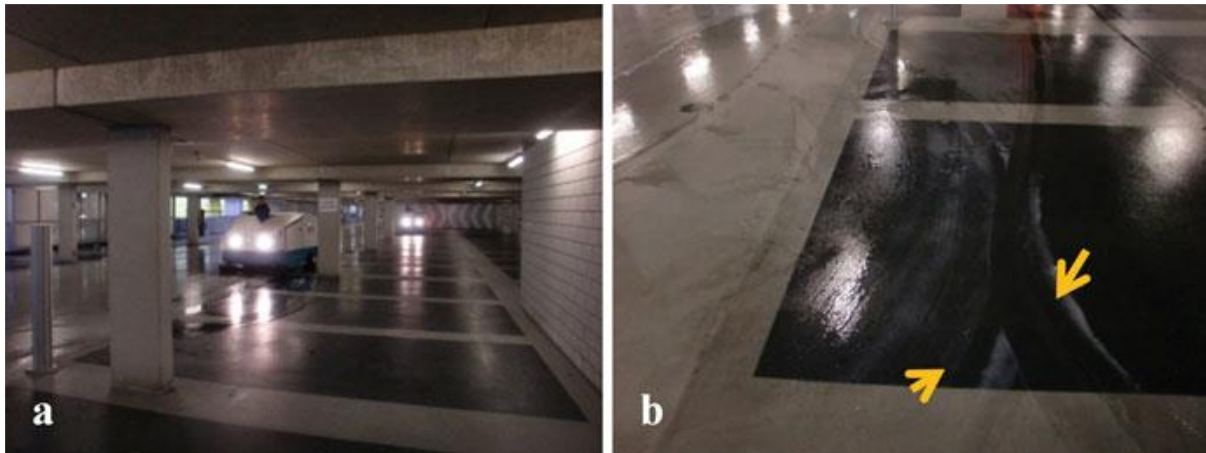


Figure 2.12 (a) Application of a liquid-based self-healing repair system in a parking garage (b) Gel formation at the surface of a crack after the application of healing solutions [85].

2.6 Concluding remarks

This literature survey is meant to give information of some important reviews related to this research work. In all the afore-mentioned studies, it is clear that the chemical and mechanical degradation of the concrete structures cannot be avoided in construction practices. If the structure fails prematurely, it might be due to a wrong design or materials being used or due to placement in a wrong environmental exposure class. When the structure is being exposed to an extreme environmental condition, transport properties of detrimental chemicals in the concrete matrix may play a major role in the degradation processes of the concrete, e.g. in relation to the capillary pore system and micro-crack development. Both have to be deliberated clearly at the design stage in order to attain a concrete structure that achieves its predicted potential.

The integration of self-healing materials in the concrete matrix can manage the otherwise detrimental occurrence of small cracks and by doing so delay the physical and chemical degradation process of the material. The aim of integrating a healing mechanism in concrete is, after damage has occurred, to regain the structures original level of performance of the structure or a level close to that. The current state of knowledge of the mechanism of bacteria-based self-healing concrete has indicated a bright prospect for crack-sealing and resistance towards degradation processes in concrete. The authors claimed that the decreased chloride ingress was a consequence of bacteria-initiated self-healing. The most common method used from the literature is to determine water permeability through cracked concrete while only a few authors measured chloride permeability. However, the chloride permeability results were based on the rapid chloride test which does not account for the impact of chloride penetration on long-term durability of cracked concrete. Furthermore, the effect of bacterial self-healing on stopping chloride ingress in concrete is also questionable in case of variable load on the structure.

An experimental program was developed in order to gain a better insight into the healing efficiency of bacteria-based self-healing concrete. The same bacteria-based self-healing agent used in the research by Jonkers et. al., 2011, was used in current study. This healing agent aims to become cost effective in such a way that self-healing concrete can minimize the operation, maintenance, and repair costs within the lifetime of the structure. An

enhanced service life of concrete structures will reduce the demand for new structures through a rational life cycle cost optimization.

3 .

Test methods to determine durability of concrete under compressive load-induced damage

“A valuable research will allow today's grossly over-simplistic deem-to-satisfy design methods to be replaced by scientifically sound probabilistic service life design methods.”

-Steen Rostam-

In Chapter 2, cracks and pore system of concrete were identified as the main adverse influence on concrete permeability which can be seriously amplified by mechanical stress. A variety of methods for assessing the effects of mechanical stress on the permeability of concrete have led to diverging conclusions in many published research studies. Therefore, this chapter aims to develop a method to determine chloride diffusion in concrete subjected to compressive loading. Under such combined actions, a more realistic characterisation of concrete durability is possible.

The background for the study of permeability of stressed concrete in chloride and carbonation environments is presented in Section 3.2. A description of the test series for investigating cracking and failure induced by compressive loading is given in Section 3.3. Techniques used in the literature to analyse microstructure and crack patterns in concrete are explained in Section 3.4. Finally, effects of combined loads on concrete service life, based on reviews of existing research, are presented and discussed in Section 3.5 and subsequently a new evaluation method for concrete under combined loads is presented in Section 3.6. Furthermore, methods for chloride profiles determination of a performed international Round-Robin Series (within the framework of the RILEM TC 246-TDC) is also presented in Section 3.7.

3.1 Introduction

Concrete is porous and therefore prone to deterioration phenomena. The pore space in concrete is uncertain as it can change due to the continuing hydration process that affects the transport properties of concrete. Variations of temperature and air pressure of the surrounding may also contribute to the complex process of transport of ions in the pore space. The pore space in concrete is partially filled with a high pH aqueous solution. The volume of the pore space depends, among others, on the water-to-cement ratio, type of cement, type and amount of admixtures used, aggregate distribution and the period of hydration [2, 6, 52]. Under service conditions, modification of the pore structure in concrete can be significant and can result in the formation of a multitude of cracks of varying connectivity.

Stresses due to mechanical and one or more environmental loads may act simultaneously or consecutively under service conditions. Therefore, it is essential to be conservative and more realistic to evaluate chloride resistance of concrete under simultaneous application of mechanical stress. Review of existing research [86] indicates that the process of damage in concrete under mechanical loads is continuous and is initiated at very low applied stresses. In most reported cases, the micro-cracks remain stable until the applied stress reaches about half its ultimate value [26, 56, 87]. As a matter of fact, however, studies on synergetic effects have not been clear and complete. In this thesis, a specific hypothesis is therefore defined as follows. Low-to-moderate compressive stress levels densify the porous structure of the concrete leading to a reduction of pore space due to elastic deformation of the pores. However, above a specific critical stress level the pore structure becomes damaged resulting in the formation of cracks that increases pore solution flow.

Therefore, from the viewpoint of durability, it is considered important to apply a more practical approach to evaluate chloride ingress in concrete under the influence of mechanical loading [25]. A comparatively high safety margin is proposed in the present research work. The load configuration, specimen size, stress level, and strength of concrete are all considered as influencing parameters and are therefore considered in this research in order to provide a more realistic service-life estimate for concrete structures.

3.2 Permeability of cracked concrete

Permeability is the most influential concrete durability parameter and is particularly controlled by an interconnecting network of capillary pores. The pores will be disconnected at a certain degree of hydration by means of the development of calcium silicate hydrate gel and calcium hydroxides which form impermeable regions. Thus, the permeability coefficient decreases with time due to ongoing hydration [26]. The hydration process requires the availability of water to react with the unhydrated cement and availability of space for deposition of hydration products [88].

In sound concrete, permeability is related to the porosity. Detrimental compounds dissolved in water such as chloride can be transported through the pore space by capillary action. Then, the dissolved ions may transport deeper into the porous material by diffusion once they have entered the pore space. However, the presence of micro cracks, e.g. induced by structural stresses, also affects ion transportation rates within the matrix. In the case of cracked concrete, specimens to be tested are usually saturated to facilitate chloride diffusion as the governing transport mechanism. Under non-saturated conditions, the transport of chlorides is a very complex process which involves the combination of many mechanisms.

The effect of cracks on the permeability of concrete has been extensively reported [7, 23, 44, 58, 60, 61, 89-102]. In the case of pre-cracked concrete specimen, the crack opening displacement (COD) threshold value is in the range of 50 – 135 μm . There was little change in concrete permeability below the threshold crack width but it increased rapidly beyond the critical crack width [89, 91]. For reinforced mortar, Sahmaran [100] found that the effect on chloride diffusion coefficient was marginal for the crack width below 135 μm and increased rapidly above that threshold. Ismail et al [95] observed no chloride diffusion occurred along the crack path below 30 μm crack width. Lu et al. [94] reported that when crack widths exceed 350 μm , it was not feasible to use an equivalent chloride diffusion model to fit the chloride profile subjected to drying and wetting cycles of chloride penetration.

Several researchers have reported similar experimental observation on the relationship between cracking and concrete permeability. Aldea et al. [98] reported cracking below 100 μm had little effect on concrete water permeability. Additionally, Song Mu et al. [44] evaluated the effect of different crack densities prepared by a non-destructive notch method and found that higher crack numbers result in a higher chloride diffusion coefficient in comparison to a single crack. Both investigations concluded that the concrete resistance to water and chloride ion penetration depends significantly on the density of cracks, and this was also discussed in [7, 58, 99]. The permeability has no effect or direct relationship with the crack length. It is mostly characterized by the COD. However, the chloride penetration in dynamic cracks is assumed not to be limited by the crack width [23].

Stitmannathum et al. [103] and Win et al. [90] also studied the effect of water- cement ratio on the chloride diffusion coefficient. It was found that there was a reasonable chloride ingress depth difference between lower and higher water- cement ratios due to different performance of the concrete matrix. However, when the crack depth was varied, it became a much more dominant factor. The variation in water- cement ratio was then less important. In static cracks, permeability is governed by the crack width but in dynamic cracks permeability is controlled by the frequency and rate of load application [23]. In addition to increasing the penetration of aggressive agents into concrete, cracking may also contribute to the change in behaviour of the concrete element and affect the strength of the structural component [7].

3.3 Permeability of stressed concrete

By using fracture mechanics, permeability can be related to the crack properties [87]. Under high sustained load, cracks grow with increasing load and the damage of the porous micro-structure of concrete is progressive as function of time [8, 104]. There is a reduction in the pore space under load up to a certain threshold compressive stress level [8, 9, 11, 23, 56, 105].

Kermani et al. [57] evaluated the effect of stress conditions on permeability of concrete. A threshold stress level of approximate 40% of 30 MPa ultimate strength was found in mortar specimens loaded in compression. Similar values were found for concrete. In [106] the measurement of concrete permeability was performed based on a steady state in flow. The stress level threshold was observed to occur at a low level of about 30% of peak stress. In a study by Desmettre and Charron [38], it was observed that the permeability coefficient was achieved at a loading of 20 to 35 MPa in normal-strength concrete mixture. It was a bit in contrast with a study conducted by Saito and Ishimori [104] on chloride permeability, where a small change was observed at the stress level up to 90% of 25 MPa peak stress. Similar studies on chloride permeability under pre-stressed systems were reported by Jiang et al. [9, 56]. It was found that cracks began to appear at a stress level of 50% to 60% of 52.5 MPa maximum load capacity of concrete and became unstable at stress level exceeding 70% to

90% during which a rapid increase of permeability can be seen. Similar results were also obtained by Wan et al. [107] in which a decrease in chloride diffusion coefficient at stress level 30% of 46 MPa peak strength was found. The coefficient rose and became close to unloaded specimen value after the stress level increased to 50% and followed by substantial increase of the diffusion coefficient at stress level 80%. A similar point of view is consistent with that reported by Wang et al. [108] for the progress of chloride ingress into loaded mortar. When the samples are compressed, pre-existing micro-cracks are closed and the size and the pore connectivity would be reduced, which significantly blocks chloride transport. In contrast, the microstructure of the samples changed gradually including the accumulation and expansion of micro-cracks when the loads increased. Subsequently, increase in porosity and pore connectivity and finally leading to a higher chloride transport property.

Using a rapid-chloride migration test, Rahman [87] examined the effects of the chloride ingress in concrete under compression load-induced cracks and found that the chloride ingress depth by percentage of the total depth was 33% in control specimen and a marginal increase to 35% was observed at 40% stress level of 55 MPa ultimate stress. A significant increase to 50% was found at stress level 75% and rapidly increased to 82% at stress level 90% of the ultimate stress. Samaha and Hover [109] reported that mass transport properties of concrete were affected at the stress level above 75% of the ultimate stress by as much as 20%. For these measurements, a rapid chloride permeability test was used. Under flexural stress it was observed that chloride diffusivity in the compression zone was lower than that in the tension zone. The acceleration of the chloride ingress in the tension zone can be attributed to the damage at the aggregate-paste interface [11]. Zhu et al. [110] studied differences in chloride penetration between compressive and tensile zones in large reinforced beam under load found that the chloride content of samples from the tensile zones was higher than that of samples from the compressive zones. The tension stress increased the micro pores in the concrete at the bottom zone, while the compressive stress reduced the micro pores in the top zone. As a result, the concrete in the tensile zone provided more space for the chloride movement.

Stitmannathum et al. [103] evaluated chloride penetration in reinforced concrete under flexural load and suggested two states of chloride diffusion. At first stage, the chloride might diffuse faster through the crack region where the chloride diffusion coefficient would be influenced by the cracks. In the second stage it would diffuse further through the uncracked concrete region governed by chloride diffusion coefficient of un-cracked concrete. Indirectly, it might be related to the effect of the crack depth. In addition to that, cyclic loaded specimens indicated a threshold stress about half of the stress at 25 MPa strength and rapidly increased at stress levels beyond this threshold [104]. Alternatively, a study on gas permeability [111] showed that the threshold stress is closer to the ultimate stress. It can be simplified that, in the growth and coalescence of cracks due to compressive stress, the water permeability is in fact more sensitive than the gas permeability [26]. The water permeability is relatively higher than gas permeability during crack development as the pore pressure gradient across the specimen increased [112]. The relative permeability of the gas increases a little as the pressure gradient increases due to the frequent occurrence of droplet entrainment and critical condensate saturation [113].

However, it should be kept in mind that in most of the results that are published, there is the disadvantage that the permeability test was conducted subsequently after the loading test. The inconsistency of the results could be attributed to the fact that the permeability experiment was conducted on the samples which were stressed and then unloaded. In addition to that, the corresponding compressive strengths of concrete in those studies above were not equal. Therefore, there is no straightforward correlation between the observed threshold level

of stress and the compressive strength of concrete [26]. In addition to that, differences in exposure time to the mechanical load may influence the results. This observation can be explained by the continuous propagation of damage of the composite structure under high sustained compressive load.

3.4 Cracking and failure in compression

In structural applications, the compressive strength of the concrete is of primary importance because the major structural elements in the building are the compression members. Sometimes, it is claimed that the compressive zone is considered to be free of microcracking [23]. Pre-existing network of pores and microcracks are already formed initially when the concrete is compressed [8, 26]. The influence of compressive load on new micro-cracks formation has been studied by several authors in the past [56, 107, 114-116].

In early evaluation of concrete cylinders subjected to uniaxial compression test, Loo [114] distinguished three different phases of microcracking. In the beginning, marginal cracking activity can be observed and this ends beyond the initiation stresses which exhibits quasi-elasticity. In the next phase, increase in localized microcracking is higher at the aggregate-cement interface than in the mortar matrix and can be observed by critical stress. Finally, substantial increase in mortar cracks can be marked with unstable crack growth. Unstable crack propagation may lead to complete disintegration of the material [86]. In this study [86], the initiation stresses were found to vary within the stress level 15 to 40% of 32.5 MPa cylinder strength and by 50% stress level, microcracking started to accelerate. Lim et al. [115] specified that the critical stress occurred when the stress level exceeded 80 to 85 % of 47.5 MPa peak and added, permeability was more sensitive to the stress applied [56].

Similar observations were recently done by Wan et al. [107]. It was found that a substantial volumetric strain recover took place at stress level 80% of 46 MPa ultimate stress. Between 70 to 95% stress level, a partial closure of microcracks is expected. A complete recovery of specific crack area at 50% stress level was noticed. It can be inferred that it is possible that microcracks completely or partially close after the specimen is unloaded. The report added that there is an elastic stage below the stress level of 30 to 50% where strain and stress develop linearly. Review of existing research [104] indicates that the propagation or growth of micro-cracks cause the increase in lateral strains and Poisson's ratio.

3.5 Analysis of load-induced damage

Several techniques have been devised to provide a quantitative view of the damage on the materials occurring during or after compression loading. Cracks in concrete can be evaluated visually by means of microscopic observations of surface cracks [7, 117]. These techniques are able to quantify the microstructure and the crack pattern inside concrete. However, it should be pointed out that the destructive method has several disadvantages. It requires great care when preparing the samples to avoid any additional cracks due to sawing and grinding operations [117, 118]. Undoubtedly, with this type of quasi-brittle materials, the crack patterns or sizes observed in samples prepared after unloading potentially differ from those observed while loading [114]. As a matter of fact, the crack after unloading was observed by two-dimensional observation from three-dimensional concrete samples under sustained load. In previous studies [118-121] of micro-cracks formation in concrete due to compressive load, it was observed by microscopic analysis that the cracks initiated at a critical stress of about 70 to 90% of ultimate stress.

The other alternative method is to detect and assess damage in concrete through their manifested effects and this is usually known as non-destructive crack characterization. These methods include surface strain measurements [107, 114, 115], ultrasonic pulse methods [3], the acoustic emission technique, a cyclic loading technique with measurements of cumulative energy dissipation and change in modulus [86], and holographic interferometry [122]. The ultrasonic methods are appropriate for crack detection but less sensitive to internal cracks in the materials [86], while the acoustic emission technique is best applied for the detection of crack initiation which corresponds to the reduction in integrity of the specimen materials recorded by acoustic signals. However, these methods have limitations in geometrical information regarding the orientation, location or sizes of cracks in concrete.

Similar results as found in destructive methods were published by studies using non-destructive testing which state that cracks growth occurred at higher stress level approaching the ultimate strength. A non-destructive cracking evaluation of damage occurring in concrete in uniaxial compression was published by Spooner and Dougill [86]. It was found that significant damage occurred during the first loading with a decrease of the initial slope of the reloading curves. The observations were done by using acoustic emission and energy dissipation measurements. This degradation corresponds to the reduction in integrity of the materials of the specimen. While at the peak stress it shows little or no consequence in terms of the progression of damage in the specimen. The results also suggest that the strength of the material is of little or no influence in terms of the propagation of damage in the specimen. [86]. In contrast, the analysis of literature on permeability has indicated that higher ingress of chloride was significant after the applied stress reaches half of its peak value. Definitely, the range of initiation stress values strongly depends on sensitivities of the crack detection techniques, even for the concrete that has identical properties. Another explanation can be due to the heterogeneous nature of concrete.

3.6 Service life of concrete under combined mechanical load and environmental actions

In practice, concrete structures are subjected to mechanical loading and at the same time or subsequently could be under severe environmental actions. These conditions may pose a serious threat to durability and service life of concrete structures. For instance, if the structure was under a sustained high compressive load, the service life may be reduced substantially [56]. In more complex cases of concrete structures subjected to flexural cracking, even if “deemed to comply” rules are satisfied, cracks may develop if higher yield strength steel bar is used [11]. The stress in the steel reinforcement needs to be limited to ensure adequate ductility of the concrete section and is related to the prescribed limit on concrete compressive strain of 0.003. Cracks generated by the mechanical load create preferential paths for fluids penetration and links to the existing pores. The cracks will accelerate the deterioration process of concrete, hence reduce the concrete service life [56, 87].

In the past, chloride ingress prediction is based on the assumption of a homogenous un-cracked concrete. In reality, concrete is a heterogeneous material and concrete structures are always subjected to heavy mechanical loading and environmental action. The mechanical loading conditions include complete rest periods and periods with varying dynamic live loads. Environmental actions are categorised in different levels of severity in accordance to Eurocode 2 (EC2), namely, mild, moderate, severe, very severe, and extreme. Many studies exist on the deterioration of concrete during crack initiation and further propagation. It was observed that

service life under combined loads is considerably shorter than under separate individual actions [10, 123]. This indicates that mechanical stress can increase the chloride transport rate and penetration depth in concrete [9]. However, the coefficients of capillary suction and chloride penetration are reduced under moderate compressive load and will increase by higher loads when micro-cracks develop further [12]. In contrast, under tensile stress both porosity and the damage index (ratio between the initial and the reduced structural integrity) increase with the increasing of tensile load [105]. Zhu et al. [110] observed the beam under three-point bending system had contributed to only about 3 months service life of the corroded beams in the tension zone and one year in the compressive zone. However, the effect of flexural cracks on the chloride content was not considered in that study as all the samples were collected at least 50 mm far from the flexural cracks. Therefore, combined mechanical and environmental loads must be taken into consideration for realistic and practical service life design of concrete structures [10].

3.7 Proposed combined method

Based on various published data, it appears that inducing damage into the specimen and then measuring its permeability subsequent to the mechanical loading test may not provide true information on the flow of liquids in quasi-brittle materials and hence, predicting service life may be wrong [26, 57]. In fact, the permeability measured under load can be less than the permeability after removing the load due to the trend of concrete becoming denser if under a lower compressive stress level [23]. Additionally, stress-induced load may be considered as the key parameter influencing the chloride profile and chloride diffusion as chloride ion diffusion in damaged concrete has been reported to increase. An application of a standard test method for combined mechanical and environmental loads can thus provide substantial insight into the durability of the concrete-based infrastructure.

The key objective of this chapter is to develop a test method that can characterize the performance of concrete under combined actions of compressive stress and chloride penetration. The validity of the proposed test method has been checked with comparative test series carried out in a number of selected laboratories in different countries under RILEM Technical Committee 246-TDC and can be found in [124].

3.7.1 Description of test rig for compression

Several setups consisting of a rig to apply load with a maximum capacity of 400 kN, in conjunction with a strain indicator (Wheatstone-bridge) to measure the applied load were used to load concrete prism specimen. The dimension of the test rig is 120 cm in height and 32 cm in width. The test rig consists of four thick boards and one thin plate in the middle as shown in Figure 3.1. A steel 'pancake' jack is sandwiched between the top board and the second board of the test rig and allowed to swell at a certain extent and locks in the pre-defined stress level position during loading of specimens. The steel jack is also used to compensate the creep deformation of the concrete and keep the applied stress approximately constant. Two concrete specimens of dimensions 100mm x 100mm x 400mm can be placed between second thick board and third thick board of the test rig vertically with a thin plate in the middle as a divider. It is essential to ensure good alignment of both ends of the specimens with the testing machine platens. To avoid any discrepancy of results produced, only one specimen which placed at the bottom of the set-up was used for this study and a dummy specimen was placed at the top.

Oil pressure is applied to the nozzle of a manifold connected to the jack and accumulator to automatically supply and regulate the balancing pressure. A load cell is placed between the third board and the base board and linked to the strain indicator system to measure the applied load inside the rig. At first loading, the applied load will decrease quite fast thus, an extra oil pressure is needed to keep the load at the pre-defined level. Later the load will decrease much slower and the connected accumulator is capable to maintain the pressure within a small limit. It was considered important to ensure that the load imposed by the testing machine was as close as possible to the pre-determined compression load throughout the period of loading. The thin plate between the second and third board is used as a divider which makes it possible to place two concrete specimens at the same time in the test rig. The compressive loading test setup is given in Figure 3.2.

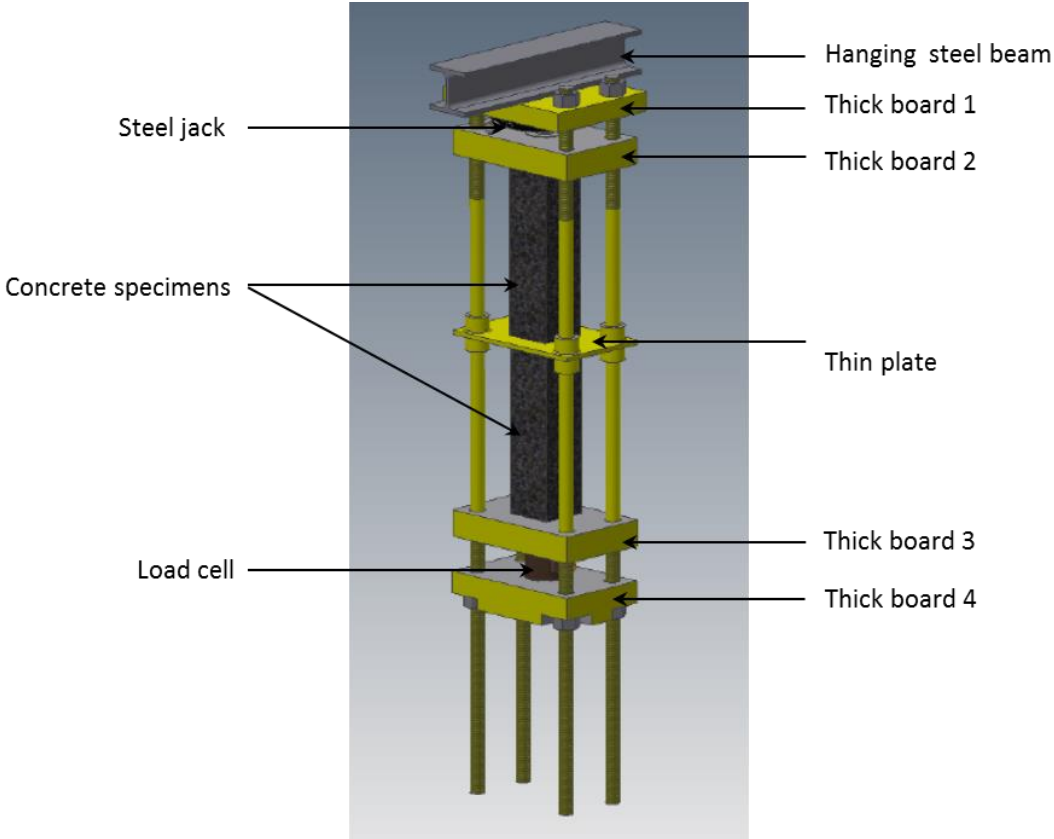


Figure 3.1 Schematic diagram of compressive loading test frame

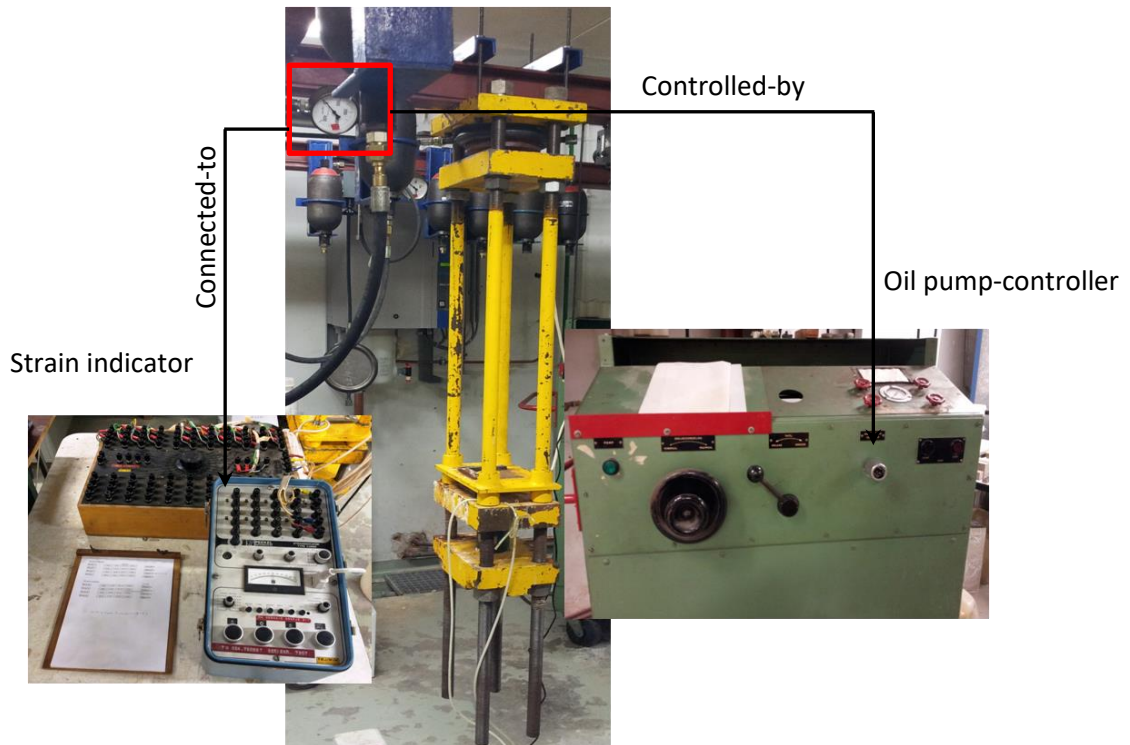


Figure 3.2 Compressive loading test setups

3.7.2 Method for preparation of samples

In Figure 3.3, the chronology of lab work for the first concrete batch is presented. After casting, the specimens were stored under plastic sheets at room temperature and at relative humidity of about 80 % to 95 % for 24 hours (h). Then, the specimens were demoulded and further cured in tap water up to 28 days.

The specimens were taken out from the water bath and subsequently saturated with calcium hydroxide, $(Ca(OH)_2)$ solution under vacuum conditions for three hours to ensure chloride penetrate into the concrete by diffusion and also to avoid leaching of $Ca(OH)_2$ during chloride testing. Afterward, the free water on the surfaces was removed with a clean dry towel. A sealing membrane of self-adhesive aluminum foil was installed immediately on the concrete surface except for one of the moulded surfaces. Here, a window was left open of a size of (80 x 160) mm. On this window the chloride solution container was fixed. The purpose of sealing of the surfaces was to ensure one-dimensional diffusion only. Then, the chosen compressive stress ratio, which is the ratio of applied stress to the compressive strength, was applied on the prismatic concrete specimens using a test rig as shown in Figure 3.1. The specimens were unloaded after designed duration, after which the specimens were ready for chloride profile determination.

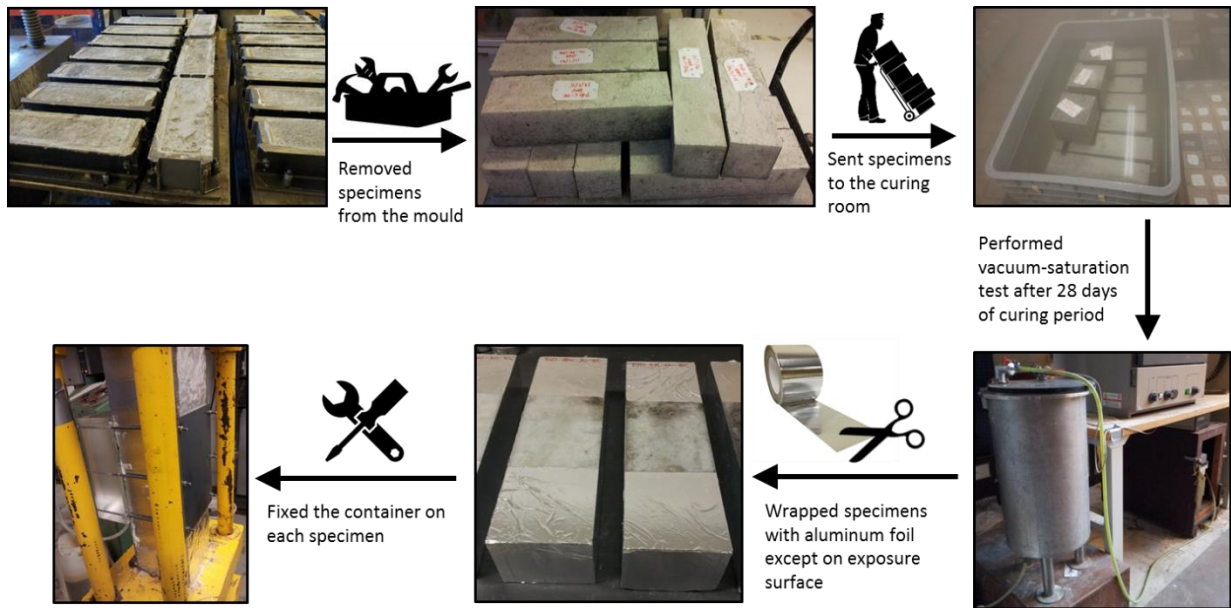


Figure 3.3 The chronology of the lab work performed

3.7.3 Vacuum saturation test

Degree of saturation or water content has a significant influence on transport mechanism of concrete [58]. In some cases, curing condition did not allow for complete saturation [88]. In several studies of the permeability test [88, 109, 125], moist curing in a fog room was also observed to be insufficient for complete saturation. The incomplete saturation may contribute to false or non-permanent self-sealing. Therefore, in the recommendation, it is proposed to use vacuum saturation of the specimens.

The vacuum tank shown in Figure 3.4 has a height of 800 mm with 250 mm of diameter. It can fit for four concrete prisms with dimension 100 mm x 100 mm x 400 mm at the same time. The specimens were left in the vacuum tank for 2 hours to extract the air, after which water was added and the vacuum was removed.



Figure 3.4 Vacuum chamber for saturation test

3.7.4 Chloride circulation setups

A saturated calcium hydroxide, $\text{Ca}(\text{OH})_2$ solution containing 3% to 3.3% of sodium chloride (NaCl) was circulated through a transparent container (which was attached at the opening area positioned at the mid-height of the concrete specimen) immediately after the specimens were loaded in compression. The container was connected to a small basin containing five liters of fresh chloride solution and equipped with a small capacity water pump. The chloride solution was circulated using the pump and recycled from a five litres capacity basin in every setup which is shown in Figure 3.5. This is to ensure that the flow rate of the solution can be easily controlled in each setup. The solution was circulated at a flow of 5 ml/s through the chloride container from the basin and monitored over time. The specimens were left under combined chloride and compression load for 2, 6, 18 and 36 weeks.

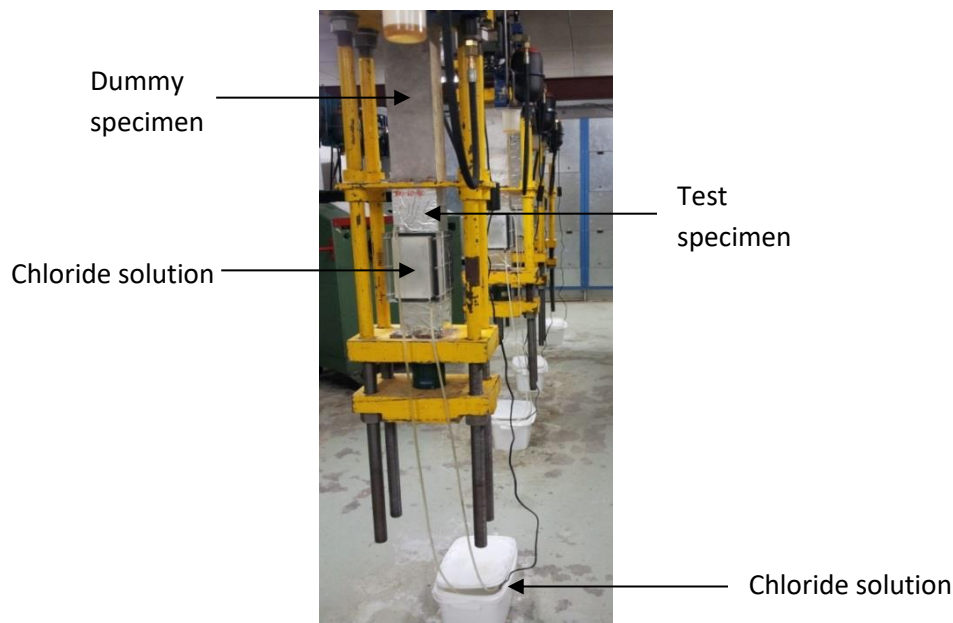


Figure 3.5 Complete set-up for combined actions testing

To produce a realistic chloride circulation, a special container device was designed. The transparent cuboid container of size $(100 \times 180 \times 60) \text{ mm}^3$ in rectangular size was attached to the opening surfaces with a thin layer of rubber sheet of approximately 2 mm thick to ensure water tightness during circulation process. A steel plate of size $(100 \times 180) \text{ mm}^2$ was clamped to the container using six steel rods and 12 nuts to bring the container into position. Finally, two tube connectors were inserted at the inlet and outlet designed at the top and bottom of the container. The inlet and outlet tube connectors were positioned diagonal to each other to initiate multi-directional chloride ingress through the specimen. The containers are durable with very fast and straight-forward installation and hence, enable it to be reused again for several times. The parts of the container and the way to assemble it are schematically shown in Figures 3.6 and Figure 3.7, respectively.

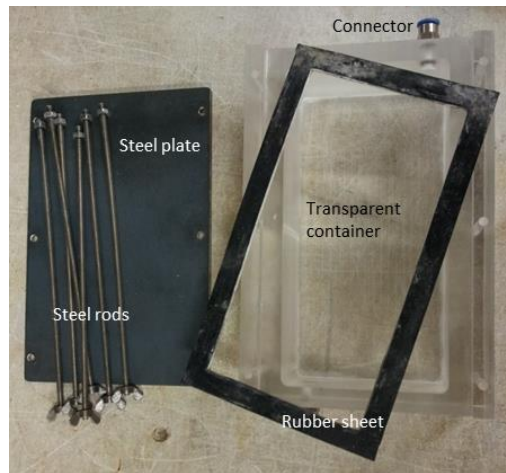


Figure 3.6 Parts of chloride permeability system

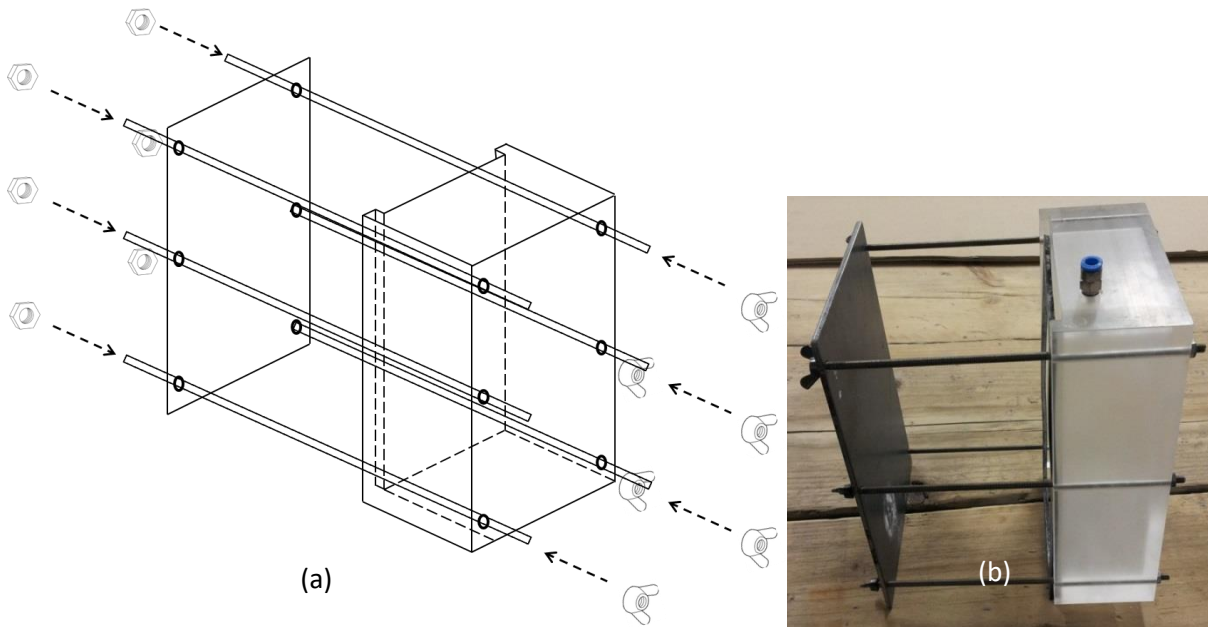


Figure 3.7 (a) Schematic diagram of container installation; (b) final installation

3.8 Determination of chloride profiles

3.8.1 Laser Induced Breakdown Spectroscopy, LIBS

Laser Induced Breakdown Spectroscopy, also known as LIBS, is a spectroscopic technique that provides information about materials elemental compositions. In this thesis, LIBS was employed to measure the total chloride content as percentage to the cement mortar of the concrete specimens. With ideally simple sample preparation, LIBS can detect elements that are present on the surface of solids, liquids or gases. A pulsed laser at highly energy density evaporates a very small part of material on the surface of the specimen to form a plasma cloud. The atomic emission spectrum was recorded and analyzed by monitoring the wavelengths and intensities of the emission lines. This action can capture more than one element at a certain time measurement. The scanning of the exposed surface of the sample is grid-like in a plane

perpendicular to the laser beam [126]. The quantitative analysis of LIBS highly depends on the accuracy of calibration methods. Several researches have been conducted to improve analytical performance of LIBS including classical calibration [15], internal standardization [16,17] and multivariate calibration [18,19]. In recent study conducted by Yuan et al. [127], a new one-point calibration method was proposed to build the calibration and improve the accuracy of determination of major elements in LIBS. The study used the determination coefficient (R^2), the root-mean-square error of cross-validation (RMSECV), the average relative error (ARE), and the average relative standard deviation (ARSD) as the evaluation parameters to determine the performance of single-sample calibration LIBS (SSC-LIBS) and found that almost all the major elements had more than 95% accuracy and even better than those calculated by using multipoint calibration LIBS (MPC-LIBS). This results indirectly provide convincing application of LIBS. The LIBS system used in this research was developed at Federal Institute for Materials Research and Testing (BAM), Berlin, Germany. Figure 3.9 shows the arrangement of the LIBS system and a sample to be tested.

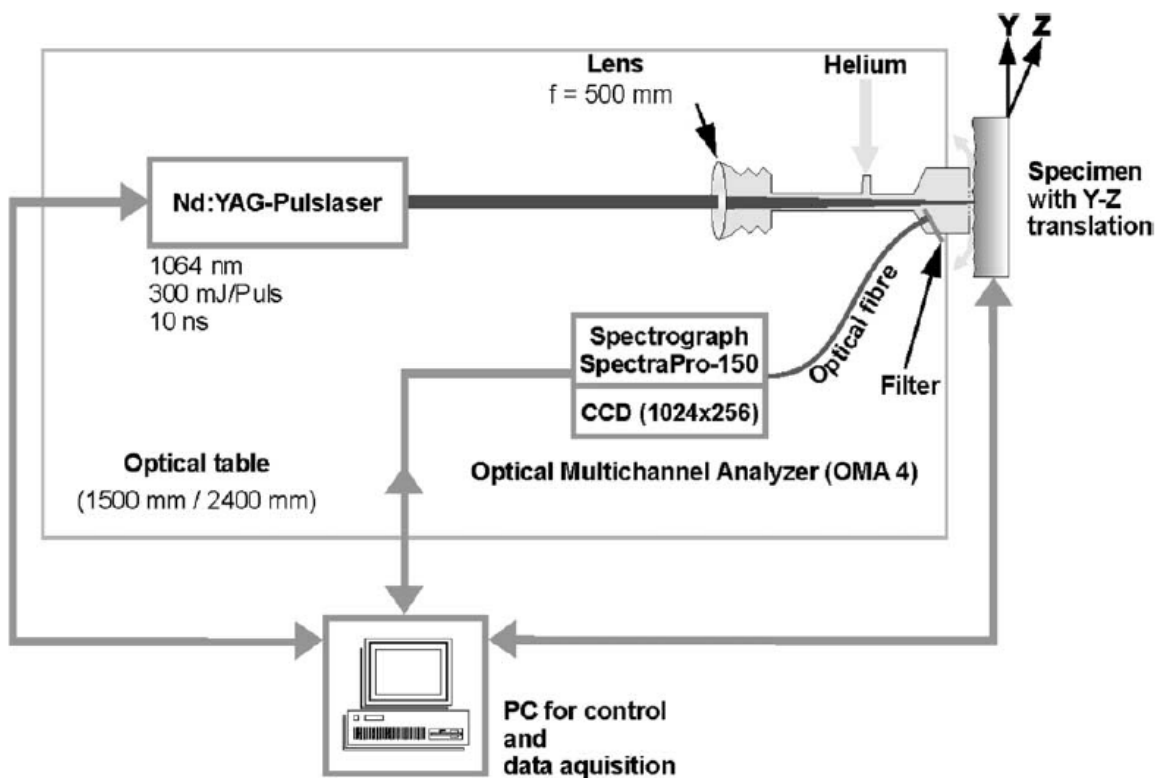


Figure 3.8 LIBS experimental set-up [126]

3.8.2 Photometric Determination

Another simple and rapid chloride analysis method is photometric determination using mercury thiocyanate/iron (III) method. The photometer identifies the optical path length of the inserted cell and immediately calculates the correct concentration. In general, the photometer is equipped with barcode-scanner system with different test kits programmed in the database. Each cell test has a barcode that enables the correct method to be selected automatically. Figure 3.10 shows photometry machine.



Figure 3.9 Photometry and cell kit box

This method also minimizes sample preparation activities prior to analysis. For chloride measurement, a minimum mass of 1000 mg sample of concrete, shredded to a grain size < 100 μm is required to mix with 3 molar nitric acid for a few minutes. The mixed solution was then heated to moderate boiling for 5 minutes. The solution was cooled down at room temperature. The cooled solution is filtered through a micro-glass fibre filter to get a clear solution and the total volume was measured. The steps are given in Figure 3.11. Only 1.0 ml from the clear filtered solution with 0.5 ml reagents was pipetted in provided test cells. The solution in the cell test was thoroughly mixed for a few seconds before placing in the photometer using a turbine mixer. Immediately the photometry will indicate the measurement value on the small display screen in the encoded form. The percentage error reported for photometric determination was about 3% at 17 mg per litre of chloride. This method is sensitive towards colour contaminants however, treatment with aluminium hydroxide can be sufficient to eliminate such interferences in most cases [128]. The linear Equation 1 was used to determine the chloride content in % for 50 ml volume of filtered solution.

$$\text{Chloride content in \%} = \frac{\text{analysis value in } \frac{\text{mg}}{\text{l}} \text{Cl} \times 5}{\text{weight of sample in mg}} \quad (1)$$

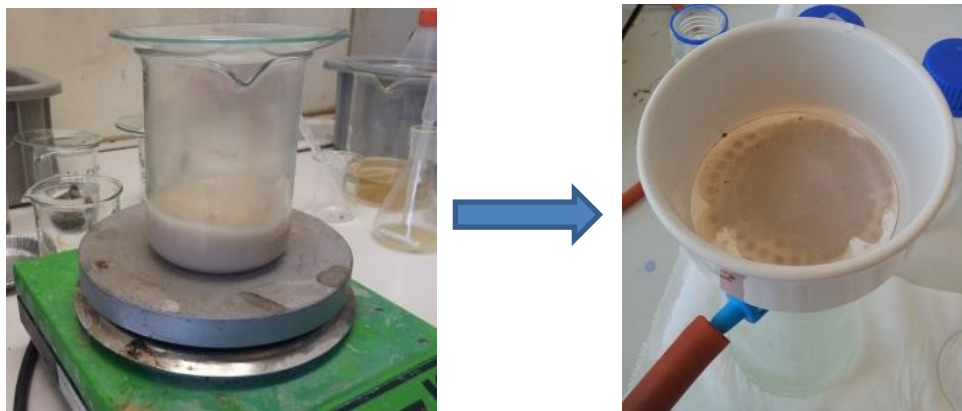


Figure 3.10 Solution sample preparation

3.9 Conclusions

Research has been undertaken to quantify permeability of cracked concrete, and the chloride ingress in cracked concrete under static load application, however, the influence of synergetic effects has received scant attention. As a matter of fact, concrete resistance towards chloride ingress is closely related to the development of micro-cracks. The ingress of chloride ions of concrete under compression increases rapidly when the applied stress exceeds a certain threshold value. However, from all the results published, it has been concluded that the threshold value for the stress level is dependent on the strength grade of the concrete as well.

The method developed in this chapter is mainly to characterize the sensitivity of a normal-strength type of concrete with respect to chloride ingress under the influence of compressive stress. Using the approach outlined in this chapter, the critical compression stress level which provides the onset of coalescence of microcracks to rise can be defined. The impact of compressive load-induced damage coupled with chloride transport on the concrete structures may be used for calculating the reduced service life of reinforced concrete structures and recommendations can be made for engineering practice.

4.

Chloride resistance of concrete with compressive load-induced cracks

“Strength and permeability of the hydrated cement paste are two sides of the same coin in the sense that both are closely related to the capillary porosity.”

-P. Kumar Mehta-

Most durability tests on concrete under laboratory conditions are done in the absence of damage properties of the concrete, i.e. propagation of cracks. A short review on this issue was given in Chapter 2. A realistic approach for durability test of concrete was presented in Chapter 3 and experimentally investigated in this chapter.¹

In the pages that follow, concrete experiments under coupled effects of chloride penetration at different compressive load levels and experimental time are presented with materials used in the sample preparation (4.2 and 4.3). The chloride profiles were analysed and the diffusion rate was determined with respect to the percentage of the cement mortar by using Laser-Induced Breakdown Spectroscopy (LIBS) method (4.5.1) and to the percentage of concrete by chemical analysis method using Photometric determination (4.5.2). The chloride profiles and chloride diffusion coefficients of each specimen from photometry analysis are determined (4.5.2).

Then, the effects of mechanical loading on the concrete with the ingress of chloride ions are discussed (4.6). The results obtained were in good accordance with the results from other labs participating in the round robin test series of RILEM TC 246-TDC [124, 129]. The chloride permeability was affected when the stress level was higher than 50% of the ultimate stress.

¹ Parts of this chapter have been published in “Balqis M.Y., Jonkers H.M., Schlangen E. “Chloride penetration into concrete with compressive load induced cracks”, *Construction Materials and Structures: Proceedings of the First International Conference on Construction Materials and Structures: ICCMATS*. Amsterdam: IOS Press, pp. 819-824, 2014.

4.1 Introduction

There is a vast interest in investigating the deterioration of concrete after crack initiation and further propagation. There are several factors which may explain this interest. One of the most significant current discussions in the deterioration of concrete structures is related to the fact that the service life designs are based on simple laboratory test results of chloride diffusion coefficients which are carried out on specimens which are not under load. By doing so, the service life of real structures is considerably overestimated [8]. Another factor that plays a role is that the prediction of chloride ingress is based on the assumption of a homogenous uncracked concrete [10, 12, 105]. Therefore, the importance of the state of stress on the transport properties has been highlighted extensively.

At present there exist several techniques to evaluate permeability of concrete subjected to compressive loading. However, limited attempts had been made to evaluate the chloride transport during a compression test. Crack characterisation or permeability testing of unloaded specimens is different from those while under load. Furthermore, combined mechanical and environmental loads may turn out to be much more severe than isolated load. As discussed earlier, load plays a role in increasing chloride penetration into concrete especially when the concrete structures are exposed to marine environment. The development of micro-cracks due to loading may facilitate the transport of chloride ions from the surrounding media [104]. An early study on chloride permeability influenced by micro-cracks has been pointed out by Mehta [130]. Concrete subjected to loading probably requires only a few hours for the chloride to reach steel as compared to concrete without loading which requires a longer time. Faster diffusion could occur through the cracked material. Therefore, it would be more appropriate to do combined loads so that a more realistic account of the concrete service life can be made. The effect of combined loads should be considered as an important factor for realistic service life design of concrete.

4.2 Materials

An investigation was carried out on concrete prisms of size 100 mm x 100 mm x 400 mm. The concrete was composed of Ordinary Portland Cement Type I, 42.5 having Blaine value of 328 m²/kg with a water/cement ratio of 0.45. Crushed gravel with nominal maximum size 16 mm was used. Superplasticizer, Cretoplast SL01 from CUGLA (Breda, the Netherlands) was used to achieve a slump value of 15-16 cm for the mixture. The materials were mixed using tap water. The composition of fresh concrete that specifically used in this study is listed in Table 4.1. The concrete mixtures were cast in steel moulds in two steps and compacted by a vibrating needle for 30 second (s). The fresh concrete surface was levelled, and the specimens were covered with plastic sheets.

Table 4.1 Mix proportion of fresh concrete (kg/m³)

w/c	Portland cement	Sand	Coarse aggregates	Tap water	Super-plasticizer
0.45	368	840	1027.5	165.5	2.6

All mixing and casting were carried out in a standard laboratory condition at a temperature of 23 ± 2°C and a humidity of 50 ± 5% RH. The specimens were demoulded after 24 hours and then cured in tap water until 28 days. Two concrete batches were made to observe different properties of chloride transport in concrete. Three concrete prisms were prepared from each batch of concrete. In the first batch, the concrete specimens were taken

out of the water bath after 28 days and were immediately sealed with aluminium foil after the surface of the specimens was dried using a cloth. In this concrete batch, the analysis of chloride was done using laser-induced breakdown spectroscopy (LIBS).

In the second concrete batch, the specimens were taken out of the water bath 28 days and subsequently saturated with calcium hydroxide, $(\text{Ca}(\text{OH})_2)$ solution under vacuum conditions for three hours. The purpose of vacuum saturation approach is to suck the trapped air within the effective pores and replacing it with solutions. This method reduces the influence of the capillary sorption in the materials. In addition, by filling the pores with solution, it will accelerate the process of chlorides transport in concrete due to the higher pore connectivity to decrease the tortuosity for the pathway of mass transfer in concrete [131]. Afterwards the free water was removed from the surface of the specimens using a dry cloth and the surface was immediately sealed with aluminum foil. For all the specimens in this batch, the photometric determination was used for the determination of the chloride profile.

4.3 Specimen under combined loads

The loading of the specimens was done according to the method proposed by RILEM TC 246-TDC, (see section 3.6) [129]. As the specimens should be under pre-selected stress level, the compressive strength of the concrete prisms was measured at the age of 28 days. The total number of prism specimens produced was 24. A total of 18 prisms were used for the chloride diffusion tests and 6 for obtaining the ultimate compressive strength. Concrete prism specimen was used in this combined load test to get an equal stress distribution for chloride exposure area which is at the middle of the test specimen. Prisms or cubes form of failure indicate that friction between the steel loading platen and the concrete restrains the ends of the test specimen (Figure 4.1) [132]. In this case, the microcracked zones were presumed uniform from the surface to deeper layers at the middle of prism and thus, the concerns of chloride exposure penetrate into concrete and meeting differently microcracked zones can be neglected.

The average values for ultimate compressive strengths obtained are given in Table 4.2. From Table 4.2, it was observed that the average values for ultimate strengths of concrete prism were about 23 % to 29 % lower in comparison to concrete cube compressive strengths presented in Section 5.3.3. It also should be noticed that basically cube test representing crushing strength of the concrete and does not representing “true” uniaxial strength of the concrete. In a study reported by Hughes and Bahramian [132], the ratio of prism strength to cube strength varied in the range of 0.59 to 0.99. In more recent study by Zhenhai Guo [133], the slightly higher value of it is used in the design code of different countries, generally in between of 0.70 to 0.92, considering the safety of the structure. In addition to that, the types of aggregates and mix proportions can both influence a relation between prism and cube strengths.

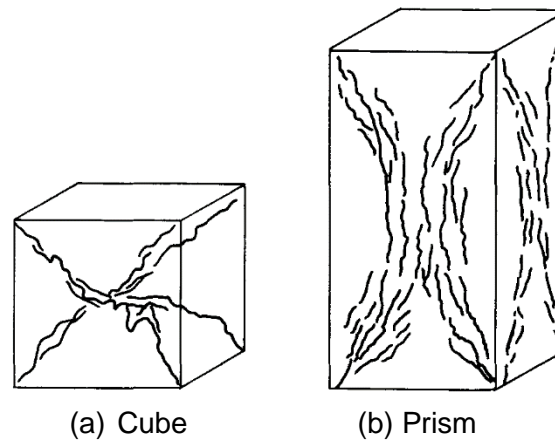


Figure 4.1 Form of failure of cube (a) and prism (b) of test specimens [132]

The specimens were placed in the compression test rigs and subjected to the stress level of 30% and 60% of peak compressive stress. Each test series had an unloaded specimen to act as a control. From the point of view of structural engineering, a building is normally designed to take service load at about 25% to 35% of the concrete ultimate strength. However, from the previous study conducted on combined load test [107], test specimen with stress level below 50% of ultimate strength demonstrated that the pore structure is being compressed, concrete was still under elastic phase and chloride penetration was lower than unloaded specimen. A slightly above 50% stress level is encouraged for this work to get a significant effect of chloride ingress into concrete under different applied load. This changing behavior agrees well with crack developing observed by Wang et al [134]. According to the authors, there is a steady development of microcracks in the interfacial transition zone at stress level of 50 % of ultimate compressive stress. However, sustained loading above 75% stress level of the concrete ultimate strength should be avoided because concrete crack systems become extremely unstable and can fail easily. Therefore, 30% and 60% stress level were selected in this study. All specimens were coded according to the nomenclature of exposure conditions code as described in Figure 4.2.

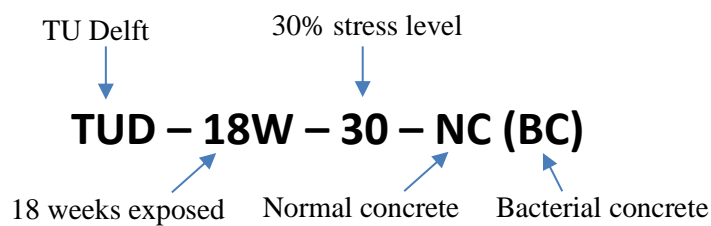


Figure 4.2 Nomenclature of specimen code

Table 4.2 Concrete batch, specimen codes and compressive strength of concrete prism at 28 days of age

Concrete batch	Specimen code	Average ultimate strength (MPa)	Standard Deviation	Coefficient of variation (%)
1	TUD-6W-0-NC	37.93	1.71	4.5
	TUD-6W-30-NC			
	TUD-6W-60-NC			
	TUD-18W-0-NC			
	TUD-18W-30-NC			
	TUD-18W-60-NC			
2	TUD-2W-0-NC	40.72	1.92	4.7
	TUD-2W-30-NC			
	TUD-2W-60-NC			
	TUD-6W-0-NC			
	TUD-6W-30-NC			
	TUD-6W-60-NC			
	TUD-18W-0-NC			
	TUD-18W-30-NC			
	TUD-18W-60-NC			
	TUD-36W-0-NC			
	TUD-36W-30-NC			
	TUD-36W-60-NC			

4.4 Sampling techniques

4.4.1 LIBS sampling method

For the LIBS method, the samples were prepared in the following way: First, the prisms were cut into three pieces consisting of top, central and bottom parts of the prism with a saw which was oiled cooled to prevent washing out of chlorides from the surface. Next, the resulting specimens were taken in a thickness of 50 mm from the central part of the prism that was exposed to the chlorides and had a size of (100 x 100) mm². The preparation of concrete cores for the LIBS measurements is schematically shown in Figure 4.3.

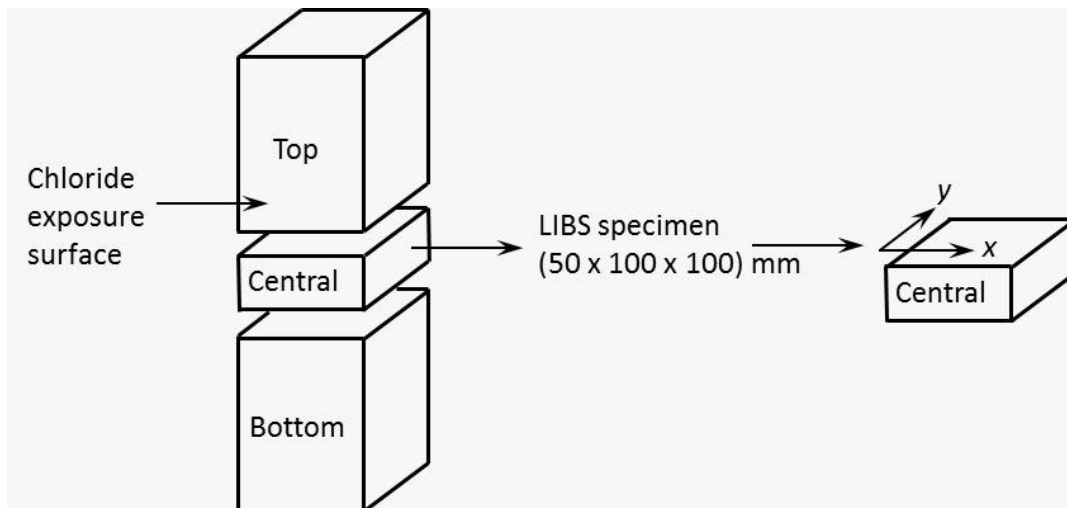


Figure 4.3 Sample preparation for LIBS

For the LIBS measurement, line scans of 0.5 mm spacing with the same 0.5 mm resolution is used to scan (100 x 30) mm grid on (100 x 100) mm concrete size. The exposure time of the detector chosen is 860 ms for all measurements. Central monochromator position was set to 837nm for concrete spectrum in the chlorine spectral line which has been reported to be well detectable and quite strong in gases and solid organic compounds, see Figure 4.4 [135]. This causes ablation of the material and the formation of sound waves and characteristics plasma. In particular, the sample does not need to be in a vacuum. Hence, it is noteworthy that pre-saturated of specimens were not applied prior to the LIBS test. The analysis using this method was limited to the sample exposure age of 6 and 18 weeks.

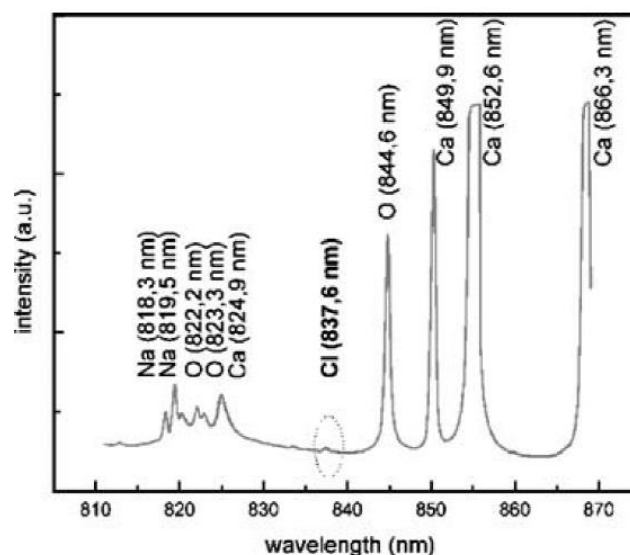


Figure 4.4 Spectrum line in the chlorine wavelength range of typical concrete [135]

4.4.2 Sampling method for photometric determination

For the photometric determination of the chloride profiles, powder samples at different layers were prepared by using a grinder. The powder samples were obtained by stepwise grinding layers with a thickness of 1 to 2 mm from the exposed surface that was in contact with the chloride solution. The grinding work took place immediately after the test period to stop the potential of the chloride to diffuse further through the pores or microcracks developed in concrete. In addition to that, the concrete surface is protected from drying before the grinding process can begin, as drying will modify the chloride profile. Ten layers were ground from each specimen at different load levels of approximately 0, 30% and 60% of the ultimate compressive load and exposure time. It is recommended that the number and thickness of the layers can be adjusted according to the expected chloride profile with a minimum of eight measuring points. Similarly, samples were also obtained at the outside of the exposed zone representing the initial chloride content of the concrete specimens. In order to avoid edge effects and an influence of the glue of the self-adhesive aluminum foil on the test results, sampling was performed on an area with a distance of 10 mm from the border of the exposure zone. The chloride content for the powder samples of each layer was determined by dissolving the powder in acid and using photometric determination (see section 3.7.2). The set-up of sample for chloride profiling on the concrete prism is shown in Figure 4.5.

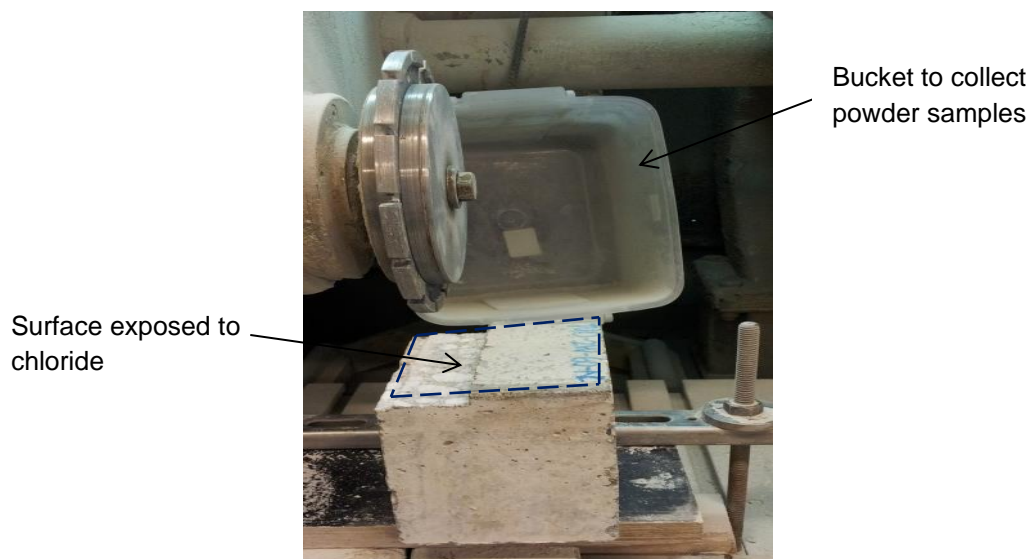


Figure 4.5 The set-up of sample profiling

4.5 Results and discussion

4.5.1 LIBS measurement and results

The chloride profile analysis was performed on a surface dimension of (100 x 30) mm area in specimen size (120 x 100 x 50) mm as depicted in Figure 4.6. The measurement starts from the chloride-exposed surface along the 100 mm dimension which is labeled as x-direction and continue until 30 mm of penetration depth which is taken as y-direction. The sample is scanned line by line (in x-direction) with line spacing of 1 mm throughout the y-direction. The resolution is 0.5 mm x 0.5 mm with a pulse frequency of 10 Hz.

LIBS is only able to detect the element chlorine which is in pure gaseous form. In concrete normally only ions of chlorine (chlorides, Cl) occur. Therefore, the signal of the chlorine peak can be implied to the total chloride concentration in concrete samples. The sensitivity of chloride line can be increased by flushing the induced plasma with helium so that the influences of atmospheric elements e.g. nitrogen or oxygen are excluded. In addition to that, it is possible to exclude the coarse aggregates to avoid influences of elements like calcium or oxygen which are detected simultaneous with the chosen wavelength range for chlorine. To which size the aggregates can be excluded depends on the chosen resolution. The higher the resolution chosen the more time is needed for the measurement. Total chloride content in concrete exposed to compressive stress and chloride environment, including free and bound chloride was collected and analyzed by a computer using chemometric software. The results are shown in Figures 4.7 and 4.8.

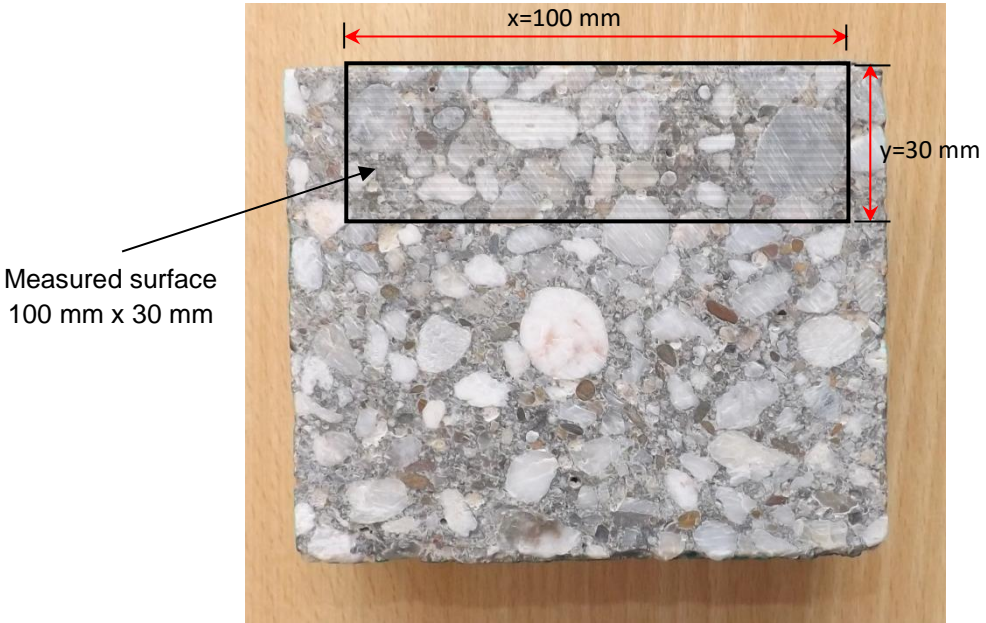
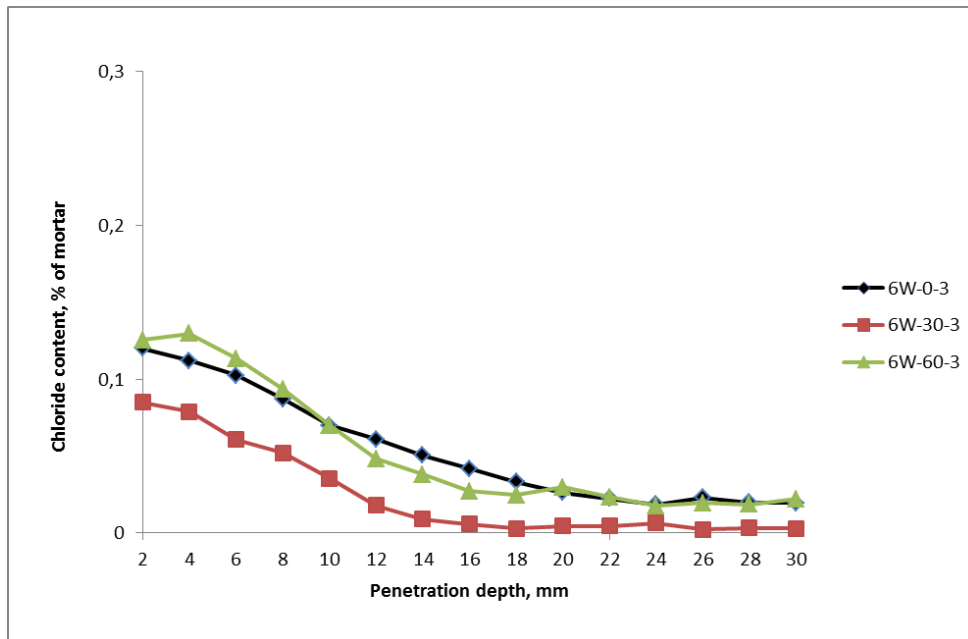
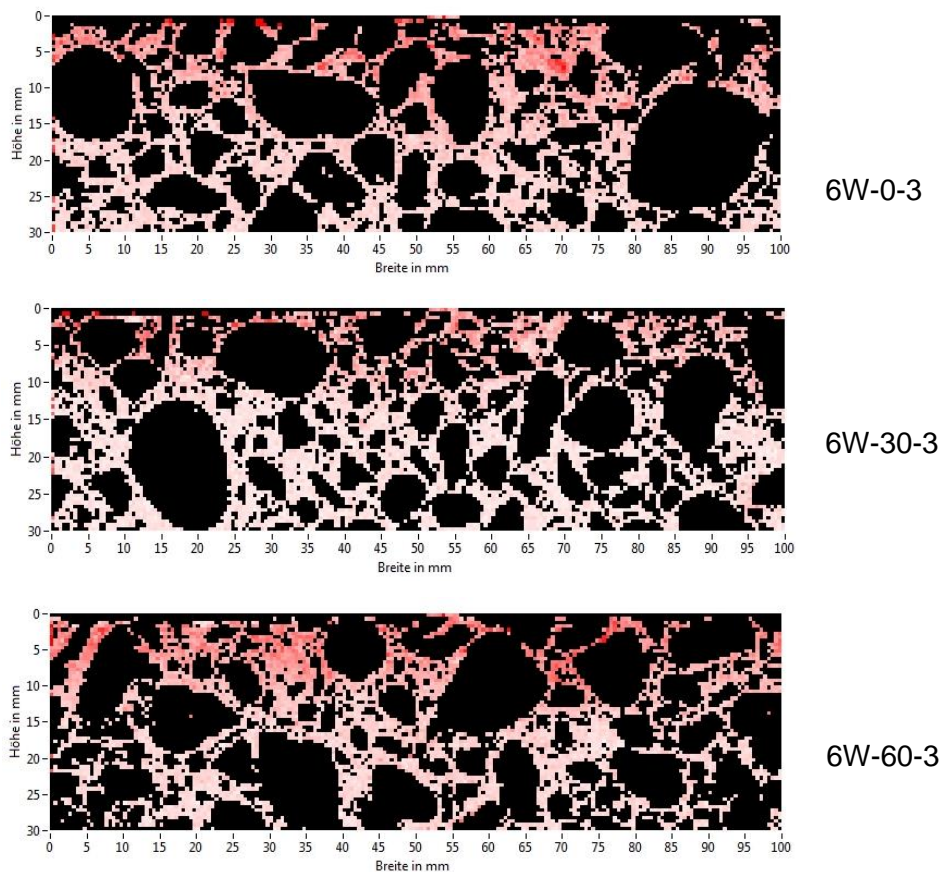


Figure 4.6 Exposed surface, X and Y area of TUD-6W-0- concrete sample

In Figure 4.7 (a), it can be seen that the chloride ingress after 6 weeks exposure for the 60% stress level was slightly increased for the first 8 mm depth of penetration. With further penetration it became somewhat lower than the stress-free specimen until equal total chloride content from both specimens was found after 20 mm of depth. For the 30% stress level, the chloride concentration was significantly lower than the stress-free specimen. However, the total chloride concentration obtained is still low at this stage, although the role of damage has been detected. Two-dimensional images of chloride distribution for 6-weeks specimens are presented in Figure 4.7 (b). Dark red represents a higher chloride intensity.



(a) Chloride profiles for 6-week specimen

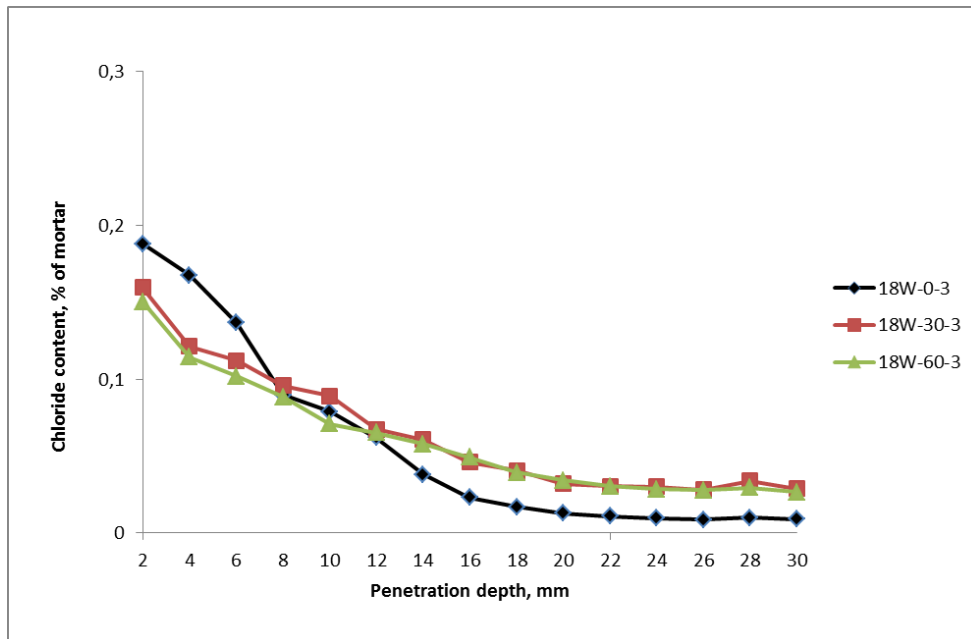


(b) Chloride distribution over sample surface with excluded coarse aggregates

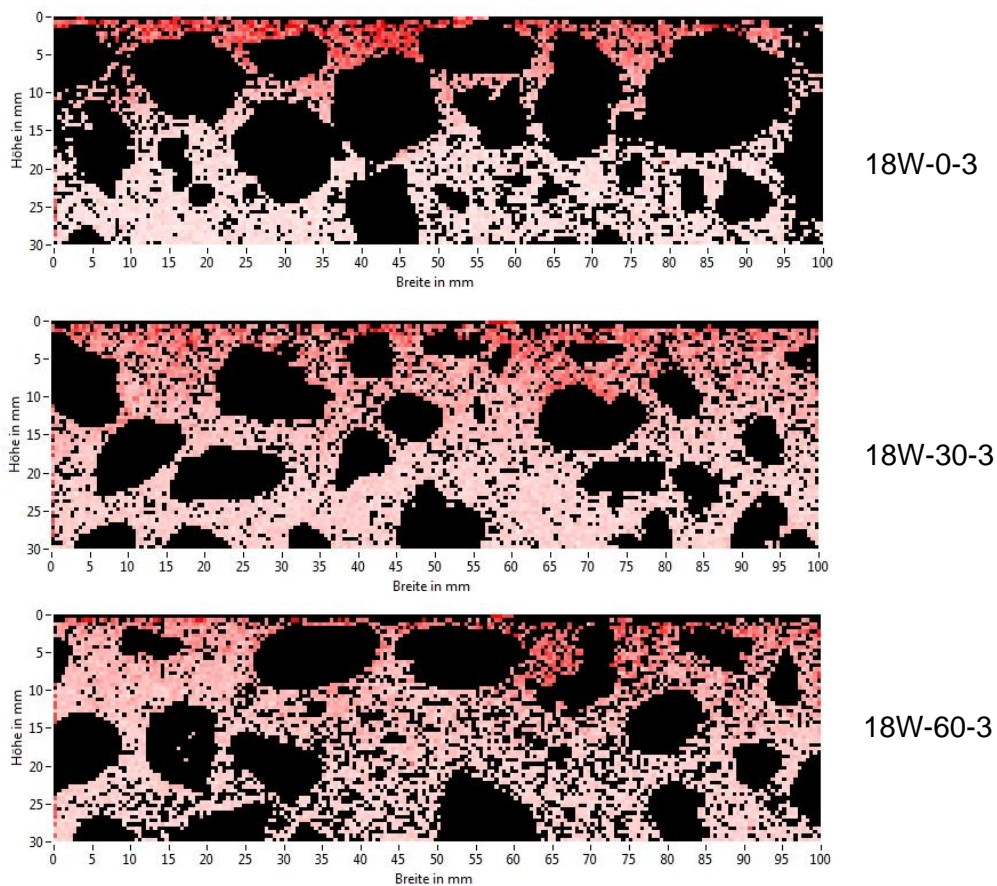
Figure 4.7 LIBS measurement of chloride analysis after 6-weeks of testing period

The difference of profile change has been observed in Figure 4.8 (a) for the specimen with the extension of time interval of 18 weeks. Initially, stress-free specimen has a higher total chloride content, but a rapid decrease took place after 8 mm penetration depth. This observation can be due to the influence of the capillary suction which could be more effective by the inherent microcracks in the concrete material than in the specimen with an applied stress where the crack opening is larger. At the distance of 10 mm, the chloride in control specimen was observed to penetrate further into the concrete matrix by the diffusion transport mechanism and the concentration was lower than the specimens under stress. The total chloride content reached an equilibrium value of approximately 0.02% by 20mm depth which coincides with the initial chloride content of the concrete before the diffusion test. Specimens with 30% and 60% of the ultimate stress show more stable chloride profiles with similar amount of chloride penetrates into the pore space of concrete. Figure 4.8 (b) shows images of chlorine distribution over the surface of 18-weeks samples with exclusion of aggregates captured from LIBS measurement.

In summary, the chloride surface concentration of 18 weeks specimens were higher than 6-weeks specimens as well as the depth of penetration. This observed become larger is partly due to internal crack and changes of pores connectivity as described previously. However, these results were not enough to summarize that the applied stresses contribute to the percentage increase of penetrates chloride into pore space of concrete by developed microcracks. Therefore, in the next concrete batch, acid soluble chloride method was used for total chloride concentration measurement at more various time intervals.



(a) Chloride profile of 18-week specimen



(b) Chloride distribution over sample surface with excluded coarse aggregates

Figure 4.8 LIBS measurements of chloride analysis after 18-weeks of testing period

4.5.2 Photometric determination

An observation on the chloride penetration was continued by photometric determination. In order to discuss on the chloride penetration profiles, the information of each profile is grouped according to the test period. In this section, the research parameters were refined which included the exposure time and minimization ingress of chloride due to capillary suction by performing saturation under vacuum condition. Prior to chloride diffusion test, pore volumes in the concrete were filled up with calcium hydroxide solution to avoid leaching of calcium hydroxide from concrete during the circulation of the chloride solution during the test. Due to that, more stable results were produced. In this method, sample with 2, 6, 18 and 36 weeks of test period were evaluated. The 2-weeks and 36-weeks of test period were added from LIBS method to get significant relationship for chloride diffusion graph.

The values of chloride concentration subjected to static compressive stress are plotted against penetration depth in Figure 4.8 (a)-(d). The chloride permeability of concrete loaded to the stress level of 30 and 60% of ultimate load is nearly equal to the unloaded specimen after 2 weeks exposed to chloride solution as represented in Figure 4.9 (a). This observation can be explained by the effect of a short overload in 2-weeks exposure concrete which rapid hydration still available hence may reduce pore space and provide a provisional impermeable surface layer. However, it appears that after 6 weeks, a significant difference in chloride permeability can be observed between stress levels, although these plots are somewhat scattered. It is also apparent from Figure 4.9 (b) that the application of 60% stress level rises the chloride concentration over the entire penetration depth.

After 18 weeks, an increase in chloride penetration depth was observed for every stress level including unloaded specimens with insignificant change of chloride surface concentration except for the 30% stress level. The chloride profile trend indicated that the specimen at 30% stress level lies slightly above the unloaded specimen and 60% stress level specimen was marginally above the 30% stress level specimen. Therefore, it can be assumed that some pores and micro-cracks are partially compressed at 30% stress level of ultimate stress after 6-weeks of exposure. Hereby limiting the ingress of chloride into concrete. However, by further exposing the concrete specimen to load even at lower stress level, it may cause a certain degree of damage as soon as microcracks attract one another and they finally coalesce. In general, the permeability should not be significantly affected by lower stress level.

The results represented in Figure 4.9 (d), which is after 36-weeks, indicate that a considerable number of cracks developed in concrete. Wittmann et al. [56] obtained experimental result showing that extensive interconnection of cracks occurred in concrete after reaching 50 % of the ultimate stress. Considering these findings, it can obviously be seen that there is a substantial gap between the chloride profile at 60% stress level and 30 % stress level and unloaded concrete specimens. When concrete is subjected to 60 % stress level, the micro-cracks begin to propagate noticeably by allowing more chloride ions to ingress. The chloride penetration rate was significantly increased at 60 % stress level. This trend is also in good accordance with observations of Jiang et al. and Wang et al. [9, 108].

In each case, load levels at higher percentage of ultimate strength increased the ingress of chloride into concrete significantly. Micro-cracks widening due to mechanical loading is also indicated by the fact that the chloride profiles at 60 % of breaking load are always the highest from week 6 onwards. It is also observed that, at load levels under 30 % of ultimate loading, the concrete becomes denser, thus having less pores available for chloride transport. The observation is in good accordance with studies reported by [9, 107] which indicated that at stress levels lower than 50 %, the concrete is in a consolidated phase. The study by [107] also reported that for stresses below 50 %, concrete exhibited elastic deformation when the strain

returned to zero after unloading from uniaxial compression test conducted on volumetric strain due to micro-cracking. Thus, significant difference can be found in chloride resistance of concrete under loading and after unloading. According to Wang et al. [134], studied on the impact of removing the load on the change in the chloride migration coefficient had found that concretes subjected to 75 % stress level of ultimate concrete strength recovered by half of the increased chloride migration coefficient when the load is released.

The plotted chloride profiles in current study clearly indicate that chloride penetration is time-dependent, and the chloride transport rate is considerably modified if the concrete is subjected to different load levels. The effects of different loads applied are more pronounced in the week 36 which indicates a larger gap between ingress profiles at 60% of stress level and the control specimen, indicating severe cracks propagation and connectivity over time.

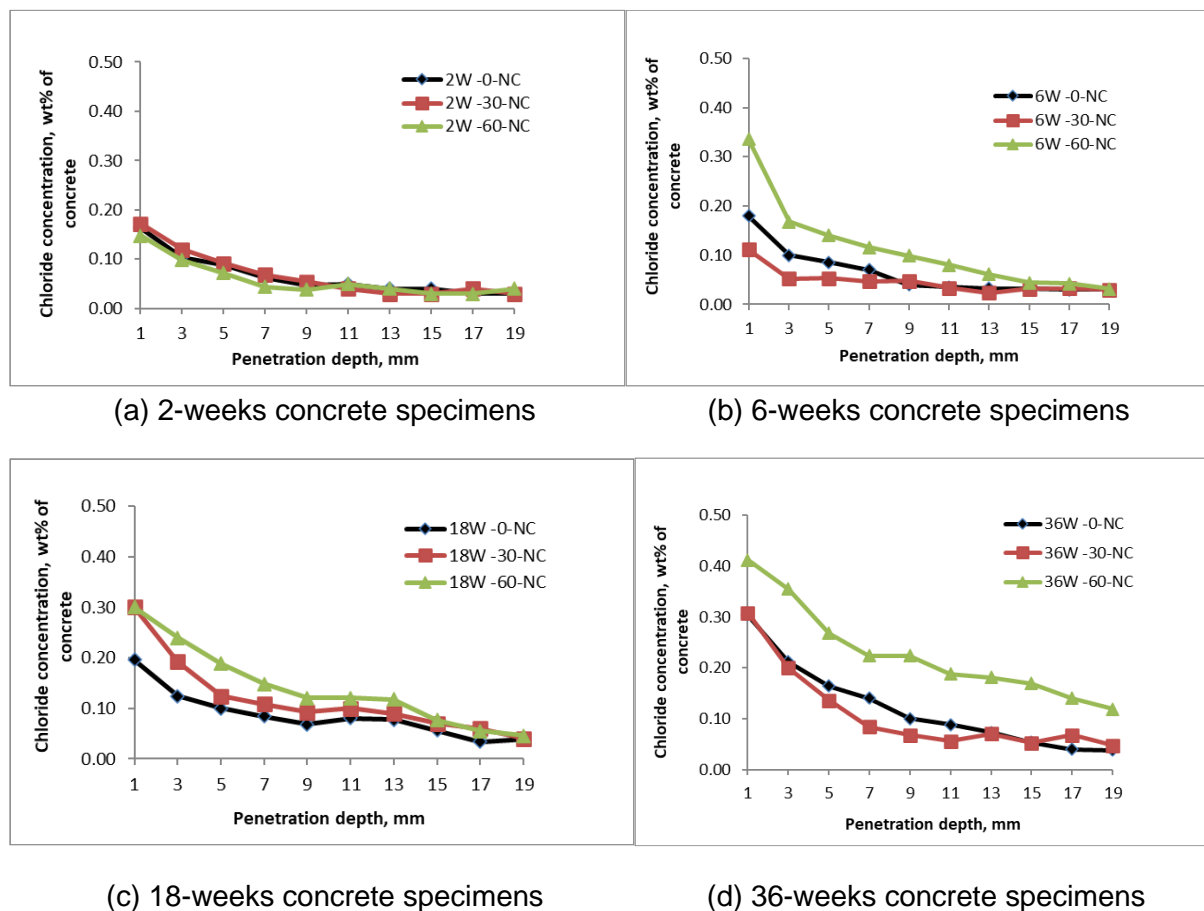


Figure 4.9 Chloride profiles determined of normal-strength concrete (-NC) in contact with chloride solution of specimen without load (-0-NC), of compressively loaded specimen at a level of about 30% (-30-NC) and 60% (-60-NC) of ultimate load.

Diffusion coefficients of chloride ions

Chloride diffusion coefficient, D_a in unit of mm^2/s can be obtained by fitting the chloride profiles using Fick's second law model proposed in Chapter 2. As well-known, chloride transport into concrete is a complex process which involves superposition of different transport modes [56]. The value of D_a determined from the best fit (represented by Equation (2.3)) of the measured

chloride profile is therefore a rough estimation to get the order of magnitude of the penetration depth. Using Matlab curve fitting toolbox, fitting analysis was performed. All fitting parameters of D_a , C_s and R^2 are listed in Table 4.3. The values obtained in Table 4.3 indicates that the distribution of total chloride content in all samples with different stress level are well fitted to the diffusion coefficient given in Equation (2.3) for normal strength concrete with the average coefficient determination (R^2) of above 0.95.

Table 4.3 Chloride diffusion coefficient

Specimens	C_s (wt%)	D_a ($10^{-6}mm^2/s$)	R^2
TUD-2W-0-NC	0.165	17.58	0.979
TUD-2W-30-NC	0.187	15.24	0.995
TUD-2W-60-NC	0.170	9.68	0.980
TUD-6W-0-NC	0.196	3.43	0.982
TUD-6W-30-NC	0.123	2.11	0.927
TUD-6W-60-NC	0.331	5.70	0.956
TUD-18W-0-NC	0.182	3.80	0.913
TUD-18W-30-NC	0.282	3.08	0.933
TUD-18W-60-NC	0.302	5.21	0.981
TUD-36W-0-NC	0.306	1.57	0.989
TUD-36W-30-NC	0.339	0.75	0.979
TUD-36W-60-NC	0.393	5.44	0.964

Theoretically, the diffusion coefficient decreases with age as shown in Figure 4.10, a behavior which is similarly observed in unloaded specimens. However, it appears that at 60% stress level the chloride diffusion coefficients drop remarkably less in the first 20 weeks diffusion time and all three specimen types exhibit almost negligible decrease after about 30 weeks. the decrease is Therefore, the influence of compressive stress on chloride diffusion should be further estimated. Additionally, it can also be observed that the chloride surface concentrations of concrete, C_s substantially increase with time and elevated compressive stress level.

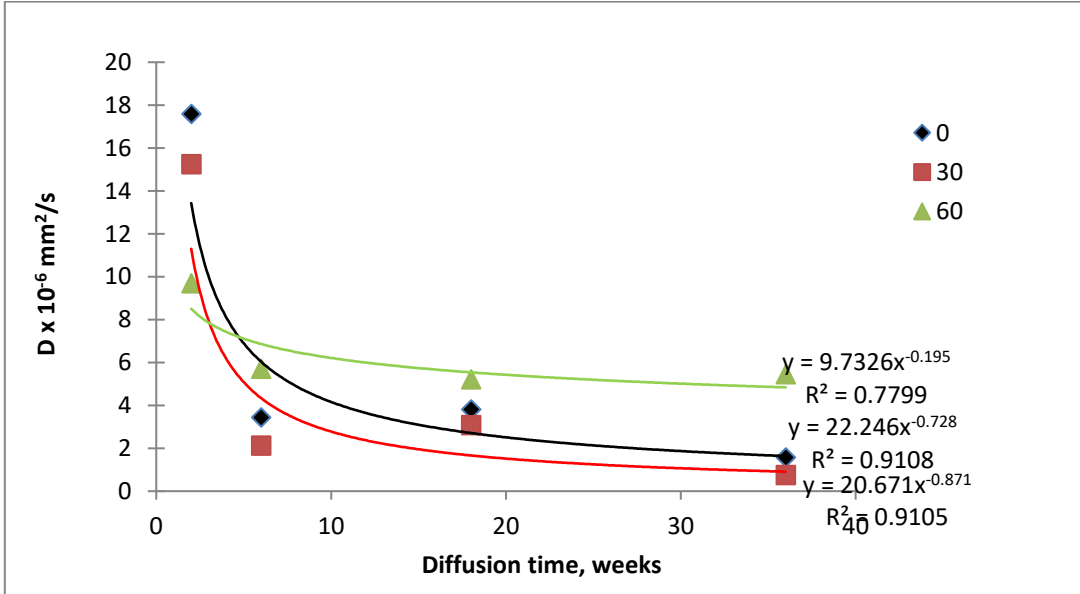


Figure 4.10 Chloride diffusion coefficient as calculated in concrete specimens with 30% and 60% of ultimate stress and stress-free specimens in time

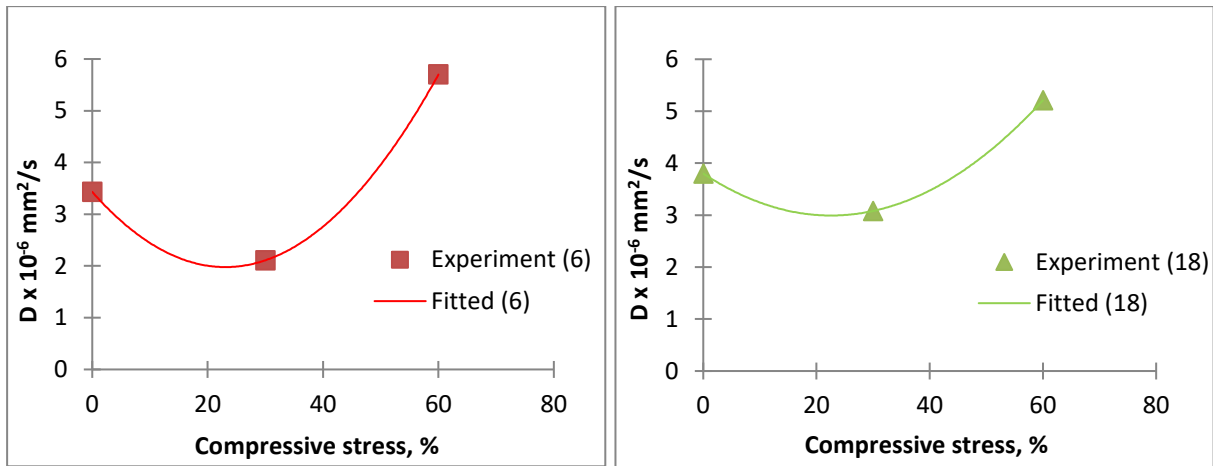
Wittmann et al. [56] evaluated the effect of an applied compressive load on chloride ingress in prismatic concrete and proposed an analytical model of effective diffusion. The relationship between stress level and chloride diffusion coefficient can be described with a polynomial function of stress effect as given in Equation (4.1)

$$D_{\sigma} = D_0 \cdot f(\sigma_c) \quad (4.1)$$

D_{σ} in the Equation 4.1 is the stress dependent chloride diffusion coefficient and D_0 is the apparent diffusion determined on unloaded specimen. $f(\sigma_c)$ is the stress function of diffusion coefficient in compressively loaded concrete specimen and can be written by a quadratic polynomial:

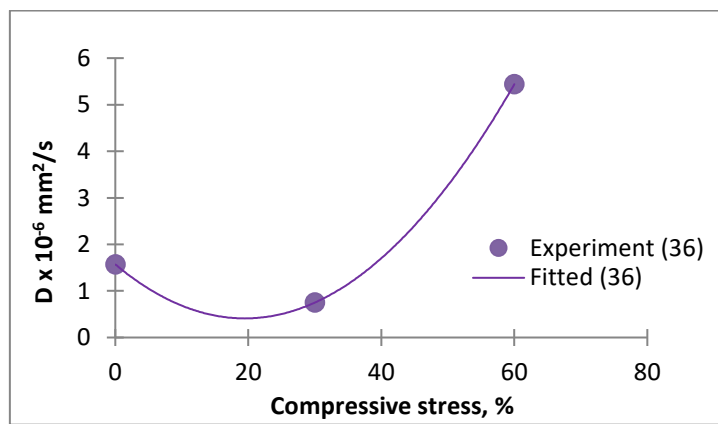
$$f(\sigma_c) = (1 + a\sigma + b\sigma^2) \quad (4.2)$$

The fitted polynomial of Equation (4.1) with chloride diffusion coefficient given in Table 4.3 is shown in Figure 4.11. The variables a and b obtained from the fitted polynomial change accordingly with the different test duration and the results are compiled in Table 4.4. Based on the results obtained on concrete specimens without load, the diffusion coefficient of concrete structures subjected to compressive load can be predicted using Equation 4.1. However, it was observed that the variables a and b change considerably at different test duration. Therefore, the calculations of chloride diffusion coefficient of concrete structures subjected to compressive load are also very much time dependent.



(a) 6-weeks concrete specimens

(b) 18-weeks concrete specimens



(c) 36-weeks concrete specimens

Figure 4.11 Experimental data and fitted polynomial of chloride diffusion coefficient in concrete

Table 4.4 Variables values for stress function obtained from the fitted polynomial

Duration of test	a	b
6-weeks	- 0.0367	0.0008
18-weeks	- 0.0188	0.0004
36-weeks	- 0.0759	0.0020

4.6 Summary of LIBS and photometric determination

Results described in both LIBS and photometric determination method indicated that the chloride ingress into concrete is affected under different load stress applied. It was observed that the total chloride content measured using LIBS are slightly lower than using photometric determination. The reason can be due to the exclusion of coarse aggregates in LIBS measurement. However, it is important to note that the trend of chloride profiles plotted between LIBS and photometric determination is similar for 6 weeks and 18 weeks of exposure time. The changes of chloride profiles under the action of an applied load can be explained in a phenomenological way at least, by now.

LIBS was used in Section 4.4.1 to get two-dimensional element mapping with high resolution on the meso-scale. At the same time, LIBS results were also used to verify the chloride profiles obtained using photometric determination method as duplicate sample was not available in this study. Only two different exposure times were considered for LIBS analyses which are 6 weeks and 18 weeks. Two more exposure time of 2 weeks and 36 weeks were added in photometric determination to get significant relationship in chloride diffusion graph.

4.7 Conclusions

The properties of concrete are influenced by its stiffness degradation at microstructure and macrostructure level, which can be characterized by the amount and the distribution of the internal pores and cracks. Chloride profiles obtained from different analysis methods show a similar tendency of total chloride ion increase at a stress level of approximate 60% of the ultimate strength. This indicates that the chloride permeability has a close relationship with the compressive stress, but this is influenced to a large extent by the stress level.

From these findings, different phases of damage induced by load can be distinguished. Initially, the penetrating chlorides into concrete may decrease during the elastic phase of the compressive loading as the porous concrete structure becomes denser. Then, micro-cracks appear with the propagation of existing cracks, resulting in a slight increase of chloride penetration at a certain threshold stress level. A significant increase of total chloride concentration and deeper penetration depth after 36-weeks of combined loads exposure is observed with the same threshold stress level value. A main contribution to this effect is the onset of macro-cracks formation by the destruction of the composite structure under sustained high compressive load. This situation is what is mostly experienced in practice. Additionally, the total chloride content gradually decreases with the increase of depth, but the decline of chloride content becomes slows at stress level of 60%. A sudden increase of chloride ingress can be expected beyond of this threshold value.

Based on the equivalent diffusion model proposed in Chapter 2, Equation (2.3), the apparent chloride diffusion coefficients for unloaded and concrete specimens loaded in compression were calculated. The profiles of total chloride ion at various test durations are in close agreement with the distribution curve of Fick's second law. In addition to that, it can be found from the fitting precision that the diffusion model is suitable for analyzing the chloride penetration at various stress level. The polynomial function of stress dependent chloride diffusion coefficient was proposed by fitting the Equation (4.1) with chloride diffusion coefficient given in Table 4.3. From the results obtained on concrete specimens without load, the diffusion coefficient of concrete structures subjected to various compressive load levels can be estimated considering the effect of exposure duration.

In the subsequent chapter, it can be hypothesized that bacteria-based healing agent is capable to regain the chloride resistance of concrete and increase the structure service life lost by load-induced cracking due to metabolically calcium carbonate precipitate occurrence.

5.

Strength development of concrete containing bacteria-based self-healing agent

A new idea is first condemned as ridiculous, and then dismissed as trivial, until finally it becomes what everybody knows.

-William James-

Chapter 5 describes how self-healing materials have been applied to cement-based systems in the past decades. It was concluded that further investigation is essential particularly in characterizing the material before applying this material in practice. The present chapter provides the strength development of concrete and mortar containing a bacteria-based self-healing agent.

The composition of the bacteria-based self-healing particles used in this study is described in Section 5.2. The influence of the healing agent on fresh concrete and mortar mix properties is experimentally investigated in Section 5.3 and 5.4 respectively. The summary and conclusion of the strength development of both bacteria-based self-healing concrete and mortar are given in Section 5.5. It was found that the optimum amount of healing agent added to mortar- or concrete mix is close to 3% by weight relative to the cement content, as 2.9% resulted in an increase in strength of 28 days cured mortar specimen while 4% resulted in a decrease of compressive strength in concrete specimens.

5.1 Introduction and research significance

Conventional concrete has a flaw as it forms cracks upon external loading, volume changes due to shrinkage, creep, thermal, chemical effects or splitting along reinforcement due to bond and anchorage failure. Cracks may cause detrimental effects, especially on structures exposed to general outdoors or aqueous media conditions. Owners of infrastructures and buildings subjected to various ways of deterioration may therefore be confronted with significant maintenance and repair costs. Furthermore, the damaging environment may also compromise the intended construction service life. Therefore, innovative cement-based materials which can improve certain material properties may result in resilient constructions with longer service life.

More and more research efforts are devoted in developing new materials for construction applications. In fact, some of these new materials have already been employed in practise. In most cases, they were applied in order to improve mechanical properties or durability of the final concrete product. With respect to durability improvement, self-healing materials target sealing of occurring cracks via deposition of crack-filling material. Thus, self-healing treatment promotes a sustainable repair methodology resulting in an increase in lifespan of concrete structures [20].

The bacteria-based self-healing agent is a healing material in which bacteria mediate the precipitation of calcium carbonate. Similar to another type of healing agent, this complex bio-healing agent must also meet several requirements in order to function optimally. This signifies that the bio-healing agent must be concrete compatible, i.e. not negatively affect concrete properties. The next criteria is that the bio-healing agent should remain potentially active in the long-term and preferably work as a catalyst to enable multiple healing events in the concrete system [17]. Due to that, several size, shape and composition, optimization of the healing agent has been investigated for its pragmatic application. It was found that healing agent modified mortar exhibited positive contribution to self-healing through precipitation of calcium-based minerals resulting in sealing of up to 0.6 mm wide cracks [18, 80, 136]. Previous studies have shown that healing agents are also able to increase compressive strength with respect to control specimens [24, 75, 76, 137].

10 years of research on alkali-resistant spore-forming bacteria has led to the development of a two-component particle consisting of bacteria and nutrients which can be produced on industrial scale at economical competitive costs. In this study, these newly developed bacteria-based particles were investigated for effect on compressive strength development of concrete and mortar specimens.

5.2 Bacteria-based self-healing concrete

Table 5.1 summarizes the weight composition of the concrete mix with the bacteria-based additive. Similar concrete mix composition was used to cast control specimen without healing agent addition. The bio-healing particle was prepared using powder compression technology. The dried bacterial spores and nutrients (both in freely flowing powder form) were mixed with 1% (weight) binder (stearic acid). This powder mixture was compressed by roller compaction and the resulting sheets were subsequently ground to coarse 1–4 mm flake sized granules. This form of compressed powder flake-shaped healing agent is hard and consists of almost fully (95 – 99%) functional healing agent components. Therefore, the applied volume of healing agent can be limited to only 1% of concrete volume or 4% of cement weight [136].

Table 5.1 Concrete mix composition required per one concrete cube with dimensions of 150 mm x 150 mm x 150 mm

Compound	Weight (g)
Cement (CEM I, 42.5)	1,304
Water	586
Aggregate Size Fraction (mm):	
0.125 – 0.25	149
0.25 – 0.5	521
0.5 – 1	744
1 – 2	744
2 – 4	819
4 – 8	1,274
8 – 16	2,367
Super-plasticizer	9
Healing agent	53

The distribution of bacteria-based self-healing particles in the concrete mix can be improved by grinding and sieving it to a smaller size. The healing particles size used for the study was confined from 2 to 4 mm as presented in Figure 5.1. The concentration of healing agent used was restricted to 15 kg per cubic meter of concrete or 4% by weight of cement. This quantity is based on the optimal amount of the healing agent without significantly affecting strength properties of the cement-based material as was reported in previous studies [83, 138].

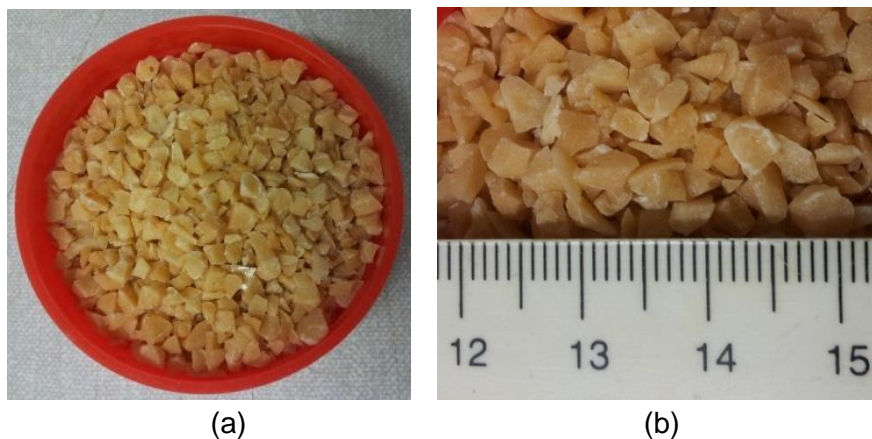


Figure 5.1(a) Flake-like shaped healing agent particles (b) 2-4 mm sized as used in concrete specimens

In order to ensure that the healing particles were thoroughly mixed and uniformly dispersed in the concrete, a standard mixing procedure with relevant mixing time was proposed. In the first phase, fine aggregates were mixed dry with the healing agent for two minutes. Subsequently, cement was added and mixed for another three minutes followed by addition of water and superplasticizer. Then, the mixture was put at rest for half a minute. Finally, the coarse aggregate was added and mixing continued to a total time of ten minutes. The summary of mixing sequence is listed in Table 5.2.

Fresh concrete mix with incorporated bacteria-based healing agent was cast in standard cubes of 150 mm x 150 mm x 150 mm. Control specimens without healing agent were also prepared in a similar method, and compressive strength of specimens was determined after 1, 3, 7, 14 and 28 days of curing. In addition to that, a slump test was

performed on the fresh concrete mix for determination of material workability and mix uniformity estimation.

Table 5.2 Summary of mixing procedure

Mixing procedure	Time (min.)
1.Dry mix fine aggregates + healing agent	2.0
2.Add cement	3.0
3.Add water + superplasticizer	1.5
4.Rest	0.5
5.Add coarse	3.0
Total time	10.0

5.2.1 Slump test

A Cretoplast SL01 type of superplasticizer from CUGLA, Breda, the Netherlands with prescribed dosage was applied into the concrete mix to provide high workability. A slump test was performed using a cone mould of 300 mm high with a small opening at the top. The cone was placed on a smooth surface before filling with fresh concrete in three layers (with 25 times of stamping with a steel rod in between each layer) immediately after discharging the concrete from the mixer. Subsequently, the cone was slowly lifted vertically to let the concrete slump naturally.

As shown in Figure 5.2, slump values of both bacterial concrete and control concrete were measured. The slump values given by the control and bacterial concretes were 150 mm and 175 mm, respectively. Higher slump indicates higher initial workability. The presence of healing agent in the mixtures is also expected not to negatively affect the potential degree of concrete packing as only a marginal decrease in bulk density of 2258 kg/m³ for bacterial concrete in comparison to 2269 kg/m³ for the control concrete batch was measured.



Figure 5.2 Slump test of (a) normal strength concrete and (b) bacterial concrete

5.2.2 Setting time of concrete

Freshly mixed concrete hardens with time. The current experimental work quantified mixture setting times and it revealed that that healing agent-containing concrete set slower in comparison to the control concrete. For this reason, healing agent-containing concrete needs

two or three days before it can be demoulded instead of 24 hours for control concrete. In addition to that, the effect is dependent on dosage of healing agent in which the higher the dosage the stronger the effect and also on type of cement used i.e., the lower the clinker content in the cement the higher the effect.

5.2.3 Strength development

As aforementioned, to comply with one of the ideal self-healing material characteristics, the presence of the bacteria-based healing agent should not have a significant negative impact on the overall performance of the system. Hence, the effect of addition of mineral-producing bacteria together with nutrients, in form of a granular healing agent, on the compressive strength of concrete was investigated. Figure 5.3 shows the 1, 3, 7, 14- and 28-days compressive strength of concrete cubes with and without healing agent. The compressive strength of healing agent-containing specimens was always lower than that of control specimens. The relative difference in strength decreased gradually with increasing setting time but ended with a slight spike on the 28 days cured specimen.

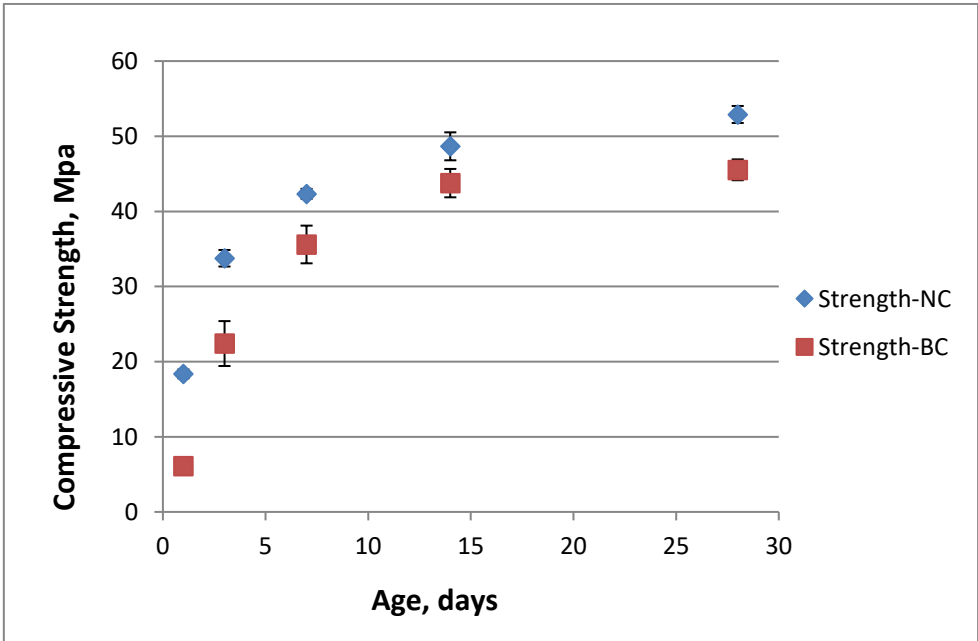


Figure 5.3 Compressive strength of reference concrete (NC) and healing agent-containing concrete (BC) specimens

The decrease in compressive strength is probably due to the organic nature of the healing agent. During the mixing period some calcium lactate is likely released from the healing agent particles which may interfere with the cement hydration process and result in delayed strength development. This effect is probably concentration dependent, similar to what has been reported for glucose [2]. In order to improve the performance of healing agent addition in terms of compressive strength development, further research on relation between healing agent concentration and development of compressive strength is required. In this study, initial compressive strength of prism specimens at 28-days were taken as reference for the calculation of 30 % and 60 % of load stress applied on specimen [124].

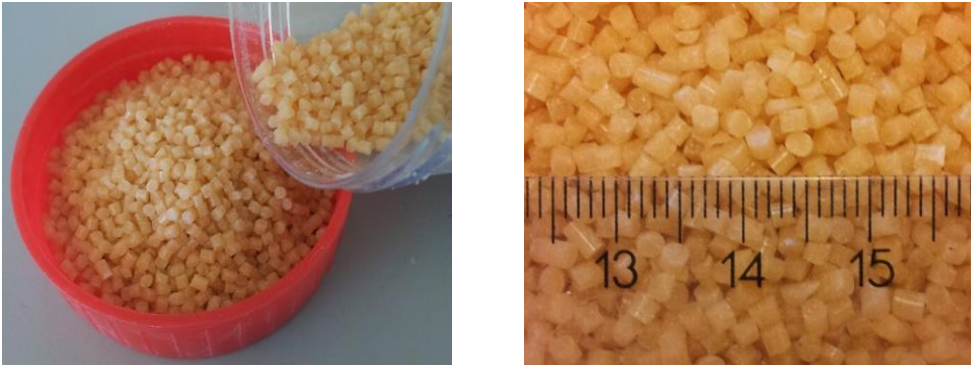
5.3 Mortar containing bacteria-based healing agent

The effect of healing agent addition on strength development was further investigated for a mortar mixture. Standard mortar prisms of dimensions 40 mm x 40 mm x 160 mm were made from ordinary Portland cement (CEM I 42.5), CEN Standard Sand and 0.5 water to cement ratio in accordance with EN196-1:2005 without any further additions (control specimens) and with bacteria-based healing particles. Table 5.3 summarizes the composition of each batch required for production of three replicate test specimens. In contrast to the concrete specimen, the concentration of the healing agent to cement ratio was lower (2.9% instead of 4%) although an equal quantity of 15 kg healing agent per cubic meter of mortar was applied, in what is attributed to the relatively higher cement content of the mortar mix in comparison to the concrete mix.

Table 5.3 Composition of mortar mix required for three test specimens

Compound	Weight (g)
Cement (CEM I, 42.5)	450
CEN Standard Sand	1350
Water	225
Healing agent	13

Three mortar prisms were tested for flexural strength and six mortar cubes of dimensions 40 mm x 40 mm x 40 mm obtained from the same samples of the flexural test were tested for compressive strength after 1, 3-, 7-, 14- and 28-days curing. As in the previous concrete experiment, the mortar prisms were left for 72 hours curing at room temperature before being un moulded. Thereafter, all samples were further cured in a fog room at 99% ± 1% relative humidity. In healing agent-containing mortar samples, more uniform sized healing agent particles were used in comparison to the concrete experiment (see and compare Figures 5.1 and 5.4). The surface to volume ratio of these cylindrical particles was smaller than that of the flake-shaped particles used in the concrete mix.



(a)

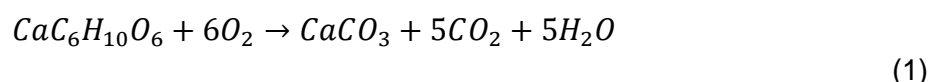
(b)

Figure 5.4 (a) Cylinder-shaped particles with (b) uniform size added to the mortar mix

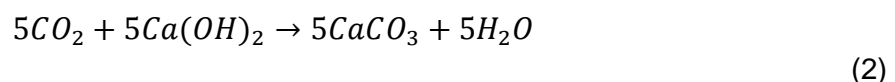
5.4 Bacteria-based self-healing agent constituents

A bio-based healing agent was applied in concrete to increase the durability and make the material more sustainable. In 2006, Jonkers [17] developed a biologically induced cement-based material in which bacteria form minerals which contribute to sealing of cracks and fractures in concrete. In this healing system, alkaliphilic spore-forming bacteria of the genus *Bacillus* were used as spores which can survive the initially extreme alkaline environment of concrete. The bacteria were obtained from the German Collection of Microorganisms and Cell Cultures (DSMZ), Braunschweig, Germany and cultivated spores were mixed with calcium lactate, acting as mineral precursor compound, and other growth requiring nutrients before incorporated into the concrete mixture [20, 139]. However, it appeared that when directly (unprotected) added to the concrete mix, the mineral-producing activity of the bacteria was limited to 2 to 4 months. Therefore, in subsequent studies, the bacterial spores were protected by encapsulation using a binder (stearic acid). The mechanism of bacterially induced self-healing is based on the metabolic conversion by activated spores of dissolved precursor compounds to filler minerals such as calcium carbonate in an alkaline environment. The filler minerals are relatively dense and can block cracks thus waterproofing the material. The bacteria thus act as a catalyst and mediate the precipitation of minerals potentially endlessly as long as nutrients are available as the bacteria are not converted in the process themselves [18]. It was also reported that a healing event not only revives bacterial spores but also potentially results in the production of fresh spores that resets the viability status [16, 18].

This two-compound healing agent, acting as a healing particle, was embedded in the concrete or mortar and thus became an integral part of the material. The calcium lactate functions as energy and carbon sources for the bacteria to grow. In some cases it was observed that the added calcium lactate not only acts as precursor compound for crack sealing minerals but also enhances concrete compressive strength [139]. The encapsulation by binder and nutrients is important to increase the potential for long-term viability of bacterial spores. This can be proven by measuring oxygen consumption due to bacterial activity in concrete specimens up to several months after concrete casting [14]. In general, the bio-conversion of calcium-lactate results in direct calcium carbonate (CaCO_3) formation according to the following reaction:



The metabolically produced CO_2 can subsequently chemically react with calcium hydroxide present in the paste matrix leading to additional or indirect CaCO_3 precipitation, according to:



These bacteria work optimally in a pH range of 8 to 11.5 and in a temperature range of 15 – 40 °C. If untouched, the bacterial spores in the healing agent can potentially stay inactive in the concrete for decades [140]. On the other hand, under suitable environmental conditions with appropriate food source available and sufficient water, the bacteria can grow exponentially and heal the cracks. Therefore, when water begins to seep into the cracks it activates the spores of the bacteria which subsequently germinate into active (vegetative) cells which metabolically convert the calcium lactate. This process consumes oxygen and results in the formation of limestone that solidifies and seals pores and cracks. The removal of oxygen is also expected to reduce the tendency of the steel reinforcement corrosion as reduced supply of oxygen usually lowers the corrosion rate of steel by oxygen oxidation. In the case of chloride

containing environment, the negatively charged chloride ions can penetrate the passive oxide layer of steel and exposed the steel surface to the environment. However, with the absent or low concentration of oxygen, the corrosion reaction will cease or proceed very slowly. The corrosion rate is limited by the rate of diffusion of dissolved oxygen. The risk for corrosion in highly concentrated chloride environment is dependent on the dissolved oxygen level, temperature and chloride content. Therefore, it can be assumed that the rate of corrosion will also decrease once the bacteria is activated in the case of chlorides entering the crack before it is healed. In addition to that, it would be expected that the bacteria will seal the crack and reduce the diffusion and stop the external chlorides penetrating concrete. Detailed information on the microbial healing concept is discussed in [136].

5.4.1 Influence of bacteria-based self-healing agent on properties of fresh mortar mix

After casting, the time taken for the healing agent-containing mortar to harden sufficiently was longer than in normal mortar. This can be observed when mortar cubes with healing agent not fully attained the shape of the mould in which it is cast after 24 h. It was only possible to attain the exact shape of the mould after 72 h. By observation, the final setting time of healing agent-containing mortar was somewhat delayed in comparison to a standard mortar without healing agent. This remark is confirmed when the addition of the bacteria-based healing agent resulted in strong decrease of early strength in this current study and also in a study reported by Mors and Jonkers [141].

5.4.2 Hydration and strength development

Aim of the second part of this study was to compare the effect of healing agent addition on strength development between concrete and mortar specimens. Figure 5.5 shows compressive strength development of the mortar cubes with and without healing agent. The incorporation of healing agent in mortar specimens resulted in a different development of compressive strength in comparison to concrete specimens. For concrete, strength of healing agent-amended specimens was always lower than in reference specimens (up to 28 days curing). However, for mortar, while the strengths of healing agent-amended specimens were lower in 1, 3, 7 and 14 days cured specimens, they were respectively equal and 7% higher in 21 and 28 days cured specimens. Apparently compressive strength of healing agent amended specimens overtakes that of reference specimens at later age.

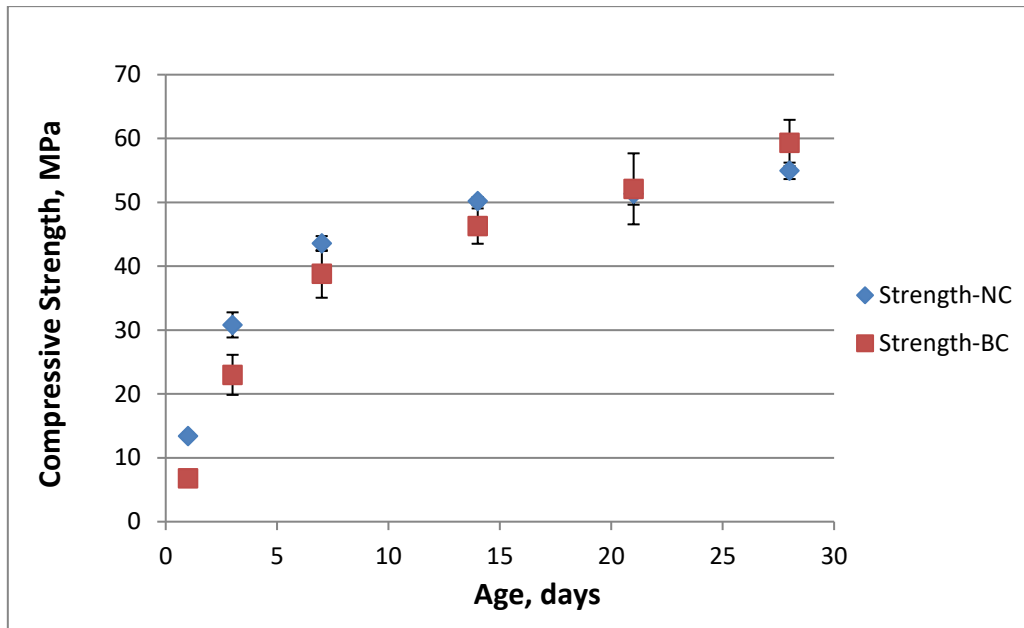


Figure 5.5 Compressive strength of mortar without (control; NC) and with bacterial healing agent addition (BC)

The development in strength of mortar samples amended with healing agent can possibly be explained by the lower healing agent to cement ratio (2.9% healing agent concentration) and additionally by the lower surface to volume ratio of the cylindrical healing agent applied to the mortar mix. Both effects apparently result in less amount of organic compound (calcium lactate) release from the healing agent particles during the mixing process, and therefore lead to reduced negative effect on compressive strength development. Also in another study an actual increase in compressive strength of older (28 days cured) specimens was found for an healing agent to cement weight ratio of around 3% [142]. In addition to that, a smaller size of healing particles may contribute to a more even dispersion of particles in the cement matrix which is attributed to crack-healing efficiency improvement of specimens. Latter potentially positive effect must however be further investigated in follow-up studies.

5.5 Conclusions

The compressive strength development of concrete and mortar specimens with incorporated bacteria-based healing agent was characterized in this study. Based on the results presented in this chapter, it is concluded that the proportion of healing agent concentration to cement content of the mix influences the strength development of specimens. The lower amount of healing agent (2.9% to cement weight in mortar mix) results in higher compressive strength of specimens at later age (28 days curing) in comparison to reference specimens, while higher amount of healing agent (4% to cement weight in concrete mix) results in lower strength at all ages (up to measured 28 days cured specimens) in comparison to reference specimens. The optimum amount of healing agent to be added to specimens appears therefore close to 3% of the applied cement weight. Further investigation is necessary to establish the crack-healing efficiency of healing agent-amended specimens which will be addressed in subsequent chapters.

6 .

Chloride transport under compressive load in bacteria-based self-healing concrete

“A crude model based on some engineering evaluation is better than no model, and certainly better than pure guesswork.”

-Steen Rostam-

In chapter 5, the compatibility of bacteria-based healing agent to mortar and concrete mixes with respect to strength development was given. To clarify the potential applicability and benefit of this self-healing agent, the influence of bacteria-based self-healing agent addition on concrete durability must also be investigated. This chapter repeats the experimental work done in Chapter 4, chloride resistance of concrete under compressive load, but now with incorporation of the bacteria-based healing agent added to the concrete mix. Aim therefore was to determine and compare the chloride diffusion coefficient of self-healing bacteria-based concrete with reference samples, both submitted to various compressive load stress levels. Materials preparation (Chapter 6.2) and methods applied (6.3) in this research are presented with marginal modification and extension of the methods used in the study described in chapter 4. Furthermore, chloride transport analysis and morphology of bacterially produced mineral precipitates as investigated by environmental scanning electron microscopy (ESEM) are presented in section 6.4. Evidence of microbial activity in healing agent-containing specimen is provided in section 6.5 through application of oxygen consumption assays. Finally, chloride ingress analyses results obtained in this chapter are compared with those obtained in Chapter 4. From the results obtained in this study it was concluded that although evidence for bacteria-mediated self-healing was found, it was insufficient to significantly decrease chloride ingress in damage-induced specimen (due to continuous compressive loading at 60% of ultimate load capacity) simultaneously subjected to chloride exposure. Further studies should clarify whether bacteria-mediated self-healing of occurring damage before exposure to chloride could help to improve the durability of chloride exposed concretes.

6.1 Introduction

Very often rapid deterioration of concrete structures already occurs after a period of ten to fifteen years, much shorter than their intended service life. It was estimated that one third of the annual budget for asset managing of large civil engineering works in the Netherlands is spent on inspection, monitoring, maintenance, upgrading and repair. This amount of money spent each year on maintenance and repairs shows a demand for quality improvement and increased durability of concrete structures, probably in most of the countries in the world. As discussed earlier, building high quality durable and at the same time sustainable structures requires the use of minimal number of finite materials at lower energy consumption rates. However, it remains a challenging task to design for a long-term service life because of the sometimes unexpected service conditions and microclimatic interactions the concrete is subjected to as outdoors conditions vary considerably from those in the climate-controlled lab environment.

Self-healing concrete appears a promising solution for increasing concrete durability by reducing the ingress rate of aggressive compounds in voids and cracks [143]. Healing will reduce compound ingress in static cracks by bridging the cracks or blocking the pores expectedly resulting in delay of e.g., chloride ingress. However, healing is limited under dynamic loading due to changes in geometry and increased solution flow. Thus, dynamic loading will reduce the scale of self-healing on the crack surfaces. This is in line with the observation by Küter et al. (2005) about a significant increase in ingress towards the crack tip of chloride profiles after 40 days exposure period, under dynamic loading, in comparison to data from the literature covering ingress in static cracks [23]. In several studies self-healing of pre-defined cracks have shown proof-of principle of the technology, however, the possibility for self-healing to occur under load-induced crack formation has not been investigated yet.

The reality of crack occurrence in concrete is undeniably. Most research studies conducted focused on change of materials properties over time due to cement hydration processes, yet not taking the occurrence of crack formation and their propagation under service loads into consideration. Effect of chloride ingress through cracks is as yet hardly considered, possibly due to the difficulty to obtain accurate measurements. The effect of chloride ingress could be even worse if cracks are continuously connected to each other as this phenomenon can greatly negatively affect the structural durability and integrity. As cracks generated by mechanical loading can serve as additional pathway for deteriorating compounds into concrete, occurrence of crack self-healing could be the mechanism to counteract this effect.

In recent years, several research studies attempts were made to incorporate a specific mechanism in concrete to enhance its self-healing properties particularly for application in aggressive environments. The effects of various parameters on the self-healing process including load-induced cracks and chloride concentration have been discussed. In one of those studies a positive contribution of fibres as healing agent to the durability of concrete was proven, as fibre reinforced concrete demonstrated a greater self-healing capacity with a reduction in water penetration of 70% in comparison to 50% for non-fibre containing concrete under static tensile loading [38]. In another study on fibre reinforced concrete a lower permeability level in comparison to plain concrete was also observed when both types of specimens were subjected to compressive stress [106, 144, 145]. In another study a water repellent agent was applied for the purpose to protect reinforced concrete in environments containing chloride. The results indicated that positive reduction of chloride penetration appeared in surface-impregnated concrete in comparison to untreated concrete submitted to more than half of ultimate compressive load. Although water repellent treatment did not

completely prevent chloride penetration, the ingress appeared significantly reduced [146, 147]. Sisomphon et al. [148] studied the self-healing potential of fibre-reinforced strain hardening cementitious composite (SHCC) and found improvement in water tightness with slight recovery of mechanical properties of the samples tested.

This chapter focuses on the effect of self-healing, due to addition of a bacteria-based self-healing agent, on chloride ingress of concrete subjected to compressive stress in a chloride environment. Based on laboratory quantification [136], self-healing functionality of samples with incorporated bacteria-based healing agent in which bacteria mediate the production of crack-filling material was found to be superior over control specimens. Healing improved the liquid-tightness of cracked concrete. As full impermeability of cracked concrete through bacterial self-healing appears unlikely, a substantial delay in chloride ingress can be expected. The healing agent particles which comprise specialized alkaliphilic bacteria and suitable growth substrates can survive incorporation in the concrete matrix and can be activated by ingress water, probably also containing chloride. Challenge of this study is to achieve bacteria-based self-healing under load-induced cracking in a chloride environment what can influence the bacteria metabolism and activation.

6.2 Experimental program and used methods

6.2.1 Bacterial specimen preparation

The self-healing concrete prisms with a size of 100 mm x 100 mm x 400 mm were prepared using similar methods and materials as given in Chapter 4 in Table 4.1. The type of bacterial healing agent described in Chapter 5 was added at a concentration of 15 kg/m³ in the current concrete mixture with the aim to enable self-healing of cracks generated by compressive loading. Precipitation of calcium carbonate within the crack on the surface of the crack walls is expected to delay the process of chloride transportation in cracked concrete, hence prolonging the service life of concrete structures.

6.2.2 Testing methods

The experimental program conducted on specimens under combined load and chloride exposure was following the procedure given in Section 3.6. The total number of bacterial prisms produced was 15 of which 12 were used for the chloride diffusivity test and 3 for ultimate compressive strength measurement. The average value of ultimate compressive strength obtained from three bacterial concrete prisms at 28 days was 22.85 MPa with a standard deviation of 1.32 and coefficient of variation of 5.8%. The compressive strength of the concrete is determined by tests on cubes after 28 days. However, the creep tests are performed on prisms. Prisms have a much lower failure load than the compressive strength when loaded in compression. The reason for this is the triaxial state of stress that is created at the two ends of the specimen as depicted in Figure 6.1 [149, 150]. In a prism this zone is much smaller compared to a cube [132]. Therefore, the failure load of a prism is lower. In the creep and chloride ingress test the load level is taken as a percentage of the failure load of the prism. In addition to that, mentioned in Section 5.3.2, normally after 24 hours of casting, the surface of bacterial concrete tends to be roughed and soft when demoulding. This effect is more pronounced with the difference in dosage of healing agent used. In the case of mortar, the dosage used to cement content was higher compared to concrete specimen, thus, resulted in strong decrease of early strength as the higher the dosage the stronger the effect. Mortar mixes have lower clinker content in cement in which may also contribute to the higher effect on strength development at early phase. In comparison to concrete specimen, mortar

specimen used different batches of healing agent in which can potentially contribute to a delay in strength development at 28 days.

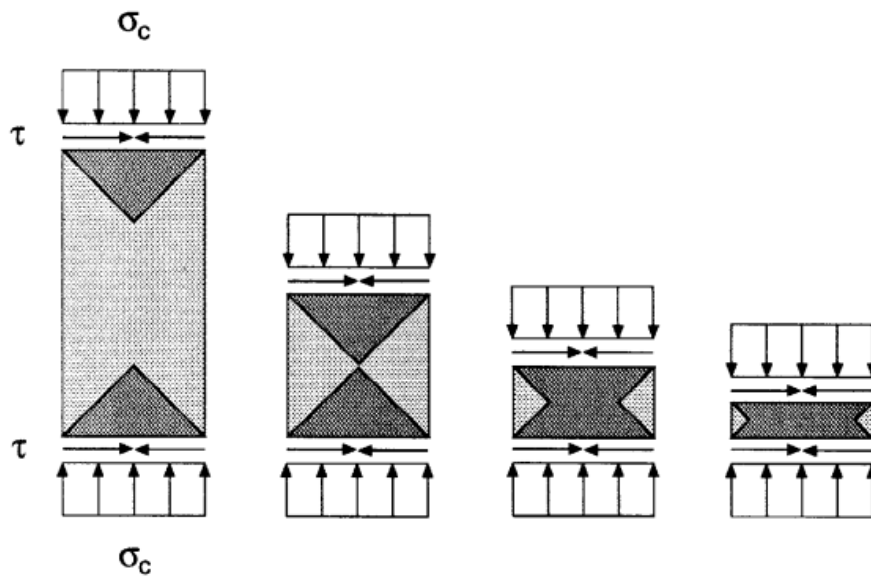


Figure 6.1 Triaxial state of stress due to frictional restraint for specimens of different slenderness [150]

The 12 remaining specimens were divided in four groups of three specimens of which one was subjected to 0%, one to 30% and one to 60% of peak compressive stress. The four groups of 3 specimens each were subsequently incubated under experimental conditions given in Section 3.7 (combined exposure to compressive loading and chloride) for 2, 6, 18 or 36 weeks respectively.

6.2.3 Chloride profiles determination

After the incubation period, chloride concentration profiles of specimens were measured by photometric determination. Here, dry drilling instead of grinding (as done with specimens in Section 4.4.2) was performed in defined steps using a rotary hammer and a diamond bit (see Figure 6.2b). The produced concrete dust was collected from the concrete surface after each drilling depth interval. This drilling procedure was chosen here as it is a less destructive sampling method and less time consuming when a large number of specimens have to be sampled. This sampling process allows a spatial resolution on a millimetre scale (2-mm depth intervals) what was considered sufficient for this study. Nine holes were drilled in each specimen at random locations at the chloride exposed surface by means of a 10-mm diameter drill as shown in Figure 6.2. The sample depth of each drilled hole was adjusted according to the expected chloride profile for each of the different specimens series. A minimum of 8 depth layers were sampled until the depth at which the chloride concentration reached a constant value, i.e. equal to the initial chloride content before external chloride exposure. The sampling was performed over a surface area of at least 2500 mm² and with a distance of 10 mm from the border of the exposure zone to avoid the influence of edge effects and disturbances from the coating [129]. The powder samples of distinct depth zones of replicate drills were combined in order to get a minimum sample weight of 5 g of concrete dust required for chloride content determination. Prior to that, the initial (background) chloride content of each concrete specimen was measured in an area that was not exposed to chloride solution. The obtained chloride

penetration profiles were used to compute the chloride diffusion coefficient by fitting the chloride profile using Fick's second law model.



Figure 6.2 (a) An example of drilled holes for determination of chloride concentration profiles at the exposed zone of specimens; (b) drill bit

The risk of erroneously pooling concrete dust samples from different depth layers was considered low as the drilling machine was mechanically secured at a fixed position from the specimen surface [129]. The depth position of the drill head was also measured using a slide gauge with an accuracy of 0.1 mm while the sample depth of distinct layers was 2.0 mm. Risk of contamination of dust samples with material from other layers was further limited as the drill hole and drill bit were cleaned between each step interval by use of a compressed air blower.

6.2.4 Determination of the concrete self-healing process

Mineral precipitation observations

Microanalysis and electron imaging were done by means of Environmental Scanning Electron Microscopy (ESEM, Philips XL30 series) and Energy Dispersive Spectroscopy (EDS). Prior to analysis, the ESEM samples were impregnated using low viscosity epoxy under vacuum for filling of remaining cracks and pores and to maintain specimen integrity. Subsequently, the specimens with dimensions of 25 mm x 40 mm x 6 mm were polished with grinding paper increasing in range from 120 to 12000 grain size using 100% Ethanol on a rotating disk plate until the surface shined like glass. The specimens were examined under ESEM to observe possible calcium carbonate precipitation on crack surfaces. Minerals formed at crack surfaces were observed by ESEM to search for bacterial imprints what provides evidence that their formation was mediated by bacteria.

Oxygen consumption measurements

Metabolic aerobic conversion of calcium lactate (one of the main ingredients of the healing agent) by bacteria requires oxygen [14]. Therefore, optical oxygen microsensors (micro-optodes) were applied to quantify oxygen consumption of samples containing bacteria-based healing agent and reference specimens without bacteria. Needle-type oxygen microsensors is ideal type for oxygen distribution profiling with a high spatial resolution (50 μ m). A stainless-steel needle is used to protect the fibre tip with its oxygen-sensitive coating of an optical fibre (Figure 6.3).

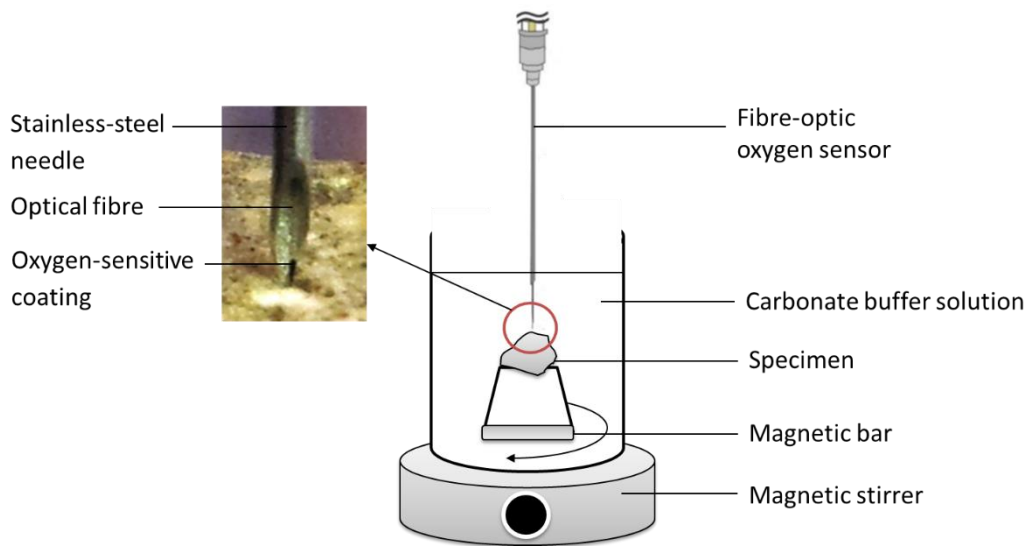


Figure 6.3 Oxygen consumption measurement system

36-weeks incubated specimens, that had been exposed to combined compressive loading and chloride, were sampled just before the test. The O_2 consumption monitoring was performed on the fresh fractured surface of these samples which were submerged in a solution of pH 10 (carbonate buffer) at room temperature. The oxygen concentration in each of the sample was measured by inserting an oxygen microsensor (Fibre optic oxygen sensor, Presens – Precision Sensing GmbH). The oxygen-sensitive tip has to be extended out of the steel needle during the measurement. Oxygen micro-profiles were obtained in vertical steps of $50\ \mu\text{m}$, from 5 mm above towards the surface of the specimen. The arrangement of an oxygen consumption rate measurement is given Figure 6.4.

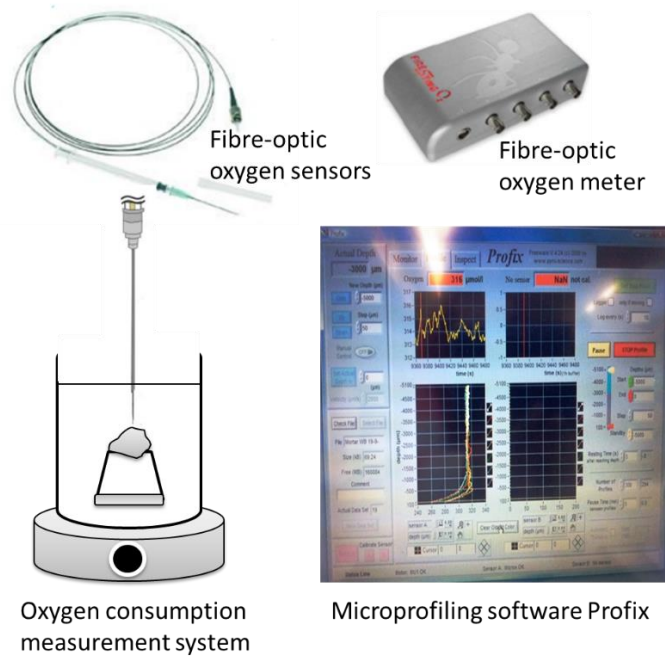


Figure 6.4 Experimental setup used for the measurement of oxygen consumption rate

6.3 Results and data collections

6.3.1 Chloride ingress in bacteria-based healing agent containing specimens

Chloride profiles for loaded and unloaded specimens after 2-, 6-, 18- and 36-weeks incubation periods are given in Figures 6.5 (a) to (d). After a 2-weeks incubation period it appears that chloride ingress in the specimen loaded at 30% of ultimate load was marginally higher than for the unloaded- and 60% loaded specimens. After 6 weeks incubation all three specimen types showed substantial increase in chloride concentration in the top 5mm layer with a specific high peak in chloride concentration in the 30% loaded specimen. Further exposure to chloride solution and compressive loading of up to 18 weeks resulted in a substantial increase of chloride concentration for all specimens from 3-mm depth down, without significant difference between loaded and unloaded specimens. The high peak of chloride concentration observed in the surface 0-3 mm layer of the 6 weeks incubated and 30% loaded specimen was much less pronounced in the 18 weeks incubated specimen and was similar to the non-loaded specimen. Particularly in the deeper layers, the 9-15 mm depth zone, it appeared that the chloride concentration of the 30% loaded specimen was somewhat lower than that of the non-loaded and 60% loaded specimens. After 36 weeks incubation the 30% loaded specimen showed lowest chloride concentrations in virtually all depth zones in comparison to the non-loaded and 60% loaded specimens. However, differences were only small, and it should be realized that these results are obtained from single specimen only.

What can be further concluded from the results shown in Figure 6.5 when considering chloride ingress over time is that chloride concentration per depth (chloride profiles) increased significantly in the incubation period from 2 to 6 weeks (compare Figure 6.5 a and b). However, incubation for longer than 6 weeks (up to 36 weeks) did not result in significant further increase in chloride concentration with depth (compare Figure 6.5 b, c, and d).

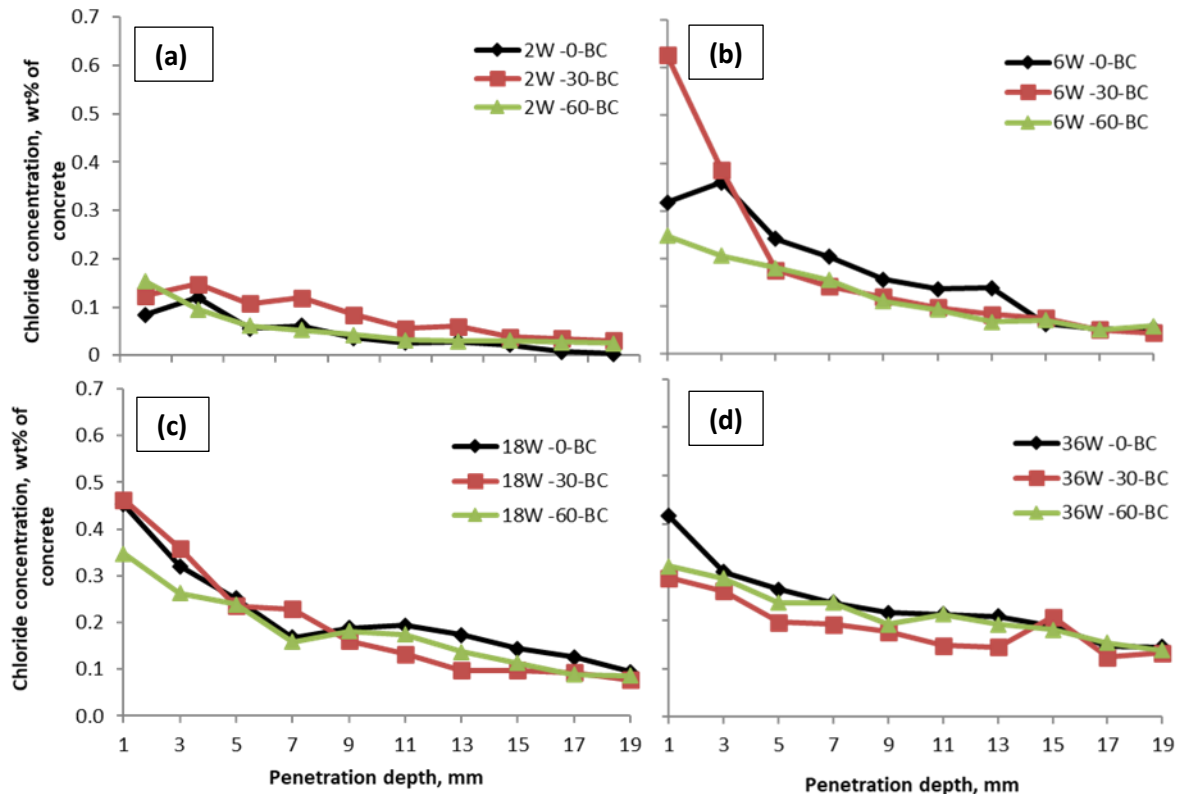


Figure 6.5 Chloride ingress profiles in bacteria-based healing agent (BC) containing concrete specimens after (a) 2 weeks; (b) 6 weeks; (c) 18 weeks and (d) 36 weeks incubation of non-loaded specimens (-0-BC), and specimens loaded at 30% (-30-BC) and 60% (-60-BC) of ultimate load.

6.3.2 Chloride ingress in reference specimens

Figure 6.6 shows the chloride ingress profiles measured in this study concerning bacteria-based healing agent containing specimens in comparison to the ones measured and discussed in chapter 4 concerning reference (no healing agent containing) specimens. Overall comparison of these profiles show that chloride ingress was substantially higher in healing agent containing specimens in comparison to reference specimens for non-loaded and 30% loaded specimens series but not significantly different in 60% loaded specimens series. The chloride ingress profiles of healing agent containing specimen for non-loaded specimens (Figure 6.6 a) and 30% loaded specimens (Figure 6.6 b) lie clearly above those of reference specimens, while they appear similar for 60% loaded specimens (Figure 6.6 c) after either 6-, 18- or 36-weeks incubation. Particularly for reference specimens (not containing healing agent) it can be seen that chloride ingress increased with incubation time for all specimens series (non-loaded, 30% or 60% loaded specimens), and that this increase was similar for reference and healing agent containing specimens loaded at 60% of ultimate load.

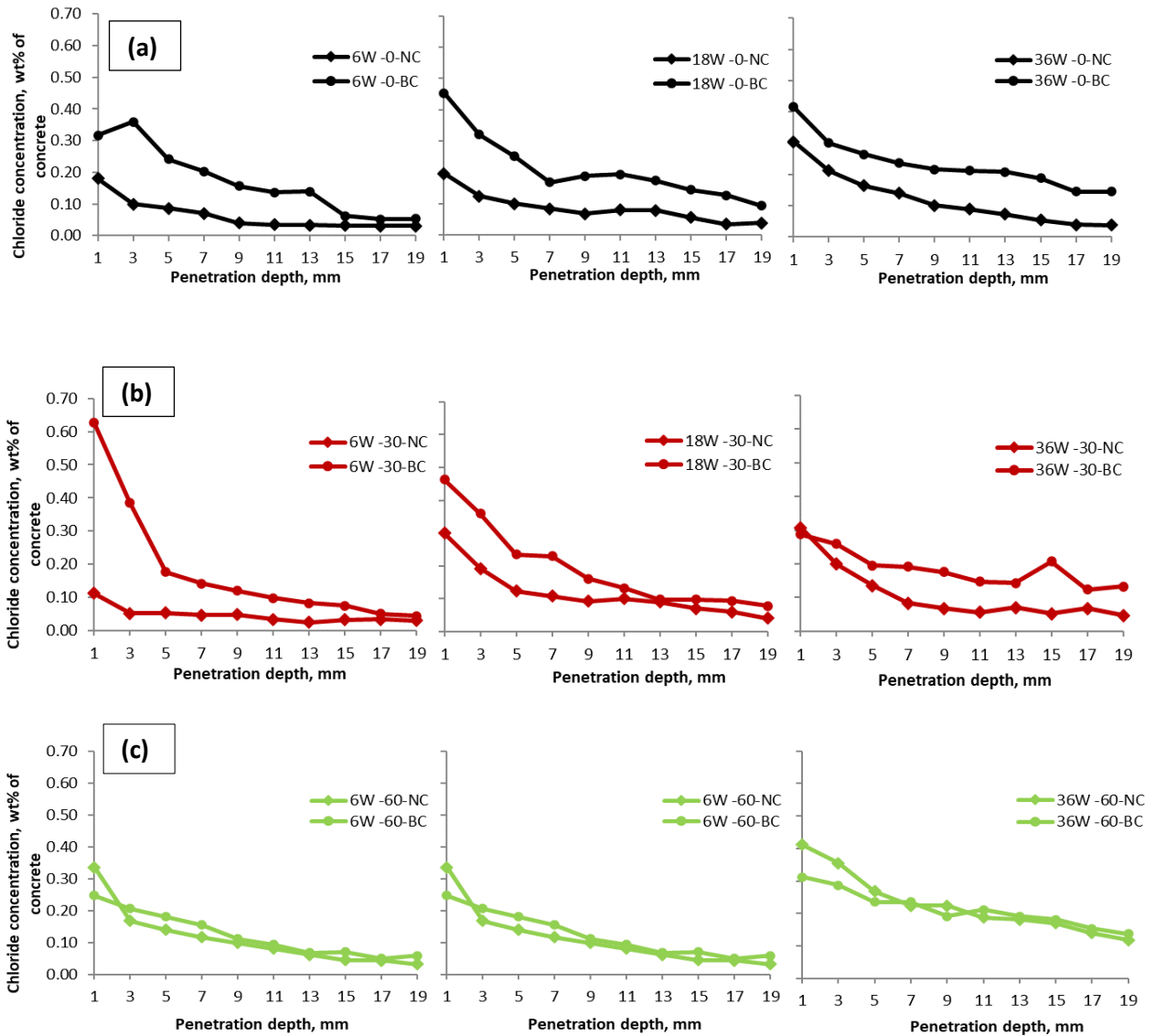


Figure 6.6 Chloride profiles of (NC) reference (no healing agent containing) and (BC) bacteria-based healing agent containing concrete specimens, (a) non-loaded or (b) loaded at 30% or (c) 60% of ultimate load and subsequently incubated and exposed to chloride for either 6, 18 or 36 weeks

6.3.3 Estimation of chloride diffusion coefficients

Using the Matlab curve fitting toolbox, fitting analysis was performed on chloride ingress profiles (as shown in Figure 6.7) and the parameters of chloride diffusion coefficient (D), chloride surface concentration (C_s) and correlation coefficient (R^2) were determined for specimens containing bacteria-based healing agent, and values are listed in Table 6.1, as well as the results obtained in Section 4.5.2, for specimens without healing agent. The values of D were obtained from the best fitted curve of the chloride profiles using Fick's second law represented by Equation (2.3). The fitted curves yielded correlation coefficients between 0.850 and 0.995 for BC (Bacterial Concrete) specimens and high correlation coefficients above 0.913 for NC (Normal Concrete) specimens. No clear trend in change of chloride surface

concentration nor diffusion coefficient versus incubation time or loading regime can be observed for Bacterial Concrete from these data.

Table 6.1 Chloride diffusion coefficient as calculated from curve fitting of chloride ingress profiles of healing agent-containing specimens

Specimen	C _s (wt%)		D (10 ⁻⁶ mm ² /s)		R ²	
	NC	BC	NC	BC	NC	BC
TUD-2W-0	0.165	0.116	17.58	17.572	0.979	0.890
TUD-2W-30	0.187	0.157	15.24	49.499	0.995	0.941
TUD-2W-60	0.170	0.175	9.68	8.517	0.980	0.992
TUD-6W-0	0.196	0.382	3.43	15.195	0.982	0.968
TUD-6W-30	0.123	0.728	2.11	3.120	0.927	0.987
TUD-6W-60	0.331	0.268	5.70	13.935	0.956	0.995
TUD-18W-0	0.182	0.401	3.80	7.475	0.913	0.923
TUD-18W-30	0.282	0.469	3.08	3.935	0.933	0.982
TUD-18W-60	0.302	0.332	5.21	8.051	0.981	0.961
TUD-36W-0	0.306	0.370	1.57	7.694	0.989	0.927
TUD-36W-30	0.339	0.272	0.75	10.605	0.979	0.852
TUD-36W-60	0.393	0.309	5.44	11.337	0.964	0.968

Figure 6.7 shows the diffusion coefficient per type of specimen against time of incubation. Fitted trend lines show a relatively high correlation coefficient for (R² = 0.8855) for the non-loaded specimens but very low ones for the 30% and 60% loaded specimens (R² = 0.2689 and 0.0172 respectively) in concrete with bacteria. However, both normal- and bacterial-concrete specimens show comparable fitted trend lines with relatively high but not decreasing chloride diffusion coefficients with time for 60% loaded specimen (green lines) but decreasing chloride diffusion coefficients with increasing incubation time for non-loaded (black lines) and 30% loaded (red lines) specimen.

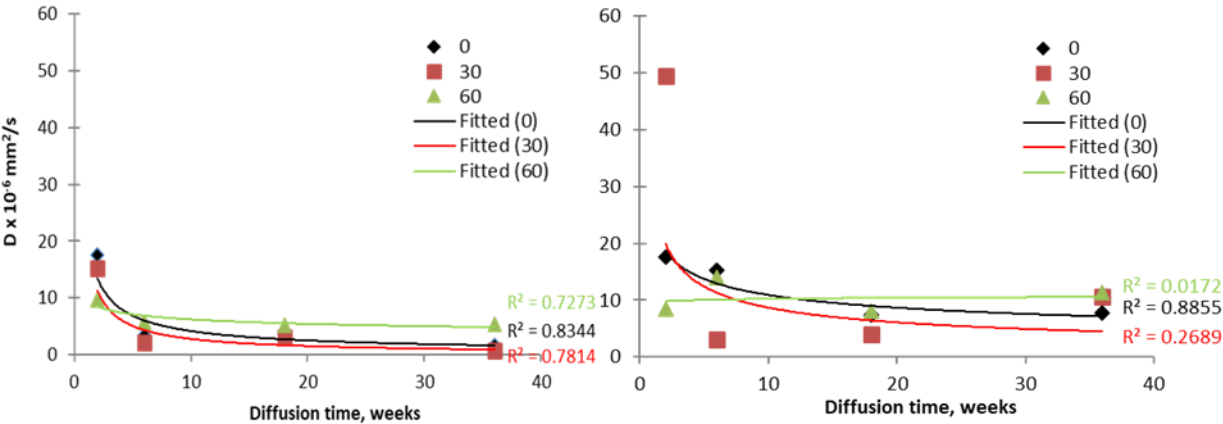


Figure 6.7 Fitted trend lines through chloride diffusion coefficients over time of non-loaded and 30% and 60% loaded normal (reference) specimen (left graph) and bacterial concrete specimen (right graph).

6.3.4 Microscopic observation of mineral formation

Mineral precipitates formed on crack surfaces of cracked concrete specimens were visualized in this study through ESEM investigation of thin sections. Figure 6.8 shows images taken from cracked bacteria-based healing agent containing concrete specimen loaded at 60% of ultimate load and incubated for 36 weeks under chloride exposure conditions. These images show that formed calcium carbonate precipitates appeared to bridge and block cracks resulting in a pattern of disconnected and smaller cracks. The precipitates were further analysed by EDAX measurements and this revealed the presence of high amounts of calcium, carbon and oxygen atoms indicating that the composition of the mineral precipitates were calcium carbonate (CaCO₃)-based. A representative plot of EDAX element analysis is shown in Figure 6.9.

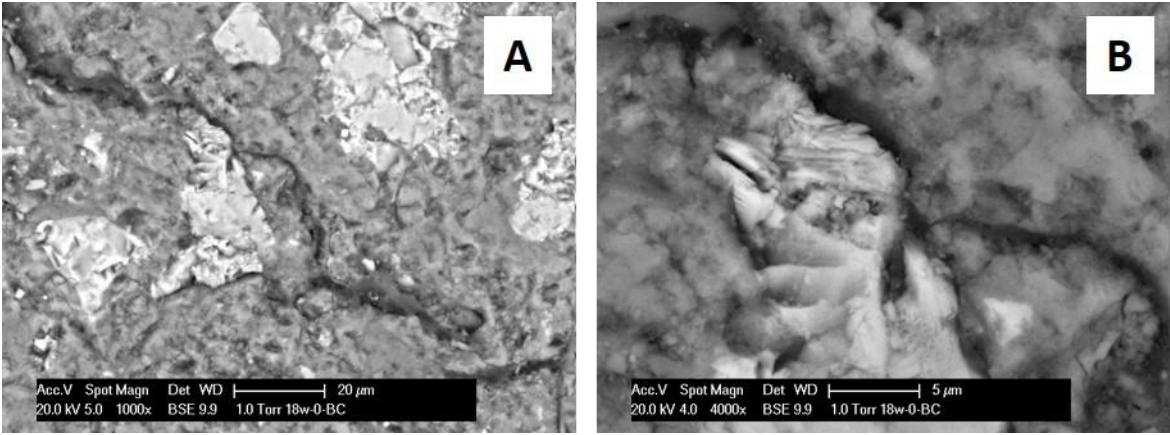


Figure 6.8 Mineral formation on the surface of a cracked bacteria-based specimen. (a) ESEM image 1000x magnification. (b) ESEM image 4000x magnification

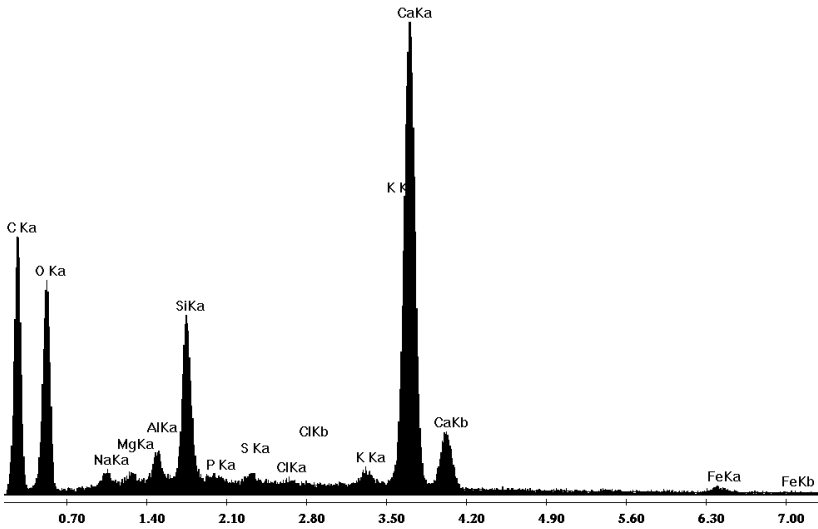


Figure 6.9 EDAX analysis of mineral precipitates occurring on crack surfaces show that the mineral composition is dominated by calcium-, carbon-, and oxygen atoms

Bacterial imprints

Evidence that calcium carbonate-based minerals were formed due to bacterial metabolic activity was found by ESEM analysis as typical bacterial imprints on the surface of precipitated minerals were found, similar as shown before in studies by Wiktor et al. [133-134], (see Figure 6.10).

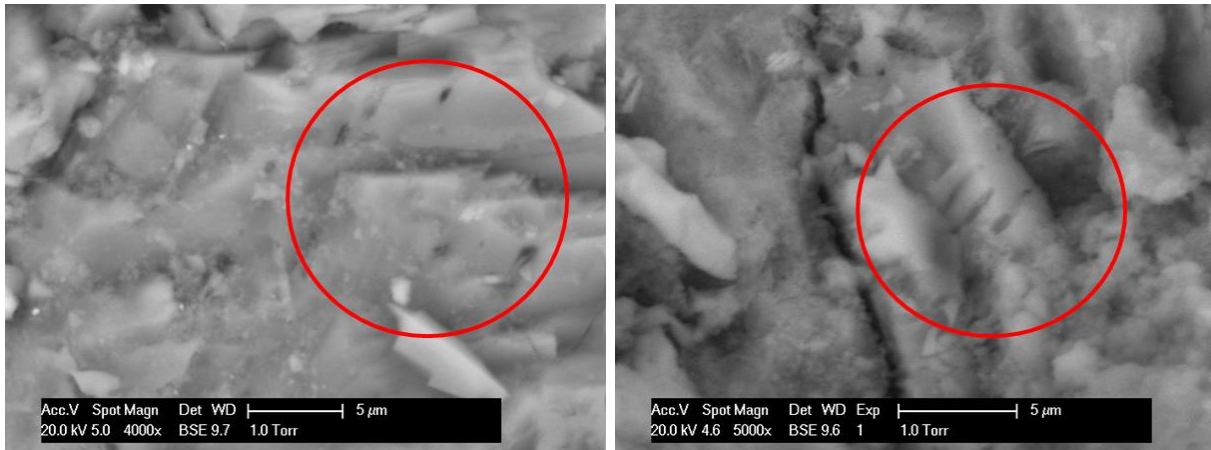


Figure 6.10 Bacterial imprints in precipitated calcium carbonate-based minerals in a cracked and healed bacteria-based self-healing agent containing concrete from this study

6.3.5 Oxygen consumption of concrete specimens

ESEM images of formed calcium carbonate-based minerals provided evidence that the process was mediated by bacterial metabolic activity due to the presence of bacterial imprints in the mineral precipitates. However, it cannot be excluded that the observed bacteria-like imprints did not originate from bacteria but occurred due to purely chemical mineral precipitating processes. Therefore, additional evidence for bacterial metabolic involvement was derived from oxygen consumption measurements as bacterial metabolism, but not chemical mineral precipitation, results in oxygen consumption. Oxygen consumption measurements were done by profiling oxygen concentration changes towards the surface of water submerged bacteria- and reference concrete samples using an oxygen microsensor. Figure 6.11 shows the oxygen profile measurements for a reference and a bacterial healing agent-containing sample after being submerged for 36 h in sodium carbonate buffered water at pH of 10.5. The oxygen concentration at the surface of the bacteria-based sample was observed to progressively decrease in the 0.9-mm water layer overlying the sample surface while the concentration remained constant near the surface of the control sample. These oxygen profiles show that oxygen consumption occurred by the healing agent containing specimen but not in the reference specimen.

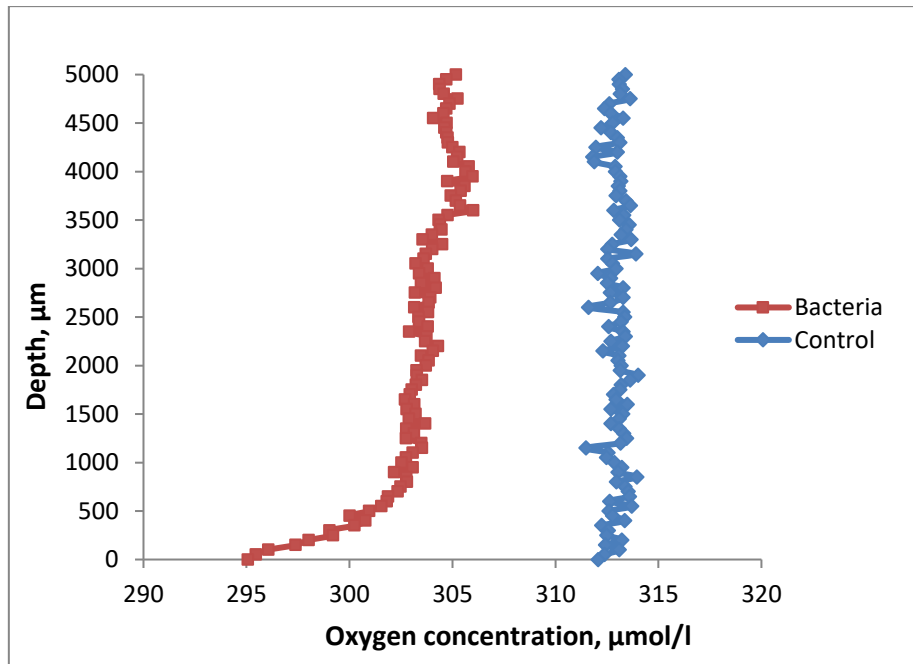


Figure 6.11 Oxygen concentration micro-profiles determined towards surfaces of water-immersed reference and bacteria-based concrete specimens. Bacterial healing agent containing specimen shows oxygen consumption as the oxygen concentration progressively decreases towards the surface of specimen while this does not occur in the reference specimen

6.4 Discussion

Chloride ingress in unloaded and loaded concrete specimens

In this study, it was hypothesised that loading of specimens at 30% and 60% of ultimate load capacity would cause (limited) damage of microstructural integrity through formation of micro-cracks which enhance ingress of chlorides. It was further hypothesized that self-healing of micro-cracks (expected to be higher in bacterial healing agent containing than in reference specimens) would result in decreased chloride ingress rates.

Interpretation of the obtained data in this study should be done with some caution as the obtained results are based on data derived from single specimen. Due to practical experimental limitations only single specimen for each set of parameters (0%, 30% or 60% continuous compressive loading during 2, 6, 18 or 36 weeks of incubation) could be handled in this study. This allows therefore only general comparison of possible difference in trends of chloride profiles of sets of specimens rather than establishing statistically significant differences between (parts) of chloride ingress profiles.

Comparison of chloride ingress in non-loaded and loaded bacterial healing agent containing specimens incubated for 2, 6, 18 and 36 weeks (shown in Figure 6.4) show that the expected increase in chloride concentration with depth only occurred to a significant extend in the period between 2- and 6-weeks incubation. Longer incubation (up to 36 weeks) did not result in substantial further increase in chloride concentration with depth. Furthermore, no significant difference (clearly different pattern) in chloride ingress between non-loaded, 30%- and 60% loaded specimens at all incubation periods could be observed.

Lack of clear difference in chloride ingress profiles between non-loaded and 30% or 60% loaded specimens suggest that the initial hypothesis that damage of the microstructural integrity results in increased chloride ingress appears therefore falsified. However, as actual occurrence of microstructural damage due to loading was not investigated in this study, it might be that occurred damage, if at all, was insufficient to lead to substantial differences in chloride ingress. The observed substantial increase in chloride ingress in the incubation period from 2 to 6 weeks but not from 6 to 36 weeks incubation can be explained by the exponentially decreasing progress of chloride ingress with depth over time. The followed methodology in this research, analysis of single specimen combined with pooling of drilled subsamples obtained from distinct depth layers, did apparently not allow sufficient distinction in chloride concentration to establish expected increase of chloride ingress over time in between 6- and 36-weeks incubation.

Second hypothesis of this study was that occurrence of self-healing of (micro)cracks would delay ingress of chloride over time. Comparison in ingress of chloride (chloride profiles) between reference and bacterial healing agent containing specimens series was therefore done (see Figure 6.5). Striking is that ingress of chloride appears substantially higher in healing agent containing specimens compared to reference specimens for non-loaded and 30% loaded specimens but not for 60% loaded specimens. This observed difference can possibly be explained by a higher porosity of intact (non-damaged) concrete matrix of healing agent containing specimens in comparison to intact reference specimens. Some increase of porosity can indeed be expected as the healing agent is relatively soft and disintegrates over time when embedded in the concrete matrix expectedly leading to pores. This leads to the conclusion that addition of healing agent increases the porosity (and permeability) of intact (non-damaged) concrete. Results in Figure 6.5 show that chloride profiles of non-loaded and 30% loaded reference species were similar and also that those of non-loaded and 30% loaded healing agent containing specimens were similar. This suggests indeed that 30% loading did not result in damage (occurrence of micro-cracks) in the concrete material matrix. However, the clear difference between chloride profiles of the 60% loaded reference specimens in comparison to those of the non-loaded and 30% loaded reference specimens strongly suggests that damage (micro-cracking) of the concrete matrix occurred at 60% load, resulting in increased chloride ingress rates. In this case (under 60% loading) chloride ingress profiles of reference and healing agent containing specimens appeared similar what suggests that on the one hand addition of healing agent does not lead to further increase in permeability of damaged specimen, but on the other hand did also not result in decrease of permeability to healing as was hypothesized in this study. The rate of (micro)crack healing was apparently too low to significantly decrease the simultaneously occurring ingress of chloride through the damaged concrete matrix during the permanently applied loading.

Evidence for bacteria mediated self-healing

Although the rate of bacteria-mediated self-healing appeared not sufficient to result in a significant decrease of chloride ingress in damaged 60% loaded specimen, evidence for the self-healing process itself was actually obtained in this study. The decrease in oxygen concentration in the water column directly above the submerged healing agent containing specimen (see Figure 6.10) showed that bacteria were metabolically active. Oxygen consumption by active bacteria occurs during metabolic conversion of the nutrients (calcium lactate) being part of the healing agent into calcium carbonate [14, 82]. This observation thus provides evidence for bacterial metabolically driven calcium carbonate precipitation in bacteria-

based healing agent-containing specimens. Further evidence was obtained from electron microscopic analysis of precipitates formed in micro-cracks of damaged concrete (Figure 6.7) as these showed imprints similar in size and shape of active bacteria as was also found in previously published studies [137, 138].

6.5 Conclusions

The study described in this chapter investigated the effect of inclusion of a bacteria-based healing agent in concrete and its effect on penetrability of chlorides in specimens under compressive load. Results show that the chloride ingress in reference concrete specimen was lower for non-loaded and 30% loaded (of ultimate load) specimen in comparison to corresponding healing agent containing specimen. However, no clear difference in chloride ingress was found for both types of specimens loaded to 60% of maximum load capacity. From these observations, it was concluded that addition of healing agent increases the permeability of intact (non-damaged) concrete but not that of damaged (due to 60% continuing load stress) concrete. In this study evidence for bacteria-mediated self-healing was found as healing agent containing specimen consumed oxygen (indicative for metabolically active bacteria) but reference specimens did not. Moreover, calcium carbonate-based precipitates formed in cracks of healing agent containing specimens showed bacterial imprints what further provided evidence for the occurrence of bacteria-mediated formation of crack-filling calcium carbonate-based precipitates. However, the rate of occurring bacteria-mediated self-healing appeared too low to result in significant decrease of chloride ingress in 60% (of maximum) loaded- and simultaneously chloride solution exposed concrete specimens. Further studies should clarify whether bacteria-mediated self-healing of occurring damage before exposure to chloride could help to improve the durability of chloride exposed concretes.

7

Durability improvement via bacteria-based self-healing of cracked mortars under compression-, carbonation- and chloride-loaded conditions

“Maintaining structures in satisfactory form and preserving pleasant visual appearance is a precondition for continued acceptance the reputation of concrete as the primarily building material for the future.”

-Steen Rostam-

The results in Chapter 6 indicate that the chloride profiles of bacterial concrete were not following the general trend as in normal-strength concrete. Higher in chloride concentration in time was noticed when samples were subjected to a higher compressive load. Although healing potential was observed at this stage, there is still insufficient information about the crack-sealing capacity of concrete amended with bacteria-based healing agent. The healing potential for improving durability aspects of cementitious materials has been further investigated in the study described in this chapter. The present chapter experimentally quantifies the healing capacity of the sustainable bio-based healing system towards chloride and carbonation ingress in crack-containing mortars.

Materials used for sample preparation and the pre-conditioning of mortar specimens are presented in Section 7.2. The methods used to evaluate healing efficiency with respect to chloride distribution and carbonation ingress into the mortar matrix are discussed in Section 7.3. The results for energy disperse spectroscopy (EDS) mapping analysis, phenolphthalein test and x-ray computed tomography are reported in Section 7.4. In addition, the crack-sealing capacity of mortar specimens observed by stereomicroscopy including image analysis of mineral formation due to metabolic activity of bacteria by ESEM is also present in Section 7.4. The oxygen consumption test, dealt with in Section 7.4, provided further evidence for bacteria-controlled crack-healing. The conclusion of this study, described in detail in Section 7.5, is that the application of bacterial healing agent improved durability properties of cracked mortars with respect to chloride ingress and carbonation.

7.1 Introduction

Addition of a bacteria-based healing agent to cementitious materials is known as an alternative self-healing treatment and is particularly applied for durability improvement of cementitious materials. Considerable research on this topic mainly assessed durability from the water permeation property aspect of bacteria modified mortar or concrete [73, 85, 136, 151, 152]. Promising results of the bio-based healing system on water permeation properties have led to further durability improvement investigations such as resistance towards degradation processes due to cracks under laboratory conditions. It demonstrated that the addition of the bacterial healing agent to mortar mixtures resulted in mitigation of degradation processes and therefore in improvement of durability aspects [69, 72, 78, 79, 153, 154].

Published research on chloride resistance of bacteria-based self-healing mortar or concrete is, however, scarce and mostly addresses rapid chloride migration investigations of undamaged (non-cracked) samples. In one study, the increased resistance towards chloride ingress through limestone production via biodeposition was observed for specimen featuring various water-cement ratios. In that specific study [69], however, the biodeposition treatment was only applied on the surface of specimens and can therefore only be regarded as a coating system. In another study by *Achal et al.* [72], a bacterial strain of the genus *Bacillus* was used to reduce chloride ion permeability in mortar specimen. Applying the process of microbially induced calcium carbonate precipitation (MICP), increased surface permeability resistance of cement-based materials was achieved. Other studies addressed investigations on the influence of bacterial limestone production on chloride resistance in concrete made with fly ash [78] and silica fume [79]. These studies also indicated improved resistance towards chloride penetration when the specific bacterium *Sporosarcina pasteurii* was applied. In addition to that, positive results were also reported for improved resistance towards carbonation of mortar specimen treated with bacteria [69, 154].

The studies referenced above indicated that bacterial treatment improved the resistance of chloride ingress and carbonation of mortar and concrete specimens. However, in most studies the healing efficiency of the applied bacteria was not fully explored as mainly surface treatment of otherwise undamaged samples were considered. Hence, the bacterial healing efficiency under extreme and aggressive environmental conditions of particularly cracked specimens has as yet not been quantified.

Therefore, in the previous Chapter 6, preliminary investigations were undertaken to evaluate the durability enhancement of bacteria-based self-healing concrete under service loading at different compressive stress levels. Despite current knowledge about the impact of compressive load-induced cracking on chloride ingress in fractured concrete, the self-healing capacity to resist the attack of harmful ions in cracked samples is not sufficiently understood. In addition, consequences of extra carbon dioxide produced by active bacteria embedded within the mortar or concrete matrix on material properties still require more attention. The influence of mineral-producing bacteria on resistance towards chloride and carbonation needs therefore further investigations.

This chapter therefore quantifies the potential of bacterial CaCO_3 precipitation for improving resistance of cracked mortar specimens towards chloride ingress and carbonation. In order to reduce some complexity, mortar samples were prepared featuring specific pre-defined cracks. In addition, mortar instead of concrete was used to eliminate the influence of coarse aggregates on ingress of chloride, as water may dissolve various minerals present in the aggregates [155]. Mortar prisms were prepared with mixes to which bacterial healing agent was added, and these were subsequently subjected to cracking and accelerated chloride penetration and carbonation. Additional experiments on oxygen consumption of bacteria-

based specimen were conducted to find further evidence for involvement of bacterially controlled carbonate mineral production for self-healing of cracks in these mortar specimens.

7.2 Materials and methods

All prismatic test specimens (40 mm x 40 mm x 160 mm) were prepared in accordance with NEN-EN 196-1: 2005 [156]. The type of cement used was Ordinary Portland cement, CEM I 42.5 and water/cement ratio applied was 0.5. The sand used was a normalized standard sand. Two mortar batches were made to produce control specimens with and without added bio-healing agent. All samples were prepared in triplicates and coded according to the nomenclature of exposure conditions code as describe in Figure 7.1.

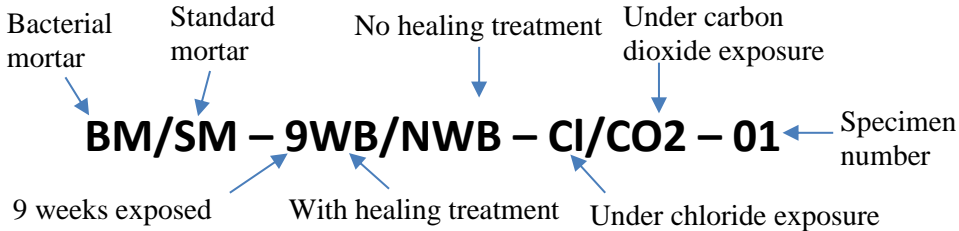


Figure 7.1 Nomenclature of sample code

After mixing, the mortar was immediately brought into moulds in two layers followed by compaction of each layer for 30 seconds on a vibrating table. The fresh mortar surface was leveled and covered with an impermeable plastic sheet. After 72h, the specimens were removed from the mould and sent to the curing room with a temperature of 20 ± 2 °C and a relative humidity of ≥ 95 % until 28 days. After 28-day curing, all specimens for chloride ingress testing were vacuum saturated for 3 h and sealed with aluminum sticking foil prior to the bending test. While specimens for carbonation testing, the prism mortars were immediately sealed after 28 days of curing time without saturation test. The surface with the crack opening was left open. Sealing was applied to prevent the uncracked sides from being exposed to the test environments.

7.2.1 Pre-conditioning of mortar specimens

A crack was introduced to the test specimens through three-point bending using an Instron machine (INSTRON 8872 Testing System) of 10 kN maximum capacity (as shown in Figure 7.2). Prior to the three-point bending test, five sides including the as-cast surface of the mortar sample were sealed with aluminum sticky tape to afterwards allow chloride and CO₂ to enter only from the cracked side of the prism. The crack width was controlled and measured using a linear variable differential transformer (LVDT). Under crack displacement control at a rate of 0.5 μm/s, a visible crack of 350 μm with ± 50 μm width after unloading was produced in 40 mortar samples. The crack self-healing potential in chloride- and carbonation environments of 9- and 18-weeks old specimens were investigated. A crack width of approximately 350 μm was chosen in order to limit the effect of crack width on the ingress rate of chloride and CO₂ [58, 84]. The specimens were reinforced with two steel wires at the tension side, as illustrated in Figure 7.3, in order to keep the crack surfaces at a distance after unloading and to avoid full

separation of prisms in halves during the bending test. The support span of the three-point bending test was 142 mm. The load and crack displacement were automatically recorded during the tests.

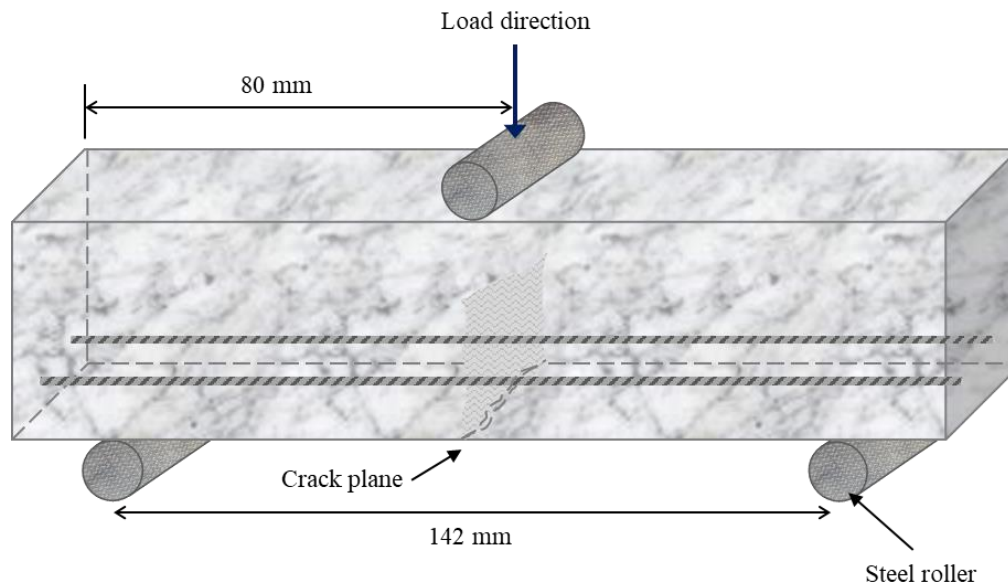


Figure 7.2 Three-point bending test

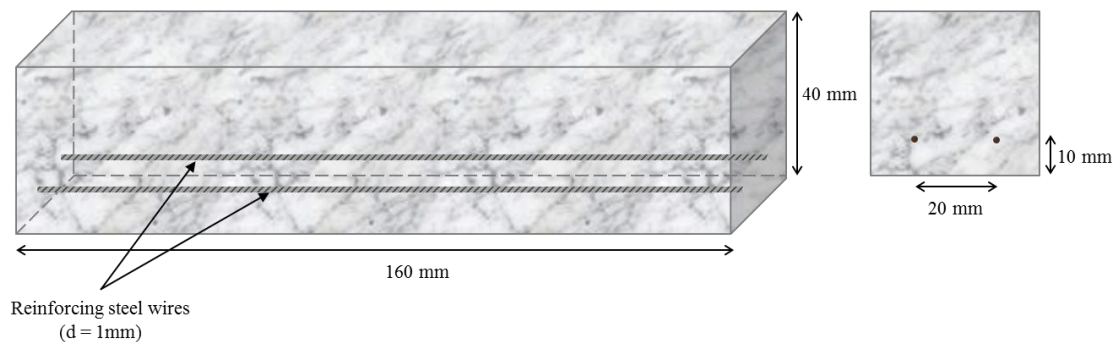


Figure 7.3 Specimens for three-point bending test

7.2.2 Healing treatment procedure and selection of bio-healing agent

After the maximum crack width was reached, the load was released and immediately crack line images were taken using a stereomicroscope. In order to promote microbially mediated CaCO_3 precipitation in the crack, mortar samples both with and without healing agent were incubated in demineralized water prior to the chloride and carbonation test as healing treatment. This study did not use tap water (in healing treatment) to avoid interference with the chloride test investigation. The specimens were removed from water after another 28 days incubation. Following this healing treatment, the images of the crack line were captured for the second time to evaluate autogenous (reference specimens) and autonomous (healing agent amended specimens) crack sealing capacity by mineral deposit formation. Next, the specimens were sent to carbonation chamber and chloride pond respectively for 9 weeks and 18 weeks exposure period. These exposure periods were selected considering the duration before and after 90 days test duration for meaningful profile to develop.

Furthermore, to observe the efficiency of the proposed healing treatment, samples from 18-weeks specimens were reserved for both chloride and carbonation testing without 28 days incubation in demineralized water. In this case, the specimens were directly taken to the chloride test immediately after the bending test. A comparison of chloride distribution with and without healing treatment is given in Section 7.4.3. A clear overview of the process flow for pre-conditioning of mortars specimen after curing process is given in Figure 7.4.

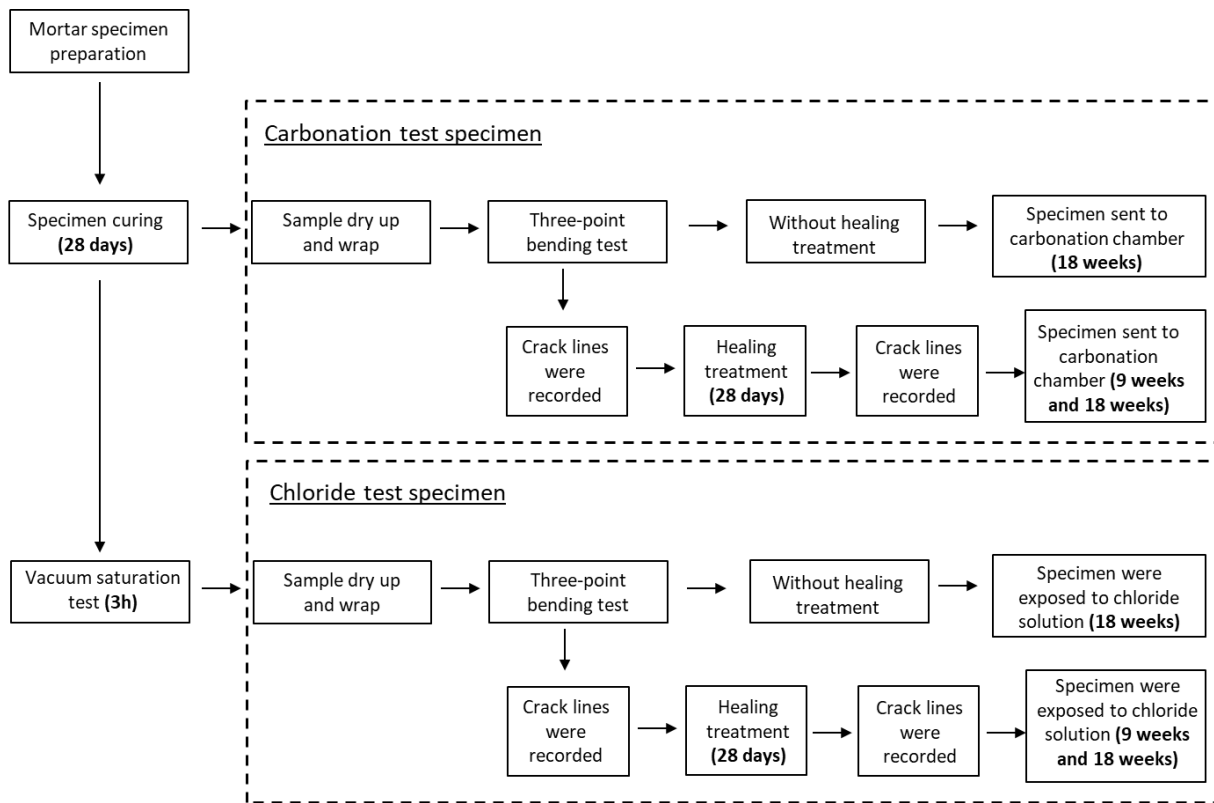


Figure 7.4 Process flow of pre-conditioning of mortars specimen for carbonation and chloride testing after 28 days of curing

Bio-healing agent featuring cylinder-shaped particles with diameter of approximately 2 mm, containing a mixture of bacterial spores, growth requiring nutrients and calcium lactate were selected for this study. The healing agent particles were coated with a polymer-based coating in order to retain integrity during mixing and were added to the standard mortar constituents at an amount of 15 kg/m³ as reported in Section 5.4. Detailed information about the healing particle constituents and its production details were reported previously by Jonkers and Mors [136].

7.3 Evaluation of healing efficiency

7.3.1 Chloride ingress in cracked mortar

After the images of surface cracks were taken for the second time, which is after being subjected to 28 days incubation period in demineralized water, the specimens were fitted into the chloride solution containing tray and partially submerged with the crack opening side facing down into chloride solution containing 3% of sodium chloride. To limit the effect of hydrostatic

pressure, the level of the chloride solution was kept constant at a height corresponding to approximately 10 mm above the crack surface of the mortar specimen. This configuration allows chloride ingress only from the bottom surface of the mortar prism permitting the flow of solution in the vertical direction as shown in Figure 7.5. In this case, the crack faces were constantly in contact with the exposure solution while the specimen was partially exposed to the solution.

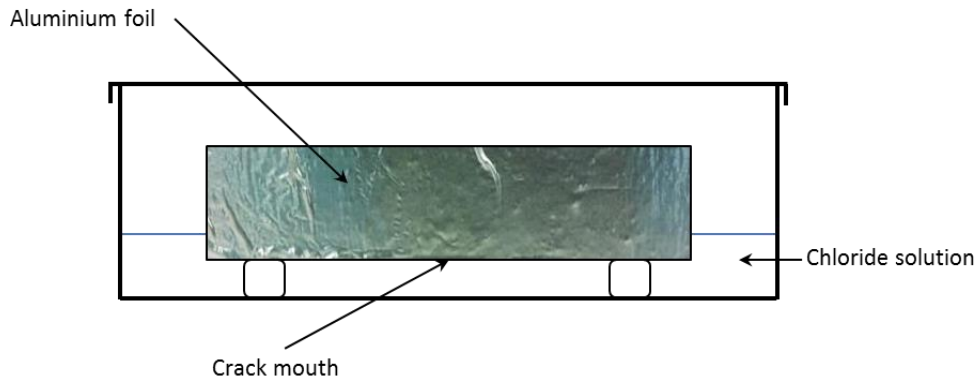


Figure 7.5 Ingress of chloride through the cracked bottom face of the mortar beams

Under this exposure condition, the chloride ingress in the cracked mortar specimen is assumed to follow two-dimensional diffusivity, in one dimension from the exposed surface and the other one perpendicular to the crack plane [103]. The specimens were laid in the solution tray up to 9 and 18 weeks with pH values in between 8 and 9.5. Specimens with and without bacteria-based healing agent were kept in separate containers to avoid cross-contamination [82].

Chloride mapping by EDS

After the chloride ingress testing period, bacterial healing agent- and control specimens were immediately sawn by using dry sawing with a spray of ethanol solution for smooth cutting and to avoid disturbance of chloride ion distribution during cutting. A single cut was made in the middle area of the crack location parallel to the wire steel with dimensions of 40 mm x 40 mm x 6 mm as shown in Figure 7.6 [90]. Both types of specimens were subsequently vacuum impregnated using low viscosity fluorescent epoxy. Prior to quantitative Energy Dispersive X-ray Spectroscopy (EDS) microanalysis in SEM, the impregnated specimens were polished by SiC paper grinding grade #500, #800, #1200 and #4000 successively using a 100% ethanol solution on a rotating disk plate until the surface was free from micro-scratches.

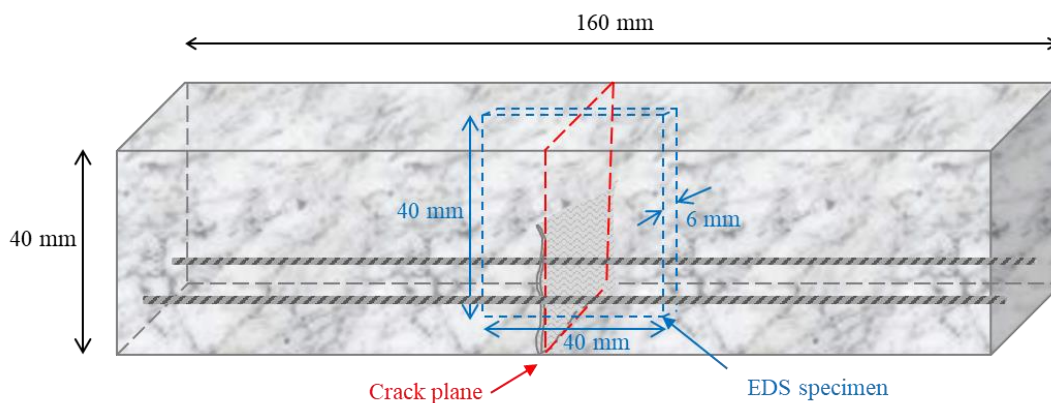


Figure 7.6 Location of specimen for EDS scanning in cracked mortar prism

EDS installed with default Noran System Six (NSS) spectral analysis software, operating at an accelerating voltage of 15 kV, was employed to measure the elemental composition of the sample. The electron beam current (spot size) in between 5.5 to 6.3 was adjusted to achieve system dead time (DT) of 20-25% for spectral artifacts minimization. The analysis provided the mass fractions or weight percent of the elements present as shown in Figure 7.7. The operating parameters applied in the default spectra and conditions being used to carry out the analysis are essential as it can limit the accuracy and precision of the results.

In this case, the distribution of chloride provided by X-ray mapping should clearly show the penetrated area of the cracked mortar. As the distribution area for chloride calculated in this study was relatively large, the mapping was run by analysis automation and the data collected were quantified by contour plotting. Figure 7.8 shows how the chloride element has been mapped from the EDS scanning images.

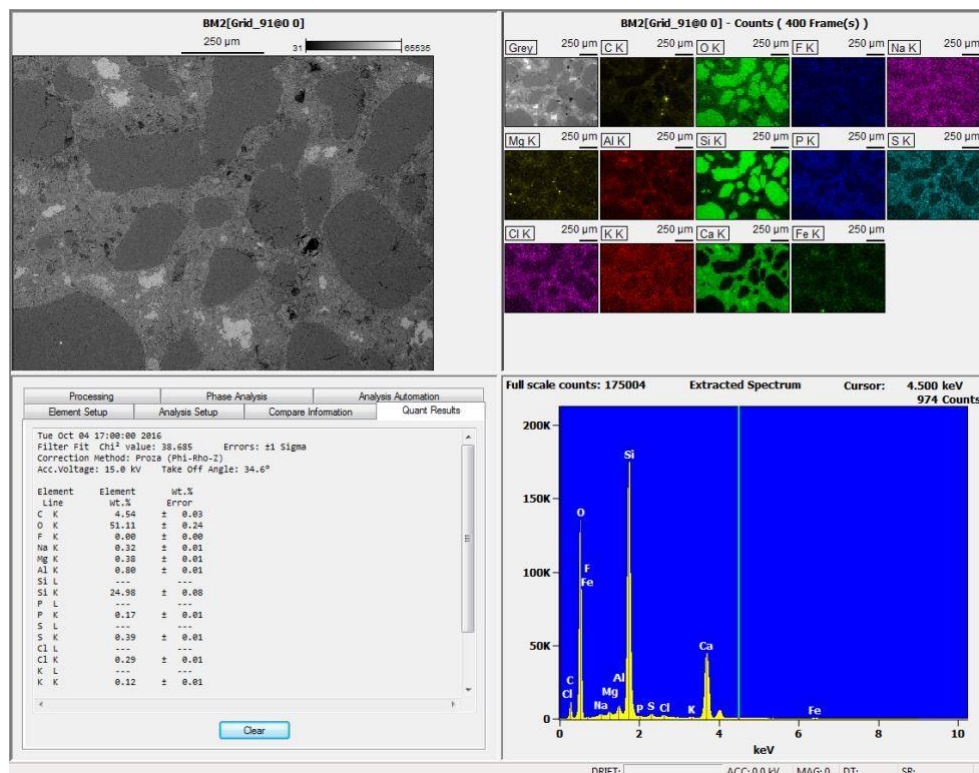


Figure 7.7 NSS spectra analysis layout

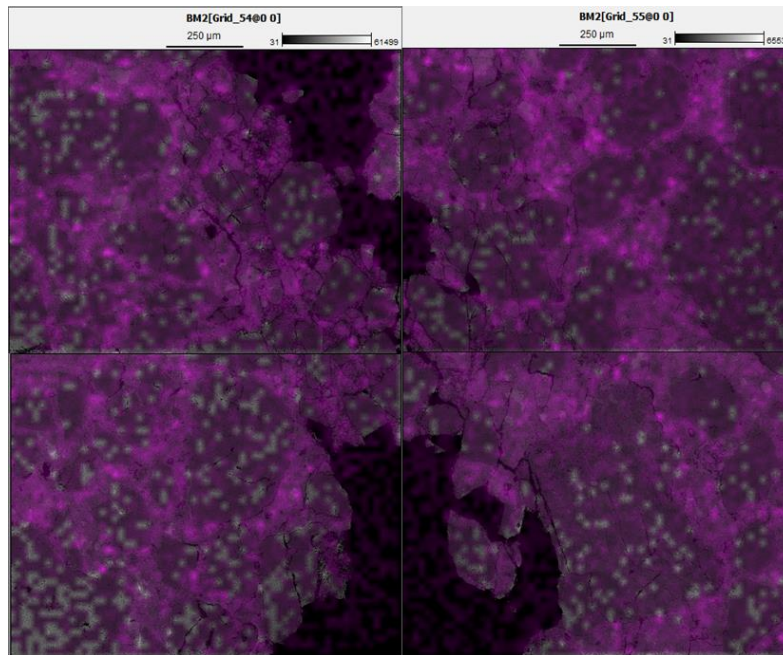


Figure 7.8 Example of stitching of EDS scanning image of chloride element (Cl⁻)

7.3.2 Carbonation rate of cracked specimen

Since carbonation is a slow long-term process, accelerated carbonation tests were performed in a carbonation chamber with pre-set parameters of 3% CO₂ concentration at a temperature of 20 ± 2 °C and a relative humidity of $70 \pm 10\%$. The mortar samples were stored in the carbonation chamber for 9 and 18 weeks. After 9 weeks, the prisms were axially split into two parts and the freshly split sections were sprayed with phenolphthalein solution for determination of the carbonation depth. For 18 weeks specimens, the effects of carbonation were examined by considering the changes of pore volume in the cement matrix between standard mortar and bacterial mortar.

7.3.3 Pore volume assessment

In addition to the phenolphthalein test, the carbonation effects were further investigated by using a helium pycnometer test for pore volume assessment of 18-week-old samples. The experiments were performed in triplicate and as explained in the following paragraph.

Helium pycnometry

The samples were cut into small cubes of 20 mm x 25 mm x 25 mm in dimension for pore volume analysis. Subsequent to that, the samples were pre-conditioned by placing them in fresh propan-2-ol for 14 days and subsequently transferred to a fresh solution of the same composition for an additional 14 days. Finally, the samples were placed in a vacuum desiccator for 7 days to remove the solvent. The volume of the solids and the matrix of samples were measured using a gas expansion pycnometer, UltraPycnometer 1000. In the configuration shown in Figure 7.9, the gas enters the specimen cell before the reference cell, however the order of the cells could be reversed without affecting the measurement. In general, the sample is activated, weighed and placed into the sample cell. Then the sample is immediately loaded

into the sample cell to avoid the uptake of moisture and other atmospheric contaminants. With the sample inside, the sample cell is subsequently dosed with a gas to an initial pressure. The gas is then allowed to expand into the reference cell, causing the pressure to drop to the final pressure [157].

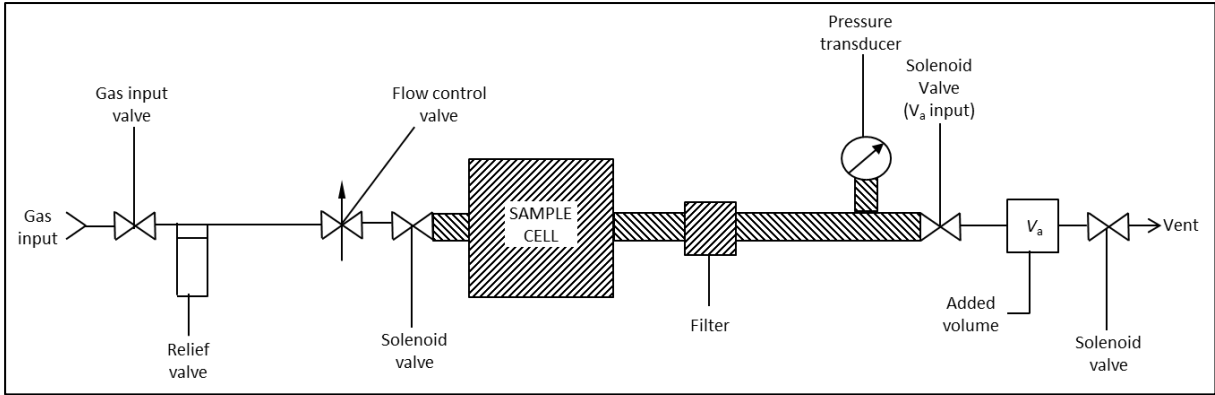


Figure 7.9 Schematic drawing of the ultra-pycnometer

Within a measuring cycle, ultra-pycnometry distinguishes three phases. In the first phase, the added volume V_a was calibrated and followed by sample cell volume calibration in the second phase. In the final phase, the pressure was applied for 30 seconds before the actual measurement was taken in each of the test runs. The accessible pore volume of the solid part was determined based on Archimedes and Boyle’s Law working principles. The working equation employed by the ultra-pycnometer is given in Equation (7.1). By measuring the volume of hardened mortar, the porosity of each sample can be calculated by applying the equation given in (7.2).

$$V_{ma} = V_c + \frac{V_a}{1 - P} \tag{7.1}$$

where, V_{ma} is the solids volume;
 V_c is the cell volume;
 V_a is the added volume and;
 P is the pressure above the ambient divided by the pressure drop

$$\phi = \frac{V_b - V_{ma}}{V_b} \tag{7.2}$$

where ϕ is the porosity and V_b is the bulk volume of hardened mortar.

7.3.4 Optical observations by ESEM and stereomicroscopy

Additional measurements were carried out to collect more evidence that the enhanced healing performance in the bacterial specimens can be attributed to the bacteria-based healing system. The surface of cracks was evaluated with a stereomicroscope to investigate the surface crack closure before and after the healing treatment and also after the exposure to the

test environments. More detailed information on the crack healing was obtained by observing the mineral precipitates along the crack surface by ESEM.

7.3.5 Oxygen consumption analysis

The healing potential investigation was continued by oxygen consumption analysis. The type of bacteria used, which are in form of spores lying dormant in the concrete matrix, should become active after activation by water entering freshly formed cracks. Activated bacteria subsequently seal cracks by the process of metabolizing nutrients which are converted to calcium carbonate precipitates, a process that requires oxygen. Similar steps from Section 6.2.4 were applied in this study on both type of specimens (control and healing agent containing) for oxygen concentration measurements. The analysis was performed on freshly fractured and dry sawn control and bacterial specimens. The crack surface with exposed healing agent was immersed in buffered (carbonate-bicarbonate) solution at room temperature with continuous stirring of the solution in an open system as shown in Figure 7.10. Profiles of oxygen concentration and oxygen uptake by specimen were measured using fibre optic oxygen sensors by moving the sensor stepwise towards the specimen surface as described in Section 6.2.4 and reference [14].

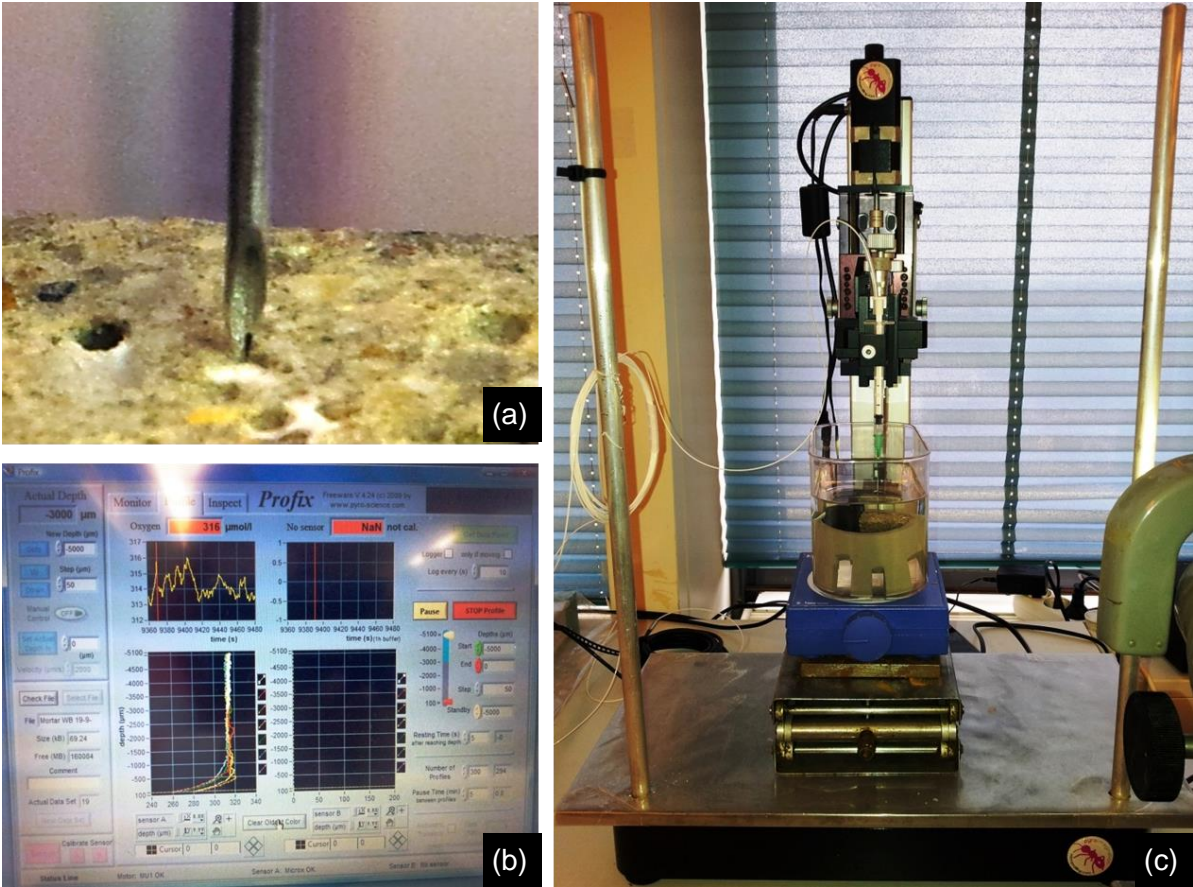


Figure 7.10(a) Oxygen micro-sensor approaching the surface with exposed healing agent; (b) Microprofiling software prefix; (c) Motorized micromanipulators with stand

7.4 Results and discussion

7.4.1 Crack opening displacement

The crack width was kept in a narrow range to limit the effect of crack width on the compound ingress rate [5]. A single crack appeared approximately in the middle of the prism with a span of 142 mm. The obtained load displacement graphs are given in Figure 7.11 for specimen of 9 weeks exposure period and Figure 7.12 for specimen of 18 weeks exposure period. The crack produced by 3-point bending was not straight but appeared more tortuous. From Figure 7.11, it can be seen that most specimens were cracked to yield about 300 μm displacements after unloading. However, a wider crack opening displacement of about 350 μm was recorded for the samples set prepared for 18 weeks exposure period in both bacterial and standard mortars (Figure 7.10).

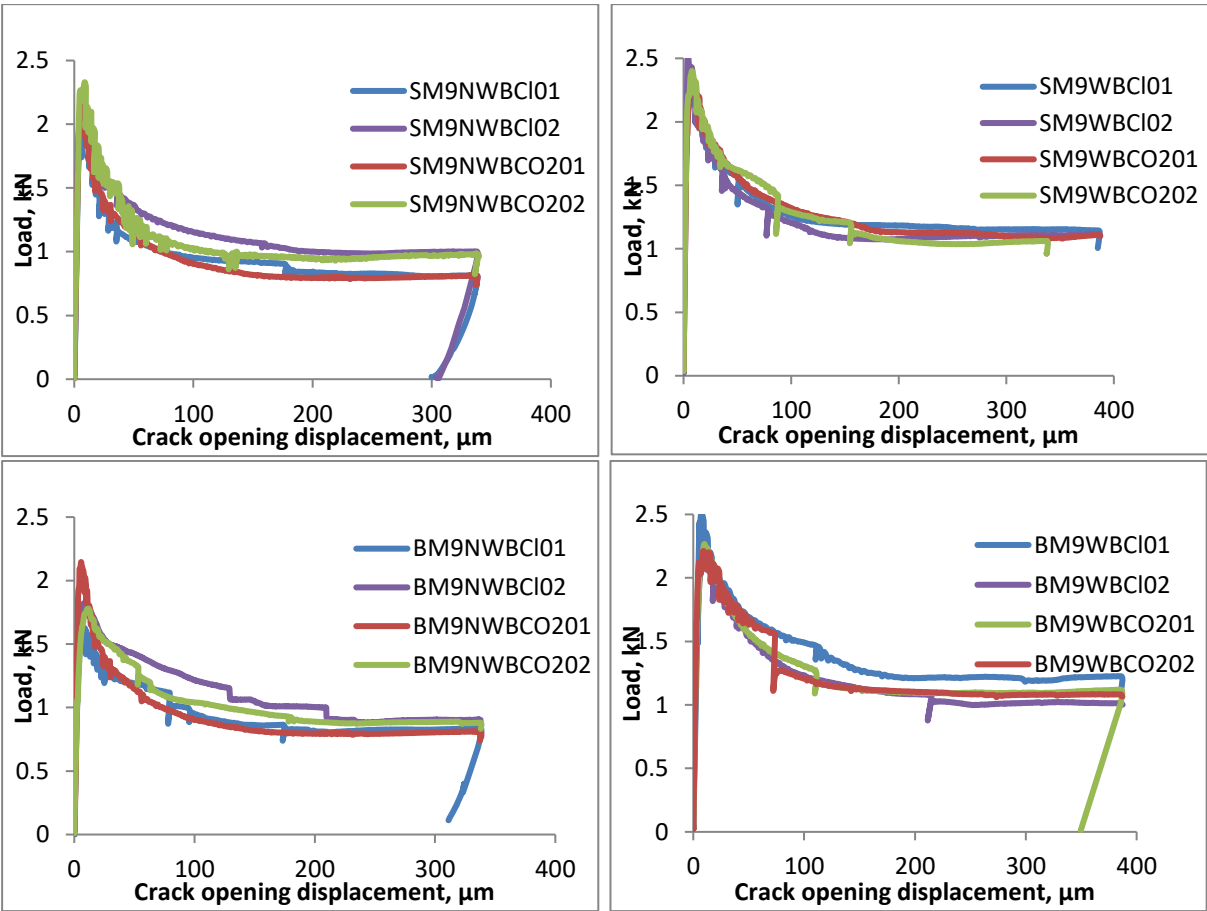


Figure 7.11 Load-displacement curves of mortar prisms prepared for 9 weeks aggressive environment exposure

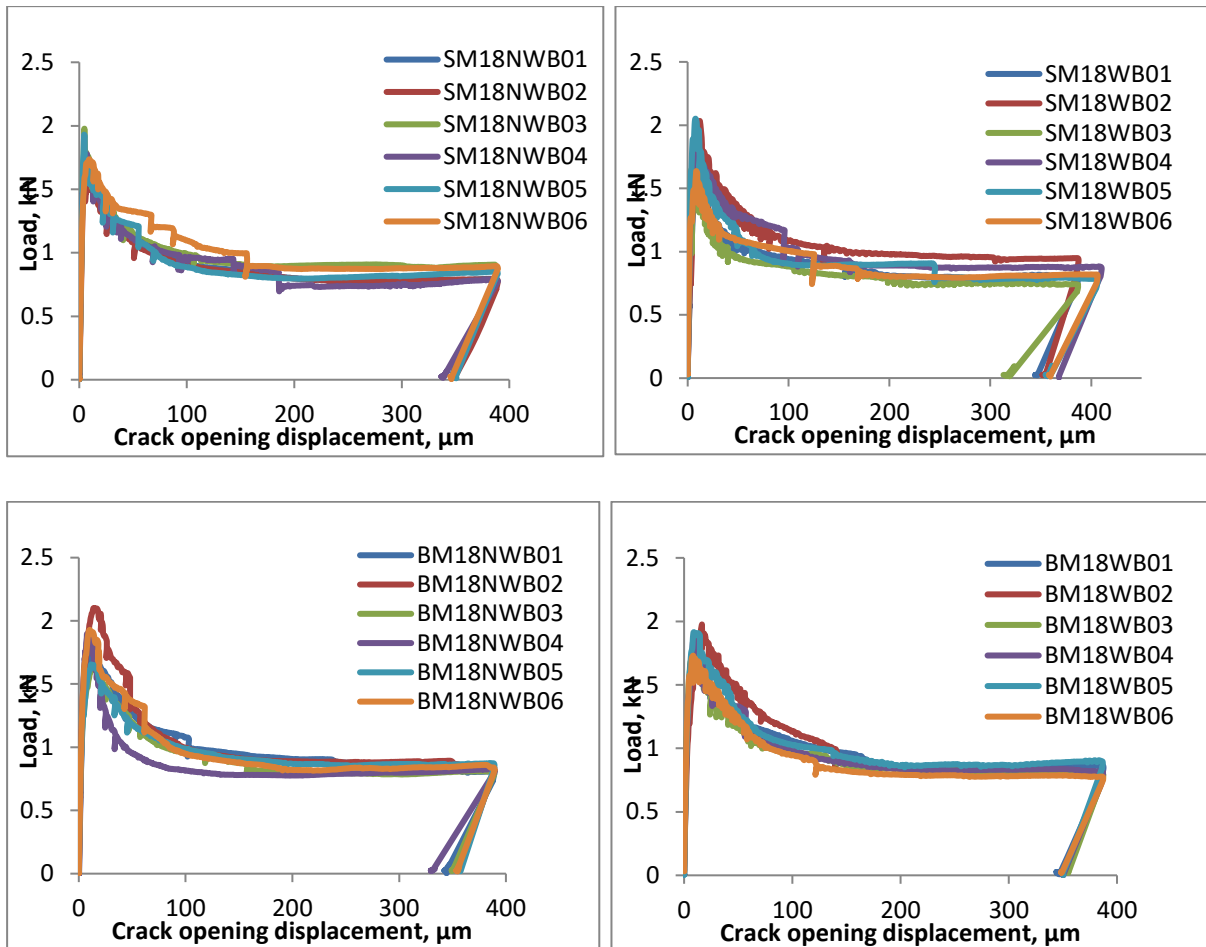


Figure 7.12 Load-displacement curves of mortar prisms prepared for 18 weeks aggressive environment exposure

7.4.2 Crack-healing capacity

Crack closure at the crack mouth from both control and healing agent-containing specimen was visualized by stereomicroscopy. Figure 7.13 (a) and (b) show healing after three and 28 days of healing treatment of reference and healing agent-containing specimens, respectively. The images were taken three days after the bending test as there was a technical problem with the images taken right after the bending test. Only images at three days and 28 days of healing treatment were available for the comparison of the healing progress before 9 weeks of chloride and carbonation test. It was observed that autonomous healing already took place within three days as mineral formation was clearly visible at the crack mouth in bacteria-based specimen. No mineral formation, i.e. autogenous healing, was detected on the crack surface of control specimen. At 28 days, the higher healing capacity of bio-healing agent-containing samples is more obvious. In a study by Wiktor et al. [4], it was observed that complete crack-sealing in bio-based concrete took substantially longer, i.e. 100 days of immersion in tap water for complete healing of 460 μm wide cracks. The longer incubation period, the higher the crack-healing percentage of bacteria-based specimen.

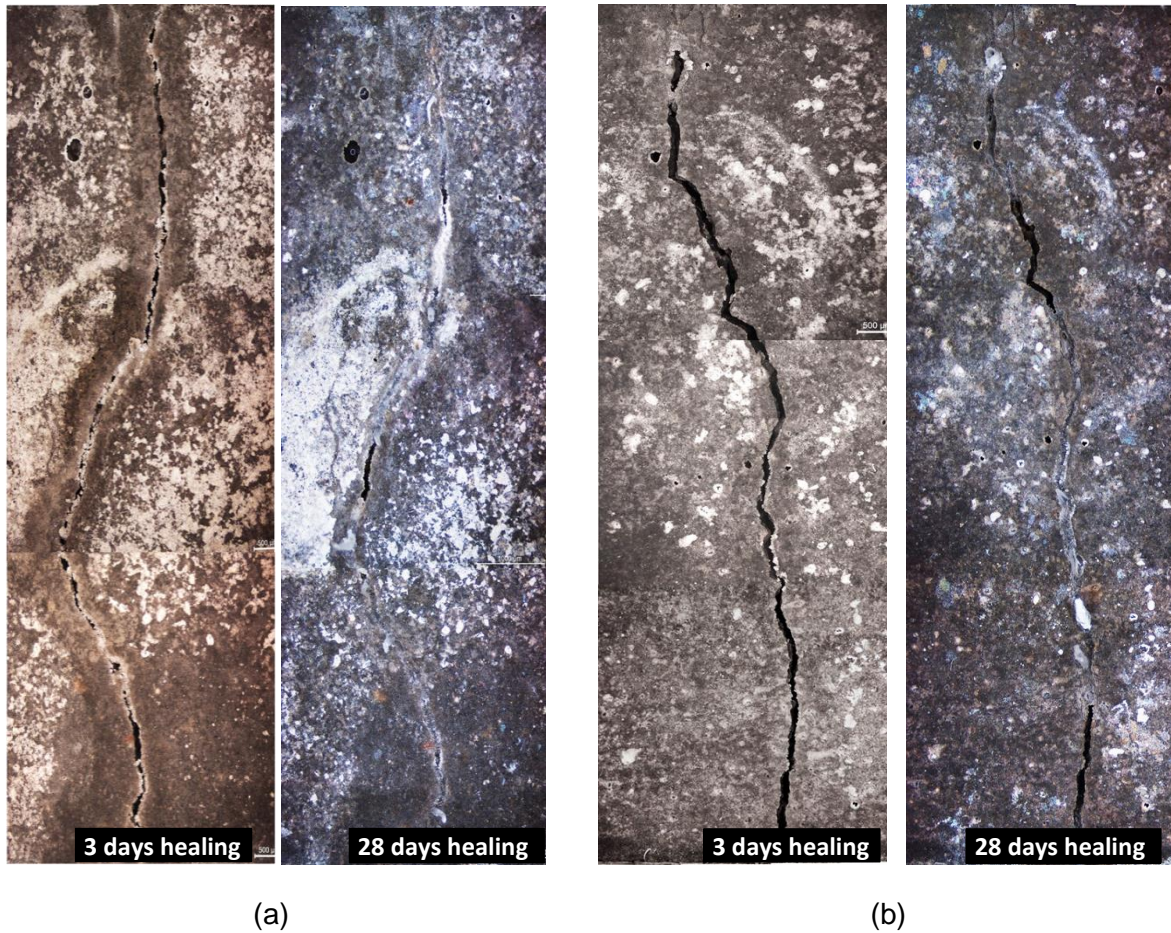
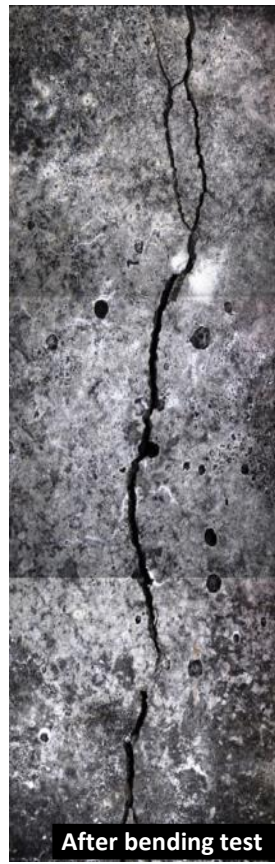


Figure 7.13 Observed crack-healing by stereomicroscopy in bacteria-based specimen (a), and in control specimen (b) for 9 weeks exposure mortar prisms.

Crack-healing was studied further in 18-weeks old specimens, and the results are shown in Figure 7.14 (a) – (f) with images taken immediately after three-point bending and after 28 days healing. A series of replicate samples was compared and from these it could be concluded that at least 50% of healing occurred in bacteria-based specimens at the end of four weeks storage under wet conditions. As a matter of fact, autogenous healing of control specimen was only effective for crack widths of less than 200 μm [26]. Furthermore, the concrete mix composition and the time of healing will have a large influence on the autogenous healing. From these observations it can be speculated that the transportation and amount of an aggressive agent such as chloride ions will be delayed due to blocking of the cracks, and that this effect is significantly more pronounced in specimen amended with bacteria-based healing agent in comparison to control specimen.



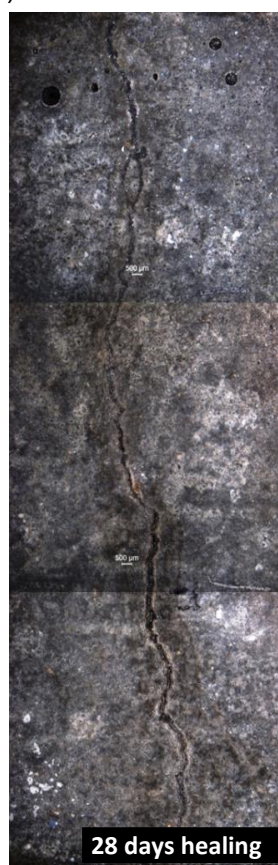
(a)



(b)



(c)



(d)

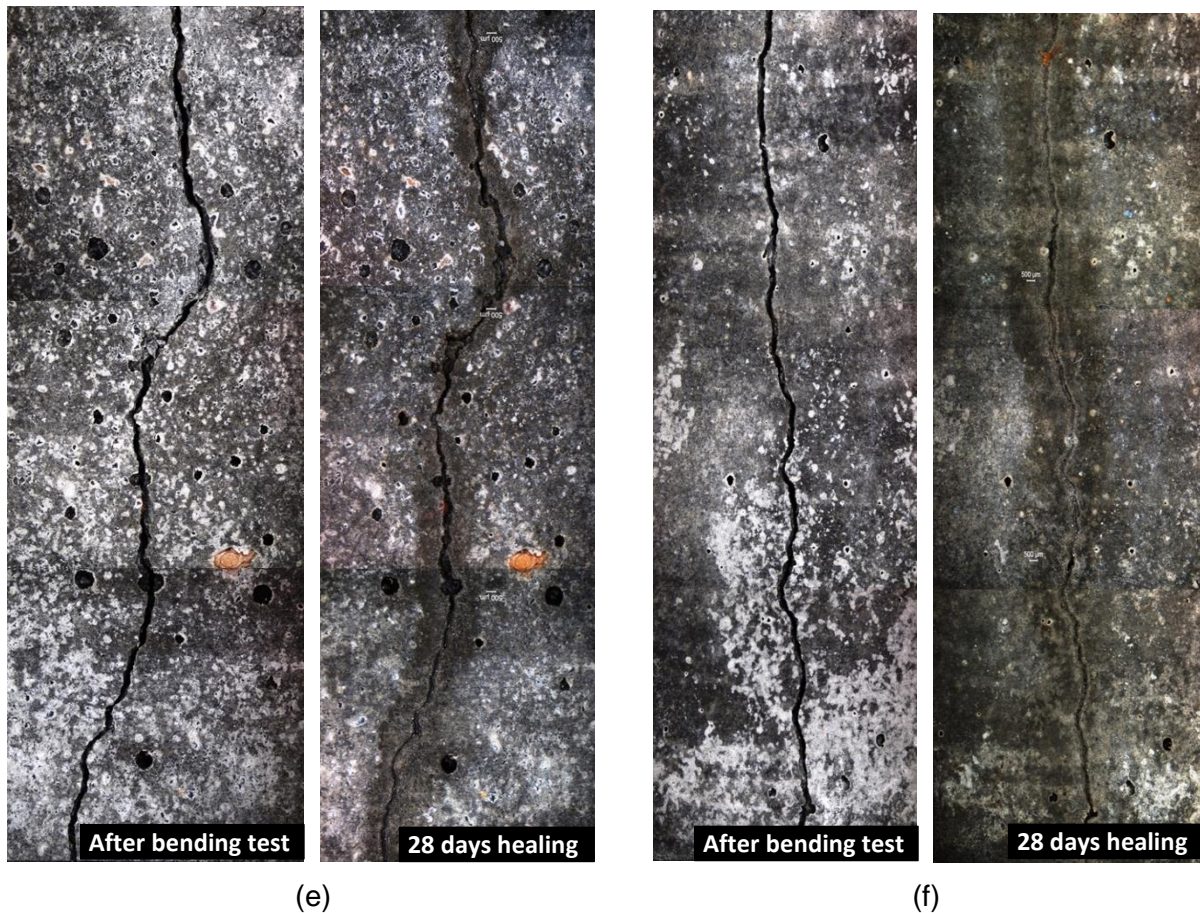


Figure 7.14 Visualization of crack-healing process on 18 weeks old mortar prisms by stereomicroscopy before and after healing treatment (a)-(c) in bacteria-based specimens and (d)-(f) in control specimens.

7.4.3 EDS mapping analysis

For microscopic visualization of crack-healing at the surface of cracked specimens is insufficient to draw conclusions on the effective functionality of the healing process, the samples were further analyzed by X-ray mapping for chloride ingress tracking. The intensity of chloride ions ingress depicted in Figure 7.15 to 7.17 were indicated by the red color gradient. Dark red represents a higher chloride concentration. The color-coding with range of value listed in the legend of the images denotes the weight percent of the chloride elements in the mortar sample obtained from the EDS scanning analysis. The results show that the distribution of chloride was clearly modified by the application of the bio-based healing system. The chloride permeability appeared, as expected, to be more pronounced at the exposed surface of both control and bacterial specimens. In the early phase of chloride exposure, i.e. during the first 9 weeks of specimens exposure to chloride solution, it was observed that the chloride ion distribution of healing agent-containing mortar specimen was higher than in the reference specimen. More dark red colour was spotted as shown in Figure 7.15 (a). This observation can be explained by the presence of extra voids in healing agent containing specimen as in these the pore size distribution was modified due to incorporation of the healing agent. It is unlikely that these voids can already become fully sealed by microbial calcite precipitation in this early phase as this process may take several months as was found in previous studies [75-77, 84].

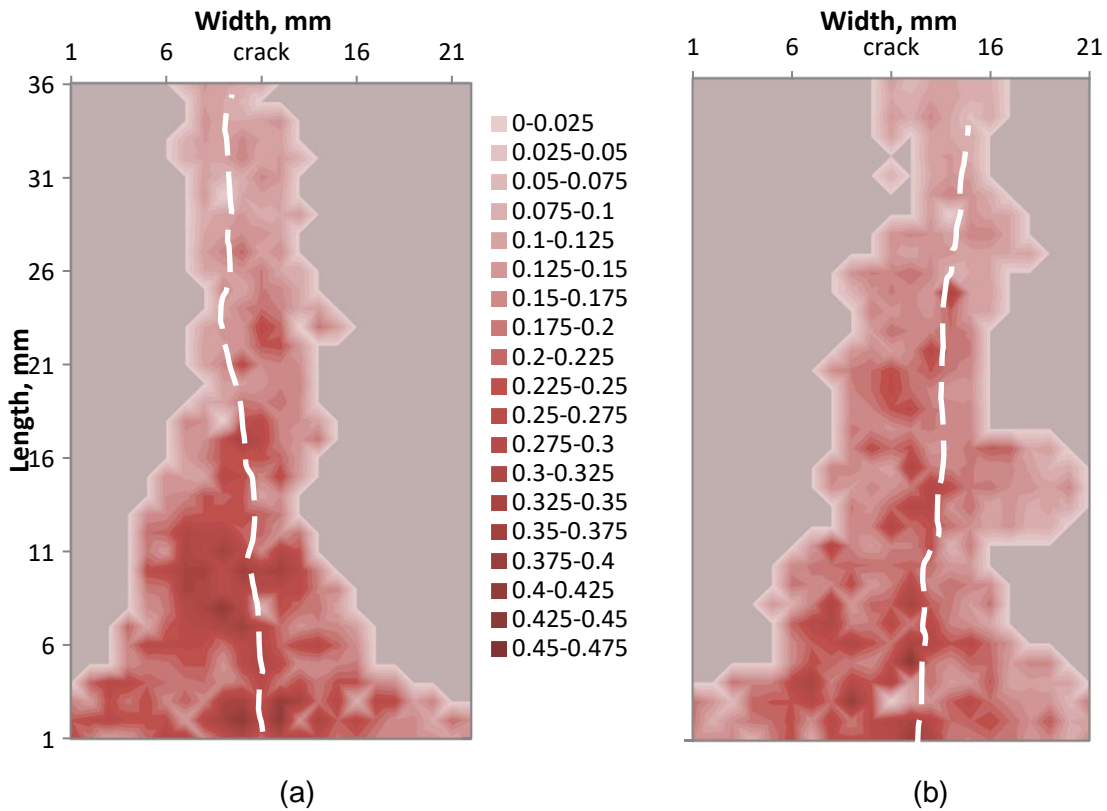


Figure 7.15 Chloride distribution in 9 weeks bacteria-based specimen (a) and control specimen (b) which were subjected to a healing treatment. (The numbers in the legend (colors) representing the weight percentage of the chloride elements).

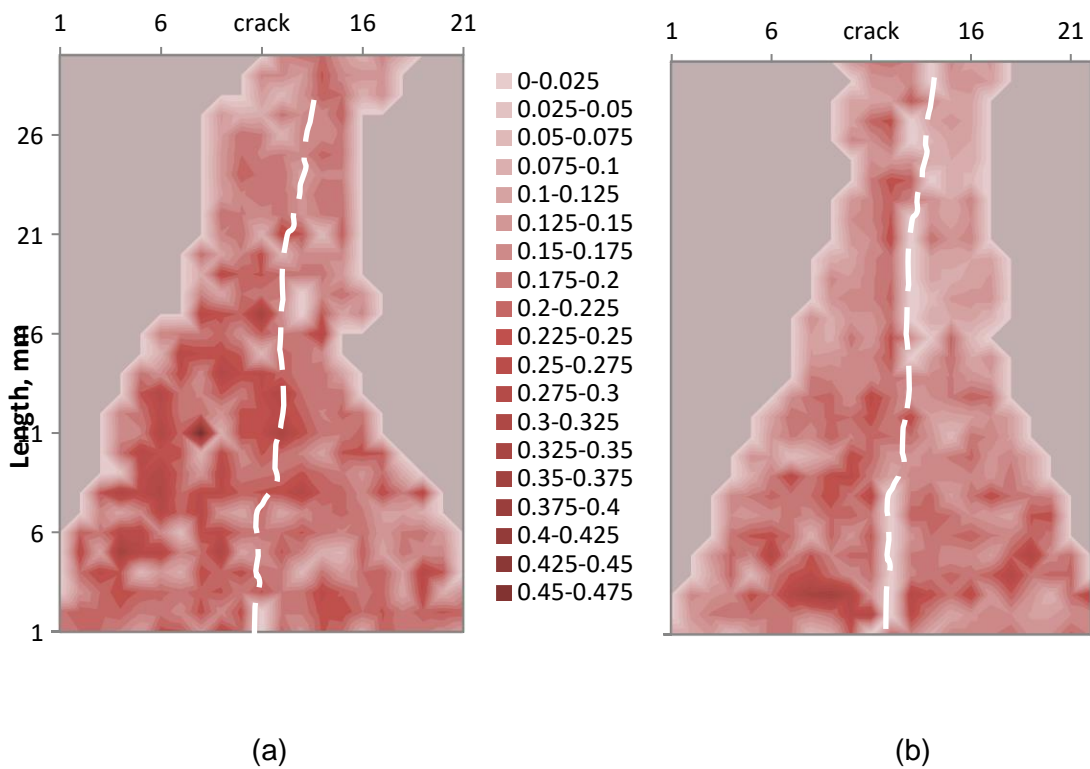


Figure 7.16 Chloride distribution in 18 weeks bacteria-based specimen (a) and control specimen (b) which were not subjected to a healing treatment

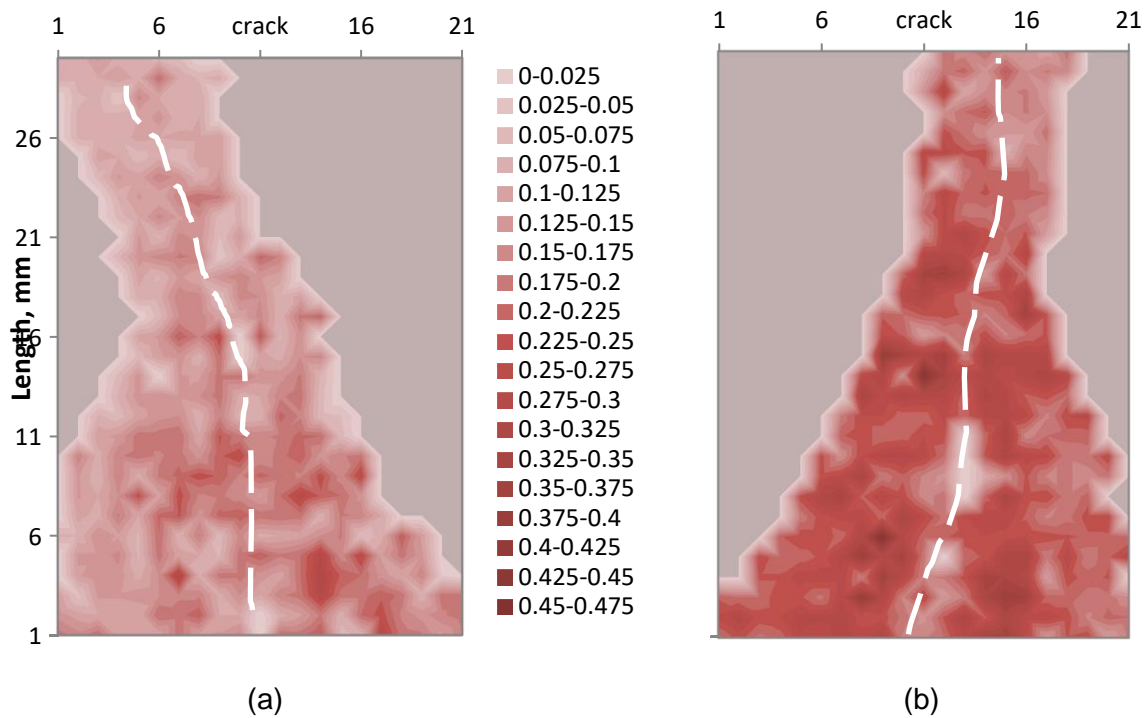


Figure 7.17 Chloride distribution in 18 weeks bacteria-based specimen (a) and control specimen (b) which were subjected to a healing treatment

Although it was not significant, the red colour gradient reduced in Figure 7.16 after exposing the samples for 18 weeks in chloride solution, in which indicated that the gradient of the chloride ions started to reduce in both control and bacteria-based cracked specimens which were not subjected to a healing treatment. However, in contrast to that, a substantial decrease of chloride concentration was noticed in cracked specimen which were subjected to 28 days of healing treatment before chloride exposure. In comparison to control specimen, bacterial specimen showed a substantial reduction in the gradient of the chloride ions as presented by low colour gradient of red in Figure 7.17 (a). The decrease was attributed to the microbially mediated calcium carbonate precipitation, which hindered the ingress rate of chloride. Adversely, substantial chloride concentration was observed in specimen without bio-healing agent with high red colour gradient spotted in Figure 7.17 (b).

The increased chloride ion concentration through the crack in an 18-week water incubated control sample may be due to the limited amount of cement hydration products formed (autogenous healing) at the surface of the crack during elapsed time. For more than three months (18 weeks sample in chloride solution) aged specimen, it was indeed expected that these would contain only a limited amount of unhydrated cement. Furthermore, as the samples were soaked in demineralized water prior to the chloride test, present calcium hydroxide may have leached out due to its solubility, a process that produces macro-porosity. Particularly in these aged specimens, it is expected that microbial calcium carbonate production leads to considerably higher self-healing (sealing) of cracks in comparison to reference specimens. The amount of chloride ingress rate is therefore also expected to be much lower in aged healing agent-containing specimen in comparison to equally aged control specimen. Due to the slow process of healing, however, it may take several weeks to months to completely fill the crack. Over time, the growth of calcium carbonate crystals seals the crack,

the rate depending on crack width and other factors. In the case of healing by bacteria, the slow process of calcium carbonate precipitation could be attributed to limited physicochemical environmental conditions for metabolic activity. For instance, limitation of oxygen availability in the deeper part of the crack or the low temperature ($< 10^{\circ}\text{C}$) or too high pH ($\text{pH} > 11.5$) or too low pH ($\text{pH} < 8$) are factors which slow down the bacterial calcium carbonate precipitation rate. Therefore, repetitive replenishment of the specimen incubation water by fresh oxygenated water could increase the rate of bacterially controlled crack sealing. The sealing of cracks reduced the permeability and prevented chloride ions from penetrating into the matrix. The network formed by interconnected internal cracks can thus be blocked from the exposed environment when the crack, which is open at the surface, becomes completely sealed.

The healing occurrence was further observed by the presence of whitish deposits along the internal crack line of epoxy impregnated samples, indicative for the healing process as shown in Figure 7.18. The area with the whitish deposit was scratched to detach it from the thin epoxy layer, thus enabling element quantification by EDS point analysis. The analysis was carried out in three distinctive areas beside the location of a white deposit to clearly distinguish the signature of the white deposit from the cement stone matrix. From the results given in Figure 7.19 it can be seen that point one (1) and three (3) exhibit higher counts for calcium- and carbon- atoms, while point two (2) indicates the area that was still covered by a thin layer of epoxy with only greater counts of carbon atoms. Qualitatively, this indicates appearance of C-S-H products at the spotted area. Moreover, as the weight percentage of oxygen atoms was three times that of calcium, it also indicates the presence of calcium carbonate-based minerals.

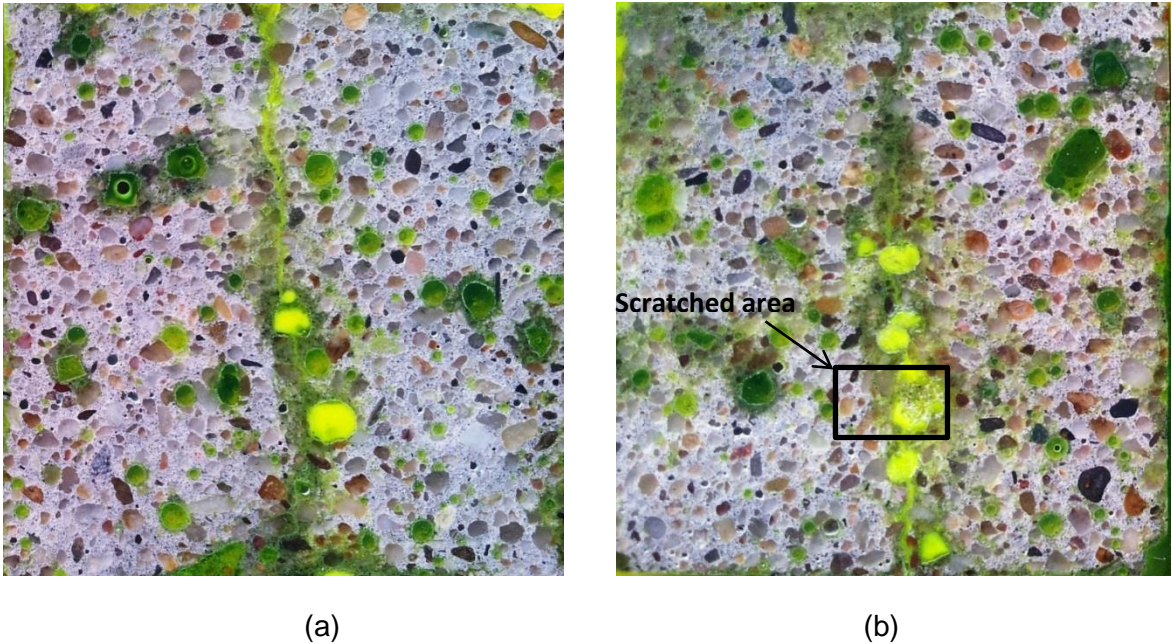


Figure 7.18 Evidence of healing spots by the presence of whitish deposits along the internal crack line (a) with indication of scratched area for EDS point analysis of epoxy impregnated samples (b)

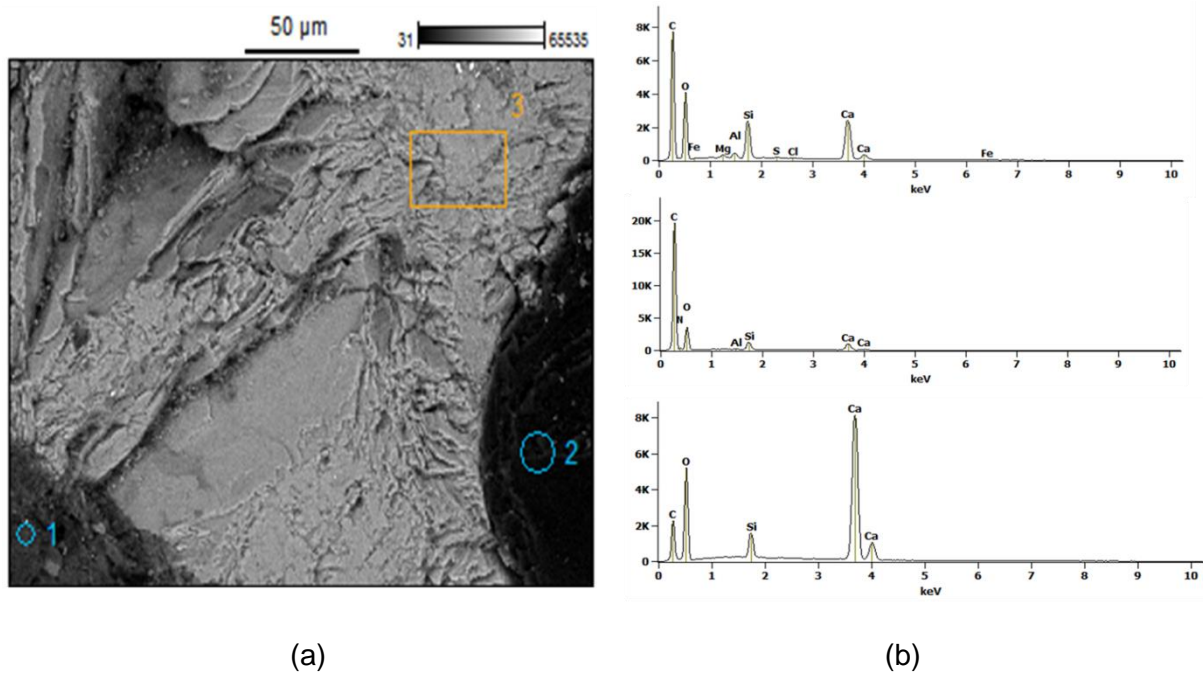


Figure 7.19 EDS point analysis in three different regions (a) with corresponding element counts (b)

7.4.4 Carbonation

In the process of carbonation, carbon dioxide from the air reacts with calcium hydroxide ($\text{Ca}(\text{OH})_2$), present in the concrete matrix to form calcium carbonate (CaCO_3), and also with the hydrated cement paste what can lead to reduction of alkalinity and to pH values as low as 8.5. Therefore, the phenolphthalein test was performed on freshly fractured samples on longitudinal sides of both control and bacterial specimens for determination of the carbonation depth. An insignificant depth of the carbonation front along the crack lines was observed in the early phase of 9 weeks exposed specimens as well as in the intermediate phase of 18 weeks carbonated specimens as visualised in Figure 7.20. Carbonation in general is a very slow process and, with low permeability of mortars made from Portland cement, the process takes a considerable long time. In recent study on influence of loads on carbonation and chloride transport in concrete phases [108], the results also showed that the effect of load on the depth of chloride ingress was more significant than the effect of carbonation. Lower penetrability of carbon dioxide into concrete was also due to water presence in the crack. The rate of dissolved inorganic carbon species diffusion is also governed by the crack width and the permeability of the crack space [158].

On the other hand, it can be seen in the 9 weeks exposed bacterial specimen that the propagation of the carbonation front was reduced by the microbial activity. In Figure 7.20 (a) localized phenomena are visualized as carbonation was only observed at a small perimeter nearby the healing particles, indicative for microbial production of carbonation. Intense carbonation may occur if all the bacterial nutrients and calcium lactate ($\text{Ca}(\text{C}_3\text{H}_5\text{O}_3)_2$) is fully metabolically converted. However, that is not always the case as it happens only locally in the crack region where the bacteria are active. Therefore, further investigations were carried out by means of helium pycnometry to more closely study the effects of carbon dioxide production in cracks of bacteria-based mortar specimen.

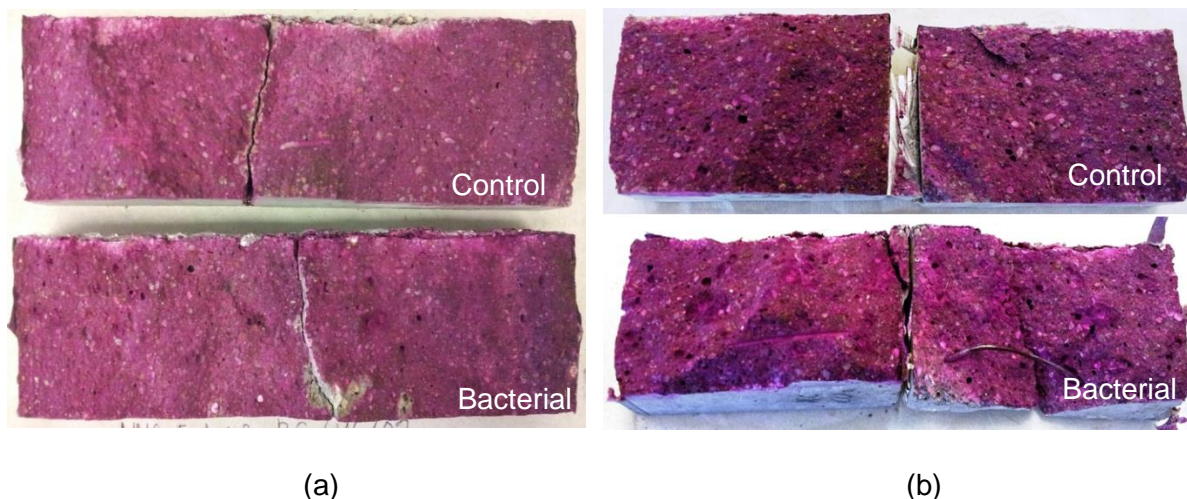


Figure 7.20 Observation of carbonation depth in 9 weeks (a) and 18 weeks (b) exposed specimens by application of the phenolphthalein test

7.4.5 Gas expansion pycnometer

The solids volume of 18-week samples exposed to carbonation are tabulated in Table 7.1. Based on Equation 7.1, the total pore volume accessible to helium is presented in Figure 7.21. Results show the porosity of control specimens were higher than that porosity in bacteria-based specimens not subjected to healing treatment. Although it was found that the bacterial specimens were more porous in early days, towards the continuous hydration process of cement, it leads to decrease in porosity consequential in increased at strength better than standard mortar. With healing treatment, however, only a marginal effect in pore volume decrease (of 2%) was detected in samples containing bacteria in comparison to a considerable reduction of 22.5% for the control samples. A negligible difference was observed between samples containing bacteria with and without additional water immersion for healing treatment. The results obtained did apparently not allow sufficient difference in the extent of CO₂ infiltration into the concrete to establish expected reduction of pore volume over time. Future studies should consider increasing the relative humidity of carbonation chamber as it could be the reason that the bacteria have inadequate moisture to be activated during the exposure period as maximum relative humidity is especially essential for bacterial spores to germinate. Additionally, the results found in control samples can possibly be explained by leaching of calcium hydroxide from samples immersed in water during healing treatment, a process that creates larger pores and subsequently increased carbonation of the CSH matrix. For the results obtained from pycnometer measurements, it should be pointed out that only relevant porosity was measured, as the relevant porosity is the porosity that provide access to moving fluids [51].

Table 7.1 Volumes of samples exposed to carbonation

Samples	Bulk-volume, V_b (cc)	Solid volume, V_{ma} (cc)
NWB-SM	13.8	11.8
NWB-BM	16.2	14.3
WB-SM	14.7	13.2
WB-BM	16.4	14.5

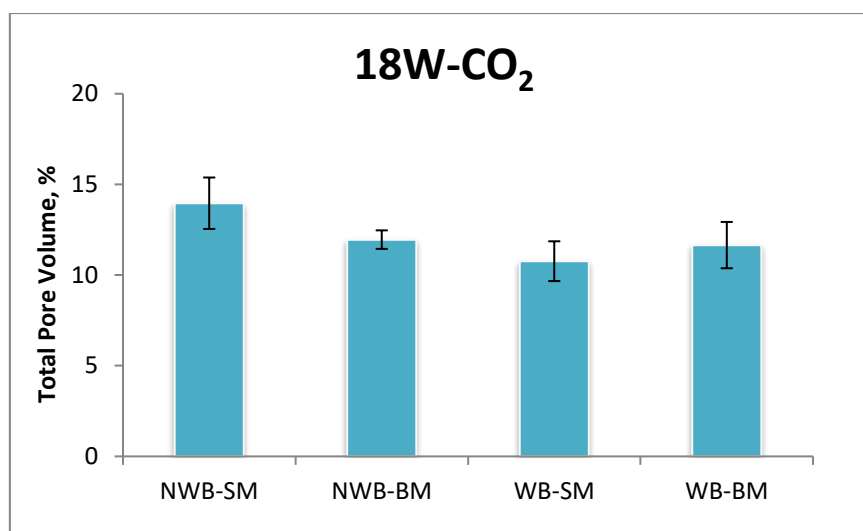


Figure 7.21 Total pore volume of 18 weeks carbonated samples without (NWB-) and with (WB-) additional underwater curing in control (-SM) and bacteria-based (-BM) specimens

7.4.6 Optical observation of bacterial imprints

Single calcite rhombohedra were formed by autogenous healing due to chemical reaction of carbon dioxide with calcium hydroxide present in the material matrix. Additives are known to have a strong effect on crystal morphology, as well as organic additives [159] and pH values [160, 161]. Thus, the influence of bacteria on calcium carbonate crystallization due to metabolic conversion of calcium lactate was studied using ESEM. In the 9 weeks cured bacterial sample, copious formation of “rosette-like” aggregates was observed near the crack surface what indicates the nucleation of CaCO_3 in the unstable form of vaterite (Figure 7.22). In addition to that, intermediate morphologies between stacks and rosettes were also noticed in the same area of observation as displayed in Figure 7.22 (a). This means in the latter case that mineral crystals become more stabilized possibly depending on the amount of free calcium ions present. However, crystallization would be less likely to occur near the crack surface due to less free calcium that is available to form calcite crystals.

No bacterial imprints were spotted in crystals present at the crack surface possibly due to overgrowth of calcite crystals on the crystal core for which formation bacteria might have been initially responsible. The search for bacterial imprints was continued close to embedded healing agent particles of the same sample. Interestingly, similar crystal morphologies of calcium carbonate polymorphs of vaterite (rosettes) were captured with a few visible imprints present as shown in Figure 7.22 (d). Bacterial imprints are indicative for formation of metabolically controlled mineral crystals at the surface of cracks.

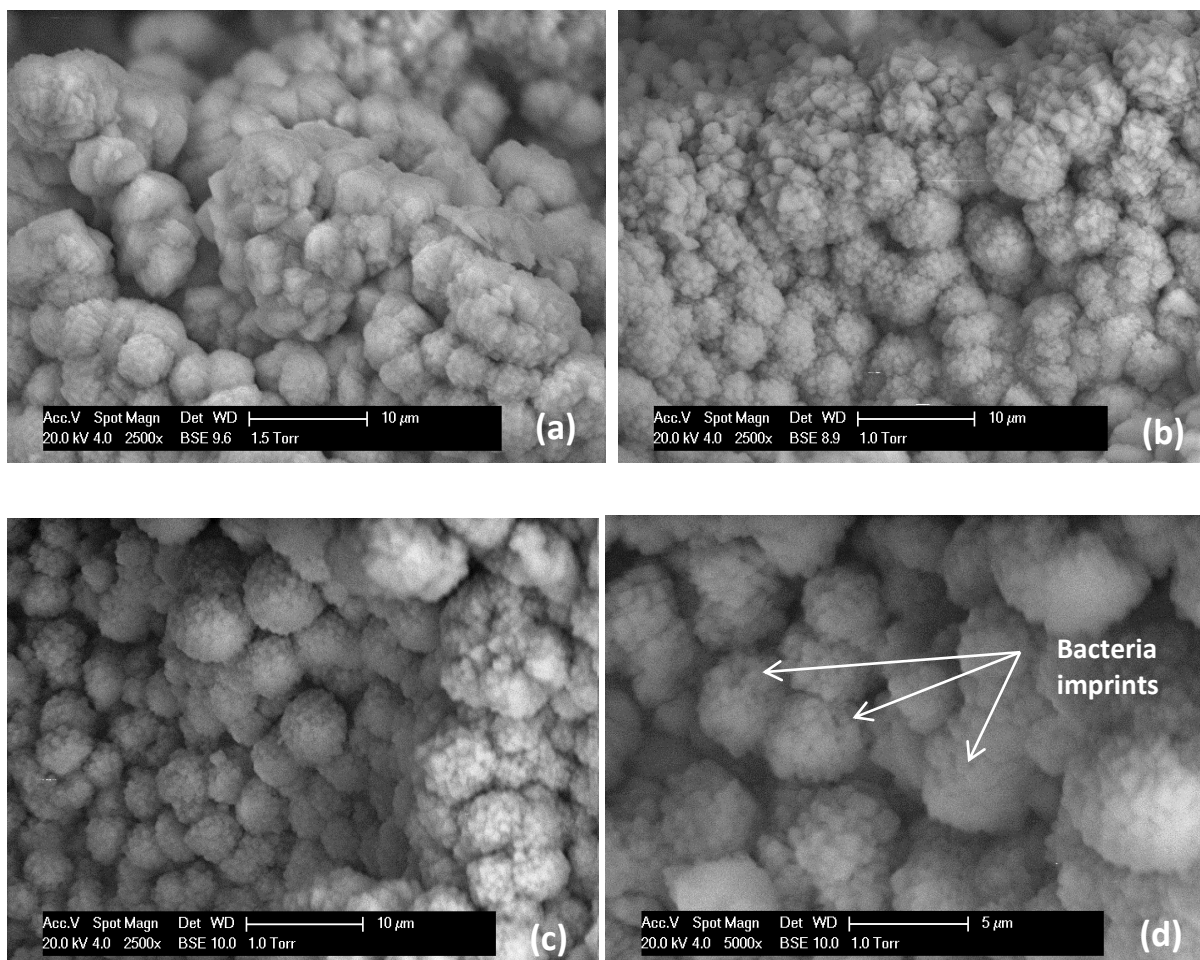


Figure 7.22 ESEM images of (a-c) bacterial calcite deposition in microcracks with (d) imprints in 9 weeks cured bacterial samples

From 9 weeks cured samples it can be learned that imprints in precipitated limestone crystals can be visible if metabolically active bacteria are present. Therefore, in older 18 weeks cured samples which featured significant oxygen consumption and limestone precipitation more visible bacterial imprints were expected to occur. Figure 7.23 shows scanning electron micrographs taken at higher magnification. Contrary to the previous ESEM images taken of 9 weeks cured specimen, calcite formed in multiple layered crystals (stacks of rhombohedra) could be observed in these aged specimens. Moreover, the imprints were clearly seen in every image taken which show a strong indication of the direct involvement of metabolically active bacteria in the calcium carbonate precipitation process.

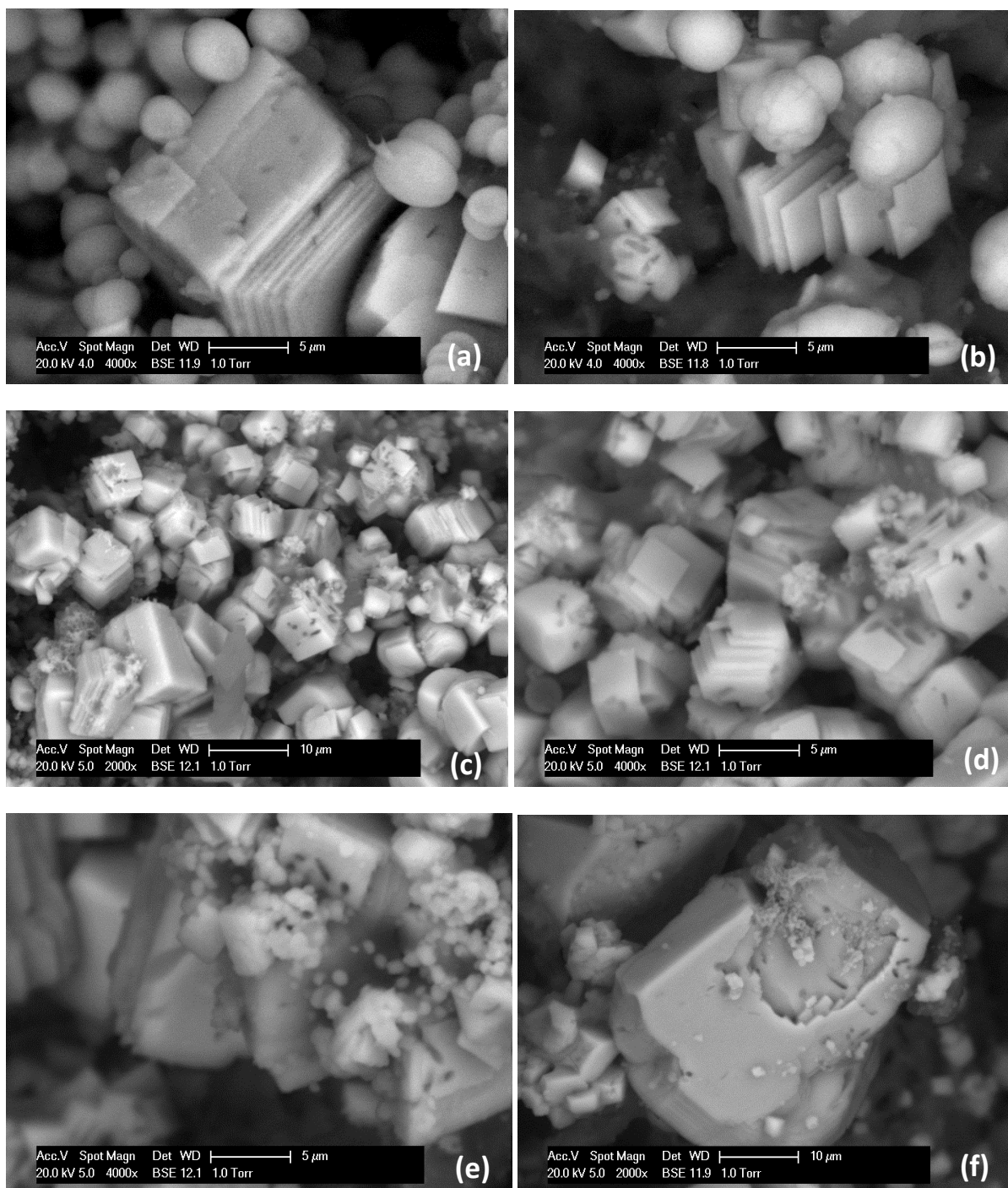


Figure 7.23 ESEM images of (a)-(b) multi-layer crystalline calcite precipitates with presence of (c)-(f) bacterial imprints in 18 weeks cured samples

The occurrence of the bacterial imprints in the formed calcite crystals provides strong evidence for metabolically controlled formation as no similar marks or shapes were identified on crystals formed in control samples. In this case, the control samples yielded single rhombohedral crystals. The materials were then further analyzed by Fourier-Transform InfraRed (FT-IR) spectrometry for identification of type of calcium carbonate-based minerals. Typical infrared frequencies for calcite, vaterite and aragonite structures in calcium carbonate polymorphs are listed in Table 7.2. As shown in Figure 7.24, the results are in good agreement with the vibrational modes associated with the FTIR peaks documented in literature review

[162, 163]. It was observed that the strong band centred at 1451 cm⁻¹, concerning asymmetric stretching mode, ν_3 of carbonate together with the narrow peak at 1085 cm⁻¹ of the symmetric stretching mode, ν_1 . The observed band at 870 cm⁻¹ and the small peaks at 750 and 712 cm⁻¹ are assigned to the out-of-plane bending, ν_2 and in-plane bending, ν_4 modes as distinct peaks seen in the calcium carbonate spectrum. The satellite bands for vaterite and calcite were indeed identified as the only crystal polymorphs present in all cases. Conclusively, this result highlighted the potential contribution of bacteria-based healing agent in hindering the ingress of chloride in crack-containing mortars.

Table 7.2 Infrared spectra (in cm⁻¹) of calcium carbonate polymorphs [147]

	ν_3	ν_1	ν_2	ν_4
Calcite	1432	1087	881	712
Vaterite	1450	1090	850 878	741 747
Aragonite	1430 1550	1087	866	703 715

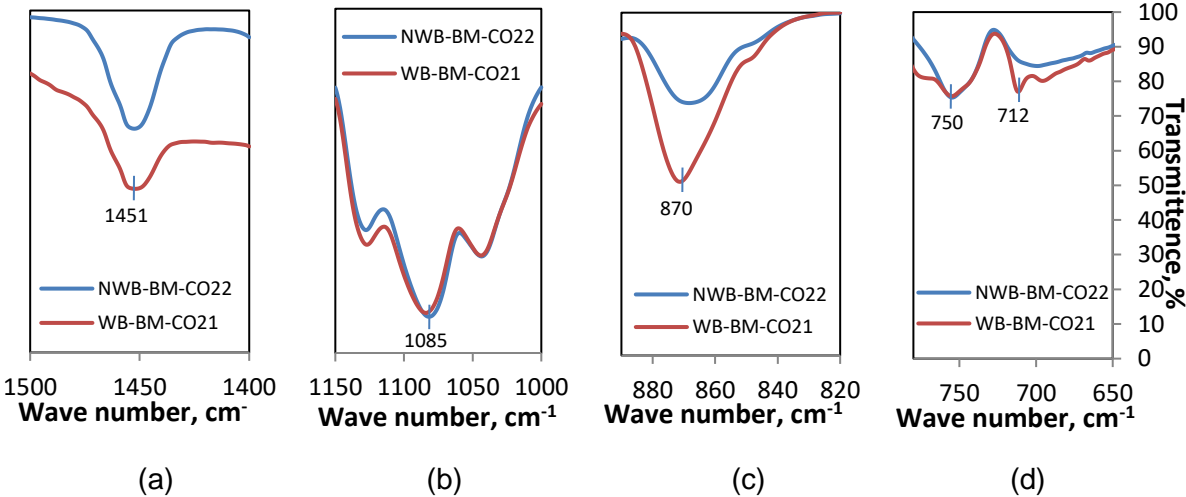


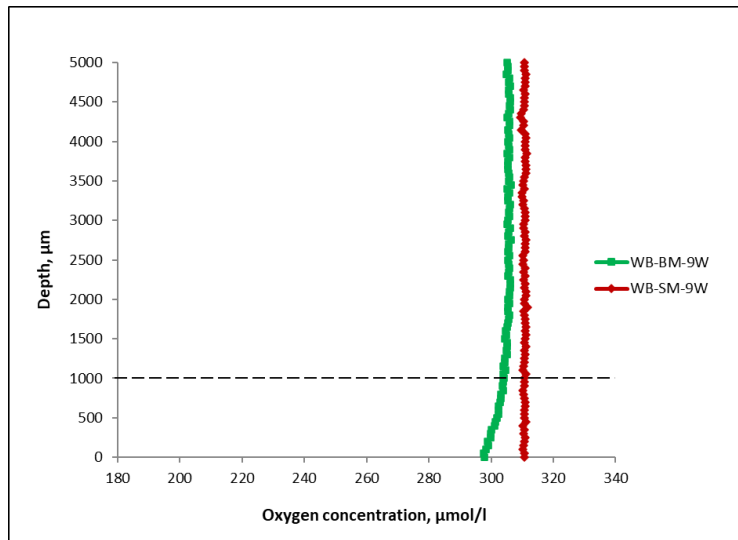
Figure 7.24 Detailed FT-IR spectra of (a) ν_3 (b) ν_1 (c) ν_2 and (d) ν_4 in 18 weeks cured samples

7.4.7 Oxygen consumption test

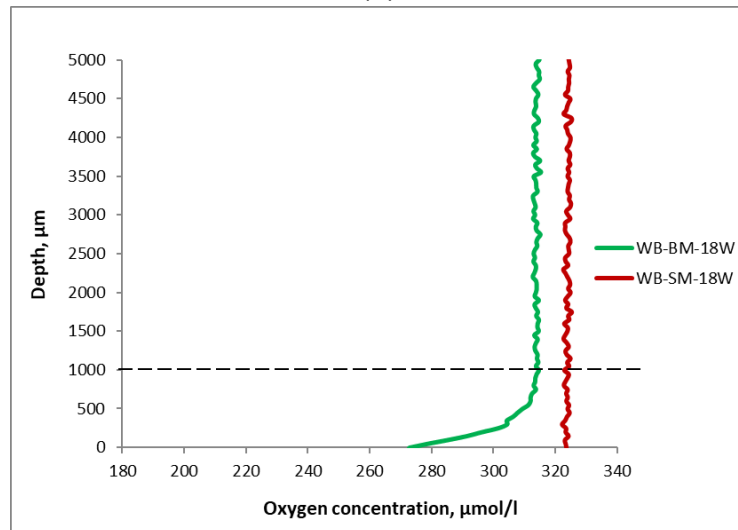
The observation of bacterial imprints confirmed that the observed calcite deposition was due to the presence of metabolically active bacteria. The additional observation of oxygen consumption further confirms the presence of metabolically active bacteria which requires oxygen during the metabolic conversion of calcium lactate. In this study, oxygen profiles were obtained from 5 mm maximum depth towards the surface of the specimen in vertical steps of 50 μm . In Figure 7.25, it can be seen that the oxygen profile for specimen without embedded bio-healing agent had constant oxygen concentration throughout the 5 mm diffusion boundary layer (indicated by the roughly vertical line). This is due to zero oxygen consumption occurring in the bacteria-free specimen. In contrast, a significant drop in oxygen concentration was revealed in the approximately 1 mm thick diffusion boundary layer of 9 weeks cured healing agent-containing specimen as shown in Figure 7.25 (a). Oxygen depletion in the local environment around bio-based healing particles contributes to evidence for the presence of

metabolically active bacteria, converting growth requiring nutrients (i.e., calcium lactate) eventually into calcium carbonate. Deeper than 1 mm, the oxygen consumption was low and constant.

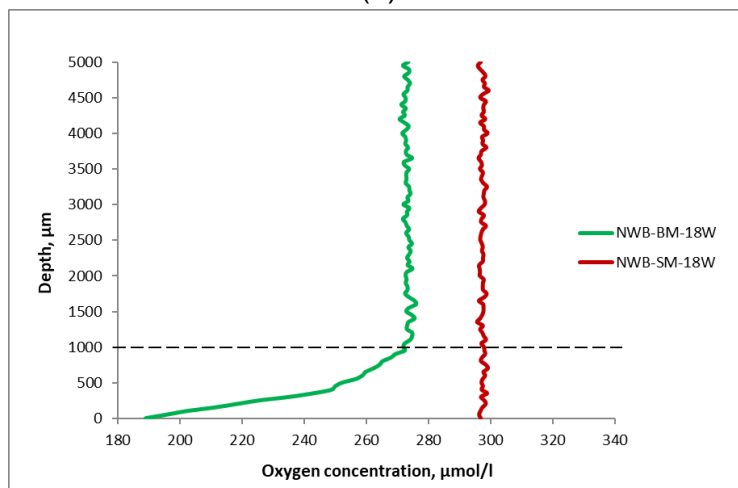
Additionally, the samples should have tested at 18 weeks of exposure duration, which is at 126 days. However, few attempts have been made and only at 140 days when another crushed sample were tested, the results started to indicate an oxygen consumption by the bacteria. Figures 7.25 (b) and (c) show substantially increased oxygen consumption rates in 140 days hardened mortar specimen, as the drop in oxygen concentration in the diffusion boundary layer was higher than in that of 9 weeks cured specimen. An even larger drop in oxygen concentration, shown in Figure 7.25 (c), occurred in a sample that was not primarily subjected to incubation under water but only at later age. This strongly suggests that healing particles present in the hardened matrix may become rapidly metabolically active when exposed to incubation water, and the high rate of observed oxygen consumption in these specimens can be explained by the still copious amount of nutrient (calcium lactate) present. In time, as nutrients are converted and their availability becomes scarce, the rate of oxygen consumption is also expected to decrease. From these results it can be concluded that although in a cracking event with the presence of water, oxygen, and nutrients, the bacteria can still remain dormant if the values of temperature and pH are not within their range of potential metabolic capacity. Therefore, a specific combination of metabolic pathway, activity, and physicochemical environmental conditions are essential for bacterial metabolically driven calcium carbonate precipitation [85].



(a)



(b)



(c)

Figure 7.25 Oxygen concentration microprofiles of healing agent-containing- and control specimen in 9 weeks samples (a) and 18 weeks samples subjected to a healing treatment (b) and 18 weeks samples not subjected to a healing treatment (c) but freshly incubated under water

7.5 Conclusions

The healing capacity of bacteria-based healing agent on cracked mortar specimen was investigated under exposure to chloride and carbonation using a variety of techniques, including stereomicroscopy, EDS mapping, helium pycnometry, environmental scanning electron microscopy, oxygen (micro)-sensor techniques and FT-IR. Cracked mortar specimens with and without the presence of bacterial healing agent were prepared and subjected to either healing treatment (water incubation) or control treatment. The obtained results from stereomicroscopic analysis showed that cracks were significantly healed in bacteria-based but healed to a minor extent in control specimen. As to provide evidence for functional crack healing concomitantly resulting in enhanced material durability, chloride ingress obtained from bacterial specimen was compared to control specimen.

Localization and development of microcracks may increase permeability of specimen, and also the addition of bacteria-based healing agent particles may initially cause extra (isolated) voids in the mortar matrix which must be more than compensated by bacterial metabolic formation of calcium carbonate in the subsequent incubation (water exposure) period. Indeed, in a short period of incubation time of 9 weeks, a higher chloride ingress was observed. However, with 4-week healing treatment and additional exposure time, the crack was almost filled with calcium carbonate resulting in lower ingress of chloride in 18-weeks bacteria-based specimen subjected to chloride solution but not in control mortar specimens. Crack filling with mineral precipitates was also observed by the presence of the whitish substance deposits along the internal crack line which was not observed in control specimen. The results of chloride distribution at the sample surface and along the crack line also showed a positive correlation between EDS mapping and photometric determination.

Because no carbonation front could be detected by the phenolphthalein test, two additional techniques were proposed for measuring the influence of carbonation on cracked mortar specimen, i.e., helium pycnometry. It was observed that sealing deposits increased on specimen that were kept immersed in water for an elapsed time of additional 28 days. This suggests that substantial crack-healing could indeed be expected during longer incubation periods. On the other hand, the carbonation process was decelerated in healing agent containing samples subjected to additional healing treatment. This observation may be explained by metabolically controlled crack-healing that prevents rapid ingress of carbon dioxide within the mortar matrix.

Formation of calcium carbonates in cracks due to metabolic activity of bacteria was confirmed through ESEM and EDS observation. The observed mineral crystals in this study were respectively vaterite- and calcite-based. The initial formation of a calcium carbonate particle composed of an aggregate of vaterite spheres was confirmed by ESEM images with mineral composition verification by FT-IR measurement. Subsequent to that, evidence for bacterial metabolic activity was found by the presence of bacterial imprints in minerals and oxygen consumption appearing in bacterial but not in control specimen.

Based on the present study it can be concluded that crack-sealing was more substantial in bacteria-based incubated specimen in comparison to equally long incubated control specimen. Further investigations are required for full quantification of healing capacity of bacteria-based in comparison to control specimen.



Conclusions and prospects

The real act of discovery is not in finding new lands, but in seeing with new eyes.

-Marcel Proust-

The bacteria-based self-healing concrete should be able to repair its crack effectively, not only improving its internal microstructure, but also to improve the mechanical properties and durability of concrete structures. This chapter remarks the works presented in this thesis. General conclusions by answering the research questions itemised in Chapter 1 are presented. In the end, suggestions for further research are given.

8.1 General conclusions

The goal of this thesis is to investigate the influence of chloride ingress and carbonation in concrete containing bacteria-based self-healing agent. To this end, the results emphasized the positive contribution of metabolic activity of alkaliphilic bacteria of the genus *Bacillus* towards enhancing the durability of building materials. Additionally, a new method that contributes to the great practical significance of durability evaluation was successfully developed in a RILEM Round Robin which reduces the risk of underestimating the service life of concrete structures. The procedures also proved to be doable, and the experiments produced results which reflect actual in-situ concrete behavior.

Based on experimental investigations carried out in the present study, the following research questions (given in Chapter 1) have been addressed.

1. *How does mechanical stress affect the chloride transport in normal concrete before it being incorporated with bacterial healing agent?*

Literature clearly indicates that concrete resistance to chloride penetration is closely related to the development of micro-cracks. Hence, a more practical technique considering chloride diffusivity of concrete subjected to monotonic compressive stress was successfully developed by a RILEM Round Robin and described in Chapter 3. The ingress of chloride ions into concrete under compression increases rapidly when the applied stress exceeds a certain threshold value. The results revealed that the chloride diffusion coefficient increases as a function of time if the structural elements are exposed to high compressive load which is in contrast with the hypothesis that the diffusion coefficient decreases with age in sound concrete specimen. It also suggests that the Fick's diffusion model can be considered in analyzing the chloride penetration at stress levels of approximate 30% and 60% of ultimate stress. Using the approach outlined in this chapter, the critical compression stress level of 60% of ultimate stress which provides the occurrence of unstable crack growth was identified. Indirectly, it indicates that measuring total chloride ingress could be used as a technique to observe damage phenomena in concrete under compressive load. However, the exact stress levels at which this change takes place depends on the microstructure of the material, the degree of hydration, the mix composition and how this material responds to the applied stress. The findings are useful for establishing a method aiming to provide a realistic quantitative service life design. The results from this study concerning chloride diffusion coefficients and its use for improved modeling of the service life of concrete is presented in the Final Report of RILEM TC 246-TDC [124].

2. *What is the influence of bacteria-based self-healing agent on the fresh properties of cementitious material?*

The effects on compressive strength of concrete and mortar cubes with incorporated bacteria-based healing agent at age of 1, 3, 7, 14, and 28 days were characterized and presented in Chapter 4. It was found that the concentration of healing agent to cement content in the mix influences the strength development of the concrete. A low amount of healing agent results in higher compressive strength of mortar at 28 days curing. A high amount of healing agent results in lower strength, compared to the reference strength, for all ages up to 28 days curing. During the mixing period some calcium lactate is likely released from the healing agent particles which may interfere with the cement hydration process and result in delayed strength development. This effect is probably concentration dependent, in which can turn the healing

agent into a bit as retarder. The optimum amount of healing agent to be added to the concrete, if only compressive strength is considered, appears to be close to 3% of the applied cement weight.

3. *How resistant is the bacterial concrete subjected to chloride and load-induced cracks?*

The beneficial effects of adding bacteria-based healing agent for increasing the durability of concrete were studied and presented in Chapter 6 using a newly developed test method. The results showed that the bacterial activity led to a denser concrete matrix, which reduced the chloride penetration. In this study, the ingress of chloride was not fully influenced by the stress level increment as the latter was already affected by the healing rate which was ongoing during the increasing deformation. The healing of (micro-) cracks became more apparent as lower chloride ingress was observed at the higher stress level as well as decreased in every testing period in comparison to unloaded specimen. Due to that, the diffusion coefficient of the bacterial specimens subjected to applied stress did not satisfy the assumptions in the Fick's diffusion model. The slower chloride ingress at elevated stress level is an indication that bacterial treatment can improve the durability of concrete. The role of the bacteria in calcium carbonate precipitation beneficial for sealing cracks was further verified by ESEM and oxygen consumption tests. It was concluded that the damage induced to concrete by an applied load can be healed over time (under the tested conditions) with bacterial treatment. The advantage of bio-healing concrete was shown to be promising. The material is capable of remediating and at the same time improving the durability of the cementitious material. Additionally, the experimental results emphasized, that the Fick's law is not applicable in the case where the bacteria close off the cracks over time and change the chloride profile. Application of immobilized spores as part of the self-healing agent could result in using less resources and energy consumption. Hence, it is not only making the concrete substantially more durable, but also more sustainable.

4. *What is the healing potential of the biogenic healing agent in cracked mortar exposed to carbonation and chloride attack?*

Further investigation for establishing the crack-healing efficiency of specimens with incorporated healing agent is addressed in Chapter 7. The chapter provides further information for evaluating the effect of metabolized mediated calcium carbonate precipitates on chloride ingress and carbonation of cracked mortar. The healing efficiency was evaluated using a variety of techniques, including stereomicroscopy, EDS mapping, helium pycnometry, scanning electron microscopy, oxygen microsensing and FT-IR. Initial observation by stereomicroscopy showed that the crack was significantly healed in the bacteria-based mortar at 28 days healing compared to the reference mortar. Contrary to the initial findings, higher chloride distribution was observed in 9-week specimen what was probably due to the extra voids created in the cement matrix by bacterial activity. However, over time, the cracks and pores were rapidly filled with calcium carbonate, thus delaying the penetration of chloride in the 18-week aged specimen. Sealing increased with time for the specimen kept under water. This suggests that substantial healing could be expected if the testing period would be longer. In summary, the crack recovery in mortar specimen could be better visualized in comparison to larger concrete beam specimens. However, the effect of chloride ingress showed a positive correlation between the results found in Chapters 6 and 7.

In the CO₂ test, the carbonation process appeared decelerated in bacterial samples stored under water. This observation may be explained by less CO₂ that is able to penetrate the mortar matrix with the bacteria are activated hence sealing the crack. Although no specific conclusion was made to the effect of extra CO₂, it was however proven that the carbonation ingress was stopped in water immersed mortar samples in comparison to non-immersed samples as in former a substantial pore volume reduction was observed due to the reaction between CO₂ and portlandite minerals present in the material matrix. In addition to that, deposition of sealing products was more rapid in specimens with healing agent compared to reference specimen which was proven by tomographic images. The results have also clearly shown that the retardation of chloride ingress and carbonation were (partly) induced by the calcium carbonate precipitation. This is proven by the observation of the enhanced sealing. The initial formation of calcium carbonate particles composed of vaterite spheres was confirmed through ESEM analyses with mineral composition verified by FT-IR measurement. Evidence of the occurrence of imprints was found in the case of active microbial activity in bacterial specimen with a higher oxygen consumption as observed by oxygen profile measurements. The outcomes reported in this chapter are, therefore, significant for the evaluation of the healing efficiency. The proposed bio-based self-healing system is recommended to be implemented in concrete structures that are not easily accessible for maintenance and repair work.

8.2 Future perspectives

The significance of this thesis is in the establishment of the influence of chloride ingress and carbonation in concrete containing bacteria-based self-healing agent. However, new materials and techniques can never be fully investigated and addressed in a single thesis. This section, therefore, presents recommendations for future work.

- *Considering a prolonged testing duration in self-healing experiments*

Significant contribution of bacteria-based healing agent to improvement of durability aspects of cementitious materials was observed in this research. Self-healing of micro-cracks in time was observed in Chapters 6 and 7. For longer testing duration, the continuing cement hydration has a minimal effect on ongoing autogenous healing and therefore the efficiency of the effect of the healing agent on additional autonomous healing can be expected to increase through significant ongoing precipitation of calcium carbonate. Due to this, a prolonged test period is encouraged to be conducted to investigate the effectiveness of applying the bacteria-based healing agent on the longer term. Therefore, considering a longer testing duration in self-healing studies is of considerable importance in order to verify active and sustainable healing throughout the service life of structures.

- *Investigating the chloride diffusivity and healing efficiency in stress-induced damaged concrete under various stress levels*

Only a minimum and maximum load level (present in real concrete structures) was considered in this study. However, a higher stress level can possibly be applied for obtaining more significant changes of mass transport properties and self-healing of cracks by bacteria. At higher stress level, the bond micro-cracks may increase in number, length and width, implying the onset of unstable micro-crack propagation. The rate of crack propagation of stresses above 75 %, could be too high for the self-healing to take place effectively. Hence, by investigating

this, the efficiency of bacteria-based healing agent as a protective measure to the ingress of harmful ions into the concrete under a stress influence can further be established.

- *To reduce the gap between laboratory conditions and in-situ conditions in self-healing studies*

It is clear that the applied stress modified the pore structure and introduced micro-cracks in concrete. As stress was not considered in most published laboratory studies, extrapolation of the state of knowledge to the concrete building is limited. Thus, it is important to reduce the gap between laboratory and in-situ conditions by considering the combined load test method in self-healing studies. Further studies could also focus on specific types of cracking patterns produced. To ensure that the produced results are reliable, the average value and the standard deviation for each parameter are required and therefore samples series of multiple replicate specimens should be included.

- *Testing the effects of mineral-producing bacteria on concrete samples with embedded steel reinforcement*

A review of existing studies indicates that carbonation and chloride induced corrosion has not attained adequate involvement of bacteria-based self-healing agent addressing reinforced concrete structures. As bacterial healing is an aerobic reaction, it is impossible to study the effect of chloride- and carbonation-induced corrosion under oxygen free conditions. Another main concern is when CO₂ (produced by the bacterial conversion of calcium lactate into calcium carbonate) can no longer interact with calcium hydroxide when the latter compound is exhausted, resulting in depassivation of the steel reinforcement by CO₂. Therefore, it is necessary to fully understand the effects of bacterial healing in reinforced concrete specimen in future studies.

- *Further work on numerical simulation to predict the efficiency of self-healing concrete*

A more detailed investigation by numerical analysis could also be beneficial to make practical application of the bio-healing material feasible. Computer simulation can reduce the amount of costly and laborious experimental work by providing an effective method to estimate the bacterial self-healing of damage in concrete. It will be useful when the mathematical model of the bacterial self-healing can include various degradation parameters in order to gain better insight into the efficiency of self-healing concrete to increase the service life of the structure. The further accumulation of relevant information will stimulate in-depth research on self-healing cement-based materials.

References

- [1] S. Shah and C. Ouyang, "Fracture mechanics for failure of concrete," *Annual review of materials science*, vol. 24, no. 1, pp. 293-320, 1994.
- [2] A. M. Neville, *Properties of concrete*. 1995.
- [3] V. S. Ramachandran and J. J. Beaudoin, *Handbook of analytical techniques in concrete science and technology: principles, techniques and applications*. Elsevier, 2000.
- [4] V. G. Papadakis, C. G. Vayenas, and M. N. Fardis, "Fundamental modeling and experimental investigation of concrete carbonation," *Materials Journal*, vol. 88, no. 4, pp. 363-373, 1991.
- [5] C.-F. Chang and J.-W. Chen, "The experimental investigation of concrete carbonation depth," *Cement and Concrete Research*, vol. 36, no. 9, pp. 1760-1767, 2006.
- [6] J. F. Lamond and J. H. Pielert, "Significance of tests and properties of concrete and concrete-making materials," 2006: ASTM West Conshohocken, PA.
- [7] A. Litorowicz, "Identification and quantification of cracks in concrete by optical fluorescent microscopy," *Cement and concrete Research*, vol. 36, no. 8, pp. 1508-1515, 2006.
- [8] H. WITTMANN and Y. ZAYTSEV, "Application of fracture mechanics to investigate durability of concrete under load," in *Proceedings of the 8 th International Conference on Fracture Mechanics of Concrete and Concrete Structures (FraMCoS-8)*, 2013.
- [9] F. X. Jiang, Y. T. Wang, T. J. Zhao, and L. L. Liu, "Chloride Penetration Resistance of Concrete Structures under Compressive Load," in *Advanced Materials Research*, 2012, vol. 479: Trans Tech Publ, pp. 120-123.
- [10] F. Wittmann, T. Zhao, P. Zhang, and F. Jiang, "Service life of reinforced concrete structures under combined mechanical and environmental loads," in *2nd International Symposium on Service Life Design for Infrastructures*, 2010: RILEM Publications SARL, pp. 91-98.
- [11] N. Gowripalan, V. Sirivivatnanon, and C. Lim, "Chloride diffusivity of concrete cracked in flexure," *Cement and Concrete Research*, vol. 30, no. 5, pp. 725-730, 2000.
- [12] Q. Cao *et al.*, "Effect of mechanical loading on chloride penetration into concrete," *Proceedings of ICDCS2008, Advances in Concrete Structure Durability (Jin WL, Ueda T and Basheer PAM (eds)). Zhejiang University Press, Hangzhou, PR China, vols*, vol. 1, pp. 283-290, 2008.
- [13] W.-m. Zhang, H.-j. Ba, and S.-j. Chen, "Effect of fly ash and repeated loading on diffusion coefficient in chloride migration test," *Construction and Building Materials*, vol. 25, no. 5, pp. 2269-2274, 2011.
- [14] V. Wiktor and H. M. Jonkers, "Quantification of crack-healing in novel bacteria-based self-healing concrete," *Cement and Concrete Composites*, vol. 33, no. 7, pp. 763-770, 2011.
- [15] H. Schlangen, H. Jonkers, S. Qian, and A. Garcia, "Recent advances on self healing of concrete," in *FraMCoS-7: Proceedings of the 7th International Conference on Fracture Mechanics of Concrete and Concrete Structures, Jeju Island, Korea, 23-28 May 2010*, 2010.
- [16] H. M. Jonkers and E. Schlangen, "Self-healing of cracked concrete: a bacterial approach," *Proceedings of FRACOS6: fracture mechanics of concrete and concrete structures. Catania, Italy*, pp. 1821-1826, 2007.
- [17] H. M. Jonkers, "Self healing concrete: a biological approach," in *Self Healing Materials*: Springer, 2007, pp. 195-204.
- [18] H. M. Jonkers and E. Schlangen, "Crack repair by concrete-immobilized bacteria," in *Proceedings of the First International Conference on Self Healing Materials*, 2007, pp. 18-20.

- [19] V. Wiktor, H. M. Jonkers, K. van Breugel, G. Ye, and Y. Yuan, "Self-healing of cracks in bacterial concrete," in *2nd International Symposium on Service Life Design for Infrastructures*, 2010: RILEM Publications SARL, pp. 825-831.
- [20] H. M. Jonkers, A. Thijssen, G. Muyzer, O. Copuroglu, and E. Schlangen, "Application of bacteria as self-healing agent for the development of sustainable concrete," (in English), *Ecological Engineering*, vol. 36, no. 2, pp. 230-235, Feb 2010, doi: 10.1016/j.ecoleng.2008.12.036.
- [21] R. B. Polder, "Critical chloride content for reinforced concrete and its relationship to concrete resistivity," *Materials and corrosion*, vol. 60, no. 8, pp. 623-630, 2009.
- [22] S. Rostam, "Service life design of concrete structures-an experience-based discipline becoming scientific," *Papers in structural engineering and materials-A Centenary Celebration, DoSEaM, TU of Denmark*, pp. 131-150, 2000.
- [23] A. Küter, M. R. Geiker, J. F. Olesen, H. Stang, C. Dauberschmidt, and M. Raupach, "Chloride Ingress in concrete cracks under cyclic loading," in *3rd International Conference on Construction Materials*, 2005.
- [24] S. Zwaag, *Self healing materials: an alternative approach to 20 centuries of materials science*. Springer Science+ Business Media BV, 2008.
- [25] S. Tang, Y. Yao, C. Andrade, and Z. Li, "Recent durability studies on concrete structure," *Cement and Concrete Research*, vol. 78, pp. 143-154, 2015.
- [26] M. Hoseini, V. Bindiganavile, and N. Banthia, "The effect of mechanical stress on permeability of concrete: a review," *Cement and Concrete Composites*, vol. 31, no. 4, pp. 213-220, 2009.
- [27] K. Van Breugel, "Is there a market for self-healing cement-based materials," in *Proceedings of the first international conference on self-healing materials*, 2007.
- [28] G. van der Wegen, R. B. Polder, and K. van Breugel, "Guideline for service life design of structural concrete—a performance based approach with regard to chloride induced corrosion," *Heron*, vol. 57, no. 3, pp. 153-168, 2012.
- [29] O. E. GjØrv, *Durability design of concrete structures in severe environments*. CRC Press, 2014.
- [30] N. Gartner, T. Kosec, and A. Legat, "Monitoring the corrosion of steel in concrete exposed to a marine environment," *Materials*, vol. 13, no. 2, p. 407, 2020.
- [31] D. Zhang, X. Gao, G. Su, L. Du, Z. Liu, and J. Hu, "Corrosion Behavior of Low-C Medium-Mn Steel in Simulated Marine Immersion and Splash Zone Environment," *Journal of Materials Engineering and Performance*, vol. 26, no. 6, pp. 2599-2607, 2017.
- [32] S. Li, Z. Jin, B. Pang, and J. Li, "Durability performance of an RC beam under real marine all corrosion zones exposure for 7 years," *Case Studies in Construction Materials*, vol. 17, p. e01516, 2022.
- [33] M. G. Richardson, *Fundamentals of durable reinforced concrete*. CRC Press, 2002.
- [34] S. Engelund, C. Edvardsen, and L. Mohr, "General Guidelines for Durability, Design and Redesign, DuraCrete, Probabilistic Performance based Durability Design of Concrete Structures," *The European Union-Brite EURam III*, 2000.
- [35] J. Cabrera, "Deterioration of concrete due to reinforcement steel corrosion," *Cement and concrete composites*, vol. 18, no. 1, pp. 47-59, 1996.
- [36] O. E. GjØrv and N. Banthia, *Concrete Under Severe Conditions 2: Environment and Loading: Proceedings of the Second International Conference on Concrete Under Severe Conditions, CONSEC'98, Tromsø, Norway, June 21-24, 1998*. CRC Press, 1998.

- [37] L. Basheer, J. Kropp, and D. J. Cleland, "Assessment of the durability of concrete from its permeation properties: a review," *Construction and building materials*, vol. 15, no. 2, pp. 93-103, 2001.
- [38] C. Desmettre and J.-P. Charron, "Water permeability of reinforced concrete with and without fiber subjected to static and constant tensile loading," *Cement and Concrete Research*, vol. 42, no. 7, pp. 945-952, 2012.
- [39] N. Build, "492. Concrete, mortar and cement-based repair materials: chloride migration coefficient from non-steady-state migration experiments," *Nordtest method*, vol. 492, no. 10, 1999.
- [40] A. Fick, "V. On liquid diffusion," *The London, Edinburgh, and Dublin Philosophical Magazine and Journal of Science*, vol. 10, no. 63, pp. 30-39, 1855.
- [41] J. Crank, *The mathematics of diffusion*. Oxford university press, 1979.
- [42] C. J. Shi, D. H. Deng, and Y. J. Xie, "Pore Structure and Chloride Ion Transport Mechanisms in Concrete," in *Key Engineering Materials*, 2006, vol. 302: Trans Tech Publ, pp. 528-535.
- [43] K. Stanish, R. Hooton, and M. Thomas, "Testing the chloride penetration resistance of concrete: a literature review," *FHWA contract DTFH61*, pp. 19-22, 1997.
- [44] S. Mu, G. De Schutter, and B.-g. Ma, "Non-steady state chloride diffusion in concrete with different crack densities," *Materials and structures*, vol. 46, no. 1-2, pp. 123-133, 2013.
- [45] R. Loser, B. Lothenbach, A. Leemann, and M. Tuchschnid, "Chloride resistance of concrete and its binding capacity—Comparison between experimental results and thermodynamic modeling," *Cement and Concrete Composites*, vol. 32, no. 1, pp. 34-42, 2010.
- [46] A. M. Neville and J. J. Brooks, *Concrete technology*. 1987.
- [47] D. Beckett, "Influence of carbonation and chlorides on concrete durability," *Concrete*, vol. 17, no. 2, 1983.
- [48] R. R. Hussain and T. Ishida, "Critical carbonation depth for initiation of steel corrosion in fully carbonated concrete and development of electrochemical carbonation induced corrosion model," *Int. J. Electrochem. Sci*, vol. 4, no. 8, pp. 1178-1195, 2009.
- [49] S. Mindess, J. F. Young, and D. Darwin, *Concrete*. 2003.
- [50] F. P. Torgal and S. Jalali, *Eco-efficient construction and building materials*. Springer Science & Business Media, 2011.
- [51] P. A. Claisse, H. El-Sayad, and I. G. Shaaban, "Permeability and pore volume of carbonated concrete," *ACI Materials Journal*, vol. 96, pp. 378-381, 1999.
- [52] H. F. Taylor, *Cement chemistry*. Thomas Telford, 1997.
- [53] P. Monteiro, Mehta Kumar, *Concrete: Microstructure, Properties, and Materials*. McGraw-Hill Publishing, 2006.
- [54] M. Setzer, M. Seter, and R. Auberg, "Basis of testing the freeze-thaw resistance—Surface and internal deterioration," *Frost resistance of concrete*, pp. 157-173, 1997.
- [55] K. L. Scrivener, A. K. Crumbie, and P. Laugesen, "The interfacial transition zone (ITZ) between cement paste and aggregate in concrete," *Interface Science*, vol. 12, no. 4, pp. 411-421, 2004.
- [56] F. Wittmann, F. Jiang, T. Zhao, and Y. Wang, "Influence of an Applied Compressive Stress on Service Life of Reinforced Concrete Structures in Marine Environment," *Restoration of Buildings and Monuments*, vol. 19, no. 1, pp. 3-10, 2013.
- [57] A. Kermani, "Permeability of stressed concrete: Steady-state method of measuring permeability of hardened concrete studies in relation to the change in structure of concrete

- under various short-term stress levels," *Building research and information*, vol. 19, no. 6, pp. 360-366, 1991.
- [58] S. Jacobsen, J. Marchand, and L. Boisvert, "Effect of cracking and healing on chloride transport in OPC concrete," *Cement and Concrete Research*, vol. 26, no. 6, pp. 869-881, 1996.
- [59] W. H. Glanville, *The permeability of Portland cement concrete*. [HM Stationery Office [printed by Harrison and sons, Limited], 1931.
- [60] C. Edvardsen, "Water permeability and autogenous healing of cracks in concrete," *ACI Materials Journal*, vol. 96, no. 4, 1999.
- [61] N. Otsuki, S.-i. Miyazato, N. B. Diola, and H. Suzuki, "Influences of bending crack and water-cement ratio on chloride-induced corrosion of main reinforcing bars and stirrups," *Materials Journal*, vol. 97, no. 4, pp. 454-464, 2000.
- [62] G. E. Jenneman, R. M. Knapp, M. J. McInerney, D. Menzie, and D. Revus, "Experimental studies of in-situ microbial enhanced oil recovery," *Society of Petroleum Engineers Journal*, vol. 24, no. 01, pp. 33-37, 1984.
- [63] M. Islam and S. Bang, "Use of Silicate and Carbonate Producing Bacteria in Restoration of Historic Monuments and Buildings," *South Dakota School of Mines and Technology*, 1993.
- [64] U. Gollapudi, C. Knutson, S. Bang, and M. Islam, "A new method for controlling leaching through permeable channels," *Chemosphere*, vol. 30, no. 4, pp. 695-705, 1995.
- [65] S. Stocks-Fischer, J. K. Galinat, and S. S. Bang, "Microbiological precipitation of CaCO₃," *Soil Biology and Biochemistry*, vol. 31, no. 11, pp. 1563-1571, 1999.
- [66] J. Dick *et al.*, "Bio-deposition of a calcium carbonate layer on degraded limestone by *Bacillus* species," *Biodegradation*, vol. 17, no. 4, pp. 357-367, 2006.
- [67] S. S. Bang, J. K. Galinat, and V. Ramakrishnan, "Calcite precipitation induced by polyurethane-immobilized *Bacillus pasteurii*," *Enzyme and microbial technology*, vol. 28, no. 4, pp. 404-409, 2001.
- [68] S. K. Ramachandran, V. Ramakrishnan, and S. S. Bang, "Remediation of concrete using microorganisms," *ACI Materials journal*, vol. 98, no. 1, pp. 3-9, 2001.
- [69] W. De Muynck, D. Debrouwer, N. De Belie, and W. Verstraete, "Bacterial carbonate precipitation improves the durability of cementitious materials," *Cement and concrete Research*, vol. 38, no. 7, pp. 1005-1014, 2008.
- [70] G. Le Metayer-Levrel, S. Castanier, G. Orial, J.-F. Loubiere, and J.-P. Perthuisot, "Applications of bacterial carbonatogenesis to the protection and regeneration of limestones in buildings and historic patrimony," *Sedimentary geology*, vol. 126, no. 1, pp. 25-34, 1999.
- [71] V. Achal, A. Mukherjee, and M. S. Reddy, "Microbial concrete: way to enhance the durability of building structures," *Journal of materials in civil engineering*, vol. 23, no. 6, pp. 730-734, 2010.
- [72] V. Achal, A. Mukerjee, and M. S. Reddy, "Biogenic treatment improves the durability and remediates the cracks of concrete structures," *Construction and Building Materials*, vol. 48, pp. 1-5, 2013.
- [73] V. Achal, A. Mukherjee, and M. S. Reddy, "Effect of calcifying bacteria on permeation properties of concrete structures," *Journal of industrial microbiology & biotechnology*, vol. 38, no. 9, pp. 1229-1234, 2011.
- [74] W. De Muynck, K. Cox, N. De Belie, and W. Verstraete, "Bacterial carbonate precipitation as an alternative surface treatment for concrete," *Construction and Building Materials*, vol. 22, no. 5, pp. 875-885, 2008.

- [75] P. Ghosh, S. Mandal, B. Chattopadhyay, and S. Pal, "Use of microorganism to improve the strength of cement mortar," *Cement and Concrete Research*, vol. 35, no. 10, pp. 1980-1983, 2005.
- [76] S. Ghosh, M. Biswas, B. Chattopadhyay, and S. Mandal, "Microbial activity on the microstructure of bacteria modified mortar," *Cement and Concrete Composites*, vol. 31, no. 2, pp. 93-98, 2009.
- [77] V. Achal, X. Pan, and N. Özyurt, "Improved strength and durability of fly ash-amended concrete by microbial calcite precipitation," *Ecological Engineering*, vol. 37, no. 4, pp. 554-559, 2011.
- [78] N. Chahal, R. Siddique, and A. Rajor, "Influence of bacteria on the compressive strength, water absorption and rapid chloride permeability of fly ash concrete," *Construction and Building Materials*, vol. 28, no. 1, pp. 351-356, 2012.
- [79] N. Chahal, R. Siddique, and A. Rajor, "Influence of bacteria on the compressive strength, water absorption and rapid chloride permeability of concrete incorporating silica fume," *Construction and Building Materials*, vol. 37, pp. 645-651, 2012.
- [80] H. M. Jonkers and E. Schlangen, "Development of a bacteria-based self healing concrete," in *Proc. int. FIB symposium*, 2008, vol. 1: Citeseer, pp. 425-430.
- [81] (2009) Hoera, mijn beton klust zelf! *Betoniek*.
- [82] M. G. Sierra-Beltran, H. Jonkers, and E. Schlangen, "Characterization of sustainable bio-based mortar for concrete repair," *Construction and Building Materials*, vol. 67, pp. 344-352, 2014.
- [83] H. Jonkers, "Bacteria-based self-healing concrete," *Heron*, 56 (1/2), 2011.
- [84] H. M. J. a. E. S. M.G. Sierra Beltran. Self-healing capacity of a strainhardening cement-based composite SHCC with bacteria
- [85] E. Tziviloglou *et al.*, "Bio-Based Self-Healing Concrete: From Research to Field Application," 2016.
- [86] D. Spooner and J. Dougill, "A quantitative assessment of damage sustained in concrete during compressive loading," *Magazine of Concrete Research*, vol. 27, no. 92, pp. 151-160, 1975.
- [87] M. K. Rahman, W. A. Al-Kutti, M. A. Shazali, and M. H. Baluch, "Simulation of chloride migration in compression-induced damage in concrete," *Journal of Materials in Civil Engineering*, vol. 24, no. 7, pp. 789-796, 2012.
- [88] N. Hearn, "Self-sealing, autogenous healing and continued hydration: What is the difference?," *Materials and Structures*, vol. 31, no. 8, pp. 563-567, 1998.
- [89] C.-M. Aldea, S. P. Shah, and A. Karr, "Effect of cracking on water and chloride permeability of concrete," *Journal of materials in civil engineering*, vol. 11, no. 3, pp. 181-187, 1999.
- [90] P. P. Win, M. Watanabe, and A. Machida, "Penetration profile of chloride ion in cracked reinforced concrete," *Cement and concrete research*, vol. 34, no. 7, pp. 1073-1079, 2004.
- [91] K. Wang, D. C. Jansen, S. P. Shah, and A. F. Karr, "Permeability study of cracked concrete," *Cement and Concrete Research*, vol. 27, no. 3, pp. 381-393, 1997.
- [92] H.-W. Reinhardt and M. Jooss, "Permeability and self-healing of cracked concrete as a function of temperature and crack width," *Cement and Concrete Research*, vol. 33, no. 7, pp. 981-985, 2003.
- [93] L. Marsavina, K. Audenaert, G. De Schutter, N. Faur, and D. Marsavina, "Experimental and numerical determination of the chloride penetration in cracked concrete," *Construction and*

Building Materials, vol. 23, no. 1, pp. 264-274, 1// 2009, doi:

<http://dx.doi.org/10.1016/j.conbuildmat.2007.12.015>.

- [94] C. Lu, Y. Gao, and R. Liu, "Effect of Transverse Crack on Chloride Penetration into Concrete Subjected to Drying–Wetting Cycles," 2014.
- [95] M. Ismail, A. Toumi, R. François, and R. Gagné, "Effect of crack opening on the local diffusion of chloride in cracked mortar samples," *Cement and concrete research*, vol. 38, no. 8, pp. 1106-1111, 2008.
- [96] A. Djerbi, S. Bonnet, A. Khelidj, and V. Baroghel-Bouny, "Influence of traversing crack on chloride diffusion into concrete," *Cement and Concrete Research*, vol. 38, no. 6, pp. 877-883, 2008.
- [97] E. d. P. Hansen, T. Ekman, and K. K. Hansen, "Durability of cracked fibre reinforced concrete structures exposed to chlorides," in *Proceedings of the eighth international conference on durability of building materials and components, Ottawa, Canada, 1999*, pp. 280-9.
- [98] C.-M. Aldea, S. Shah, and A. Karr, "Permeability of cracked concrete," *Materials and structures*, vol. 32, no. 5, pp. 370-376, 1999.
- [99] A. Konin, R. Francois, and G. Arliguie, "Penetration of chlorides in relation to the microcracking state into reinforced ordinary and high strength concrete," *Materials and structures*, vol. 31, no. 5, pp. 310-316, 1998.
- [100] M. Şahmaran, "Effect of flexure induced transverse crack and self-healing on chloride diffusivity of reinforced mortar," *Journal of Materials Science*, vol. 42, no. 22, pp. 9131-9136, 2007.
- [101] A. Akhavan and F. Rajabipour, "Quantifying the effects of crack width, tortuosity, and roughness on water permeability of cracked mortars," *Cement and Concrete Research*, vol. 42, no. 2, pp. 313-320, 2012.
- [102] C.-Q. Li and S. Yang, "Prediction of concrete crack width under combined reinforcement corrosion and applied load," *Journal of engineering mechanics*, vol. 137, no. 11, pp. 722-731, 2011.
- [103] B. Stitmannathum, H. Q. Vu, and M. Van Tran, "Chloride Penetration into Reinforced Concrete Structure," in *3 rd International Conference on Sustainable Construction Materials and Technologies,-claisse. info*.
- [104] M. Saito and H. Ishimori, "Chloride permeability of concrete under static and repeated compressive loading," *Cement and Concrete Research*, vol. 25, no. 4, pp. 803-808, 1995.
- [105] F. Jiang, F. Wittmann, and T. Zhao, "Influence of mechanically induced damage on durability and service life of reinforced concrete structures," *Restoration of Buildings and Monuments*, vol. 17, no. 1, pp. 25-32, 2011.
- [106] N. Banthia and A. Bhargava, "Permeability of stressed concrete and role of fiber reinforcement," *ACI materials journal*, vol. 104, no. 1, p. 70, 2007.
- [107] f. H. W. Xiaomei Wan , Tiejun Zhao, Fuxiang Jiang, "Chloride Penetration into Concrete after Uniaxial Compression," *Journal of Frontiers in Construction Engineering*, vol. 2, no. 3, pp. 66-74, 2013.
- [108] Y. Wang *et al.*, "Influence of axial loads on CO₂ and Cl⁻ transport in concrete phases: Paste, mortar and ITZ," *Construction and Building Materials*, vol. 204, pp. 875-883, 2019.
- [109] H. R. Samaha and K. C. Hover, "Influence of microcracking on the mass transport properties of concrete," *Materials Journal*, vol. 89, no. 4, pp. 416-424, 1992.

- [110] W. Zhu, R. François, Q. Fang, and D. Zhang, "Influence of long-term chloride diffusion in concrete and the resulting corrosion of reinforcement on the serviceability of RC beams," *Cement and Concrete Composites*, vol. 71, pp. 144-152, 2016.
- [111] T. Sugiyama, T. W. Bremner, and T. A. Holm, "Effect of stress on gas permeability in concrete," *Materials Journal*, vol. 93, no. 5, pp. 443-450, 1996.
- [112] V. Picandet and A. Khelidj, "Gas and water permeability of cracked concrete," in *ICPCM, A new Era of Building*, 2003.
- [113] X. Wang and K. Mohanty, "Pore-network model of flow in gas/condensate reservoirs," *SPE Journal*, vol. 5, no. 04, pp. 426-434, 2000.
- [114] Y. Loo, "A new method for microcrack evaluation in concrete under compression," *Materials and Structures*, vol. 25, no. 10, pp. 573-578, 1992.
- [115] C. Lim, N. Gowripalan, and V. Sirivivatnanon, "Microcracking and chloride permeability of concrete under uniaxial compression," *Cement and Concrete Composites*, vol. 22, no. 5, pp. 353-360, 2000.
- [116] Y. T. Wang, W. Z. Chen, and F. X. Jiang, "Development and Evaluation for Microdamage of Concrete under Uniaxial Compressive Load," in *Applied Mechanics and Materials*, 2014, vol. 507: Trans Tech Publ, pp. 226-229.
- [117] F. O. Slate and S. Olsefski, "X-rays for study of internal structure and microcracking of concrete," in *Journal Proceedings*, 1963, vol. 60, no. 5, pp. 575-588.
- [118] T. T. Hsu, F. O. Slate, G. M. Sturman, and G. Winter, "Microcracking of plain concrete and the shape of the stress-strain curve," *Journal of the American Concrete Institute*, vol. 60, no. 2, pp. 209-224, 1963.
- [119] S. P. Shah and S. Chandra, "Critical stress, volume change, and microcracking of concrete," in *Journal Proceedings*, 1968, vol. 65, no. 9, pp. 770-780.
- [120] K. Krishnaswamy, "Strength and microcracking of plain concrete under triaxial compression," in *Journal Proceedings*, 1968, vol. 65, no. 10, pp. 856-862.
- [121] Y. Niwa, W. Koyanagi, and K. Nakagawa, "Failure processes of concrete under triaxial compressive stress," in *Proc. JSCE*, 1971, no. 185, pp. 31-41.
- [122] M. Light and A. Luxmoore, "Detection of cracks in concrete by holography," *Magazine of Concrete Research*, vol. 24, no. 80, pp. 167-172, 1972.
- [123] M. Van Tran, B. Stitmannathum, and T. Nawa, "Chloride penetration into concrete using various cement types under flexural cyclical load and tidal environment," *The IES Journal Part A: Civil & Structural Engineering*, vol. 2, no. 3, pp. 202-214, 2009.
- [124] Y. Yao *et al.*, "Test methods to determine durability of concrete under combined environmental actions and mechanical load: final report of RILEM TC 246-TDC," *Materials and Structures*, vol. 50, no. 2, p. 123, 2017.
- [125] R. K. Dhir, P. C. Hewlett, and Y. N. Chan, "Near surface characteristics of concrete: intrinsic permeability," *Magazine of Concrete Research*, vol. 41, no. 147, pp. 87-97, 1989.
- [126] G. Wilsch, F. Weritz, D. Schaurich, and H. Wiggenhauser, "Determination of chloride content in concrete structures with laser-induced breakdown spectroscopy," *Construction and building materials*, vol. 19, no. 10, pp. 724-730, 2005.
- [127] R. Yuan *et al.*, "Accuracy improvement of quantitative analysis for major elements in laser-induced breakdown spectroscopy using single-sample calibration," *Analytica chimica acta*, vol. 1064, pp. 11-16, 2019.

- [128] H. Coll, "SPECTROPHOTOMETRIC DETERMINATION OF CHLORIDE ION," Louisiana State University and Agricultural & Mechanical College, 1957.
- [129] Y. Yao *et al.*, "Recommendation of RILEM TC 246-TDC: test methods to determine durability of concrete under combined environmental actions and mechanical load," *Materials and Structures*, vol. 50, no. 2, p. 155, 2017.
- [130] P. Mehta, "Durability of concrete exposed to marine environment--a fresh look," *Special Publication*, vol. 109, pp. 1-30, 1988.
- [131] L. Liu, W. Sun, G. Ye, H. Chen, and Z. Qian, "Estimation of the ionic diffusivity of virtual cement paste by random walk algorithm," *Construction and Building Materials*, vol. 28, no. 1, pp. 405-413, 2012.
- [132] B. Hughes and B. Bahramian, "Cube tests and the uniaxial compressive strength of concrete," *Magazine of concrete research*, vol. 17, no. 53, pp. 177-182, 1965.
- [133] Z. Guo, *Principles of reinforced concrete*. Butterworth-Heinemann, 2014.
- [134] J. Wang, P. M. Basheer, S. V. Nanukuttan, A. E. Long, and Y. Bai, "Influence of service loading and the resulting micro-cracks on chloride resistance of concrete," *Construction and Building Materials*, vol. 108, pp. 56-66, 2016.
- [135] F. Weritz, D. Schaurich, A. Taffe, and G. Wilsch, "Effect of heterogeneity on the quantitative determination of trace elements in concrete," *Analytical and bioanalytical chemistry*, vol. 385, no. 2, pp. 248-255, 2006.
- [136] H. M. Jonkers and R. Mors, "Full scale application of bacteria-based self-healing concrete for repair purposes," in *Concrete Repair, Rehabilitation and Retrofitting III: 3rd International Conference on Concrete Repair, Rehabilitation and Retrofitting, ICCRRR-3, 3-5 September 2012, Cape Town, South Africa, 2012*: CRC Press, p. 349.
- [137] W. De Muynck, N. De Belie, and W. Verstraete, "Microbial carbonate precipitation in construction materials: a review," *Ecological Engineering*, vol. 36, no. 2, pp. 118-136, 2010.
- [138] R. M. Mors and H. M. Jonkers, "Bacteria-based self-healing concrete: Introduction," in *Proceedings pro083: 2nd International Conference on Microstructural-related Durability of Cementitious Composites, Amsterdam, The Netherlands, 11-13 April 2012, 2012*: RILEM Publications SARL.
- [139] H. M. Jonkers and E. Schlangen, "A two component bacteria-based self-healing concrete," 2009.
- [140] H. G. Schlegel, C. Zaborosch, and M. Kogut, *General microbiology*. Cambridge University Press, 1993.
- [141] R. Mors and H. Jonkers, "Feasibility of lactate derivative based agent as additive for concrete for regain of crack water tightness by bacterial metabolism," *Industrial crops and products*, vol. 106, pp. 97-104, 2017.
- [142] R. Mors, "Personal Communication," ed, 2016.
- [143] S. Jacobsen and E. J. Sellevold, "Self healing of high strength concrete after deterioration by freeze/thaw," *Cement and Concrete Research*, vol. 26, no. 1, pp. 55-62, 1996.
- [144] 堀口 and 佐伯, "1124 INFLUENCE OF STRESS ON CHLORIDE PENETRATION INTO FIBER REINFORCED CONCRETE," *コンクリート工学年次論文集*, vol. 25, no. 1, pp. 779-784, 2003.
- [145] Y. Sakoi and T. Horiguchi, "Loading effects on chloride penetration of fiber reinforced concrete," in *Proceedings of the 2nd International fib Congress*, 2006.
- [146] F. H. W. F.X. Jiang, T.J. Zhao, "Influence of sustained compressive load on penetration of chloride ions into neat and water repellent concrete," in *Proceeding of the first internal*

- conference on performance-based and life-cycle structural engineering*, Hong Kong, 2012, pp. 992-997.
- [147] F. H. W. F.X. Jiang, T.J. Zhao, F. Li, S. Gao, "Chloride penetration into the cracked tensile zone of reinforced concrete structures before and after water repellent treatment," in *Proceedings of the 2nd International Symposium on Service Life Design for Infrastructures*, 2010: RILEM Publications SARL, pp. 875-882.
- [148] K. Sisomphon, O. Copuroglu, and E. Koenders, "Effect of exposure conditions on self healing behavior of strain hardening cementitious composites incorporating various cementitious materials," *Construction and Building Materials*, vol. 42, pp. 217-224, 2013.
- [149] J. Van Mier *et al.*, "Strain-softening of concrete in uniaxial compression," *Materials and Structures*, vol. 30, no. 4, pp. 195-209, 1997.
- [150] M. A. van Vliet and J. M. van Mier, "Experimental investigation of concrete fracture under uniaxial compression," *Mechanics of Cohesive-frictional Materials: An International Journal on Experiments, Modelling and Computation of Materials and Structures*, vol. 1, no. 1, pp. 115-127, 1996.
- [151] R. Mors and H. Jonkers, "Reduction of water permeation through cracks in mortar by addition of bacteria based healing agent," in *Proceedings of the 5th International Conference on Self-Healing Materials, ICSHM, Durham, USA, June 22-24, 2015. Extended abstract*, 2015.
- [152] K. Van Tittelboom, N. De Belie, W. De Muynck, and W. Verstraete, "Use of bacteria to repair cracks in concrete," *Cement and Concrete Research*, vol. 40, no. 1, pp. 157-166, 2010.
- [153] W. De Muynck, N. De Belie, and W. Verstraete, "Improvement of concrete durability with the aid of bacteria," in *Proceedings of the first international conference on self healing materials*, 2007: Springer.
- [154] H. Afifudin, M. S. Hamidah, H. Noor Hana, and K. Kamaruddin, "Microorganism precipitation in enhancing concrete properties," in *Applied Mechanics and Materials*, 2011, vol. 99: Trans Tech Publ, pp. 1157-1165.
- [155] O. M. Jensen, P. F. Hansen, A. M. Coats, and F. P. Glasser, "Chloride ingress in cement paste and mortar," *Cement and Concrete Research*, vol. 29, no. 9, pp. 1497-1504, 1999.
- [156] *NEN-EN 196-1: 2005. Methods of testing cement - Part 1: Determination of Strength*, February 2005.
- [157] H. G. T. Nguyen, J. C. Horn, M. Bleakney, D. W. Siderius, and L. Espinal, "Understanding material characteristics through signature traits from helium pycnometry," *Langmuir*, vol. 35, no. 6, pp. 2115-2122, 2019.
- [158] M. T. Liang, W. J. Qu, and Y. S. Liao, "A study on carbonation in concrete structures at existing cracks," *Journal of the Chinese Institute of Engineers*, vol. 23, no. 2, pp. 143-153, 2000.
- [159] M. Díaz-Dosque *et al.*, "Use of biopolymers as oriented supports for the stabilization of different polymorphs of biomineralized calcium carbonate with complex shape," *Journal of Crystal Growth*, vol. 310, no. 24, pp. 5331-5340, 2008.
- [160] M. F. Butler, N. Glaser, A. C. Weaver, M. Kirkland, and M. Heppenstall-Butler, "Calcium carbonate crystallization in the presence of biopolymers," *Crystal growth & design*, vol. 6, no. 3, pp. 781-794, 2006.
- [161] Y. S. Han, G. Hadiko, M. Fuji, and M. Takahashi, "Crystallization and transformation of vaterite at controlled pH," *Journal of crystal growth*, vol. 289, no. 1, pp. 269-274, 2006.

- [162] C. Weir and E. Lippincott, "Infrared studies of aragonite, calcite, and vaterite type structures in the borates, carbonates, and nitrates," *J. Res. Natl. Bur. Stand. US, Sect. A*, vol. 65, pp. 173-183, 1961.
- [163] M. Sato and S. Matsuda, "Structure of vaterite and infrared spectra," *Zeitschrift fur Kristallographie*, vol. 129, no. 5-6, pp. 405-410, 1969.

Appendix A

Test methods to determine durability of concrete under combined environmental actions and mechanical load: final report of RILEM TC 246-TDC

Yan Yao · Ling Wang · Folker H. Wittmann · Nele De Belie · Erik Schlangen · Hugo Eguez Alava · Zhendi Wang · Sylvia Kessler · Christoph Gehlen · Balqis Md. Yunus · Juan Li · Weihong Li · Max. J. Setzer · Feng Xing · Yin Cao

Received: 11 October 2016 / Accepted: 9 December 2016
© RILEM 2016

Abstract At present several methods are available to predict the durability of reinforced concrete structures. In most cases, one dominant deterioration process such as carbonation or chloride penetration is taken into consideration. Experimental results as well as observations in practice show that this is not a realistic and certainly not a conservative approach. In order to test more realistically, RILEM TC 246-TDC, founded in 2011, has developed a method to determine the durability of concrete exposed to the combined action

of chloride penetration and mechanical load. In this report, a test method is presented which allows determination of realistic diffusion coefficients for chloride ions in concrete under compressive or tensile stress. Comparative test results from five different laboratories showed that the combination of mechanical and environmental loads may be much more severe than a single environmental load without mechanical loading. Modelling and probabilistic analysis also showed that the obvious synergetic effects cannot be neglected in realistic service life prediction.

This final report was reviewed and approved by all members of the RILEM TC 246-TDC. TC Membership: TC Chairlady—Yan Yao, China; TC Secretary—Ling Wang, China. Members: Folker H. Wittmann, Germany; Nele De Belie, Belgium; Erik Schlangen, The Netherlands; Christoph Gehlen, Germany; Hugo Eguez Alava, Ecuador; Max Setzer, Germany; Carmen Andrade, Spain; Rui Miguel Ferreira, Finland; Erika Elaine Holt, Finland; Gideon Van Zijl, South Africa; Feng Xing, China; Tiejun Zhao, China; Michal A. Glinicki, Poland; Xiaomei Wan, China; R. G. Pillai, India; Klaas Van Breugel, The Netherlands.

Keywords Concrete durability · Service life prediction · Chloride ion diffusion · Compressive stress · Tensile stress · Combined actions

Zhendi Wang, Yin Cao, Balqis Md Yunus and Juan Li are Ph.D. students who have contributed substantially to the TC.

1 Introduction

The design of load bearing structures has a long history in civil engineering. In Europe it is now based on Eurocode 2 [1]. Similar codes for structural design exist in other regions (see for example [2–4]). In the

Y. Yao · L. Wang (✉) · Z. Wang · J. Li · Y. Cao
State Key Laboratory of Green Building Materials, China
Building Materials Academy, Beijing 100024, China
e-mail: 626043162@qq.com;
wangling@cbmamail.com.cn

N. De Belie · H. Eguez Alava
Ghent University, Ghent, Belgium

E. Schlangen · B. Md. Yunus
Delft University of Technology, Delft, The Netherlands

F. H. Wittmann
Aedificat Institute Freiburg, Freiburg im Breisgau,
Germany

S. Kessler · C. Gehlen
Technical University of Munich, Munich, Germany

last decade, a Model Code for service life design [5] has been set up analogous to Eurocode 2. In this approach the stress is replaced by environmental actions such as carbonation, chloride penetration, and freeze–thaw attack with and without de-icing agents. The mechanical resistance is replaced by the resistance of concrete to environmental actions such as carbonation, chloride penetration or freeze–thaw cycles.

Based on this concept, the following limit states can be formulated: (1) corrosion initiation induced by chloride ingress or carbonation, (2) cracking due to steel corrosion, (3) spalling of concrete cover due to steel corrosion, and (4) structural collapse due to corrosion of reinforcement. The Model Code provides four different options for service life design: (1) full probabilistic approach, (2) semi-probabilistic approach, (3) deemed to satisfy rules, and (4) avoidance of deterioration. Based on the Model Code, the safety of structures exposed to environmental actions can be expressed in terms of a reliability index β in a similar way to common practice in structural design.

The actual service life of reinforced concrete structures, and of bridges in particular, is in many cases significantly shorter than the designed service life (see for example ASCE 2013 Report Card [6]). According to this report, more than 20% of bridges in the United States are structurally deficient or functionally obsolete. A similar situation exists in many industrialized countries. As a consequence, it has become difficult to keep pace with the growing costs for maintenance and repair of the aging infrastructure.

The Model Code for service life design [5] may be considered to be a significant step forward because durability and service life of reinforced concrete structures can be taken into account during the design stage. According to the Model Code, the necessary material parameters such as the inverse carbonation

resistance or the chloride migration coefficient have to be determined under well-defined laboratory conditions. In recent years, however, it has been shown that these parameters also depend on an applied stress. For example, the rate of chloride penetration can be doubled [7, 8] under the effect of an applied tensile stress. Hence, if the effect of an applied stress is not taken into consideration, the prediction of service life will not be realistic.

Before relevant comparative tests were started by members of the TC 246-TDC the state-of-the-art of this topic was carefully investigated. As a result, a comprehensive annotated bibliography was published in 2013 [9]. These publications served as a starting point for the investigations described in this article.

2 Experiments and materials

2.1 Preparation of specimens

Research groups in five laboratories participated in the comparative test series: (1) Chinese Building Materials Academy (CBMA), (2) Ghent University (UGent), (3) Delft University of Technology (TU Delft), (4) Technical University of Munich (TUM), and (5) Dalian University (DALIAN U.) They were asked to prepare concrete specimens with identical geometry and dimensions. It was suggested that Portland cement Type I, corresponding to Chinese National Standard GB 175 [10], EN 197 [11] or ASTM should be used. All the groups were asked to add an amount of polycarboxylate superplasticizer to the fresh concrete necessary to produce a slump of approximately 15 cm.

Concrete prisms with dimensions $100 \times 100 \times 400$ mm were produced for tests under compression. Dumbbell specimens as shown in Fig. 1 were produced for tests under tension.

Except TUM, the compressive strength of the concrete prisms was usually determined at an age of 28 days. The results are shown in Table 1. The tensile strength of the dumbbell specimens at an age of 28 days determined at CBMA was 3.3 MPa. As can be seen, a wide range of compressive strengths is covered.

The internal faces of all moulds were covered with a thin Teflon film to avoid the water repellent effect of demoulding oil. After casting, the specimens were

W. Li
Dalian University, Dalian, China

Max. J. Setzer
WISSBAU® Consultant Engineering Corporation, Essen,
Germany

F. Xing
Shenzhen University, Shenzhen, China



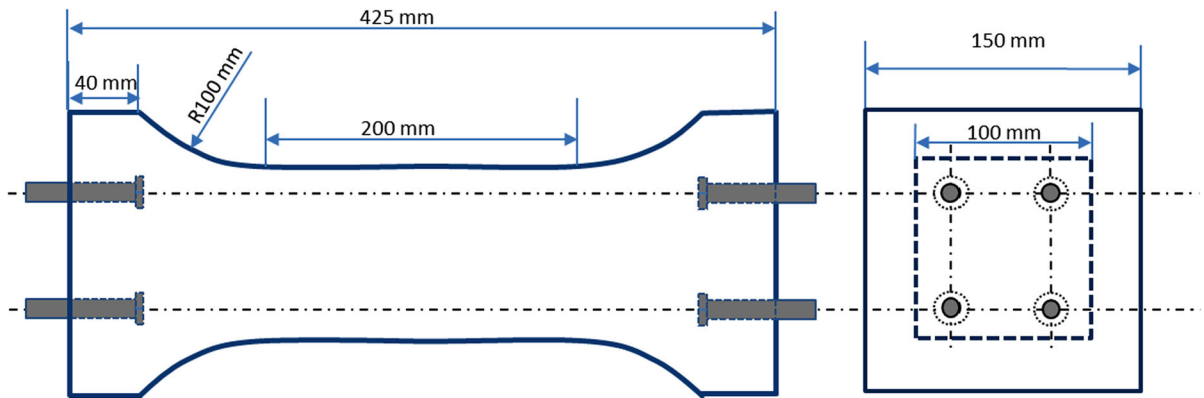


Fig. 1 Shape and dimensions of dumbbell specimen for tests under tension

Table 1 Compressive strength at 28 days of concrete prepared in five different laboratories

Laboratory	CBMA	UGent	TU Delft	TUM ^a	DALIAN U.
Prism strength (MPa)	36.6	56.9	40.7	34.0	26.2

^a Prism strength of TUM was determined at an age of 146 days, just before the prisms were subjected to the combined loading regime (mechanical load and chloride loading)

stored for 24 h under plastic sheets in a climatic chamber maintained at 20 °C and a relative humidity of about 95%. The specimens were then de-moulded and stored in tap water at 20 °C until testing.

Before testing, the specimens were taken out of the water bath and the excess surface water removed with a clean, dry towel. The surfaces were immediately sealed with two layers of self-adhesive aluminium foil. A window with dimensions 80 × 160 mm² on one moulded side surface was left open. This surface was temporarily covered to prevent drying until a plastic tank containing salt solution was attached to the surface. The tank with inner dimensions of 80 × 160 × 50 mm was glued or clamped to the specimens, covering the open window. As soon as the tank was filled with salt solution, chloride could penetrate into the concrete by diffusion. Due to incomplete saturation and further hydration of cement, capillary absorption could not be completely avoided. Nevertheless, the apparent diffusion coefficients obtained from chloride profiles in this experiment characterize the diffusion of chloride in water-saturated concrete. For the prediction of chloride penetration into real concrete structures the environmental climatic conditions have to be taken into consideration.

2.2 Test methods

2.2.1 Specimens under compression

Compressive stress was applied to the concrete prisms using a test rig as shown in Fig. 2, which fulfils the requirements of the Appendix of RILEM TC 107-CSP [12]. The compressive stress ratio, i.e. ratio of applied stress to compressive strength, was chosen to be 0, 30, and 60%. A 3 wt% aqueous sodium chloride solution was circulated from a reservoir through the plastic tank at a rate of 5 ± 1 ml/s. The concentration of the solution was checked regularly and at least once a week during the whole exposure period. The reservoir was sealed with a lid to avoid evaporation and contamination. The specimens were unloaded after exposure times of 2, 6, 18 and 36 weeks, or any other given duration, after which the specimens were ready for chloride profile determination.

2.2.2 Specimens under tension

In order to connect the dumbbell specimens to the testing rig, four bolts were fixed at each end of the mould before casting (Fig. 1). A special test rig was designed for application of a given tensile stress. The

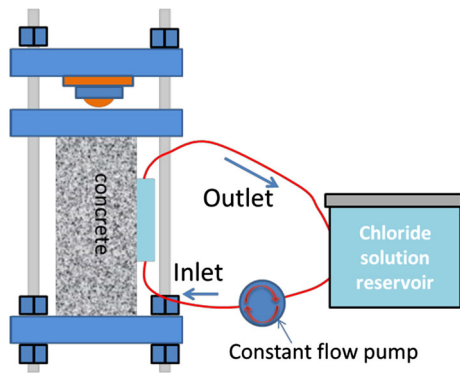


Fig. 2 Experimental setup for determination of chloride diffusion into concrete under compression

bolts on the ends of the dumbbell specimens were screwed to two steel plates joined to the spherical hinges of the test rig (Fig. 3). In this way, any eccentricity of the tension specimens could be avoided as much as possible. Similar test rigs following the same principle can also be used in other cases. Tensile stress ratios, i.e. ratio of applied tensile stress to the ultimate tensile stress, of 0, 50 and 80% were used in the experiments. The operation of the tensile setup is described in more detail in Ref. [13]. The chloride solution was circulated to the open windows of the dumbbell specimens in the same manner and rate as for the specimens under compression. The circulation of the salt solution was stopped and the dumbbell

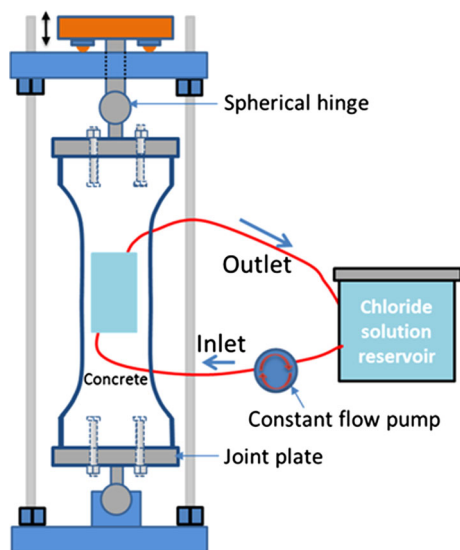


Fig. 3 Experimental setup for tension tests

specimens were unloaded after exposure times of 2, 6, 18 and 36 weeks. Chloride profiles in the concrete specimens were then determined. For other applications different periods of chloride penetration under tensile stress can be chosen.

2.3 Determination of chloride profiles

First the plastic tank was removed from the unloaded specimens. Care must be taken that the concrete surface is protected from drying before the milling process begins, because drying will modify the chloride profile. Powder samples from the exposed surface of all specimens were obtained by milling layers in steps with a thickness of 1–2 mm. The number and thickness of the layers was adjusted according to the chloride profile expected. A minimum of eight measuring points should be distributed on the descending branch of the profile. In order to avoid edge effects, and the effect of the glue on the self-adhesive aluminium foil, sampling was performed over an area with at a distance of 10 mm from the border of the exposed region. Particles with a diameter of more than 1 mm may exist in powder which is obtained by milling or crushing with subsequent grinding. In this case special care has to be taken to assure sufficient time for the extraction of the chloride from the powder using acid. The powder was digested in acid before chemical analysis of chloride content has been made according to EN 14629 [14]. It is recommended that the tests are performed at least in triplicate for the determination of average chloride ion diffusion coefficients.

3 Test results

3.1 Effect of compressive stress

3.1.1 Chloride profiles as measured at stress ratios of 0 and 30%

The chloride profiles obtained in different laboratories at stress ratios of 0 and 30% are presented in Figs. 4, 5, 6 and 7. The results obtained at UGent are shown separately (Figs. 4 for 0%, 5 for 30% stress ratio) because of the different exposure times and higher number of data points obtained per profile. The latter was considered to be important especially for longer

diffusion periods and for high stress ratios. Moreover, the scatter of values obtained in one laboratory can be estimated from these figures, because profiles measured with two similar specimens are shown.

As apparent in Figs. 4 and 5, all chloride profiles show a smooth decrease in chloride content with increasing distance from the surface. Near the surface, however, more scatter is observed. After longer exposure times a plateau is present adjacent to the surface. This clearly underlines the well-known fact that chloride penetration cannot be explained by pure diffusion. A series of different mechanisms, such as capillary absorption, chemical reactions with the porous matrix, sorption processes on the huge surface of hydration products, all affect the transport of ions through the pore space of concrete. Nevertheless, it can be seen that significantly less chloride penetrates into concrete under the influence of an applied compressive stress.

Figure 6 presents the chloride profiles obtained with unloaded specimens obtained at the other four laboratories involved in the comparative test series and Fig. 7 the chloride profiles for a stress ratio of 30%. It is not surprising that a large scatter of the chloride profiles occurs because the compressive strengths of the tested concrete specimens are different. In addition, values from DALIAN U. represent the water soluble chloride content while the other values were obtained by acid extraction.

3.1.2 Chloride profiles measured at 60% stress ratio

Figure 8 shows typical profiles determined at UGent at a stress ratio of 60%. In particular after longer exposure times, the chloride profiles differ from the usual shape Fig. 8. A plateau is present at small distances from the surface. As mentioned above, this cannot be due to a simple diffusion process alone. This

zone near the surface may be referred to as the convection zone. Most authors suggest that only the values behind the convection zone should be used for the determination of an apparent diffusion coefficient. Thus the values to the right of the vertical lines serve as a basis for fitting the error function.

The results shown in Fig. 8 underline again the fact that chloride penetration is not a pure diffusion process. Determination of a diffusion coefficient is a simplification of a complex process. The values obtained may nevertheless be used for comparison of different types of concrete.

The chloride profiles as determined by the four other groups for an applied stress ratio of 60% are plotted in Fig. 9. A large scatter of the data is apparent. This is, among other effects, also due to the different quality of the concretes tested (Table 1). Nevertheless, fitting the data with Fick's second law may be considered to be a reasonable approximation. Information on how to perform the fitting procedure is given in EN 12390-11: 2015 Annex F [15]. Recommendations on how to present and evaluate the chloride profiles are provided in the Recommendation of RILEM TC 246-TDC Influence of Applied Stress on Chloride Diffusion [13].

3.1.3 Diffusion coefficients and surface concentrations from profiles determined in five laboratories

The diffusion coefficient D and the surface concentration C_s obtained by the five participating laboratories: UGent, CBMA, TU Delft, TUM, and DALIAN U. are presented in Fig. 10. The diffusion coefficients and surface concentrations were determined by curve fitting according to EN 12390-11: 2015 Annex F [15]. The large scatter of the values is mainly due to the fact that the quality of the tested concrete was not the same.

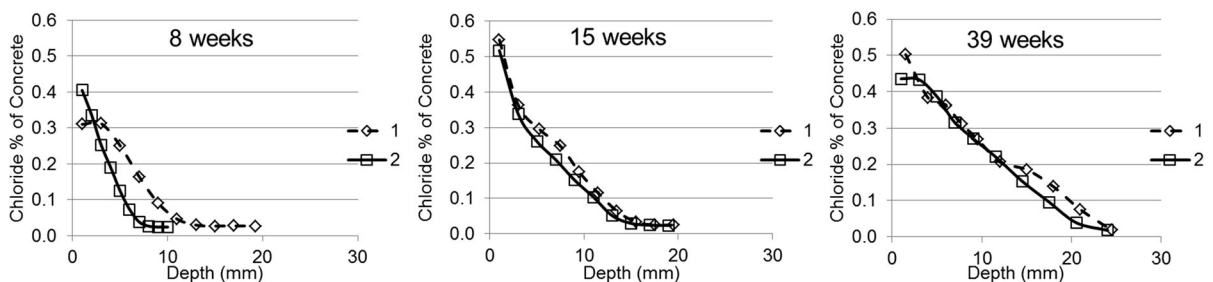


Fig. 4 Chloride profiles measured at UGent after 8, 15 and 39 weeks for similar concrete specimens without applied stress

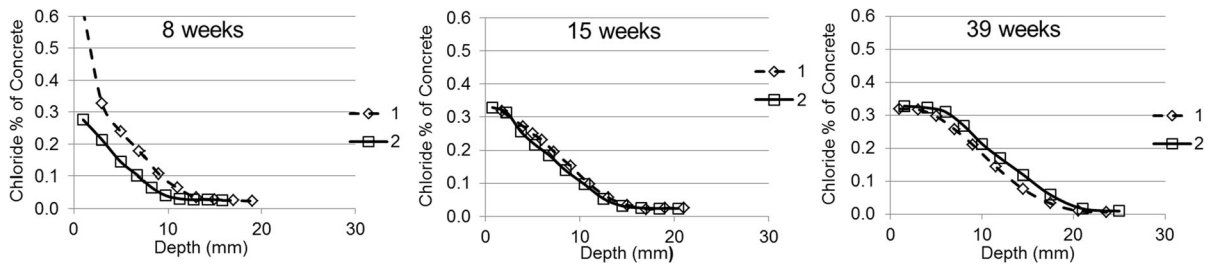
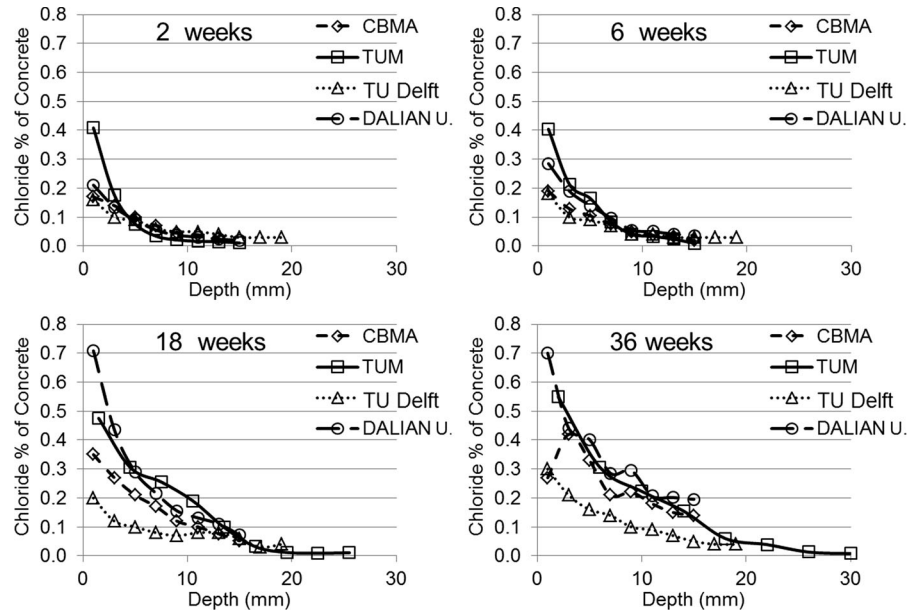


Fig. 5 Chloride profiles measured at UGent after 8, 15 and 39 weeks for similar concrete specimens at a compressive stress ratio of 30%

Fig. 6 Chloride profiles measured in four different laboratories after exposure times of 2, 6, 18 and 36 weeks for specimens without applied stress



From Fig. 10 it can be concluded that the diffusion coefficients tend to decrease with exposure time while the calculated surface concentrations increase. All the values for the diffusion coefficients tend to stabilize at values approaching $(3 \sim 4) \times 10^{-12} \text{ m}^2/\text{s}$ for long exposure time (36 weeks). The calculated surface concentration stabilizes around 0.5% for the same exposure age.

At a load of 30% of the ultimate failure load, the diffusion coefficients were usually similar or lower than in the unloaded situation. At a load of 60%, the situation was less clear. Similar, higher or lower diffusion coefficients were determined in the different laboratories. In some cases, a convection zone near the surface formed as apparent in Figs. 8 and 9. The data therefore partly agree with the literature which states that chloride diffusion under moderate compressive

load is slower, but increases if the applied load is over half of the ultimate load [9].

3.2 Effect of tensile stress

3.2.1 Chloride profiles at tensile stress ratios of 0, 50 and 80%

The chloride profiles determined for concrete specimens under tensile stress are shown in Fig. 11. The profiles were determined after exposure times of 2, 6, 10, 18 and 36 weeks. It can be clearly seen that the chloride content increases steadily with increasing exposure time. The chloride content at a given depth increases significantly when tensile stress is applied. This result was expected since the pore space or the micro-cracks are widened under tensile stress.

Fig. 7 Chloride profiles measured in four different laboratories after exposure times of 2, 6, 18 and 36 weeks for specimens at a stress ratio of 30%

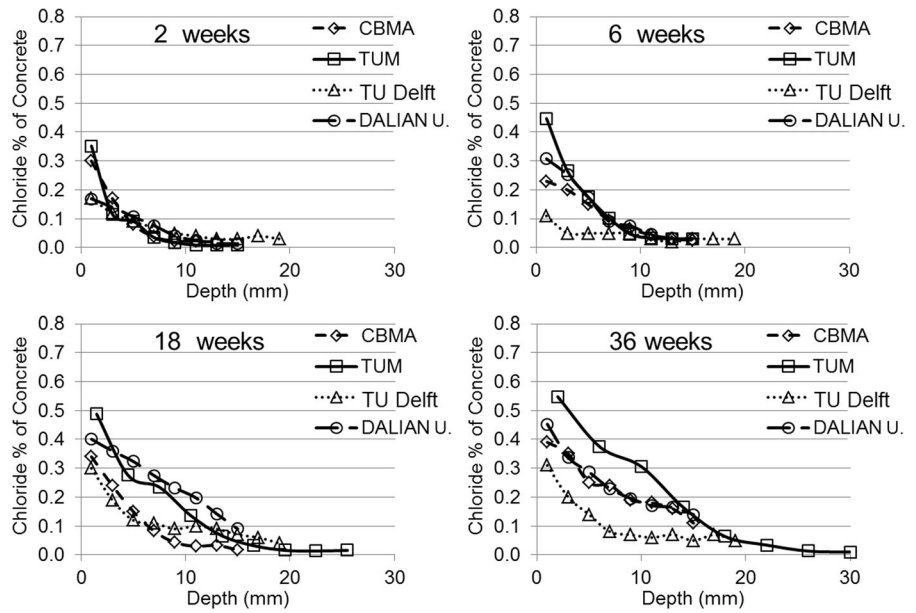
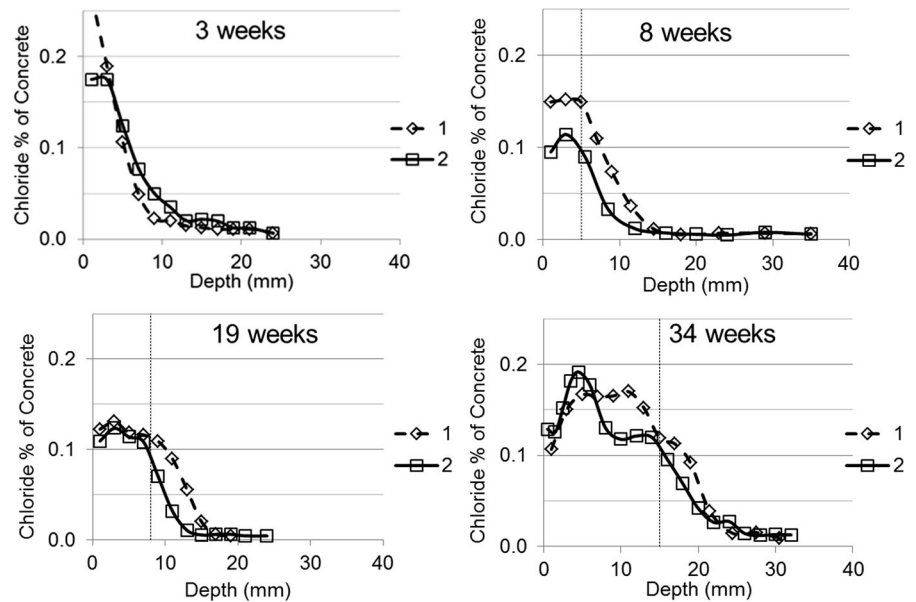


Fig. 8 Chloride profiles measured at UGent after exposure times of 2, 8, 19 and 34 weeks for specimens at a compressive stress ratio of 60%



3.2.2 Diffusion coefficients and surface concentrations measured under tensile stress

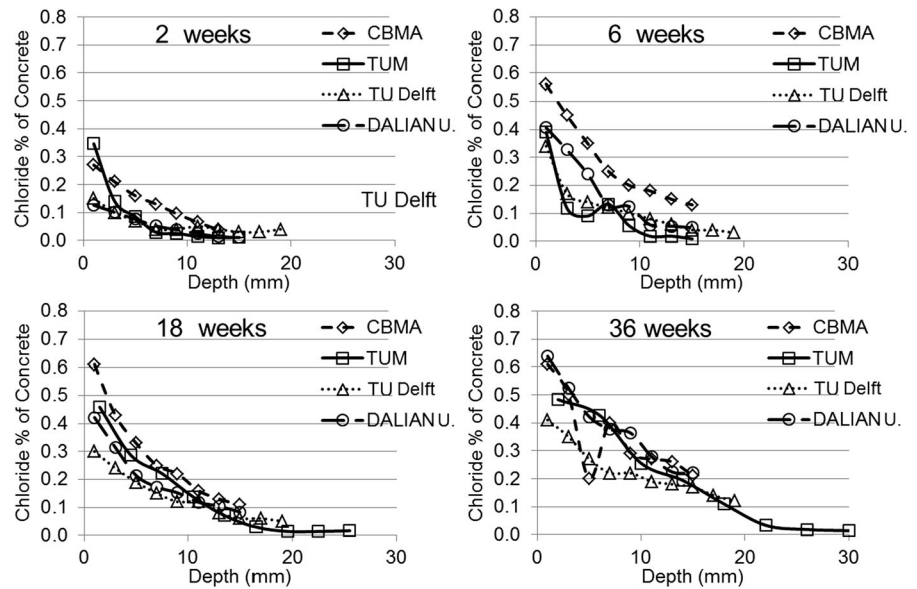
As mentioned above, the penetration of chloride into concrete is a complex process which may be simulated by assuming that diffusion represents the combination of several transport mechanisms. This must be kept in

mind when diffusion coefficients are determined. The diffusion coefficients and calculated surface concentrations are shown in Fig. 12.

It is apparent in Fig. 12 that the diffusion coefficient of concrete under tension increases with increasing stress ratio and decreases significantly with exposure time. Application of tensile stress accelerates



Fig. 9 Chloride profiles measured in four different laboratories after exposure times of 2, 6, 18 and 36 weeks at a compressive stress ratio of 60%



chloride diffusion in concrete. Despite the large scatter, it can be seen that the calculated surface concentration increases slightly with increasing exposure time.

4 Modelling and prediction

4.1 Modelling

Reinforced concrete structures which are exposed to de-icing salt or seawater can be damaged by chloride induced reinforcement corrosion. The fib Model Code for Service Life Design, fib bulletin 34 [5], provides a transport model for predicting the time-dependent probability that reinforcement corrosion is initiated. The transport model considers the time at which a critical chloride content at the depth of the reinforcement is reached in dependence of the concrete characteristics and chloride exposure. Further explanations on relevant input data and example calculations are available in fib bulletin 76 [16]. According to [5] and [16], transport of chlorides into concrete can be modelled with Eqs. 1–3, [16]. Here, Eq. 2 was extended by a so-called stress factor k_1 which takes the actual stress condition of the structural member into account.

$$C(c_{\text{nom}}, t_{\text{SL}}) = C_i + (C_s - C_i) \cdot \left[\text{erf} \left(\frac{c}{\sqrt{D_{\text{app,A}}(t_0) \cdot t}} \right) \right] \quad (1)$$

$$D_{\text{app,A}}(t) = k_e \cdot k_1 \cdot D_{\text{app}}(t_0) \cdot \left(\frac{t_0}{t} \right)^{\alpha_A} \quad (2)$$

$$k_e = \exp \left(b_e \cdot \left(\frac{1}{T_{\text{ref}}} - \frac{1}{T_{\text{real}}} \right) \right) \quad (3)$$

c_{nom} is the nominal concrete cover; t_{SL} the design service life; C_i the initial chloride content; C_s the chloride content at the concrete surface; c the concrete cover; $D_{\text{app,A}}$ the apparent chloride diffusion coefficient; t_0 the reference point in time; t the time; k_e the transfer parameter; α_A the aging exponent; b_e the temperature coefficient; T_{ref} the reference temperature; T_{real} the temperature of the structural element or the ambient air.

In the following study the service life (given by the time to corrosion initiation) is compared for concrete components which are not loaded and components subjected to compressive and tensile stress.

The study corresponds to a case study already presented in [16], Table A.2-15 which has been considered due to its similarity in concrete material (CEM I-concrete of $w/c = 0.45$, unloaded). The case

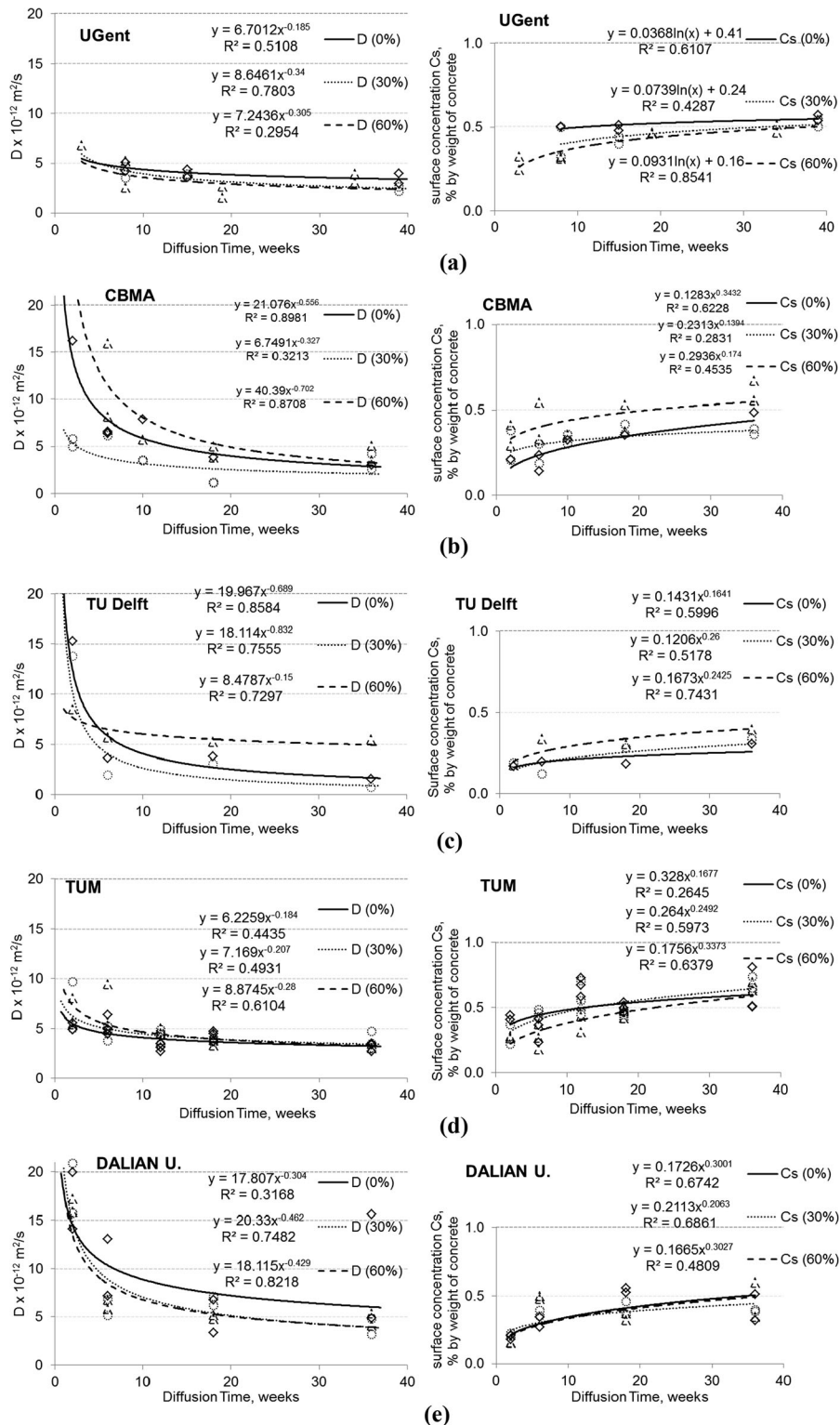


Fig. 10 Chloride diffusion coefficients and surface concentrations determined from experimental data obtained in five laboratories. **a** UGent, **b** CBMA, **c** TU Delft, **d** TUM, **e** DALIAN U



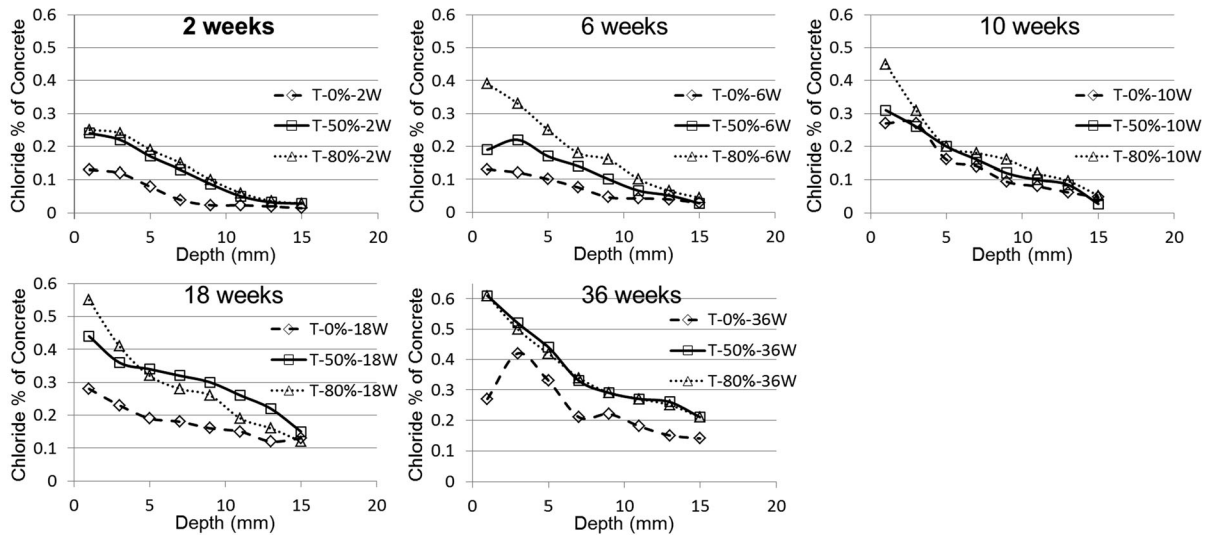
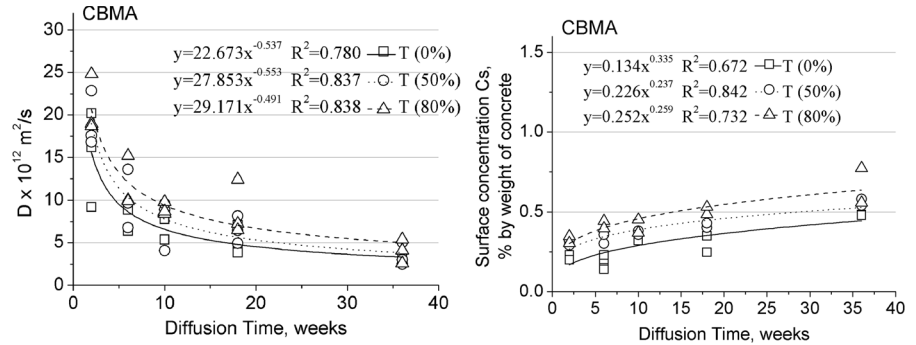


Fig. 11 Chloride profiles determined after 2, 6, 10, 18 and 36 weeks under tensile stress with stress ratios of 0, 50 and 80%

Fig. 12 Chloride diffusion coefficients and calculated surface concentrations of concrete under tension



study in fib bulletin 76, which is recalculated here for loaded concrete members, represents a typical XS2-exposure (member immersed in seawater) in Portugal (Europe). Most of model input parameters, especially the variables characterizing the environmental load, were taken from Table A.2-15 of fib bulletin 76. However, input variables to characterize the concrete material ($D_{app}(t)$) were derived from the above experiments. The material parameters used in the recalculation was averaged data of all five laboratories (CBMA, UGent, TU Delft, TUM and DALIAN U.) participating in the experimental program. The average diffusion coefficient determined after six weeks ($t_0 = 0.115$ years) for unloaded specimens was taken as the reference value (the mean was 6.52×10^{-12} m²/s, the standard deviation was 2.88×10^{-12} m²/s), Table 2. All the other load conditions were calculated with a stress factor k_1 , in

which $k_1 = 1$ for the reference, $k_1 = 0.80$ for stress ratio 0.3 (compression), $k_1 = 1.17$ for stress ratio 0.6 (compression), $k_1 = 1.25$ for stress ratio 0.5 (tension) and $k_1 = 1.53$ for stress ratio 0.8 (tension).

In order to determine an age exponent, the exposure time should be as long as possible (minimum 2 years). However in this study, the maximum exposure time was only 36 weeks. In total 15 series were investigated (five labs, 3 different stress levels), Thus 15 “short term” age exponents, Fig. 10, could be calculated according to [16], approach A. Table 2 contains not only information on α_A , but also shows the general input parameters in accordance with [5].

4.2 Prediction

The reliability of chloride-exposed concrete members without load and under compressive stress or tensile



Table 2 Input parameters for the service life prediction

Parameter	Unit	Distribution type	Mean	Standard deviation	a	b
$D_{app}(t_0)$	$10^{-12} \text{ m}^2/\text{s}$	Normal	6.52	2.88	–	–
α_A	–	Beta	0.39	0.18	0	1
t_0	Years	Constant	0.115	–	–	–
t	Years	Constant	50	–	–	–
T_{ref}	K	Constant	293	–	–	–
T_{real}	K	Normal	288	5.0	–	–
b_e	K	Normal	4800	700	–	–
$C_{S, \Delta}$	wt%/cem	Lognormal	3.0	1.0	–	–
Δx	mm	Constant	0	–	–	–
C_{crit}	wt%/cem	Beta	0.6	0.15	0.2	2.0
c	mm	Normal	50	6	–	–

stress, is given in Fig. 13. All calculations of this exemplifying case study are performed using the software STRUREL (Structural Reliability Analysis Software).

In order to obtain values on the effect of loading on service life, the service life was defined to be reached when the reliability drops below a defined minimum reliability of $\beta = 0.5$. Based on this definition, the service life was determined for each of the five curves in Fig. 13 and the relative service life calculated with respect to the reference, Fig. 14. Figure 14 shows that the service life of elements loaded by 30% of compressive strength was on average prolonged by a factor of 1.36 compared to the reference; the service life of elements loaded by 60% of compressive strength was on average shortened by the factor of

0.82 in comparison to unloaded elements. It should be pointed out that at compressive stress ratio of 60% only two out of the five laboratories found a remarkable increase in diffusion coefficient (which is linked to shortened service life), the others found a small decrease in diffusion coefficient. From the data presented here we may conclude that further tests will be needed to get more precise information on the effect of loading condition on service life of reinforced concrete elements. It should be underlined in this context that the main aim of RILEM TC 246-TDC was to develop a suitable test method.

If tensile stress was applied, the service life was shortened compared to the reference by a factor of 0.70 (50% tensile strength stress) and 0.53 (80% tensile strength).

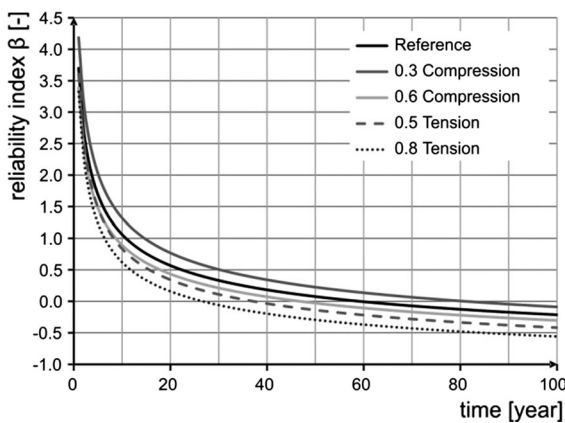


Fig. 13 Calculated reliability index for chloride-exposed concrete members without load (reference) and under compressive or tensile load (two stress ratios)

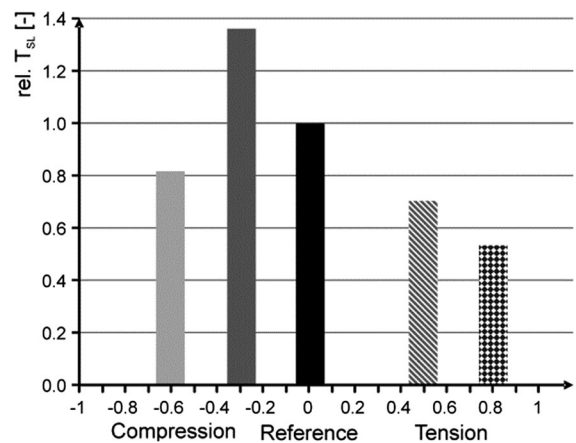


Fig. 14 Relative service life (rel. T_{SL}) of chloride-exposed concrete members without load (reference) and under compressive or tensile load (two stress ratios)

5 Conclusions and outlook

The main task of RILEM TC 246-TDC was to develop a test method to study the effect of applied compressive and tensile stress on the rate of chloride penetration. The experimental results presented in this report show that the state of stress should be taken into consideration in order to make durability and service life design more reliable and realistic.

As mentioned in the introduction of this report already, RILEM TC 246-TDC has opened a new field of research aimed at making the design of reinforced concrete structures with respect to durability and service life more realistic and reliable by taking the combination of applied mechanical stress and environmental load into consideration. It was initially clear that this task could not be finished within the duration of one single RILEM TC. Despite this a start has been made which now requires a well-structured continuation. The effect of an applied stress on chloride diffusion was measured and a recommendation for the test method was formulated. The results obtained already allow an estimation of the effect of an applied stress on durability and the service life of reinforced concrete structures exposed to a chloride containing environment. If the recommended test method is applied, the specific behaviour of different types of concrete subjected to stress can be taken into consideration.

In the future, more work will be necessary in order to investigate the effect of an applied stress, for instance on the rate of carbonation and freeze–thaw resistance. Results described in the final report of RILEM TC 246-TDC clearly show the need for follow-up investigations. Future technical committees could have the common task of providing a solid basis for taking the effect of an applied stress on durability and service life into consideration. In this manner, the actual situation of the built infrastructure in many countries could be substantially improved in a systematic way. The next step should be to perform similar test series on concrete exposed to carbonation and to formulate a standard method that will allow determining the effect of an applied tensile or compressive stress on the rate of carbonation.

For a generally realistic and reliable service life prediction the effect of cyclic stress has to be taken into consideration too. So far, however, only very limited data exist on this topic [9].

In this report an experimental method to study the effect of mechanical load on chloride penetration into the pore space of cement-based materials is described in detail. In fact, the service life of reinforced concrete structures depends on a multitude of possible combinations of mechanical load and environmental actions, including freeze–thaw cycles. Frost action has been studied in detail by two RILEM TCs, TC 176-IDC [17] and TC 117-FDC [18]. Recommendations published by these two RILEM TCs were based on a series of comparative test series and results were evaluated according to ISO 5725 [19]. Now the essential results of these two TCs are part of European standardization. The cracks formed during freeze–thaw cycles and frost suction in particular will have to be taken into consideration in future tests on combined environmental and mechanical loading [20].

In order to achieve a better understanding and a systematic description of the effect of the combination of mechanical load with environmental actions on the durability and service life of reinforced concrete structures, a numerical model for damage processes in the composite structure of concrete has to be developed. This model could be tested by comparison with appropriately measured data. It could be helpful to predict the behaviour under different load combinations.

As well as experimental test series and numerical simulations, the actual method of predicting durability and service life has to be developed further in order to enable easy use of experimental data for a realistic service life prediction.

Acknowledgements The financial support from the following four organizations is gratefully acknowledged: (1) National Natural Science Foundation of China (Grant No. 51320105016), (2) the Ecuadorian National Secretary for Science and Technology “SENESCYT”, (3) ESPOL University (Ecuador) and Magnel Laboratory for Concrete Research of Ghent University (Belgium), (4) Ministry of Higher Education Malaysia (MOHE) and Universiti Teknologi MARA (UiTM).

References

1. Eurocode 2 (2004) Design of concrete structures, Part 1-1: General rules and rules for buildings, EN 1992-1-1
2. ACI 318-14 (2014) Building code requirements for structural concrete and commentary
3. JSCE Guidelines for Concrete No. 15 (2007) Standard specifications for concrete structures—design



4. GB 50010 Chinese National Standard (2010) Code for design of concrete structures
5. Schießl P, Bamforth P, Baroghel-Bouny V, Corley G, Faber M, Forbes J, Gehlen C et al (2006) Model code for service life design. *fib bulletin* 34
6. ASCE (2013) 2013 Report card for America's Infrastructure
7. Wittmann FH, Zhao T, Jiang F, Wan X (2012) Influence of combined actions on durability and service life of reinforced concrete structures exposed to aggressive environment. *Restor Build Monum* 18:105–112
8. Wan X, Wittmann FH, Zhao T (2011) Influence of mechanical load on service life of reinforced concrete structures under dominant influence of carbonation. *Restor Build Monum* 17:103–110
9. Yao Y, Wang L, Wittmann FH (eds) (2013) Publications on durability of reinforced concrete structures under combined mechanical loads and environmental actions. An Annotated Bibliography, RILEM TC 246-TDC
10. GB 175 Chinese National Standard (2007) Common Portland Cement
11. BS EN 197-1 Cement (2011) Composition, specifications and conformity criteria for common cements-part 1: cement
12. RILEM TC 107-CSP Recommendation (1998) Measurement of time-dependent strains of concrete. *Mater Struct* 31:507–512
13. Recommendation of RILEM TC 246-TDC: Influence of applied stress on chloride diffusion. Submitted to *Materials and Structures*
14. EN 14629 (2007) Products and systems for the protection and repair of concrete structures—test methods—determination of chloride content in hardened concrete
15. EN 12390-11 (2015) Determination of the chloride resistance of concrete, unidirectional diffusion
16. Gehlen C, Bartholemew M, Edvardsen C, Ferreira MV, Greve-Dierfeld S, Gulikers J, Helland S, Markeset G, McKenna P, Papworth F, Pielstick B, Rahimi A (2015) Benchmarking of deemed-to-satisfy provisions in standards, *fib bulletin* 76: ISBN: 978-88394-116-8, May 2015
17. Setzer MJ, Heine P, Kasperek S, Palecki S, Auberg R, Feldrappe V, Siebel E (2004) Internal damage of concrete due to frost action. *Mater Struct* 31:743–753
18. RILEM TC 117-FDC Recommendation (1996) CDF test—test method for the freeze thaw and deicing resistance of concrete—tests with sodium chloride (CDF). *Mater Struct* 29:523–528
19. ISO 5725-1 (1994) Accuracy (trueness and precision) of measurement methods and results
20. Setzer MJ, Development of the Micro-Ice-Lens Model, Setzer MJ, Auberg R, Keck H-J (2002) Frost resistance of concrete. In: *Proceedings of Intern. RILEM Workshop, Essen 2002. RILEM Proceedings of 24. RILEM Publ. S.A.R.L., Cachan-Cedex, France*, pp 133–146

Appendix B

Recommendation of RILEM TC 246-TDC: test methods to determine durability of concrete under combined environmental actions and mechanical load

Test method to determine the effect of applied stress on chloride diffusion

Yan Yao · Ling Wang · Folker H. Wittmann · Nele De Belie ·
Erik Schlangen · Christoph Gehlen · Zhendi Wang · Hugo Eguez Alava ·
Yin Cao · Balqis MD Yunus · Juan Li

Received: 15 December 2016 / Accepted: 24 January 2017
© RILEM 2017

Abstract The combination of environmental actions and mechanical load has obvious synergetic effects on the durability of concrete. But these effects have been widely neglected so far. For a realistic service life prediction the effect of an applied mechanical load on chloride penetration has been taken into consideration as a first and important step in RILEM TC 246-TDC since 2011. This recommendation focuses on the test method to determine the effect of applied compressive stress and tensile stress

on chloride diffusion. It includes detailed experimental procedure to receive consistent results of chloride profile and the apparent chloride ion diffusion coefficient of concrete under compressive and tensile stress.

Keywords Concrete durability · Compressive stress · Tensile stress · Chloride ion · Diffusion coefficient

This recommendation was prepared by a working group within RILEM TC 246-TDC: Yan Yao, Ling Wang, Folker H. Wittmann, Nele De Belie, Erik Schlangen, Christoph Gehlen, Zhendi Wang, Hugo Eguez Alava, Yin Cao, Balqis MD Yunus, Juan Li, and further reviewed and approved by all members of the RILEM TC 246-TDC.

Acknowledgement: This recommendation has been prepared within RILEM TC 246-TDC. The contribution of all TC members in discussion during preparation of the draft of this recommendation and their final reading and approval of the document is gratefully acknowledged.

TC Membership:

TC Chairlady: Yan Yao, China.

TC Secretary: Ling Wang, China.

Members: Folker H. Wittmann, Germany; Nele De Belie, Belgium; Erik Schlangen, The Netherlands; Christoph Gehlen, Germany; Zhendi Wang, China; Hugo Eguez Alava, Ecuador; Yin Cao, China; Balqis MD Yunus, Malaysia; Juan Li, China; Max Setzer, Germany; Carmen Andrade, Spain; Rui Miguel Ferreira, Finland; Erika Elaine Holt, Finland; Gideon Van Zijl, South Africa; Feng Xing, China; Tiejun Zhao, China; Michal A. Glinicki, Poland; Xiaomei Wan, China; R. G. Pillai, India; Klaas Van Breugel, The Netherlands.

Y. Yao · L. Wang (✉) · Z. Wang · Y. Cao · J. Li
China Building Materials Academy, Beijing, China
e-mail: wangling@cbmamail.com.cn

F. H. Wittmann
Aedificat Institute Freiburg, Freiburg, Germany

N. De Belie · H. E. Alava
Ghent University, Ghent, Belgium

E. Schlangen · B. MD Yunus
Delft University of Technology, Delft, The Netherlands

C. Gehlen
Technical University of Munich, Munich, Germany

Zhendi Wang, Yin Cao, Balqis MD Yunus and Juan Li: Ph.D students who have contributed substantially to this manuscript.

1 Introduction

Several methods to predict durability of reinforced concrete structures exist at present. In most cases, one dominant deteriorating process such as carbonation or chloride penetration is taken into consideration. Experimental results as well as observations in practice show, however, that this is not a realistic and certainly not a conservative approach. The combination of much more severe than the sum of the individual mechanical load and environmental actions may be contributions.

There are obvious synergetic effects which have been widely neglected so far. With the aim of developing more realistic test methods, a first RILEM Technical Committee (RILEM TC 246-TDC) on the determination of durability and service life of concrete under combined environmental actions and mechanical load was set up in 2011.

To establish a solid basis for the following experimental studies, an annotated bibliography containing publications on the durability of reinforced concrete structures exposed to mechanical load and environmental actions was first compiled [1]. This publication presents the state-of-the-art in this specific field. This document is now available for all interested colleagues.

Based on the annotated bibliography and the specific experience of TC members, well-defined comparative test series have been carried out and evaluated. As a first step, the combination of mechanical load and chloride penetration was investigated. It became obvious that for a realistic service life prediction the effect of an applied mechanical load on chloride penetration has to be taken into consideration [2]. Other combinations of mechanical load and environmental actions will be studied in detail in several follow-up technical committees. At a later stage, the results of all follow-up committees will be critically compiled and implemented in national and international codes. In this way, the average service life of the built infrastructure can be extended significantly.

From the wide range of possible combinations of mechanical stress and environmental actions in practice, a few combinations were chosen as a first step. For obvious reasons, this work has to be extended considerably in order to make service life design more reliable in the future.

2 Scope and applications

Among the numerous possible combinations of mechanical load and environmental actions, the effect of compressive load and tensile load on chloride penetration into the pore space of concrete was selected as a first and most important example. This is a simplified case of the many different possible load combinations which may occur in field practice. As expected, a strong effect of an applied mechanical load on chloride penetration was observed. It was found that the chloride penetration is significantly accelerated under an applied tensile stress. The reduction of service life of reinforced concrete structures due to this combination can now be estimated. A more sophisticated method to take combined loads into consideration is being developed. The application of a compressive stress which is higher than half the ultimate strength also accelerates chloride penetration [1–3].

One major aim of RILEM TC 246-TDC was to develop a test method which allows determination of the effect of combined mechanical load and environmental actions. A proposed test method was critically checked by comparative test series run by members of the TC. Up to six laboratories in different countries participated in these comparative test series. The originally proposed test method was developed further and refined based on the first experience with the comparative test methods. Now, the proposed test method can be applied by others based on the detailed recommendation.

3 Equipment, specimens and test procedure

3.1 General

In this section, the principle of the test, the recommended loading rigs, the procedure for preparation, and initial curing of the specimens are described. After preparation, the specimens are mechanically loaded under compression or tension up to a certain stress ratio. During sustained loading the specimens are subjected to chloride ingress. The method for applying the chloride solution to the surface of the specimen is explained. Furthermore, the test procedure and the method for determination of the chloride profiles are given.

3.2 Test equipment

The applied load may be either compressive or tensile. The specimens for both loading cases are different as well as the loading rigs. The specimen geometry and preparation are discussed in Sect. 3.3. The principle of the loading rig for compression is shown in Fig. 1. The compressive load is applied on a prismatic concrete specimen using a test rig similar to test rigs used for creep loading and described in RILEM recommendation of TC 107-CSP [4]. Different loading rigs are used for the creep tests. The hydro-pneumatic accumulator shown in Fig. 1 is recommended.

Test rigs, which have the same principle and function and fulfil the requirements of RILEM recommendation of TC 107-CSP can be used as well. All the test rigs shall be mechanically stable during the entire loading period. A test rig with a fixed container for the chloride solution is shown in Fig. 2a. The method of fixing the container to the test specimens is shown in detail in Fig. 2b.

The test rig shown in Fig. 3 is recommended for tensile loading. Two plates attach the four bolts on each end face of the dumbbell tension specimens (Fig. 4) to the spherical hinges which are employed to minimize the uniaxial eccentricity of the tension specimen. Any other test rig based on the same principle may also be used. Strain gauges with an accuracy of $\pm 1 \mu\text{m}$ should be glued to the steel frame for monitoring the applied load. They can be mounted on the steel bars connecting the two end plates or on the steel pins connected to the spherical hinges. The strain gauges attached to the frame should be

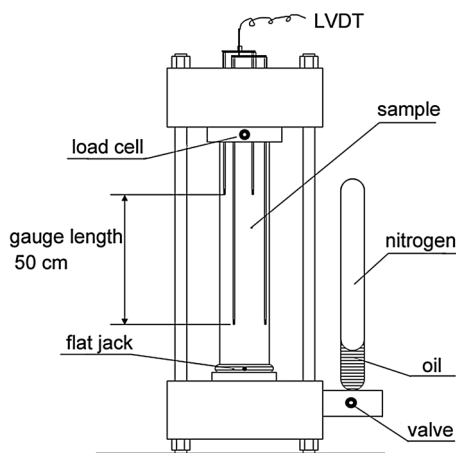


Fig. 1 Schematic representation of test rig for compression [4]

calibrated using dead loads or a loading frame equipped with load cells to convert the measured strain into stress.

To apply the chloride solution to the surface of the loaded specimen, a plastic container shall be used as shown in Figs. 2 and 3. The container shall have an inner dimension of $80 \times 160 \times 50 \text{ mm}^3$; the

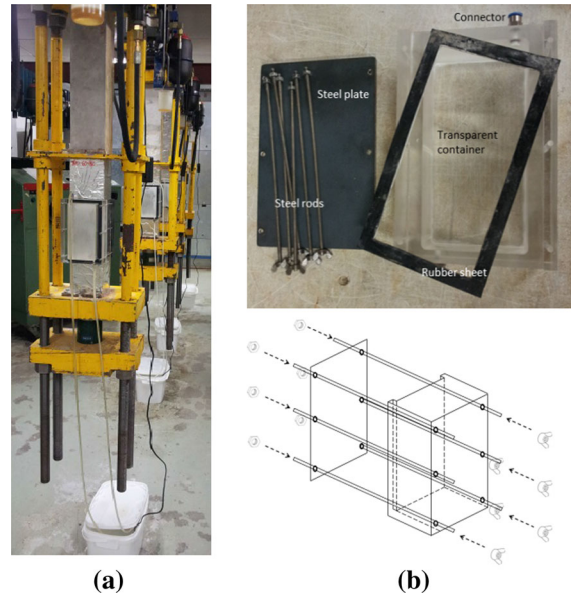


Fig. 2 Details of test equipment: a example of test rig with specimens including attached container for chloride solution, and b container and principle for fixation of container

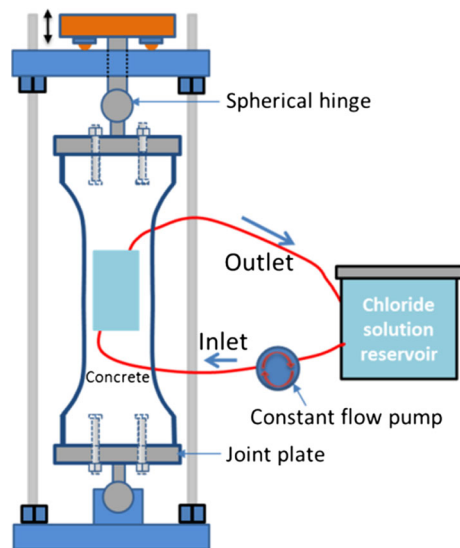
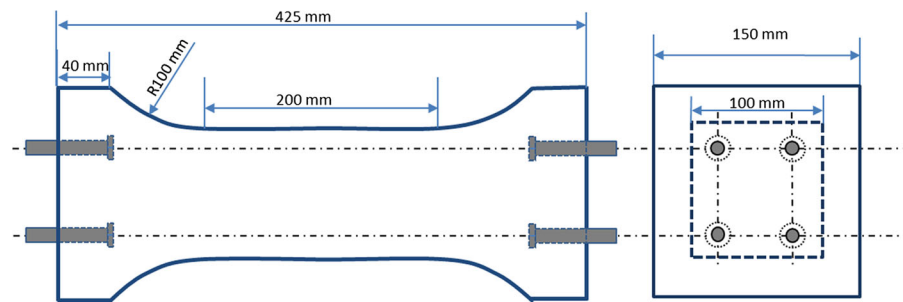


Fig. 3 Test rig for tension and dumbbell specimen with chloride solution container and reservoir for chloride solution

Fig. 4 Geometry and dimensions of dumbbell specimens for tension tests



minimum thickness of the container shall be 5 mm. The container is transparent in order to enable continuous observation of the circulation of the chloride solution. To connect the container with the specimen, a clamping system as shown in Fig. 2b is used. The container shall be connected to a reservoir by an inlet and an outlet hose. The volume of the reservoir should be at least 25 l. It must be resistant to the aqueous chloride solution. A pump with a small capacity should be used to circulate the solution at a constant flow rate of 5 ± 1 ml/s. The flow rate shall be checked regularly.

3.3 Preparation of concrete specimens

For the preparation of the specimens, the internal dimensions of the steel moulds are required with a tolerance of ± 1 mm. For the compression tests the concrete shall be cast into $100 \times 100 \times 400$ mm³ prisms. Dumbbell specimens for tension tests shall be cast with the dimensions given in Fig. 4. To connect the specimen with the tensile testing rig, four bolts shall be embedded at each end of the mould for dumbbell specimens before pouring. The raw materials and mix composition of the concrete are chosen for each specific project and should be similar to the mix used on site or as prescribed in the project specifications. Concrete with a slump between 12 and 15 cm is recommended for easy casting. The specimens shall be cast according to EN 206 [5].

A thin film or foil of Teflon shall be applied to all internal faces of each mould in order to avoid the disturbing effects of demoulding oil. The fresh concrete shall be cast in two layers. After spreading each layer of concrete uniformly, each layer shall be compacted on a vibration table.

After casting, the specimens shall be stored in a room maintained at 20 °C and not <95% relative

humidity (RH) for 24 h. Afterwards, the samples shall be demoulded. For further curing two alternative procedures are available:

- *Procedure A* immersion the specimens in tap water saturated with $\text{Ca}(\text{OH})_2$ at a temperature of 20 °C.
- *Procedure B* placement of the specimens in a moist curing chamber at a temperature of 20 ± 2 °C and a relative humidity not <95%.

After curing, specimens shall be removed from the curing procedure for testing at an age of 28 days.

All specimens shall be vacuum saturated with $\text{Ca}(\text{OH})_2$ solution before the application of the mechanical load and beginning the chloride diffusion test. The vacuum apparatus shall consist of the following.

- A container with a capacity for at least three specimens.
- A pump that is capable of maintaining an absolute pressure of <50 mbar (5 kPa) in the container.

The prisms shall be placed under vacuum ($p < 5$ kPa) for 2.5 h. Then the pressure shall be gradually increased to atmospheric pressure as water is let in and the samples left in the container for another 24 h.

After vacuum saturation, the water on the surfaces of the specimens shall be removed with a dry towel. Then the surface shall be immediately sealed with two layers of self-adhesive aluminium foil. The chloride container should also be attached immediately on a window with dimensions 80×160 mm² left open on one moulded surface with the following.

The preparation of specimens for compression and tension tests shall be identical.

3.4 Test procedure

A flow chart of the test procedure is shown in Fig. 5.

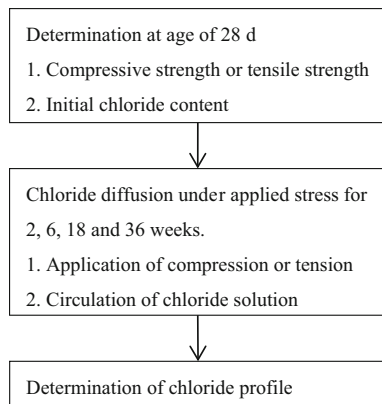


Fig. 5 Flow chart of the test procedure

The compressive strength of the concrete prisms and the tensile strength of the dumbbell specimens at an age of 28 days shall be determined on specimens with the same dimensions as those used for the chloride diffusion test. The average value based on at least three specimens shall be considered to be the reference strength. For the determination of the reference compressive strength, a servo-controlled testing machine with an accuracy of ± 0.1 kN shall be used. For the reference tensile strength, it is recommended to use the same test rig as used for the tests under sustained load.

The initial chloride content of the concrete shall be determined by chemical analysis on cubes prepared from the same fresh concrete as used for the compression or tension specimens and cured in an identical way. The test procedures shall be in accordance with EN 14629 [6]. The powder required for chemical analysis can be obtained by drilling or by milling starting at a side surface of the cubes. Milling is recommended. In the case of drilling, at least three points on one side surface shall be selected. The average value as obtained from the three points shall be considered to be the initial chloride content C_i .

Compressive stress shall be applied on the prismatic concrete specimens. Tensile stress shall be applied on the dumbbell specimens. The applied stress shall be controlled regularly and kept constant for the entire duration of the test.

The stress ratio is the ratio of applied stress and the reference strength. For compression tests, the three following stress ratios shall be used: 0, 30 and 60%. For tension tests, the following stress ratios shall be used: 0, 50 and 80%.

After a particular stress is applied, the container shall be fixed immediately onto a side surface of the specimens and connected with the reservoir by the inlet and outlet hoses. The reservoir should contain at least 25 l of aqueous salt solution (3 wt% NaCl) or sea water. Then the pump to circulate the solution is started.

The concentration of the solution should be checked regularly, at least once a week during the whole exposure period and corrected if necessary. The chloride solution in the reservoir must be isolated from the atmosphere by a lid to avoid evaporation and contamination.

The specimens shall be unloaded after an exposure time of 2, 6, 18 and 36 weeks, or any other predetermined duration. The solution tank is then removed from the specimens. The specimens are then ready for the determination of the corresponding chloride profile. The scheme of the procedure for chloride profile is shown in Fig. 6.

Sampling for the determination of chloride profiles must start immediately after removal of the solution tank from the unloaded specimen. Sampling of the material for the chloride analysis can be performed in three different ways namely, (a) milling, (b) drilling or (c) cutting and subsequent crushing. The procedures for each method shall be in accordance with Ref. [7]. The recommended procedure is milling. Powder from the exposed surface of all specimens shall be obtained stepwise by milling layers with a thickness of 1–2 mm. Do not sieve the powder obtained after milling to avoid any change in the material to be analysed. The thickness of the layers should be adjusted to the expected depth of the chloride profile so that a minimum of eight points can be obtained for each profile between the exposed surface and the depth

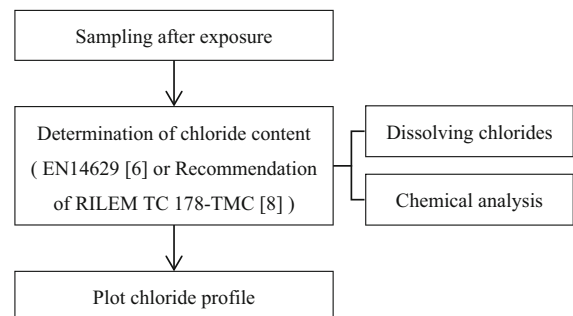


Fig. 6 The scheme of the procedure for chloride profile

where the initial chloride content is reached. Each layer should produce at least 5 g of powder. The sampling area shall not exceed $60 \times 140 \text{ mm}^2$ in the centre of the exposed surface area in order to avoid the edge effects and disturbances by the adhesive on the aluminium foil.

The chloride content of each sample shall be determined by chemical analysis according to EN 14629 [6] or the Ref. [8]. Longer time shall be needed for chloride extraction when there are particles with a diameter larger than 1 mm in the powder.

All tests shall be run at least in triplicate. The apparent chloride ion diffusion coefficient for each specimen shall be calculated by fitting the error function obtained as a solution of Fick's 2nd law. An average value of the apparent chloride ion diffusion coefficient shall be determined from at least three specimens.

4 Presentation and evaluation of test results

The chloride surface concentration and the apparent diffusion coefficient shall be determined according to Annex F of EN12390-11: 2015 [9]. Test results shall be presented in Tables 1, 2 and 3 and as graphical representation as shown below.

In particular, it has been observed that for applied compressive stress ratios higher than 50% and after longer exposure times, the obtained values of the chloride profile do not agree well with values predicted by Fick's 2nd law of diffusion. This is a clear indication that chloride penetration into concrete is a complex process in which diffusion combines with chemical reactions, interactions of the dissolved ions with the porous material (filter effect), and the effect of capillary forces. Fick's 2nd law is considered to be an approximation which describes the combined effect of the different processes. In view of this problem it is usually recommended to neglect the values obtained near the surface. It is recommended to use this approach until a more realistic model is available. A

Table 2 Parameters for chloride profiles for each concrete specimen

C_s or $C_{s,\Delta x}$
D_a
R^2
Δx
Number of layers
Number of neglected layers near the surface
The number of neglected layers near the surface shall be indicated

Table 1 Input data for chloride profiles

Test duration, t				
Initial chloride ion content, % m/m concrete				
Stress category				
Stress ratio				
Layer	Beginning of layer, mm, from exposed layer	End of layer, mm, from exposed surface	Average depth of layer, mm, from exposed surface	Average chloride ion content of layer, % by weight of concrete
L01				
L02				
L03				
L04				
L05				
L06				
L07				
L08				
L09				
L...				



Table 3 Chloride profiles as affected by stress ratio and exposure time

Stress category	Stress ratio	Exposure time, w	C_s or $C_{s\Delta x}$, wt.%	$D_a \times 10^{-12} \text{m}^2/\text{s}$	R^2	
Compression	0	2				
		6				
		18				
		36				
	30%	2				
		6				
		18				
		36				
	60%	2				
		6				
		18				
		36				
Tension	0	2				
		6				
		18				
		36				
	50%	2				
		6				
		18				
		36				
	80%	2				
		6				
		18				
		36				

typical example is given in Figs. 5 and 6. Values near the surface can be higher or lower than predicted by diffusion alone and therefore may be neglected in the data fitting process. An apparent diffusion coefficient can be determined by fitting the descending branch of the chloride profile with the error function.

The regression analyses are performed on the measured chloride profiles using the error-function solution to Fick's 2nd law as expressed by Eq. (1):

$$C_x = C_i + (C_s - C_i) \cdot \left(1 - \operatorname{erf} \frac{x}{2\sqrt{D_a \cdot t}} \right) \quad (1)$$

The initial chloride content, C_i , is determined according to Sect. 3.4. Then Eq. (1) still contains two unknown parameters, i.e. C_s and D_a . These parameters are to be determined by fitting Eq. (1) to measured chloride profiles.

The output of the regression analysis is provided in terms of C_s , D_a and the correlation coefficient, R^2 .

The calculated set of apparent diffusion coefficient, D_a , and the surface concentration, C_s , as determined on load-free and loaded samples shall be evaluated to determine the effect of the external load as well as the exposure time.

Table 1 contains the basic input information on the depth intervals of the concrete layers, the measured chloride content C_m of each layer, as well as the initial chloride content, C_i , and the duration of the test, t .

The parameters can be calculated by fitting the experimental data with the following slightly modified equation.

$$C(x, t) = C_i + (C_{s\Delta x} - C_i) \left(1 - \operatorname{erf} \left[\frac{x - \Delta x}{\sqrt{4D_a t}} \right] \right) \quad (2)$$

Here $C(x, t)$, is the chloride content measured at average depth x and exposure time t for $x > \Delta x$, % by mass of concrete; C_i , is the initial chloride content, % by mass of concrete; $C_{s\Delta x}$, is the calculated surface chloride content at the convection zone (surface region in which capillary suction and drying affect the chloride profile), % by mass of concrete; Δx , is the depth of the convection zone; D_a , is the apparent chloride diffusion coefficient, $m^2 s^{-1}$; x , is the depth below the exposed surface to the mid-point of the milled layer, m; t , is the exposure time, s.

A typical example for the measured and fitted chloride profiles as function of depth is presented in Fig. 7 where the values measured near the surface is neglected by the fitting process. Another example is shown in Fig. 8. In this case the values determined near the surface are lower than predicted by simple diffusion. These values are neglected for the determination of an apparent diffusion coefficient.

For the application and interpretation of results obtained by means of this recommendation it must be kept in mind that all tests are performed using water

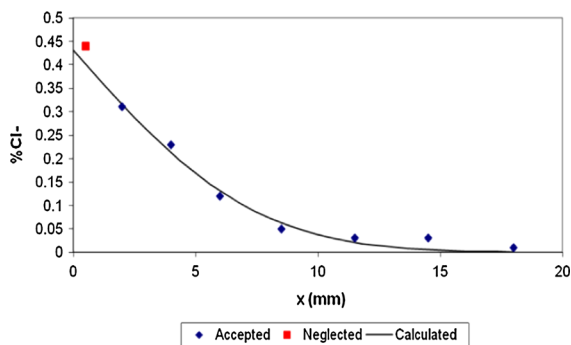


Fig. 7 Measured and fitted chloride profiles, an example

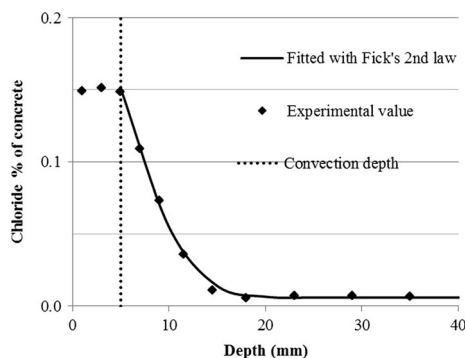


Fig. 8 Measured and fitted chloride profiles with “convection”

saturated specimens. This condition was chosen in order to provide a well-defined situation in which chloride diffusion dominates all other transport mechanisms such as capillary absorption and intermediate drying. Under these conditions the effect of an applied load on chloride penetration can be determined. The test results obtained under well-defined conditions can be considered to be a reliable indication of the durability of reinforced concrete structures in aggressive environments. In practice, however, the real situation is more complex. For realistic service-life prediction the results obtained following this recommendation have to be corrected with respect to the real conditions of exposure.

In Table 2, the output of the regression analysis is provided in terms of the fitted chloride content of exposed concrete surfaces C_s , the apparent diffusion coefficient D_a and the correlation coefficient R^2 , and Δx the depth of the convection zone.

In Table 3, results obtained on all concrete specimens are summarized.

5 Test report

The test report shall contain at least the following information.

- Reference to the method as described here
- Brief description of the test rig
- Composition of the concrete
- Selected stress ratios
- Concentration of the chloride solution
- Test results showing as Tables 1, 2 and 3 and Figs. 7 or 8, rounded to the nearest 0.001% for chloride content
- Any deviation from the procedure described in this method
- Evaluation of test results with respect to specific applications.

References

- Yao Y, Wang L, Wittmann FH (eds) (2013) Publications on durability of reinforced concrete structures under combined mechanical loads and environmental actions, An Annotated Bibliography, Aedification Publ.Freiburg. doi:10.12900/B14-0001



2. Yan Yao, Ling Wang, Folker H. Wittmann, Nele De Belie, Erik Schlangen, Hugo Eguez Alava, Zhendi Wang, Sylvia Kessler, Christoph Gehlen, Balqis MD Yunus, Juan Li, Weihong Li, Max. J. Setzer, Feng Xing, Yin Cao(2017)Test Methods to Determine Durability of Concrete under Combined Environmental Actions and Mechanical Load—Final report of RILEM TC 246-TDC, Mater Struct. doi:[10.1617/s11527-016-0983-5](https://doi.org/10.1617/s11527-016-0983-5)
3. Jiang F, Wan X, Wittmann FH, Zhao T (2011) Influence of combined actions on durability of reinforced concrete structures. Restor Build Monum 17:289–298
4. Rilem TC (1998) 107-CSP: creep and shrinkage prediction models: principles of their formation—recommendation: measurement of time-dependent strains of concrete. Mater Struct 31:212
5. EN 206 (2013) Concrete. Specification, Performance, Production and Conformity
6. EN 14629 (2007) Products and systems for the protection and repair of concrete structures—test methods—determination of chloride content in hardened concrete
7. Rilem TC (2013) 178-TMC, recommendation on methods for obtaining dust samples by means of grinding concrete in order to determine the chloride concentration profile. Mater Struct 46(3):337–344
8. Rilem TC (2002) 178-TMC: testing and modelling chloride penetration in concrete—recommendation: analysis of total chloride content in concrete. Mater Struct 35:583–585
9. EN 12390-11 (2015) Determination of the chloride resistance of concrete, unidirectional diffusion

SUMMARY

Everything we hear is an opinion, not a fact. Everything we see is a perspective, not the truth.

-Marcus Aurelius-

Under service conditions and because of environmental and climate changes, the concrete is at risk due to crack-induced durability problems. The consequences can be even more pronounced when concrete is exposed to specifically aggressive environmental conditions. This has been portrayed by rapid deterioration of relatively young concrete structures such as the ones no older than fifteen years, which obviously are much shorter than their estimated service life. As such, crack-closing ability is needed in these concrete constructions to prolong their service life.

Numerous studies have been reporting on the autogenous healing of cracks in cement-based materials. However, an active or rapid micro-crack healing is not always the case in the most critical parts of exposed structures. In this thesis, a new formulation of cement-based materials, by integrating selected bacteria and suitable organic mineral precursor compounds, was used to investigate its potential for enabling multiple crack healing events on load-induced cracked and pre-cracked concrete samples. For this purpose, chloride ingress in concrete subjected to compressive loading was investigated through laboratory experiments. Furthermore, investigation was also carried out on cracked mortar under chloride and carbon dioxide environments for healing-potential evaluation.

Methodology and Materials Development

Chapter 3 describes the method used in this study for determining chloride ingress in concrete subjected to compressive loading. Under such combined action, a more realistic characterisation of durability aspects, or a fundamental chloride-induced deterioration mechanism, of real structures is possible. This relates thus more directly to concrete in the field, which is often in certain load-induced- and environmental-stressed states. Therefore, it is considered important to understand the relationship between load-induced cracking and chloride penetrability in concrete. An attempt is made in Chapter 4 to characterize the strength development of concrete and mortar specimens containing a bacteria-based self-healing agent. The results showed that the proportion of healing agent concentration to cement content of the mix influences the strength development of specimens. The lower amount of healing agent (3% to cement weight in mortar mix) results in higher compressive strength of specimens at later age (28 days curing) in comparison to reference specimens, while higher amount of healing agent (4% to cement weight in concrete mix) results in lower strength at all ages (up to measured 28 days cured specimens). The optimum amount of healing agent to be added to specimens appears close to 3% of the applied cement weight.

Concrete Durability Assessment

In Chapter 5, chloride diffusivity into fractured concrete subjected to monotonically compressive loading was estimated. Concrete beams in dimensions of 100 x 100 x 400 mm were prepared with a 0.45 water-to-cement ratio. After 28 days of curing, the beams were

placed under pre-defined stresses at 30% and 60% of the ultimate stress, and also non-stressed (0% of the ultimate load) which acted as a control specimen. At the same time, saturated $\text{Ca}(\text{OH})_2$ solution containing 3% of weight concentration of sodium chloride (NaCl) was circulated at the mid height of the beam. Resulting chloride profiles were obtained by LIBS and an acid-solubility methodology followed by wet chemical analysis. The results present evidence that the ingress rate of chloride ions into the concrete appear reduced at compressive stress levels whereby pores are compressed. However, at higher levels of compression chloride ion ingress appears accelerated due to micro-cracking of the concrete matrix. These results indicate that the ingress of chloride shows a close relationship with compressive stress levels which are a direct consequence of the different stress level applied. The results also confirm that the chloride diffusion coefficient does not decrease but instead increases as a function of time if the structural elements are exposed to a high compressive load. This contrasts with the hypothesis that the diffusion coefficient decreases with age in sound concrete specimen.

In Chapter 6 new findings on an initial investigation in which the effect of adding a bacteria-based self-healing agent to the concrete mix and its consequences for effects of compressive loading and chloride ion penetration were reported. It was found that the healing process of cracks is strongly dependent on surrounding (environmental) conditions in which temperature and pH are the main factors controlling the bacterial metabolic capacity. External (crack ingress) water is essential for activation of the matrix-embedded bacterial spores and furthermore mineral precursor compounds are needed which are soluble in water in order to become available to the activated bacteria. As bacterial healing (metabolic conversion of precursor compounds into calcium carbonate) is an aerobic reaction, oxygen is needed for effective healing to occur.

In bacteria-based concrete, the chloride ingress is not only influenced by the stress applied but also by crack healing which occurred effectively under load-induced deformation. This became particularly apparent in concrete specimens which were subjected to 60% ultimate load and 36 weeks exposure to chloride solution. Results also showed a tendency for decrease of chloride surface concentration at higher stress level and exposure time, what suggests that increased microbial activities took place in a fracture over time. Furthermore, the healing is effective at surfaces due to ample supply of oxygen. The values of the chloride diffusion coefficient of specimens subjected to stress levels of 30% and 60% of ultimate load were found not to comply with the theory that the diffusion coefficient decreases with age due to decline of chloride surface concentration over time.

In addition to ESEM observations, oxygen micro-profiles are also presented for establishing metabolic activity of bacteria. In summary, a chloride ingress hindrance was observed in biologically induced cement-based materials as a result of microbial metabolic activities which promote precipitation of calcium carbonate. By 36 weeks, the self-healing concrete appears to be less penetrable than the normal concrete at the same level of stress. In addition to that, it also indicates that the applied chloride diffusion test assay can be considered as a reliable technique which can observe damage phenomena of concrete under compressive load what other non-destructive techniques can hardly do. However, the results are limited to certain material properties.

Quantification of healing capacity

The healing potential for improving durability aspects of cementitious materials has been further investigated in Chapter 7. This chapter presents the analysis of healing capacity with respect to carbonation and chloride transport in cracked mortar featuring incorporated

bacteria-based self-healing agent. Mortar specimens with Ordinary Portland Cement (OPC) were fabricated with dimensions of 40 x 40 x 160 mm. Cracking of mortar was performed using three-point bending under controlled crack opening displacement. The specimens were conditioned under different environmental action and were subsequently analysed using a variety of techniques, including stereomicroscopy, EDS mapping, helium pycnometry, environmental scanning electron microscopy, oxygen micro-sensing and FT-IR.

Results obtained in Chapter 7 were in line with those obtained in Chapter 6 as significant healing of cracks was observed specifically under prolonged incubation conditions. Since the addition of bacteria-based healing agent caused extra voids in the mortar matrix, higher chloride ingress was observed in 9-week exposed samples as derived from EDS mapping analysis. However, with healing treatment (under water incubation) and additional exposure time, the matrix crack configuration was partially blocked by the deposition of calcium carbonate, hindering the ingress of chloride in 18-week chloride solution-incubated bacteria-based mortar specimens. The influence of carbonation on microbial modified mortar was investigated by means of helium pycnometer testing. The results showed that the microbial self-healing is effective in carbonation environments but is not fast due to the lower pH in concrete. Another reason for observed relatively slow healing could be due to the low relative humidity used for incubation of specimen, which was lower than the optimum range for bacterial self-healing. From the ESEM observations and FT-IR analysis, the observed morphologies of minerals deposited were respectively vaterite- and calcite polymorphs of calcium carbonate-based crystals. In addition, the presence of imprints of bacteria in calcium carbonate precipitates in samples showing high oxygen consumption rates, as derived from oxygen concentration profile measurement, shows direct involvement of bacteria in calcium carbonate precipitation.

In conclusion, results from this thesis indicate that the applied bacteria-based healing agent offers a promising sustainable alternative repair system for concrete buildings. By blocking the route through which harmful substances ingress into concrete, their rate, e.g., of ingress chloride ions, can be substantially decreased. With the knowledge gathered in this thesis, the benefits of applying the bacterial healing agent in cementitious building materials are supported. Applying this technology not only provides better-performing structures, but more importantly also leads to potential economic gains.

SAMENVATTING

Alles wat we horen is een mening, geen feit. Alles wat we zien is een perspectief, niet de waarheid.

-Marcus Aurelius-

Tijdens de gebruiksfase, en versterkt door milieu- en klimaatveranderingen, kan beton scheuren waardoor duurzaamheidsproblemen kunnen ontstaan. De gevolgen kunnen nog groter zijn wanneer beton wordt blootgesteld aan specifiek agressieve omgevingsomstandigheden. Dit wordt zichtbaar door de snelle achteruitgang van relatief jonge betonconstructies, soms niet ouder dan vijftien jaar, waardoor de levensduur korter zal uitvallen dan beoogd. Daarom is in voor deze betonconstructies scheurherstel nodig om toch de beoogde levensduur te kunnen halen.

In eerdere studies is reeds gerapporteerd over het fenomeen van autogene scheurherstel in op cement gebaseerde materialen. Een actieve of snelle mate van autogeen zelfherstel van microscheurtjes komt echter niet altijd voor in de meest kritieke delen van betonconstructies. In dit proefschrift is daarom de potentie van autogeen scheurherstel in door belasting veroorzaakt gescheurd beton onderzocht. Autogeen scheurherstel wordt in dit geval gerealiseerd door kalksteen-producerende bacteriën die samen met geschikte organische minerale precursorverbindingen aan het betonmengsel worden toegevoegd. Middels laboratoriumexperimenten werd chloride-indringing in aan drukbelasting onderworpen beton onderzocht. Daarnaast is ook onderzoek gedaan aan het scheurherstellende vermogen van mortelproefstukken in chloride- en kooldioxide-houdende omgevingen.

Methodologie en materiaalontwikkeling

Hoofdstuk 3 beschrijft de methode die in dit onderzoek is gebruikt voor het bepalen van het binnendringen van chloride in beton dat is blootgesteld aan drukbelasting. Onder een dergelijke gecombineerde belasting is een realistischere karakterisering van duurzaamheidsaspecten van echte betonconstructies mogelijk. Daarom wordt het belangrijk geacht om de relatie tussen door belasting veroorzaakte scheuren en chloride-indringing in beton te begrijpen. In hoofdstuk 4 wordt de sterkteontwikkeling van beton- en mortelmonsters waaraan een op bacteriën gebaseerd zelfherstellend middel is toegevoegd onderzocht. De resultaten toonden aan dat het gehalte zelfherstelmiddel ten opzichte van het cementgehalte in het betonmengsel de sterkteontwikkeling beïnvloedt. Lagere hoeveelheden zelfherstelmiddel (3% van het cementgewicht in mortelmengsels) resulteert in een hogere druksterkte van proefstukken op latere leeftijd (28 dagen uitharding) in vergelijking met referentieproefstukken, terwijl een hogere hoeveelheid zelfherstelmiddel (4% van het cementgewicht in betonmengsels) resulteert in een lagere sterkte op alle leeftijden (tot 28 dagen uitgeharde proefstukken). De optimale hoeveelheid zelfherstelmiddel die aan mengsels wordt toegevoegd, lijkt daarom rond 3% van het toegepaste cementgewicht te bedragen.

Betonduurbaarheidsbeoordeling

In hoofdstuk 5 werd de indringingssnelheid van chloride in onder druk-belast gescheurd beton geschat. Betonbalken met afmetingen van 100 x 100 x 400 mm gemaakt met een water-cementverhouding van 0,45 werden na 28 dagen uitharden onder vooraf gedefinieerde drukbelasting van 0% (controle), 30% en 60% van de maximale drukspanning geplaatst. Tegelijkertijd werd een verzadigde $\text{Ca}(\text{OH})_2$ oplossing met 3% gewichtsconcentratie natriumchloride (NaCl) ter hoogte van het midden van de balken gecirculeerd. De resulterende chlorideprofielen werden verkregen door LIBS en door oplossen van beton in zuur gevolgd door natte chemische analyse. De resultaten tonen aan dat de indringing van chloride-ionen in het beton verminderd lijkt bij drukbelastingsniveaus waarbij de betonporiën worden samengedrukt. Bij hogere niveaus van drukbelasting lijkt de chloride-indringing echter versneld ten gevolge van microscheurvorming in de betonmatrix. Deze resultaten geven aan dat het binnendringen van chloride een sterke relatie vertoont met de verschillende toegepaste drukbelastingen. De resultaten bevestigen ook dat de chloride diffusiecoëfficiënt niet afneemt, maar in plaats daarvan toeneemt als functie van de tijd, wanneer de constructieve elementen worden blootgesteld aan een hoge drukbelasting. Dit is in tegenstelling met de hypothese dat de diffusiecoëfficiënt met oplopende leeftijd afneemt in onbeschadigde betonproefstukken.

Hoofdstuk 6 rapporteert over eerste onderzoeksbevindingen betreffende het effect van toevoegen van een op bacteriën gebaseerd zelfherstelmiddel aan onder druk-belaste en aan chloride blootgestelde betonproefstukken. Hier uit bleek dat het zelfherstelproces van scheuren sterk afhankelijk is van omgevingsomstandigheden zoals temperatuur en pH die de metabole activiteit van de bacteriën bepalen. Extern (scheurindringend) water blijkt essentieel voor activering van de aan het betonmengsel toegevoegde bacteriesporen en voor het oplossen (beschikbaar maken) van de eveneens toegevoegde minerale precursorverbindingen. Ook blijkt de aanwezigheid van zuurstof essentieel voor de microbiële metabole omzetting van precursorverbindingen in calciumcarbonaat om scheurherstel te bewerkstelligen.

In op bacteriën-gebaseerd beton wordt het binnendringen van chloride niet alleen beïnvloed door de toegepaste drukbelasting, maar ook door scheurherstel die effectief plaatsvond onder door belasting veroorzaakte vervorming. Dit werd vooral duidelijk bij betonproefstukken die werden blootgesteld aan 60% ultieme drukbelasting en 36 weken blootstelling aan chloride-oplossing. De resultaten toonden ook een afname van de chloride-oppervlakteconcentratie bij een hoger drukbelasting en blootstellingstijd, wat suggereert dat er in de loop van de tijd verhoogde microbiële activiteit plaatsvond in scheuren. Bovendien is zelfherstel effectief bij oppervlakken gekenmerkt door een ruime zuurstoftoevoer. De waarden van de chloridediffusiecoëfficiënt van proefstukken die zijn onderworpen aan drukbelastingsniveaus van 30% en 60% van de maximale belasting bleek niet te voldoen aan de theorie dat de diffusiecoëfficiënt met de leeftijd afneemt als gevolg van een afname van de chloride-oppervlakteconcentratie in de tijd.

Naast ESEM-waarnemingen worden ook zuurstofmicroprofielen gepresenteerd om de metabole activiteit van bacteriën vast te stellen. Samenvattend werd een chloride-indringingsafname waargenomen in biologisch geïnduceerde cement-gebaseerde materialen als gevolg van microbiële metabole activiteiten die de vorming van calciumcarbonaat bevorderen. Na 36 weken lijkt het zelfherstellende beton minder doordringbaar voor chloride dan het normale (referentie) beton belast op druk of hetzelfde niveau. Daarnaast geven de resultaten ook aan dat de toegepaste chloridediffusietest kan worden beschouwd als een betrouwbare methode om de schadeverschijnselen van beton onder drukbelasting waar te

nemen, wat andere niet-destructieve technieken minder kunnen. De resultaten zijn echter beperkt tot bepaalde materiaaleigenschappen.

Kwantificering van zelfherstelcapaciteit

Het zelfherstelpotentieel voor het verbeteren van duurzaamheidsaspecten van cementgebonden materialen is verder onderzocht in hoofdstuk 7. Dit hoofdstuk presenteert de analyse van het zelfherstellende vermogen met betrekking tot carbonatatie en chlorideindringing in gescheurde mortelproefstukken met toegevoegde op bacteriën gebaseerd zelfherstelmiddel. Mortelproefstukken op basis van Ordinary Portland Cement (OPC) met afmetingen van 40 x 40 x 160 mm zijn vervaardigd. Het scheuren van proefstukken werd uitgevoerd door driepuntsbuiging onder gecontroleerde opening van de scheur. De proefstukken werden geconditioneerd onder verschillende omgevingsomstandigheden en werden vervolgens geanalyseerd met behulp van verschillende technieken, waaronder stereomicroscopie, EDS-mapping, heliumpyknometer, environmental-scanning-elektronenmicroscopie, zuurstof microsensing en FT-IR.

De resultaten verkregen in hoofdstuk 7 waren in overeenstemming met die verkregen in hoofdstuk 6, aangezien significant zelfherstel van scheuren specifiek werd waargenomen onder langdurige incubatieomstandigheden. Aangezien de toevoeging van op bacteriën gebaseerd zelfherstelmiddel extra poriën veroorzaakt in de mortelmatrix, werd een hoger chloride-indringing waargenomen in 9 weken blootgestelde proefstukken zoals afgeleid van EDS-mapping analyse. Bij zelfherstelbehandeling (bij incubatie onder water) en extra blootstellingstijd werd de configuratie van de matrixscheur gedeeltelijk geblokkeerd door de afzetting van calciumcarbonaat, wat het binnendringen van chloride belemmerde gedurende 18 weken blootstelling van de proefstukken aan de chlorideoplossing. De invloed van carbonatatie op microbiëel gemodificeerde mortel werd onderzocht door middel van heliumpyknometertesten. De resultaten toonden aan dat het microbiële zelfherstel effectief is in carbonatatieomgevingen, maar niet snel is vanwege de lagere pH van het beton. Een andere reden voor het waargenomen relatief langzame zelfherstelproces kan te wijten zijn aan de lage relatieve vochtigheid die werd gebruikt voor de incubatie van proefstukken, die lager was dan het optimale bereik van scheurzelfherstel door bacteriën. Uit de ESEM-waarnemingen en FT-IR-analyse bleek dat de waargenomen vormen van de afgezette kalksteenmineralen duiden op vateriet- en calciëtpolymorfen van calciumcarbonaatkristallen. Bovendien toont de aanwezigheid van afdrukken van bacteriën in het gevormde calciumcarbonaat op directe betrokkenheid van bacteriën bij het proces van calciumcarbonaatprecipitatie.

Concluderend geven de resultaten van dit proefschrift aan dat toepassing van op bacteriën gebaseerd zelfherstelmiddel een veelbelovend duurzaam alternatief reparatiesysteem voor betonconstructies biedt. Door de route te blokkeren waardoor schadelijke stoffen in beton binnendringen, kan de snelheid van bijvoorbeeld binnendringende chloride-ionen aanzienlijk worden verlaagd. Met de kennis die in dit proefschrift is verzameld, worden de voordelen van het toevoegen van het bacteriële zelfherstelmiddel in cementgebonden bouwmaterialen ondersteund. Het toepassen van deze technologie leidt niet alleen tot beter presterende betonconstructies, maar ook tot potentiële economische voordelen.

Curriculum Vitae

Name: Balqis Md Yunus

Date of Birth: 27 November 1982

Place of Birth: Kuala Lumpur, Malaysia

Email: balqis1157@uitm.edu.my
bmdyunus@gmail.com



- | | |
|-------------|---|
| 2013 – 2022 | Phd Candidate in Civil Engineering, Microlab
Delft University of Technology, The Netherlands |
| 2008 – 2013 | Educator,
Universiti Teknologi MARA, Malaysia |
| 2007 – 2008 | MSc Candidate in Civil Engineering
Universiti Teknologi MARA, Malaysia |
| 2006 – 2007 | Teaching Assistant,
Universiti Teknologi MARA, Malaysia |
| 2000 – 2005 | Diploma and BSc Candidate in Civil Engineering
Universiti Teknologi MARA, Malaysia |

List of Publications

Journal publications

1. **Md Yunus, Balqis**, and Mohd Raizamzamani Md Zain. "Comparison of Metakaolin and Glass Powder as Supplementary Cementitious Materials (SCM) in Rubberized Concrete." *Iranian Journal of Science and Technology, Transactions of Civil Engineering* (2022): 1-9.
2. M Mohamad, OC Lian, MRM Zain, **BM Yunus**, NH Sidek, "Student Attainment Measurement System in Civil Engineering Undergraduate Programme: A Satisfaction Survey," *Asian Journal of University Education*, v17 n2 p191-202 Apr 2021
3. **B. Yunus**, E. Schlangen, and H. M. Jonkers, "Bio-based self-healing mortar," *International Journal of Integrated Engineering*, vol. 10, 2019
4. Mohd Raizamzamani Md Zain, Norrul Azmi Yahya, Lee Siong Wee, Oh Chai Lian, **Balqis Md Yunus**, *Experimental study on the bearing capacity of concrete blocks loaded through square and circular steel plates*, IOP Conference Series: Materials Science and Engineering, vol. 513, no. 1, p. 12, 2019.
5. Yan Yao, Ling Wang, Folker H. Wittmann, Nele De Belie, Erik Schlangen, Hugo Eguez Alava, Zhendi Wang, Sylvia Kessler, Christoph Gehlen, **Balqis Md. Yunus**, Juan Li, Weihong Li, Max J. Setzer, Feng Xing, Yin Cao *Test methods to determine durability of concrete under combined environmental actions and mechanical load: final report of RILEM TC 246-TDC*, Materials and Structures, vol. 50, no. 2, p. 123, 2017.
6. Yan Yao, Ling Wang, Folker H. Wittmann, Nele De Belie, Erik Schlangen, Hugo Eguez Alava, Zhendi Wang, Sylvia Kessler, Christoph Gehlen, **Balqis MD Yunus**, Juan Li, Weihong Li, Max J. Setzer, Feng Xing, Yin Cao, *Recommendation of RILEM TC 246-TDC: test methods to determine durability of concrete under combined environmental actions and mechanical load*, Materials and Structures, vol. 50, no. 2, p. 155, 2017.
7. Z Ahmad, SZ Othman, **B Md Yunus**, A Mohamed, *Behaviour of masonry wall constructed using interlocking soil cement bricks*, World Academy of Science, Engineering and Technology, vol. 60, issue. 12, p. 1263, 2011.

Book contributions

1. **M.Y. Balqis**, H.M. Jonkers, E. Schlangen, *Proceedings of the First International Conference on Construction Materials and Structures*, IOS Press Ebooks: Construction Materials and Structures, 2014.
2. **Balqis Binti Md Yunus**, *PhD Conference on Structural Engineering*, Structural Synergy, 2013.

Conference proceedings

1. MY Balqis, HMK Saiful, MMZ Raizamzamani, *Ettringite: Influence of Steam Curing and Excessive Sulphate Content*, Proceedings of the 5th International Conference on Sustainable Civil Engineering Structures and Construction Materials. Lecture Notes in Civil Engineering, vol 215. Springer, Singapore, 2022.
2. **B Binti Md Yunus**, E Schlangen, HM Jonkers, *Chloride transport under compressive load in bacteria-based self-healing concrete*, Proceedings of the 5th International Conference on Self-Healing Materials, ICSHM, Durham, USA, June 22-24, 2015.
3. **MY Balqis**, EMG Aruan, NH Mohd, *Chemical and physical characterizations of dried and pulverized sewage sludge/clay as lightweight aggregates*, 2011 3rd International Symposium & Exhibition in Sustainable Energy & Environment (ISESEE), Melaka, pp. 106-109, 2011.